

**UNIVERSIDAD AUTÓNOMA DE MADRID
FACULTAD DE CIENCIAS
DEPARTAMENTO DE BIOLOGÍA**

**ESPECIACIÓN Y DISTRIBUCIÓN DE MERCURIO
EN PLANTAS COMO BASE CIENTÍFICA
PARA FITOTECNOLOGÍA**

**SPECIATION AND DISTRIBUTION OF MERCURY
IN PLANTS AS SCIENTIFIC BASES
FOR PHYTOTECHNOLOGY**

TESIS DOCTORAL

SANDRA CARRASCO GIL

MADRID 2011

Memoria presentada para optar al Grado de Doctor en Ciencias
dentro del programa "Biología Vegetal: Aspectos Moleculares,
Fisiológicos y Biotecnológicos"

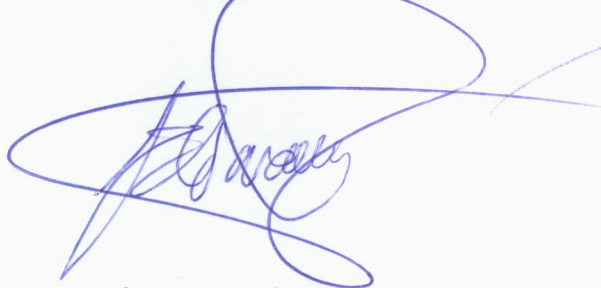
Madrid, Abril de 2011

La doctoranda:



Fdo.: Sandra Carrasco Gil
Licenciada en Ciencias Ambientales

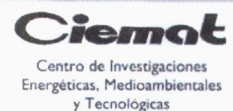
LOS DIRECTORES:



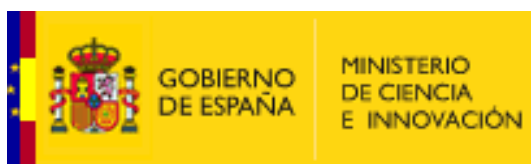
Dr. Luís E. Hernández Rodríguez
Profesor Titular de Universidad
Departamento de Biología
Universidad Autónoma de



Dra. Rocío Millán Gómez
Investigadora Titular de OPIs
Departamento de Medio Ambiente
CIEMAT



Este trabajo ha sido financiado por:



El Ministerio de Ciencia e Innovación a través de los proyectos:

RECUPERACIÓN DE SUELOS CONTAMINADOS POR MERCURIO:
RECOMENDACIONES DE USOS DE SUELOS Y PLANTAS EN LA COMARCA DE
ALMADÉN (CTM2005-04809/TECNO-REUSA).

PROSPECCIÓN DE BIOMARCADORES DE RESPUESTA A METALES (AGL2010-
15151-PROBIOMET).



La Fundación Ramón Areces a través del
proyecto: CARACTERIZACIÓN DE LOS
MECANISMOS DE RESISTENCIA DE LAS PLANTAS A
METALES PESADOS



Junta Comunidades Castilla-La Mancha a través del proyecto:

FITORREMEDIACIÓN DE EMPLAZAMIENTOS AFECTADOS POR MERCURIO EN LA
COMARCA DE ALMADÉN CON PLANTAS DE USO AGRÍCOLA (FITOALMA2,
POII10-0087-6458).

Agradecimientos/Acknowledgements

Han pasado casi cinco años desde el día que decidí apostar por el duro, pero sin embargo, apasionante mundo de la investigación, y gracias a él, he tenido la suerte de conocer gente excepcional que me ha acompañado en el camino. Por ello, no puedo pasar sin agradecer el apoyo, la ayuda y los ánimos que todos ellos me han aportado en todo este tiempo.

En primer lugar me gustaría agradecer a mis directores de tesis su apoyo, gracias al cual, este trabajo ha salido adelante. A Rocío, por la oportunidad que me brindó con la beca FPI del Ministerio de Ciencia e Innovación, gracias por creer en mí, y ayudarme a que todo fuera más fácil. A Luís, por inculcarme esa curiosidad por las cosas, por estar siempre ahí cuando le he necesitado y por animarme en los momentos difíciles.

A mi gente del Ciemat: Maite, Adrian, Aída, Javierinchi, Avelino, Thomas, Ana, Vergelina, Miguel, José, Juliana... a todos los “vecinos” de la “biblioteca-comedor-gymnasio”: Laura, Julio, Juan Luís, José Manuel, Javi... a Luisa, gracias por animarme con TODO, y por fomentar esos minutos de relax que nos han hecho pasar tan buenos momentos... a Mari José, mi compi de despacho con la que tantas cosas he compartido y a la que aprecio tanto... a Carmen, por nuestras charlillas en el laboratorio...a mi ND: Marcos, Antonio y Celia, a los que considero compañeros pero sobre todo AMIGOS, gracias por animarme SIEMPRE, por la ayuda, por las risas, por las rutas en bici, por los torneos “paquete”, por los pinchitos de tortilla...cómo se os echa de menos...

A mi gente del labo de fisio vegetal que tan bien me acogisteis. Primeramente a Paquita, por ser tan estupenda con todo y hacerme sentir desde el primer día como una más. A Juan, por ser tan paciente conmigo, y enseñarme tantas cosas. A mis niñas, Laura y Belén por tantos ratos divertidos y por las plantulitas de alfalfa que me regalabais. A Cristina, por estar siempre disponible cuando he necesitado ayuda o consejo. A David por su entusiasmo, sus ganas de aprender y su positividad contagiosa. A María por ayudarme con el invernadero y ser tan dispuesta para todo. A mis vecinos de enfrente: Sole, Ángel y Youness por los ánimos. Y a la gente con la que compartí laboratorio y ya no está, Laura, Sara, Diego.

Al grupo de Javier y Monona Abadía del Aula Dei-CSIC de Zaragoza, gracias a los dos por acogerme siempre tan bien. Y por supuesto a Aurora, Rubén, Ruth, Jorge, Hamdi, Irene, Giuseppe, Saúl y Ana Flor siempre disponibles para echar una mano cuando lo he necesitado, y especialmente a Ana, por ser para mí, un ejemplo a seguir como profesional, de la que he aprendido tantas cosas.

Thanks to people of California State University, East Bay: primarily to Danika, thanks for giving me the opportunity to work in the synchrotron, for helping me with all I needed and for your enjoyable Thursday's meeting. To Lisa and Gina for your sympathy and help in the lab. To Wren and Jennifer, for sharing those nights working at SSRL, for the dinners, for sharing beam time... thanks to everybody for being so kind to me.

Agradecimientos/Acknowledgements

Also thanks to SSRL people: To Piero, Florian, Yijin, Sam and Cynthia, for your help and especially to Joy, for making easier my stay, for helping with everything and for making me fell like home.

A Hagar por hacer sacar el máximo partido a mi estancia en California y por los buenos ratos, con un café en la mano, charlando sobre la vida en los Estados Unidos.

Y por supuesto a todos mis amigos de SIEMPRE: a David, Sergio, Tony, Tole, Silvi, Anita, Cesar, Sara... a mis chicas, Luni y Olga que siempre me decían ¿pero cuándo vas a terminar esto?, pues ¡YA!. A Caro por estar siempre tan orgullosa de mí y “venderme” como si fuera mi manager, que para ella, todo lo que hago siempre está bien. A Javi churri, que ha sido para mí un ejemplo de tenacidad y tesón. Gracias por ser mis amigos incondicionales, apoyarme en todo lo que hago y confiar en mí.

A mi GRAN AMIGA María, que siempre me acompaña y comparte los buenos y malos momentos. Por esos días de codo con codo en los que no veíamos nunca el fin de todo esto, por los días que quedan por llegar y disfrutar...gracias por ser la mejor.

A Leta, José Carlos, Chus, Dolores y Chefas a los que les tengo un especial cariño, y siempre han estado ahí para darme ánimos e interesarse por mis cosas.

Y ESPECIALMENTE, a Toti por hacerme ver que lo que hacía era IMPORTANTE, por su ánimo constante, su apoyo incondicional y su cariño durante todos estos años. A mi hermana Vanessa y a Javi, que siempre han estado dispuestos a ayudarme y apoyarme; a Paula y Adrian que consiguen sacar mi mejor sonrisa incluso en los momentos duros y sobre todo, a mis padres, Lina y Luís; por animarme y apoyarme en todo lo que hago y por estar siempre tan orgullosos de mí.

Gracias

A mis padres

RESUMEN

El mercurio (Hg) y la mayoría de sus compuestos son altamente tóxicos para las personas y para los ecosistemas. Es considerado un contaminante global debido a su alta movilidad y extremada persistencia en el medio ambiente. Un factor muy importante de los efectos del mercurio en el medio ambiente es su capacidad para acumularse en organismos y ascender por la cadena alimentaria convirtiéndose en una seria amenaza para la población humana.

El área minera de Almadén, situada al sur de España (Ciudad Real), ha sido durante siglos la zona de mayor producción de Hg a nivel mundial. El cese de la producción de Hg ha impuesto la necesidad de promover otras actividades económicas, tales como la agricultura y la ganadería las cuales se han visto debilitadas por el contenido de Hg en los suelos agrícolas de la zona. Por tanto, era importante evaluar el riesgo potencial para la salud humana y el medio ambiente considerando la absorción y distribución de Hg en cultivos que se adapten a las condiciones de la zona. En este sentido, se propuso el uso de la alfalfa (*Medicago sativa*) como cultivo alternativo y/o como planta para fitotecnologías en la comarca de Almadén, la cual podría ayudar a eliminar o estabilizar contaminantes evitando a su vez, erosión y pérdida de fertilidad en los suelos. No obstante, para la utilización de alfalfa en fitotecnologías es preciso conocer en detalle aspectos como la especiación y distribución de contaminantes dentro de la planta, para determinar el posible uso agronómico de éstas. Además, para favorecer la producción de biomasa y permitir una adecuada revegetación de los suelos contaminados es necesario determinar la influencia de la fertilización por nitrato (NO_3^-), principal nutriente limitante en los suelos problema, con respecto a la tolerancia a Hg.

El Hg se acumuló principalmente en la raíz, concretamente en la fracción celular particulada, mayoritariamente de pared celular. Se determinó asimismo la especiación del Hg soluble mediante cromatografía líquida de alta resolución (HPLC) acoplada a un espectrómetro de masas de tiempo de vuelo (TOFMS), lo que nos permitió identificar fitoquelatinas (PCs) y homofitoquelatinas (hPCs) unidas a Hg en plantas tratadas con Hg 30 μM . Estos biotioles están considerados como uno de los más importantes mecanismos de defensa de las plantas frente a metales pesados, siendo sintetizados en las células vegetales a partir de glutatión (GSH) u homoglutatión (hGSH, existente en algunas leguminosas). La enzima que cataliza la reacción es la fitoquelatina sintasa, que se activa post-traduccionalmente por la acumulación del metal, y produce una familia de

péptidos con la estructura general (Glu-Cys)_n-Gly, donde *n* varía según el tiempo de exposición al metal y su dosis. Esta identificación también fue llevada a cabo en plantas de maíz y cebada para investigar posibles diferencias entre especies vegetales. En este sentido, se detectaron 11 nuevos complejos no descritos anteriormente, formados por Hg y metil-Hg unidos a PCs y hPCs. Para comprobar la importancia de estos biotioles en la detoxificación de Hg se utilizaron plantas mutantes de *Arabidopsis thaliana* deficientes en la producción de PCs, *cad1-3*, y en el nivel de GSH, *cad2-1*, apreciándose que la falta de formación de complejos Hg-PC disminuye la tolerancia a Hg.

Para estudiar la localización de Hg a nivel de tejido se empleó micro Fluorescencia de Rayos-X con fuente Sincrotrón (μ -SXRF), estableciéndose que el Hg estaba localizado posiblemente en los conductos vasculares de raíz, tallo y hojas de alfalfa, de plantas que fueron crecidas en un medio hidropónico puro para aumentar la concentración y la señal de fluorescencia. Paralelamente se estudió la localización de Hg en plantas de marrubio (*Marrubium vulgare*) muestreadas en un suelo contaminado ubicado en una antigua planta metalúrgica, donde se obtenía Hg a partir del mineral cinabrio. Los resultados revelaron que si bien las plantas crecidas hidropónicamente absorbían el metal a través de los ápices de las raíces translocándolo a parte aérea, las plantas naturales presentaron un comportamiento excluyente, reteniendo el Hg en la raíz sin translocación a parte aérea.

Mediante la técnica de Absorción de Rayos-X (EXAFS) se identificaron los enlaces de coordinación en torno al Hg, cuando éste es absorbido por la planta. Este análisis, al igual que el de localización de Hg, se llevó a cabo en raíz, tallo y hoja de alfalfa y raíz y hoja de marrubio. Mientras que en alfalfa, más del 79% del Hg estaba unido a azufre orgánico (enlaces Hg-Cys), en el marrubio más del 60% del Hg estaba unido a azufre inorgánico, posiblemente de partículas de suelo adheridas al tejido. Además, se procedió a estudiar a nivel subcelular la distribución de Hg analizando muestras de alfalfa mediante Microscopía de Transmisión Electrónica (TEM), que permitió detectar depósitos densos, debido a la presencia de Hg, en la pared celular de raíces de la epidermis y xilema, lo que concuerda con los resultados de fraccionamiento subcelular realizados.

Por último, se estudió la influencia de la fertilización nitrogenada sobre la absorción de Hg por la alfalfa y sobre parámetros de estrés como peroxidación de lípidos, contenido en clorofilas, actividad enzimática de enzimas glutatión reductasa (GR) o ascorbato peroxidasa (APX). El estudio se realizó previamente bajo condiciones controladas en

semihidropónico y posteriormente se llevó a maceta con suelo contaminado de Almadén, para aproximarse paulatinamente a condiciones reales de campo. En ambos casos, se observó que la fertilización con NO_3^- reducía el estrés oxidativo en las raíces. Sin embargo la fertilización con un abono NPK del suelo de Almadén hizo que la planta acumulara en la parte cosechable, niveles de Hg por encima de lo permitido legalmente, poniendo de manifiesto la importancia del estudio de la absorción de Hg para evitar riesgos en la salud humana.

Un conocimiento preciso de los mecanismos de detoxificación y tolerancia de metales tóxicos es importante para optimizar las estrategias de descontaminación mediante fitorremediación. El trabajo de investigación que se presenta abre nuevas perspectivas hacia la aplicación de técnicas avanzadas para estudiar el comportamiento del Hg y su dinámica en plantas, con el objetivo último de poder aplicar estos conocimientos a fitotecnologías. En concreto, el empleo de plantas de alfalfa, podría permitir la estabilización de contaminantes, y facilitar la revegetación de suelos contaminados, evitando a su vez, erosión y pérdida de fertilidad como pueden ser el caso de Almadén. A su vez, es interesante destacar la importancia de una adecuada nutrición nitrogenada para mejorar la tolerancia a contaminantes, si bien ha de realizarse una monitorización de los cultivos para evitar el riesgo de introducir el Hg en la cadena trófica, y llegar a suponer un problema para la salud humana.

INDEX

CHAPTER 1. Advances in the characterization of mercury speciation and distribution in plants using novel approaches	1
Mercury is a problem for human health and the environment	2
Toxic effects of mercury in plants	2
Chemical species of mercury in the environment	4
Distribution and speciation of Hg in plants	5
Use of Mass Spectrometry technique for the identification of Hg-containing compounds in plants	7
Speciation and localization of Hg in the plant using a synchrotron source: X-ray absorption spectroscopy (XAS) and X-ray fluorescence (XRF)	10
Phytoremediation technologies	14
Concluding remarks and future perspectives	16
References	17
CHAPTER 2. Objectives	23
CHAPTER 3. Complexation of Hg with phytochelatins is important for plant Hg tolerance	25
ABSTRACT	25
INTRODUCTION	26
MATERIAL AND METHODS	28
Plant material	28
Tolerance to Hg assay	28
Tissue fractionation	29
Anion exchange chromatography of root soluble fractions	29
Biothiol analysis	29
Mercury analysis	30
Preparation of biothiol and Hg-biothiol complex standard solutions	30
Biothiol and Hg-biothiol analysis by HPLC-ESI-TOFMS	30
Synchrotron X-ray fluorescence microprobe (μ -SXRF)	31
Extended X-ray absorption fine structure (EXAFS)	32
Statistical analysis	33
RESULTS	33
Plant growth and Hg distribution in tissues	33
Subcellular fractionation and association of soluble Hg with biothiols in roots	33
Detection of Hg-biothiol complexes by HPLC-ESI-TOFMS	34
<i>In vivo</i> X-ray spectroscopy of Hg in alfalfa roots	41
Tolerance analysis of <i>A. thaliana cad1-3</i> and <i>cad2-1</i> mutants	42
DISCUSSION	47
REFERENCES	51

CHAPTER 4. Mercury localization and speciation in hydroponic culture and natural plants	57
ABSTRACT	57
INTRODUCTION	58
MATERIAL AND METHODS	60
Plant material	60
Mercury analysis	61
Synchrotron X-ray fluorescence microprobe (μ -SXRF) and X-ray computed micro-tomography (SR- μ CT)	62
Extended X-ray absorption fine structure (EXAFS) and X-ray Absorption Near Edge Structure (XANES)	62
Transmission X-ray Microscopy (TXM)	63
Transmission Electronic Microscopy analysis (TEM)	64
RESULTS	64
Plant growth and Hg concentration in tissue	64
Localization of Hg and other elements in <i>Medicago sativa</i>	65
Mercury speciation in <i>Medicago sativa</i>	71
Localization of Hg in <i>Marrubium vulgare</i>	73
Mercury speciation in <i>Marrubium vulgare</i>	75
DISCUSSION	77
CONCLUSIONS	81
REFERENCES	82

CHAPTER 5. Attenuation of mercury phytotoxicity with a high nutritional level of nitrate in alfalfa plants grown in a semi-hydroponic system	87
ABSTRACT	87
INTRODUCTION	88
MATERIAL AND METHODS	90
Plant material, growth conditions and treatments	90
Mercury analysis	90
Nitrogen in plants	90
Oxidative stress indexes	91
Preparation of non-protein thiol standard solutions	92
Analysis on non-protein thiols	92
Determination of in vitro nitrate reductase activity	93
Glutathione reductase and ascorbate peroxidase	93
Statistical analysis	94
RESULTS	94
Mercury concentration and biometric parameters	94
Nitrogen assimilation	95
Stress indexes	96
Biothiols analysis	98
DISCUSSION	99

CONCLUSIONS	103
REFERENCES	103

CHAPTER 6. Influence of nitrate fertilisation on Hg uptake and oxidative stress parameters in alfalfa plants cultivated in a Hg-polluted soil 107

ABSTRACT	107
INTRODUCTION	107
MATERIAL AND METHODS	111
Chemical and soil analysis	111
Experimental design, plants and growth conditions	111
Sampling	112
Mercury determination	112
Nitrogen in plants	113
Metal stress indexes	113
Glutathione reductase and ascorbate peroxidase	114
Preparation of non-protein thiol standard solutions	115
Analysis on non-protein thiols	115
Statistical analysis	116
RESULTS	116
Soil	116
Mercury concentration and distribution in alfalfa plants	117
Biometric parameters	118
Nitrogen content in alfalfa plants	119
Oxidative stress parameters	119
Analysis of non-protein thiols	121
DISCUSSION	122
CONCLUSIONS	124
REFERENCES	125

CONCLUSIONES GENERALES 127

APPENDIX I. Supplementary Table 1. LC—ESI/MS(TOF) analysis of biothiols and Hg biothiols complexes standard solutions.

APPENDIX II. Curriculum vitae



CHAPTER 1

CHAPTER 1

Advances in the characterization of mercury speciation and distribution in plants using novel approaches

ABSTRACT

In this chapter we summarize the recent findings about the distribution, localization and speciation of mercury (Hg) in higher plants. Lately, state-of-the-art analytical techniques, such as mass spectrometry coupled with high performance liquid chromatography and X-ray fluorescence with a synchrotron light source, are paving the way for a better understanding of Hg dynamics in plants. The behavior of Hg in plants will also shed some light to characterize the phytotoxic mechanisms and detoxification tools available for improved phytoremediation of soils polluted with Hg.

Mercury is a problem for human health and the environment

Mercury is one of the most toxic and hazardous metals to the environment, capable of compromising seriously human health. The expression "mad as a hatter" was popular in England in the 19th century, which reflected the neurotoxic symptoms observed in hat makers who inhaled Hg vapours released from mercuric nitrate solutions to felt furs. Such symptoms probably inspired the well known Mad Hatter character in Lewis Carroll's *Alice in Wonderland*. In more recent times, there have been several cases of human intoxication, frequently occurring after the ingestion of food contaminated with methyl-Hg, one of the most toxic chemical form of Hg. One of the worst episodes of Hg poisoning occurred in Minamata Bay and the Agano River (Japan) in 1956 as a consequence of a continuous spillage of Hg from a chemical factory. Mercury accumulated in phytoplankton, shellfish and fish as methyl-Hg, which contaminated those animals feeding from them. Domestic and wild-life animals showed erratic behaviour and nervous tremors, anteceding the tremendous effects on the local population, which suffered severe neurologic, renal and hepatic diseases and death (Naito, 2008). Another massive intoxication with Hg occurred in Iraq in the early 1970s, owing to the consumption of 95,000 tons of seeds treated with organomercurial fungicides that were used for bread baking (WHO, 1976). It has also been detailed that exposure to methyl-Hg may occur in some crops cultivated under anoxic (flooded) conditions, such as rice (Feng et al., 2008; Zhang et al., 2010). Thankfully, poisoning by

Hg is quite rare nowadays. In United State the only reported cases in the past 35 years involved a family that consumed the pork meat of animals fed with a methyl-Hg fungicide, and a professor of Chemistry in Dartmouth College (New Hampshire, USA) was accidentally exposed to a few drops of dimethyl-Hg during her experiments in the laboratory, causing her death (Nierenberg et al., 1998).

Because the referred data and other examples, Hg is considered a very hazardous and potent pollutant, with high potential to bio magnify in the food chain, characteristics that prompted a drastic reduction in its usage and trade in several countries. The Provisional Tolerable Weekly Intake (PTWI) of Hg recommended by the Joint FAO/WHO Expert Committee on Food Additives (JECFA) is $5 \mu\text{g kg}^{-1}$ and the EPA has established a limit of 0.002 mg L^{-1} for mercury in drinking water. Regarding forage use, the accepted maximum Hg concentration is 0.1 mg kg^{-1} of feeding mass (EC Directive, 2002). In 2005, the European Union (EU) drew up a strategy called “Community Strategy concerning Mercury” that was accompanied by specific actions, aimed mainly at reducing the quantity and the circulation of Hg within the EU and throughout the World as well as human exposure to this substance. This strategy is based on six objectives: (1) limiting Hg emissions, (2) reducing the supply and demand of Hg, (3) managing and controlling existing amounts of Hg used in manufactured products or kept stored, (4) protecting against its exposure, (5) improving understanding of Hg dynamics and toxic effects to implement solutions, and (6) promoting action on Hg at an international scale (European Commission, 2005).

Toxic effects of mercury in plants

Mercury accumulates in the roots of higher plants with a higher extent than in above ground tissues, indicating that the translocation to shoots is generally low (Wang and Greger, 2004; Israr et al., 2006). Mercury has not know biological activity in plants, and at relatively low concentrations can cause several phytotoxic effects, similarly as other non-essential heavy metals like Cd or Pb (Van and Clijters, 1990). Growth inhibition is one of the typical toxic effects that appear shortly after Hg exposition (Rellán-Álvarez et al., 2006b; Zhou et al., 2007; Israr et al., 2006; Cargnelutti et al., 2006; Patra and Sharma, 2000). For example, alfalfa seedlings growth was inhibited by 25% when treated with $3 \mu\text{M HgCl}_2$ for 6 h (Ortega-Villasante et al., 2005). Mercury inhibits water uptake via Hg-sensitive aquaporins on plasma membranes and consequently affects the transpiration (Zhang and Tyerman, 1999; Savage and Stroud, 2007; Cárdenas-

Hernández et al., 2009). Exposure to Hg can also alter the levels of some nutrients due to changes in membrane integrity and transport processes (Godbold et al., 1991; Shieh and Barber, 1973; De Filippis, 1979). Furthermore, it has been reported that Hg decreases the levels of photosynthetic pigments like chlorophylls and carotenoids, and inhibits photosynthetic electron transport chain (Cargnelutti et al., 2006; Cho and Park, 2000; Bernier and Carpentier, 1995; Bernier et al., 1993).

Although the precise mechanisms of toxicity are not known in detail, the high affinity of Hg for sulfhydryl groups (–SH) of proteins could explain its high reactivity. Once Hg is bound to proteins, their native structure is disturbed losing their function (Clarkson, 1972). However, so far there are few proteins identified that interact specifically with Hg in higher plants, apart from the already mentioned plasma membrane aquaporin-1 (Murata et al., 2002).

The root cell wall is directly in contact with metals in soil or nutrient solution, thus the proteins that are in cell wall and at the surface of the plasma membrane are the first targets for heavy metal toxicity. The role of the cell wall as a mechanism of Hg tolerance is supported by the fact that more than 90% of the Hg up taken by plants is accumulated in the cell wall of root cells (Valega et al., 2009; Carrasco-Gil et al., 2011). Exposition of Hg may stimulate the production of intermediate free radicals and peroxides called reactive oxygen species (ROS), that may damage and membrane resulting in oxidative stress (Ortega-Villasante et al., 2005; Rellán-Álvarez et al., 2006b; Sobrino-Plata et al., 2009). It has been reported that after the addition of diphenyleneiodonium chloride (DPI), which is an inhibitor of the enzyme NADPH oxidase, the H₂O₂ production was reduced in *Medicago sativa* seedling treated with Hg. This enzyme is present in the plasma membrane and is involved in H₂O₂ generation after metal exposition (Ortega-Villasante et al., 2007). To this end, an analysis of Hg localization is very important to elucidate what cellular process may be altered.

Plants have developed a defence system composed of antioxidant enzymes and antioxidant metabolites, that help to maintain the redox balance of the cell interrupting the cascades of uncontrolled oxidation (Foyer et al., 1997). The toxic action of Hg may also be related to an alteration of this antioxidant enzyme activities such as superoxide dismutase (SOD), ascorbate peroxidase (APX) or glutathione reductase (GR) (Ortega-Villasante et al., 2005; Sobrino-Plata et al., 2009; Zhou et al., 2007; Elbaz et al., 2010). Glutathione is a tripeptide constituted by glutamic acid, cysteine and glycine (γglu-cys-

gly) which is considered as one of the most important antioxidant metabolite involved in the defence against ROS. It is present mainly in reduced form (GSH), localized in all cell compartments: cytosol, endoplasmic reticulum, vacuole, mitochondria, chloroplast, peroxisomes and apoplast (Mittler and Zilinskas, 1992; Jimenez et al., 1998). The balance between GSH and GSSG in the ascorbate-glutathione cycle is the key for maintaining cellular redox state (Foyer and Noctor, 2005). However, Hg may alter this balance in plants as was observed with diminution in the cellular concentration of reduced glutathione (GSH) versus its oxidized form (GSSG; Rellán-Álvarez et al. 2006a; Ortega-Villasante et al., 2007; Sobrino-Plata et al., 2009). Moreover, GSH is the substrate for the biosynthesis of phytochelatins (PCs) which play an important role in Hg tolerance as we will discuss below. Therefore, the presence of a high GSH concentration increases the ability of plants to support metal-induced oxidative stress as it was observed with plants exposed to Cd (Metwally et al., 2005; Sun et al., 2007).

Chemical species of mercury in the environment

Mercury has three oxidative states: elemental or metallic ($\text{Hg}(0)$ or Hg^0), monovalent (mercurous, $\text{Hg}(\text{I})$, Hg_2^{2+}) or divalent (mercuric, $\text{Hg}(\text{II})$, Hg^{2+}). The properties and chemical behavior of Hg strongly depend on their oxidative state. Hg^0 is normally present in the atmosphere and may also be present in aqueous media, although Hg^0 species is very rare in aquatic natural ecosystems. The vapor pressure of Hg^0 depends strongly on temperature, and it vaporizes readily under ambient temperature in most natural ecosystems in some seasons. $\text{Hg}(\text{II})$ and $\text{Hg}(\text{I})$ can form several inorganic and organic chemical compounds, but $\text{Hg}(\text{I})$ is less abundant due to its low stability in natural environments (EPA, 1997). Inorganic mercuric compounds such as mercuric chloride (HgCl_2), mercuric hydroxide ($\text{Hg}(\text{OH})_2$) and mercuric sulfide (HgS) are the most common Hg compounds in the environment. They are white powder or crystal except for HgS which is red and turns black when is exposed to light. HgCl_2 is sufficiently volatile to be transformed into inorganic Hg gas. However, due to its water solubility and chemical reactivity, the inorganic Hg gas is deposited faster than the elemental Hg, with a shorter atmosphere lifetime. When Hg is bound to carbon, the compounds formed are organomercurials such as methylmercuric chloride (CH_3HgCl), methylmercuric hydroxide (CH_3HgOH) or small fractions of other organomercurials (dimethylmercury and phenylmercury) (UNEP, 2002). Mercury is slightly soluble in water and trends to associate with soft bases like S (S^{2-} , SH), I, organic S, P and N (Stumm and Morgan, 1981). As a result of coordination selectivity, Hg prefers S-donors

to O-donors as a ligand. Mercury, in contrast to other metals, tends to form covalent rather than ionic bonds. Under moderately oxidizing conditions above pH 5, the predominant Hg species in solution is non-dissociated Hg^0 , under mildly reducing conditions, Hg can be precipitated as sulfide and, under strongly reducing conditions may increase the solubility somewhat by converting the mercuric ion to free metal (Schuster, 1991).

Mercury is considered a global pollutant because it is present in all environmental compartments: water, soil, sediments, atmosphere and biota. Most of the Hg that is present in the atmosphere is Hg^0 vapour, where may circulate for up to one year, and hence can be dispersed very far away from the emission origin (Mason et al., 1994). However, HgS , HgCl_2 and methyl-Hg forms are predominant in water, soil, sediments and biota. Once mercury has been liberated from natural or anthropogenic sources (municipal waste combustors, chlor-alkali plants, coal-fired and Hg mines) the activity of some microorganisms and natural processes can change the oxidation state and the speciation of Hg in the environment.

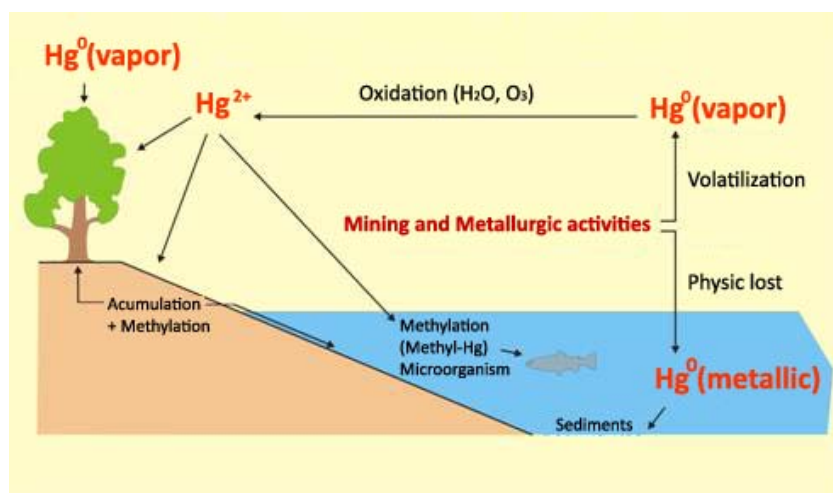


Fig 1. Shows the mercury (Hg) cycle in the biosphere, where are described the most abundant chemical species in each compartment.
(http://www.ucm.es/info/crismine/HTML_Almaden/Almaden_contaminacion.htm)

Mercury has a strong tendency to build complexes with Cl^- , OH^- and S-containing functional groups of organic ligands. Cl^- and OH^- anions occur in all natural soil and water systems, and are considered as the most mobile and persistent complexation agents for Hg. Moreover, the high affinity for $-\text{SH}$ groups explain the accumulation of Hg in organic-rich, upper soil horizons where several processes as chelating, ionic exchange, adsorption, and co-precipitation may occur (Schnitzer and Kerndorff, 1981) and are depending on the type of humic substances and the pH. The degree of metal

immobilization is strongly dependent on complex stability, and only very stable complexes exist at low pH. The influence of pH becomes less important with increasing ligand concentration (Schuster, 1991). In general, the strong binding to organic and mineral materials results in a low availability and mobility of Hg in the soil. Many experiments concluded that plant uptake and leaching were relatively insignificant in topsoil with mixed organic and mineral components (Gracey and Stewart, 1974, Kloke, 1985; Cappon, 1986). Nevertheless under certain conditions, translocation and leaching may occur where pH and Cl^- concentrations are favourable for the formation of Cl^- complexes (Frimmel, 1983; Behra, 1986).

Distribution and speciation of Hg in plants

Since terrestrial plants can absorb Hg from the soil or the atmosphere, they play an important role in the Hg cycle in many natural and humanized ecosystems. In addition, how we will discuss in the following section, Hg accumulation in plants, especially in crops or forage, could exert an impact on the food chain (Ferrara et al., 1991). The content of Hg in plants depends on its bioavailability in the soil and on the atmospheric deposition. Inorganic Hg in the soil compartment is bound to the soil particles and is not easy bioavailable to plants or organisms. In fact, the uptake of gaseous Hg^0 through leaves is much more efficient than the uptake of Hg^{2+} by roots. Generally, Hg accumulation in the root of natural plants is not transferred to the aerial part (Maserti and Ferrara, 1991). In soil, Hg uptake by plants depends on Hg concentration in soil, pH, clay content and types of minerals, organic matter, cation exchange capacity, redox conditions, CaCO_3 , the ambient temperature, and the plant species. All these aspects show the complex mechanism of Hg uptake by plants, which involve both the root and the leaf system. Therefore, it is necessary to consider both soil-root interaction as well as air-leaf interaction (Ferrara et al., 1991). Previous studies on gramineous species and crop plants grown in polluted areas have been performed to elucidate the origin of Hg accumulation, absorbed from the soil or from the atmosphere, but not clear conclusions were reported. Most studies revealed that Hg translocation is rather limited from roots to the aboveground parts of plants (Beauford et al., 1977; Cavallini et al., 1999; Patra and Sharma 2000). These studies found that 95–99% of the Hg taken up by the roots was immobilized and did not eventually reach the shoots (Beauford et al. 1977; Godbold & Huttermann 1986). However, other studies reported that Hg absorbed by leaves accumulated in shoot without translocation to root (Suszcynsky and Shann, 1995). Therefore, Hg is an extremely immobile element that binds strongly to certain

cellular components, leading to its retention in the cells and tissues that get in contact with.

As we will discuss in next sections, one of the most important mechanisms for Hg detoxification in plants is the chelating of Hg^{2+} by the sulfhydryl group of phytochelatin. For the identification of these Hg complexes in plants, it is necessary to ensure that the existing complexes are stable under the acidic analytical conditions used for complex extraction and liquid chromatography separation. Van Der Liden and Beers (1973) studied the complex formation of Hg(II) with the twenty essential amino acids (present in all proteins), in aqueous solutions in the pH range 2.7-8.5. Results showed that cysteine (Cys) had the highest stability constant (39.4), attributed to the binding with the sulfhydryl (thiol) group. Another strong bound was the amino carboxylate group, but was significantly more labile than Hg-S bounds. In addition, Moreover, Stary and Kratzer (1988) analyzed the stability constant of Hg (II)-Cys complex in the pH range from 2.0 to 8.4, and they reported an average value of 40.0 ± 0.2 . Also, they compared the stability constant of Hg^{2+} and CH_3Hg^+ bound to Cys being 2.6 times higher for Hg-(Cys)₂ complex. From all these experiments, it was concluded that the Hg-thiol complex was stable in the pH range between 2.0 to 8.6.

Use of Mass Spectrometry technique for the identification of Hg-containing compounds in plants

Mass spectrometry (MS) is an analytical technique that is used to measure the (m/z) of molecular ions originating from ionized or fragmented molecules, and a plot of ion abundance (intensity) versus m/z is drawn. With the appropriate settings, it is capable of providing information of particle mass, and when is used in tandem mass spectrometry MS, this technique can help to elucidate the chemical composition of complex molecules, such as (Boggess, 2001). The identification of Hg-containing compounds in plants is based in obtaining a mass spectrum of the characteristic natural mixture of stable isotopes of this metal. Mercury exists in a fixed proportion of isotopes, consisting in seven peaks with constant relative abundances: 0.15% ¹⁹⁶Hg, 10.02% ¹⁹⁸Hg, 16.84% ¹⁹⁹Hg, 23.13% ²⁰⁰Hg, 13.22% ²⁰¹Hg, 29.8% ²⁰²Hg, and 6.85% ²⁰⁴Hg (Fig. 2A). Normally, the m/z of Hg-containing substances is given respect to the ²⁰²Hg isotope signal, which is the most abundant one. When a molecule, such as occur with peptides, binds to Hg the resulting m/z comes from the addition of the ligand mass plus the Hg mass [$(\text{Hg}_m + \text{peptide}_m)/z$]. Therefore, the m/z scatters following the abundance of stable isotopes, producing a

characteristic isotopic signature that can be used to identify unambiguously Hg-ligand complexes (Fig. 2B).

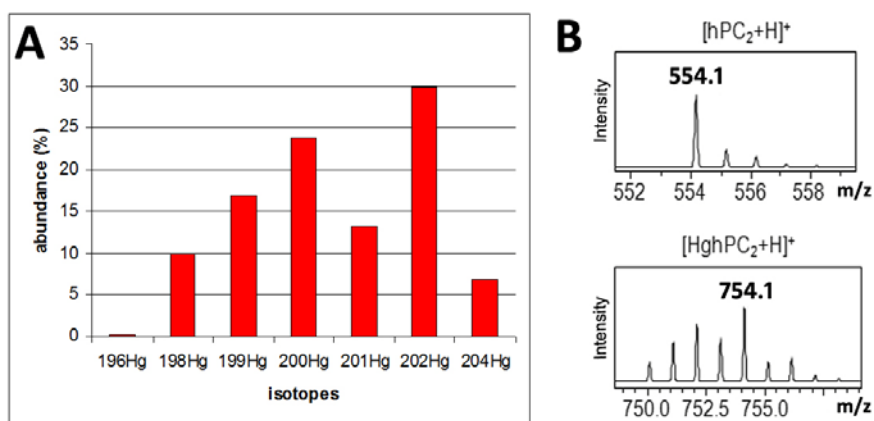


Fig. 2. (A) Abundance of stable Hg isotopes in nature. (B) Experimental m/z spectra of homophytochelatin-2 (γ GluCys- γ GluCys-Ala or hPC₂) ligand an Hg-hPC₂ complex standard. The 745.1 m/z correspond to the most abundant ²⁰²Hg isotope.

There are three main components of a mass spectrometer: an ionization source, a mass analyzer and a detector. The ionization is the most important process in MS, consisting in the conversion analytes of interest into gas-phase ions. Nowadays, the ionization techniques most used are electrospray ionization (ESI) and matrix assisted laser desorption/ionization (MALDI; Glish, 2003). Electrospray ionization is a conservative technique that permits the ionization of molecules with high m/z , maintaining the structure of the molecule of interest without fragmentation. Therefore, ESI allows the analysis of complexes containing non-covalent bonds, as may occur with metal complexes (Smith et al., 1997; Di marco and Bombi, 2006). However, the most useful property of ESI is its ability to couple MS and liquid techniques (LC) to separate compounds from biological matrices. However, despite the power of ESI, it has two shortcomings: sample is constantly being consumed and the matrix can suppress the ionization of the target analyte (Glish, 2003). The other component of MS is the analyser, and its precision in the measurement is related to the resolution that corresponds with the ability to resolve two adjacent peaks. Time-of-flight (TOF) analyser is the simplest one. Ions are all formed at the same time and place in the ion source and then accelerated through a fixed electric potential into the TOF drift tube. As all ions with the same charge obtain the same kinetic energy after acceleration, the

lower m/z ions achieve higher velocities than the higher m/z ions. Thus, by measuring the time it takes to reach the detector after the ion is formed, the m/z of the ion of interest can be determined. TOF offers isotopic mass resolution and the mass range is theoretically unlimited. Therefore, ions that have m/z ratios higher than several hundred thousand can be analysed, that is significantly above the range of the other common mass analyser. For example, every Hg can potentially be bound to an SH group from one biothiol and to an SH group from another biothiol, and this may be repeated a number of times, generating in theory an $\text{Hg}_n\text{-biothiol}_m$ multicomplex, which should be heavy enough to be out of the m/z ranges of conventional MSs (Iglesia-Turiño et al., 2006). However with a TOFMS analyser it is possible to identify an array of Hg-containing multicomplexes.

One of the most important mechanisms in heavy metal tolerance of plants is the chelating of reactive free metal ions to reduce toxic symptoms in the cytosol (Hall, 2002). This role is played by phytochelatins (PCs), which are able to form stable complexes with several toxic metals. These molecules are a family of peptides that have a general structure $(\gamma\text{-Glu Cys})_n\text{-Gly}$ where $n=2-11$, and are rapidly induced in plants by Hg treatment among other heavy metals (Grill *et al.* 1989; Cobbett and Goldsbrough, 2002). Phytochelatins are synthesized from glutathione (GSH) and homologous biothiols precursors in a post-translational process by the enzyme phytochelatase when plants are exposed to heavy metals (PCS; Ha *et al.*, 1999; Vatamaniuk *et al.*, 1999). PCS condenses the γ -glutamyl-cysteine (GC) moiety of a GSH molecule with the glutamic acid residue of a second GSH, releasing glycine and increasing the length of the PC molecule (Vatamaniuk *et al.*, 2004). The chelation of heavy metals in the cytosol by PCs ligands is potentially a very important mechanism of heavy metal detoxification and tolerance (Cobbett and Goldsbrough, 2002). It is thought that Hg^{2+} is bound to PCs through the sulfhydryl group ($-\text{SH}$) of cysteine moiety. The final step in heavy metal detoxification, involves the storage of the heavy metal-PC complex in the vacuole, so through appropriate membrane transporters these complexes cross the tonoplast (Leitenmaier and Küpper, 2010).

Several recent works have used HPLC-ESI-MS techniques to characterise Hg-biothiols complexes, thought to detoxify Hg. Iglesia-Turiño et al. (2006) used HPLC-MS/MS with a triple quadrupole analyser to identify phytochelatins (PCs) in *Brassica napus* exposed to different Hg concentrations (0-1000 μM HgCl_2). The identification of PCs *in vitro* and *in vivo* experiments was only possible after the addition of the chelating

agent DMPS (sodium 2,3-dimercaptopropanesulfonate monohydrate). The only PC identified in root was PC₂, assuming that this bi thiol was involved in Hg chelation process in rape plants. Krupp et al. (2008) developed a technique for the separation and molecular identification of Hg and Methyl-Hg (MeHg) complexes with cysteine (Cys) and glutathione (GS): Complexes, such as HgCys₂, MeHgCys, HgGS₂ and MeHgGS, were analysed in standard solutions or spiked in root and shoot extracts of *Oryza sativa*. These complexes were identified by HPLC-ESI-MS equipped with an ion trap. Simultaneous detection with ICP-MS was performed to Hg-selective determination after separation by HPLC, as the accuracy of ICP-MS over ESI-MS permits the quantification of Hg concentration in a particular HPLC fraction. Subsequently, HPLC-ICP-MS and HPLC-ESI-MS were applied to identify Hg-biothiol complexes that accumulated *in vivo* in *Oryza sativa* and *Marrubium vulgare* plants exposed to 50 µM Hg or 50 µM. MeHg. HgPC₂, Hg(des-Gly)PC₂, Hg(Ser)PC₂ and Hg(Glu)PC₂ complexes were identified in *O. sativa* roots, whereas Hg(des-Gly)PC₂ and Hg(Glu)PC₂ were identified in *M. vulgare* roots (Krupp et al., 2009). Similar analytical approach was undertaken by Chen et al. (2009) to detect Hg-PC complexes in *Brassica chinensis* L. exposed to 200 µM HgCl₂ or HgCys₂, with and without addition of 1.5 mg g⁻¹ humic acid. The detection of oxidized PC₂, oxidized PC₃, oxidized PC₄, together with HgPC₂, HgPC₃, HgPC₄ and Hg₂PC₄ in *B. chinensis* roots, suggests that the conditions to prepare plant extracts were not appropriate. We have developed a new method using HPLC-ESI-TOFMS that allowed the identification of a wide array of PCs bound to Hg in root soluble fraction of *Medicago sativa*, *Zea mays* and *Hordeum vulgare* (see chapter 3). Thanks to the superior resolution of *m/z* of TOF versus MS/MS quadrupole, we could identify several new Hg multicomplexes that previous analysis could not. The usage of a neutral pH extraction solution to prepare soluble fractions from roots permitted a better preservation of endogenous Hg-biothiol complexes, as few ligands and Hg-PC complexes were oxidized.

Speciation and localization of Hg in the plant using a synchrotron source: X-ray absorption spectroscopy (XAS) and X-ray fluorescence (XRF)

Mercury speciation is important to understand the dynamics of this pollutant in organisms contaminated ecosystems, information that may prevent risks for the environment and human health (Harris et al., 2003). Commonly, plant analysis speciation is carried out by spectroscopic techniques such as flame atomic absorption spectrometry (FAAS), inductively coupled plasma atomic emission spectrometry (ICP-

AES), inductively coupled plasma mass spectrometry (ICP-MS), high performed liquid chromatography coupled to time of flight mass spectrometry (HPLC-TOFMS). Nevertheless all of them require sample preparation that involves the total destruction of the matrix by an acidic oxidative mineralisation reaction (Marguí et al., 2009). Despite this disadvantage, these techniques are needed because of the high precision and accuracy in the analysis.

X-ray absorption spectroscopy (XAS) and X-ray fluorescence (XRF) are techniques developed by users of synchrotron radiation light sources that provide interesting information about the coordination chemistry of metals, and generate 2D-image of the metal distribution within the plants with minimal sample pre-treatment. To this end, several studies of phytoremediation have used successfully these techniques (Gardea-Torresday et al., 2003; Pickering et al., 2003; Webb et al., 2003 and De la Rosa et al., 2004). Concretely, several studies of Hg speciation in plants have been performed (Riddle et al., 2002; Rajan et al., 2008; Patty et al., 2009; Carrasco-Gil et al., 2011), but are still a minority compared to the broad information available of other toxic metals like Cd or As.

There are more than 50 synchrotron lightsources in operation around the world (www.lightsources.org). A synchrotron source produce X-ray of tunable energy up to 25 keV or white light with brightnesses several orders of magnitude greater than can be achieved by conventional means. This results in much more rapid data collection and immensely increased resolution. The access to a synchrotron facility is not easily available to the general researcher's community. Previously, the researcher has to submit a proposal of the research work that subsequently is evaluated by a scientific committee. After the approval of the proposal, the synchrotron facility assigns the called "beam time" to perform the analysis. Generally, these beam times are very short (between 8 hours and 3 days). Because of the collection of one elemental map of 2 x 2 mm can consume more than 6 h, depending on the image resolution. The best option for a beginner user is joining to other group that is working on the same topic, and has experience enough to help in data acquisition and analysis.

The main features and advantages of XAS over other techniques are the following: **i)** It is an elemental specific method that allows the focused study of selected element, excluding at wish others (low interference), **ii)**, samples require in general minimal preparation; thus the sample analysed is close to its natural state, even samples may be

analysed under *in situ* conditions without chemical or physical alteration; **iii**) the quantity of sample that is needed is small (< 1g) due to the beam size; and **iv**) the technique is non-destructive, so samples can be recovered after analysis (Lombi and Susini, 2009; Kim, 2006).

X-ray absorption near-edge structure (XANES) and extended X-ray absorption fine structure (EXAFS)

The XAS spectrum generally is divided into three different regions based on the energy range of the X-ray beam compared to the absorption edge (Fig. 3). The first region is called the pre-edge, where no ionisation occurs, only transition to higher unfilled or half filled orbitals. The X-ray absorption near-edge structure (XANES) is the next region and the position of the edge and the assignment of peaks near or on the edge give information about oxidation state, covalence, molecular symmetry of the site and coordination number. The main feature of this region is the presence of a slight “shoulder” in the case of Hg compounds. Finally, the third region is called extended X-ray absorption fine structure (EXAFS) and provides local structural information about the oxidation state and atomic neighbourhood of the target element such as number of ligands, the identity of the ligand atoms and the radial distance. The features of this region are in form of oscillations generated by the constructive and destructive interferences between the outgoing and backscattered photoelectron wave. There are different absorption edges called K, L and M, which depend on the core excited electron. Every absorption edge (K, L and M) corresponded with a principal quantum number (1, 2 and 3) respectively. Most XAS studies of Hg investigate the core level binding energy of the L_3 electron located in the 2p orbital of Hg. The electron binding energy of the L_3 electron is 12284 eV (E_0). Spectra data can be collected either in transmission mode or using fluorescence, the later in case of low metal concentration. For Hg L_3 edge, $L_{\alpha 1}$ fluorescence is usually collected at 9989 eV. Some beam lines has a cryostat that kept the sample frozen during the analysis. Low temperatures reduce the formation of free radicals by the high energy X-ray beam, which can cause photoreduction of the sample. Temperatures lower than 10K are used for EXAFS analysis, to minimize molecular movement and variation in bond length (Andrews, 2006).

The use of XANES spectra for Hg speciation analysis is less accurate than EXAFS analysis, since Hg XANES region is short of distinctive diagnostic pre-edge features by

which to clearly identify the proportion of different oxidation states that may be present (Kim, 2006). However, EXAFS analysis requires high metal concentration to collect acceptable Hg spectra. Therefore, XANES analysis is applied to samples with relatively low Hg concentration, as normally occurs in many plant and biological tissues.

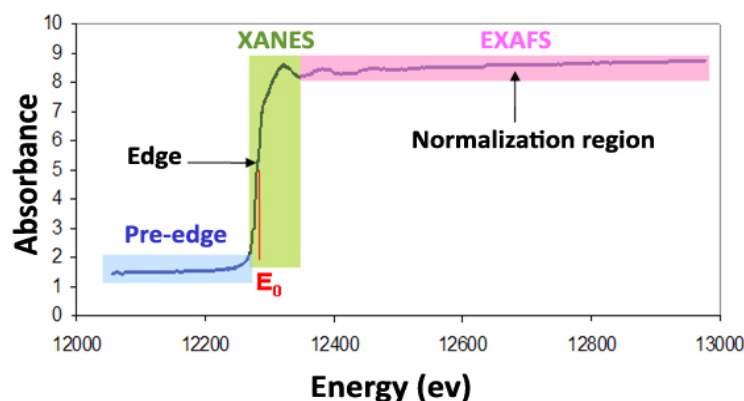


Fig. 3. Hg L_3 X-ray absorption spectrum of Hg-glutathione complex indicating the three regions: the pre-edge, the X-ray absorption near edge structure (XANES) and X-ray absorption fine structure (EXAFS).

The method to identify various metal species using both analytical approaches consists basically in the comparison of the spectrum of an unknown sample with data bases of reference spectra collected from homogeneous standard compounds (Kim et al., 2000). If the Hg concentration in the specimen under analysis is high enough ($> 100 \text{ mg kg}^{-1}$), EXAFS analysis is more recommended. EXAFS analysis is normally much easier when larger differences in composition and structure of Hg bonds occur between the unknown sample and the standard. The model compounds used as standard spectra should be collected under the same experimental conditions as those used for the unknown samples, even using the same beam line whenever possible. Concretely, EXAFS spectrum collected from a natural sample containing multiple Hg species can be decomposed, using a linear least-square fitting (LSF) method, into the sum of individual components composing the spectrum, through direct comparison with the model compounds spectra. In addition, LSF method determines the relative proportion of the contribution of each model compound spectra in the sample.

On the other hand, XANES and EXAFS analysis have several limitations. The relatively high metal concentration in the samples, mentioned before and necessary to collect quality data, leave out of these kind of analysis many environmental samples. Moreover, the goodness of the fit will depend on the quality and the number of the

model compounds in the library: Only known Hg species present in the library will be identified in an unknown sample.

Synchrotron X-ray Fluorescence microprobe (μ -SXRF)

X-ray fluorescence is a technique with considerable potential in the field of phytoremediation since it can simultaneously measure the emitted X-ray fluorescence of multiple elements in a sample following the absorption of high energy synchrotron X-rays (Punshon *et al.*, 2009). The μ -SXRF analysis generates detailed elemental maps in relation to its oxidative state, chemical bonding and correlation plots of Hg with other elements. This is very useful with respect to Hg speciation since it allows distinguish between particulate Hg, adsorbed or complexed Hg species. The spatial-resolved XRF maps may provide the distribution and localization of Hg hot spots in a given sample, It also permits μ -XANES or μ -EXAFS analysis at the selected high intense areas of metal localization to avoid physical alteration (ground samples), reducing the risk of possible artefact that disturb the analysis (Manceau *et al.*, 2002). There are other XRF techniques such as Scanning Electron Microscope with Energy Dispersive X-Ray Analysis (SEM-EDXA) and Particle induced x-ray emission (PIXE) that also permit mapping and quantification of the elements present in a sample at cellular level, although they are less sensitive and require more aggressive pre-treatment sample than SXRF. Finally, synchrotron X-ray computed μ -tomography (SR- μ CT) is a version of μ -SXRF that permits the localization and distribution of an element of interest in the internal structure without the need of physically sectioning. This technique is useful for environmental samples since do not produce neither physical nor chemical alteration, therefore the risk of generating artefact during the handling is reduced (Lombi and Susini, 2009).

Phytoremediation technologies

There are efficient technologies to clean soils contaminated with toxic metals, such as mechanical separation, isolation, containment and chemical stabilization of polluted horizons. However, utilization of these techniques is very expensive, labour intensive, and may cause serious alteration of soil structure and fertility. Using plants for metal extraction, degradation or immobilization is a promising alternative that can be used in polluted soil and water (Mulligan *et al.*, 2001). Phytoremediation comprises a series of alternative procedures, and the selection of a specific technical approach would depend on the pollutant and the particular characteristics of the soils to clean (see Table 1).

Tabla 1. Phytoremediation techniques (from Yang et al., 2005)

Techniques	Mechanism involved	Contaminated compartment
Phytoextraction	Direct accumulation of contaminants into plants aboveground organs with subsequent harvesting and disposal	Soil
Rhizofiltration	Pollutants accumulation in roots, by absorption or adsorption processes	Surface and groundwater
Phytostabilization	Accumulation in the rhizosphere, rendering the metals less soluble	Groundwater, soil, mine tailings
Phytovolatilization	Plants evaporate volatile metals, possibly after reduction of metal ions	Soil, groundwater
Phytodegradation	Degradation of the pollutant by microbial metabolism at the rhizosphere	Soil and groundwater
Phytotransformation	Alteration of plant accumulated contaminants	Surface and groundwater
Removal of aerial contaminants	Uptake of volatile organics by leaves	Air

To improve the efficiency of phytoremediation technologies, it is important to learn about the physiological processes involved in the plants including the metal content, translocation, tolerance mechanism and rhizosphere processing. The advances in XRF and XAS techniques will help to improve the research in this area (Gardea-Torresday et al., 2005). Thus, there are many studies that have identified plants capable of accumulating uncommonly high metal levels of Zn, Ni or Se (Salt et al., 1999; Krämer et al., 2000; Freeman et al., 2006). Following this singularity, many studies have been conducted to elucidate the physiology and the biochemistry of metal hyperaccumulation in plants (Yang et al., 2005). Nevertheless this technology has to overcome some limitations to become efficiently and cost-effective on a commercial scale (Khan et al., 2000). A good candidate for phytoremediation has to be fast growing and easy to harvest, have high biomass and extensive root system and tolerate high concentrations of metals accumulated in their harvestable organs. To date, there no natural plant hyperaccumulators that fulfil such requirements for phytoremediation applications in a broad scale, as most heavy metal accumulating plants identified so far have poor root penetration in polluted soils and a small biomass. Whereby remediating a contaminated area within a reasonable period of time, metal uptake and plant yield have to be enhanced considerably (Raskin et al., 1997). In contrast, high biomass and fast growing non-accumulators can be engineered to achieve some of the properties of the

hyperaccumulators (Clemens et al., 2002). However, to achieve such goal better understanding about the molecular mechanism of metal uptake, tolerance, accumulation and translocation is needed (Yang et al., 2005).

Concluding remarks and future perspectives

Some recent results indicate that GSH metabolism is important for Hg tolerance, either as an antioxidant or as a precursor of PCs. Synchrotron X-ray fluorescence and LC-ESI-TOFMS techniques can provide valuable data about accumulation, localization, and speciation of Hg, necessary to understand the dynamics of Hg and its detoxification in plants. Such studies should be focused to provide functional evidences about the relevance of GSH metabolism in Hg detoxification by using pharmacological, i.e. specific inhibitors of pathways (for example buthionine sulfoximine), or genetic approaches, i.e. mutants defective in altered components of the detoxification machinery under study (*Arabidopsis thaliana cad1-3* or *cad2-1* mutants). In parallel, genetic engineering could generate transgenic plants with improved characteristics, such as increased cellular sulphur assimilation metabolism or higher cellular concentration of GSH, with a similar aim. It should be noted that most of the current information about Hg detoxification processes comes from single pollutant assays, whereas in real soil contamination cases a multi-pollution problem is frequent. Therefore, future research should also consider the interaction between different metals, in pilot soil experiments where complex equilibrium with soil components would occur, affecting the dynamics of Hg in the plants.

References

- Andrews J.C. (2006) Mercury speciation in the environment using X-ray absorption spectroscopy. In: *Recent Developments in Mercury Science*, pp. 1-35.
- Beauford W., Barber J. & Barringer A.R. (1977) Uptake and distribution of mercury within higher plants. *Physiology Plantarum*, **39**, 271-275.
- Behra P. (1986) Migration or retention of mercury II salt when percolating through a porous medium constituted of a natural quartz sand? In: *2nd International Conference of Environmental Contamination*, pp. 318-320, Amsterdam.
- Bernier M. & Carpentier R. (1995) The action of mercury on the binding of the extrinsic polypeptides associated with the water oxidizing complex of photosystem-II. *FEBS Letters*, **360**, 251-254.
- Bernier M., Popovic R. & Carpentier R. (1993) Mercury inhibition at the donor side of photosystem II is reversed by chloride. *FEBS Letters*, **321**, 19-23.
- Bogges B. (2001) Mass Spectrometry Desk Reference (Sparkman, O. David). *Journal of Chemical Education*, **78**, 168-null.
- Cappon, C.J. (1987). In: Schuster, E, 1991: The behaviour of mercury in the soil with special emphasis on complexation and adsorption processes. A review of the literature. *Water, Air and Soil Pollution*, **56**, 667-680.

- Cárdenas-Hernández J.F., Moreno L.P. & Magnitskiy S.V. (2009) Effect of mercury on cellular transport of water in plants. A review. *Revista Colombiana de Ciencias hortícolas*, **3**, 250-261
- Cargnelutti D., Tabaldi L.A., Spanevello R.M., Jucoski G.D., Battisti V., Redin M., Linares C.E.B., Dressler V.L., Flores E.M.D., Nicoloso F.T., Morsch V.M. & Schetinger M.R.C. (2006) Mercury toxicity induces oxidative stress in growing cucumber seedlings. *Chemosphere*, **65**, 999-1006.
- Carrasco-Gil S., Álvarez-Fernández A., Sobrino-Plata J., Millán R., Carpena-Ruiz R.O., LeDuc D.L., Andrews J.C., Abadía J. & Hernández L.E. (2011) Complexation of Hg with phytochelatin is important for plant Hg tolerance. *Plant, Cell and Environment* (in press)
- Cavallini A., Natali L., Durante M. & Maserti B. (1999) Mercury uptake distribution and DNA affinity in durum wheat (*Triticum durum* Desf.) plants. *Science of The Total Environment*, **243/244**, 119-127.
- Chen L., Yang L. & Wang Q. (2009) *In vivo* phytochelatin and Hg-phytochelatin complexes in Hg-stressed *Brassica chinensis* L. *Metallomics*, **1**, 101–106.
- Clarkson T.W. (1997) The toxicology of mercury. *Critical Reviews in Clinical Laboratory Sciences*, **34**, 369-403.
- Clemens S, Palmgren MG, Krämer U. (2002). A long way ahead: understanding and engineering plant metal accumulation. *Trends in Plant Science*, **7**, 309-315.
- Cobbett C. & Goldsbrough P. (2002) Phytochelatin and metallothioneins: roles in heavy metal detoxification and homeostasis. *Annual Review Plant Biology*, **53**, 159–182.
- Coughtrey, P.J. & Martin, M.H. (1978). Tolerance of *Holcus lanatus* to lead, zinc and cadmium in factorial combination. *New Phytologist.*, **81**, 147-54.
- De Filippis L.F. (1979) The effect of heavy metal compounds on the permeability of *Chlorella* cells. *Z. Pflanzenphysiologie*, **92**, 39-49.
- De la Rosa G., Peralta-Videa J.R., Montes M., Parsons J.G., Cano-Aguilera I. & Gardea-Torresdey J.L. (2004) Cadmium uptake and translocation in tumbleweed (*Salsola kali*), a potential Cd-hyperaccumulator desert plant species: ICP/OES and XAS studies. *Chemosphere*, **55**, 1159–1168.
- Di Marco V.B. & Bombi G.G. (2006) Electrospray mass spectrometry (ESI-MS) in the study of metal-ligand solution equilibria. *Mass Spectrometry Reviews* **25**, 347-379.
- EC Directive, (2002). Directive of The European Parliament and of the Council of 7 May 2002 on Undesirable Substances in Animal Feed 2002/32/EC.
- Elbaz A., Wei Y.Y., Meng Q., Zheng Q. & Yang Z.M. (2010) Mercury-induced oxidative stress and impact on antioxidant enzymes in *Chlamydomonas reinhardtii*. *Ecotoxicology*, **19**, 1285-1293.
- EPA U.S. (1997) Mercury Study to Congress. Volume III: Fate and Transport of Mercury in the Environment (ed EPA-452/R-97-005), Washington, DC.
- European Commission (2005). Community Strategy concerning Mercury. Summaries of EU Legislation. (http://europa.eu/legislation_summaries/internal_market/single_market_for_goods/chemical_products/128155_en.htm)
- Feng X.B., Li P., Qiu G.L., Wang S., Li G.H., Shang L.H., Meng B., Jiang H.M., Bai W.Y., Li Z.G. & Fu X.W. (2008) Human exposure to methylmercury through rice intake in mercury mining areas, Guizhou province, China. *Environmental Science & Technology*, **42**, 326-332.
- Ferrara R., Maserti B. & Breder R. (1991) Mercury in abiotic and biotic compartments of an area affected by a geochemical anomaly (Mt. Amiata, Italy). *Water, Air, & Soil Pollution*, **56**, 219-233.
- Foyer C.H. & Noctor G. (2005) Oxidant and antioxidant signalling in plants: a re-evaluation of the concept of oxidative stress in a physiological context. *Plant Cell and Environment*, **28**, 1056-1071.
- Foyer C., Noctor G. & MorotGaudry J.F. (1997) Oxygen: Friend or foe for plants. *Biofutur*, 27-29.

- Freeman J.L., Zhang L.H., Marcus M.A., Fakra S., McGrath S.P. & Pilon-Smits E.A.H. (2006) Spatial imaging, speciation, and quantification of selenium in the hyperaccumulator plants *Astragalus bisulcatus* and *Stanleya pinnata*. *Plant Physiology*, **142**, 124-134.
- Frimmel, F.H., Geywitz, J., & Velikov, B.L. (1983). In: Schuster, E, 1991: The behaviour of mercury in the soil with special emphasis on complexation and adsorption processes. A review of the literature. *Water, Air Soil Pollut.* **56**, 667-680.
- Gardea-Torresdey J.L., Gomez E., Peralta-Videa J.R., Tiemann K.J., Parsons J.G., Trolani H. & Yacaman M.J. (2003) Use of XAS and TEM to determine the uptake of gold and silver and nanoparticle formation by living alfalfa plants. *Proceedings of the 225th American Chemical Society National Meeting, Division of Environmental Chemistry*, **43**, 1016–1022.
- Gardea-Torresdey J.L., Peralta-Videa J.R., de la Rosa G. & Parsons J.G. (2005) Phytoremediation of heavy metals and study of the metal coordination by X-ray absorption spectroscopy. *Coordination Chemistry Reviews*, **249**, 1797-1810.
- Glish, G.L. (2003). The basics of mass spectrometry in the twenty-first century. *Nature Reviews. Drug Discovery*, **2**, 140-150.
- Godbold D.L. (1991) Mercury-induced root damage in spruce seedlings. *Water, Air, and Soil Pollution*, **56**, 823-831.
- Godbold D.L. & Hüttermann A. (1986) The uptake and toxicity of mercury and lead to spruce (*Picea abies* karst. seedlings. *Water, Air and Soil Pollution*, **31**, 509-515.
- Gracey H.I. & Stewart J.W.B. (1974) *The fate of applied mercury in soil*. Paper presented at the Land for Water Management, Ottawa, Ontario.
- Grill E., Löffler S., Winnacker E.L. & Zenk M.H. (1989) Phytochelatins, the heavy-metal-binding peptides of plants, are synthesized from glutathione by a specific γ -glutamylcysteine dipeptidyl transpeptidase (phytochelatin synthase). *Proceedings of the National Academy of Sciences USA* **86**, 6838-6842.
- Ha S.B., Smith A.P., Howden R., Dietrich W.M., Bugg S., O'Connell M.J., Goldsbrough P.B. & Cobbett C.S. (1999) Phytochelatin synthase genes from *Arabidopsis* and the yeast *Schizosaccharomyces pombe*. *The Plant Cell* **11**, 1153-1164.
- Harris H.H., Pickering I.J. & George G.N. (2003) The chemical form of mercury in fish. *Science*, **301**, 1203-1203.
- Iglesia-Turiño S., Febrero A., Jauregui O., Caldelas C., Araus J.L. & Bort J. (2006) Detection and quantification of unbound phytochelatin 2 in plant extracts of *Brassica napus* grown with different levels of mercury. *Plant Physiology*, **142**, 742–749.
- Israr M., Sahi S., Datta R. & Sarkar D. (2006) Bioaccumulation and physiological effects of mercury in *Sesbania drummondii*. *Chemosphere*, **65**, 591-598.
- Jimenez A., Hernandez J.A., Pastori G., del rio L.A. & Sevilla F. (1998) Role of the ascorbate-glutathione cycle of mitochondria and peroxisomes in the senescence of pea leaves. *Journal of Plant Physiology*, **118**, 1327-1335.
- JECFA (Joint Food and Agriculture Organization of the United Nations/World Health Organisation (FAO/WHO) Expert Committee on Food Additives). Sixty-seventh meeting Rome, 20–29 June 2006: summary and conclusions; 2006. (<http://www.who.int/ipcs/food/jecfa/summaries/summary67.pdf>)
- Khan A.G., Keuk C., Chaudhry T.M., Khoo C.S. & Hayes W.J. (2000) Role of plants, mycorrhizae and phytochelators in heavy metal contaminated land remediation. *Chemosphere*, **41**, 197-207.
- Kim C.S. (2006) Speciation of mercury using synchrotron radiation. In: *Mercury: Sources, Measurements, Cycles and Effects* (ed R. Bowell), pp. 1-24.
- Kim C.S., Brown G.E. & Rytuba J.J. (2000) Characterization and speciation of mercury-bearing mine waste using X-ray absorption spectroscopy. *Science of the Total Environment*, **261**, 157–168.
- Kloke, A. (1985). In: Schuster, E, 1991: The behaviour of mercury in the soil with special emphasis on complexation and adsorption processes. A review of the literature. *Water, Air and Soil Pollution*, **56**, 667-680.

- Kramer U., Pickering I.J., Prince R.C., Raskin I. & Salt D.E. (2000) Subcellular localization and speciation of nickel in hyperaccumulator and non-accumulator *Thlaspi* species. *Plant Physiology*, **122**, 1343-1353.
- Krupp E.M., Milne B.F., Mestrot A., Meharg A.A. & Feldmann J. (2008) Investigation into mercury bound to biothiols: structural identification using ESI-ion-trap MS and introduction of a method for their HPLC separation with simultaneous detection by ICP-MS and ESI-MS. *Annals of Bioanalytical Chemistry*, **390**, 1753–1764.
- Krupp E.M., Mestrot A., Wielgus J., Meharg A.A. & Feldmann J. (2009) The molecular form of mercury in biota: identification of novel mercury peptide complexes in plants. *Chemical Communications*, **28**, 4257–4259.
- Leitenmaier B. & Küpper H. (2010) Cadmium uptake and sequestration kinetics in individual leaf cell protoplasts of the Cd/Zn hyperaccumulator *Thlaspi caerulescens*. *Plant Cell and Environment* (doi: 10.1111/j.1365-3040.2010.02236.x)
- Lombi E. & Susini J. (2009) Synchrotron-based techniques for plant and soil science: opportunities, challenges and future perspectives. *Plant and Soil*, **320**, 1-35.
- Macnair MR. (1990). The genetics of metal tolerance in natural populations. In: Shaw AJ, ed. *Heavy metal tolerance in plants: evolutionary aspects*. Boca Raton, FL, USA: CRC Press, 235–253.
- Manceau A., Marcus M.A. & Tamura N. (2000) Quantitative speciation of heavy metals in soils and sediments by synchrotron X-ray techniques. In: *Reviews in Mineralogy and Geochemistry* (eds P. Fenter & N.C. Sturchio), pp. 341-428. Mineralogical Society of America, Washington, DC.
- Marguí E., Queralt I. & Hidalgo M. (2009) Application of X-ray fluorescence spectrometry to determination and quantitation of metals in vegetal material. *TrAC Trends in Analytical Chemistry*, **28**, 362-372.
- Maserti B. & Ferrara R. (1991) Mercury in plants, soil and atmosphere near a chlor-alkali complex. *Water, Air, & Soil Pollution*, **56**, 15-20.
- Mason R.P., Fitzgerald W.F. & Morel F.M.M. (1994) The biogeochemical cycling of elemental mercury: Anthropogenic influences. *Geochimica et Cosmochimica Acta*, **58**, 3191-3198.
- Metwally A., Safronova V.I., Belimov A.A. & Dietz K.J. (2005) Genotypic variation of the response to cadmium toxicity in *Pisum sativum* L. *Journal of Experimental Botany*, **56**, 167-178.
- Mittler R. & Zilinskas B.A. (1992) Molecular cloning and characterization of a gene encoding pea cytosolic ascorbate peroxidase. *Journal of Biological Chemistry*, **267**, 21802-21807.
- Mulligan C.N., Yong R.N. & Gibbs B.F. (2001) Remediation technologies for metal-contaminated soils and groundwater: an evaluation. *Engineering Geology*, **60**, 193-207.
- Murata K, Matsuoka K, Hirai T, Waltz T, Agre P, Heymann JB, Engel A, Fujiyoshi Y (2002) Structural determinants of water permeation through aquaporin-1. *Nature*, **40**, 599-605
- Naito W. (2008) Ecological Catastrophe. In: *Encyclopedia of Ecology* (eds J. Sven Erik & F. Brian), pp. 983-991. Academic Press, Oxford.
- Nierenberg D.W., Nordgren R.E., Chang M.B., Siegler R.W., Blayney M.B., Hochberg F., Toribara T.Y., Cernichiari E. & Clarkson T. (1998) Delayed cerebellar disease and death after accidental exposure to dimethylmercury. *New England Journal of Medicine*, **338**, 1672-1676.
- Ortega-Villasante C., Hernandez L.E., Rellan-Alvarez R., Del Campo F.F. & Carpena-Ruiz R.O. (2007) Rapid alteration of cellular redox homeostasis upon exposure to cadmium and mercury in alfalfa seedlings. *New Phytologist*, **176**, 96-107.
- Ortega-Villasante C., Rellan-Alvarez R., Del Campo F.F., Carpena-Ruiz R.O. & Hernandez L.E. (2005) Cellular damage induced by cadmium and mercury in *Medicago sativa*. *Journal of Experimental Botany*, **56**, 2239-2251.
- Patra M. & Sharma A. (2000) Mercury toxicity in plants. *Botanical Review*, **66**, 379-422.
- Patty C., Barnett B., Mooney B., Kahn A., Levy S., Liu Y.J., Pianetta P. & Andrews J.C. (2009) Using X-ray Microscopy and Hg L-3 XAMES To Study Hg Binding in the Rhizosphere of *Spartina* Cordgrass. *Environmental Science & Technology*, **43**, 7397-7402.

- Pickering I.J., Wright C., Bubner B., Ellis D., Persans M.W., Yu E.Y., George G.N., Prince R.C. & Salt D.E. (2003) Chemical form and distribution of selenium and sulphur in the selenium hyperaccumulator *Astragalus bisulcatus*. *Plant Physiology*, **131**, 1460–1467.
- Punshon T., Guerinot M.L. & Lanzirotti A. (2009) Using synchrotron X-ray fluorescence microprobes in the study of metal homeostasis in plants. *Annals of Botany* **103**, 665–672.
- Rajan M., Darrow J., Hua M., Barnett B., Mendoza M., Greenfield B.K. & Andrews J.C. (2008) Hg L-3 XANES study of mercury methylation in shredded *Eichhornia crassipes*. *Environmental Science and Technology*, **42**, 5568-5573.
- Raskin I., Smith R.D. & Salt D.E. (1997) Phytoremediation of metals: using plants to remove pollutants from the environment. *Current Opinion in Biotechnology*, **8**, 221-226
- Rausser W.E. & Meuwly P. (1995) Retention of cadmium in roots of maize seedlings. *Plant Physiology*, **109**, 195–202.
- Rellán-Álvarez R., Hernández L.E., Abadía J. & Álvarez-Fernández A. (2006a) Direct and simultaneous determination of reduced and oxidized glutathione and homogluthathione by liquid chromatography-electrospray/mass spectrometry in plant tissue extracts. *Analytical Biochemistry*, **356**, 254-264.
- Rellán-Álvarez R., Ortega-Villasante C., Álvarez-Fernández A., del Campo F.F. & Hernández L.E. (2006b) Stress responses of *Zea mays* to cadmium and mercury. *Plant and Soil*, **279**, 41-50.
- Riddle S.G., Tran H.H., Dewitt J.G. & Andrews J.C. (2002) Field, laboratory, and X-ray absorption spectroscopic studies of mercury accumulation by water hyacinths. *Environmental Science & Technology*, **36**, 1965-1970.
- Salt D.E., Prince R.C., Baker A.J.M., Raskin I. & Pickering I.J. (1999) Zinc ligands in the metal hyperaccumulator *Thlaspi caerulescens* as determined using X-ray absorption spectroscopy. *Environmental Science and Technology*, **33**, 713-717.
- Savage D.F. & Stroud R.M. (2007) Structural basis of aquaporin inhibition by mercury. *Journal of Molecular Biology*, **368**, 607-617.
- Schnitzer M. & Kerndorff H. (1981) Reactions of fulvic acid with metal ions. *Water, Air, and Soil Pollution*, **15**, 97–108.
- Schuster E. (1991) The behavior of Mercury in the soil with special emphasis on complexation and adsorption processes- A review of the literature. *Water, Air, and Soil Pollution*, **56**, 667-680.
- Shieh Y.J. & Barber J. (1973) Uptake of mercury by *Chlorella* and its effect on potassium regulation. *Planta*, **109**, 49-60.
- Smith, R.D., Bruce, J.E., Wu, Q., Lei, Q.P. (1997). New mass spectrometric methods for the study of noncovalent association of biopolymers. *Chemical Society Reviews*, **26**, 191-202.
- Sobrinho-Plata J., Ortega-Villasante C., Flores-Caceres M.L., Escobar C., Del Campo F.F. & Hernandez L.E. (2009) Differential alterations of antioxidant defenses as bioindicators of mercury and cadmium toxicity in alfalfa. *Chemosphere*, **77**, 946-954.
- Stary J. & Kratzer K. (1988) Radiometric determination of stability constants of Mercury species complexes with L-Cysteine. *Journal of Radioanalytical and Nuclear Chemistry*, **126**, 69-75.
- Stumm W. & Morgan J.J., eds (1981) *Aquatic Chemistry: an Introduction Emphasizing Chemical Equilibria in Natural Waters*. Wiley-Interscience, Toronto.
- Sun Q., Yec Z.H., Wang X.R. & Wong M.H. (2007) Cadmium hyperaccumulation leads to an increase of glutathione rather than phytochelatin in the cadmium hyperaccumulator *Sedum alfredii*. *Journal of Plant Physiology*, **164**, 1489-1498.
- Suszcynsky E.M. & Shann J.R. (1995) Phytotoxicity and accumulation of mercury in tobacco subjected to different exposure routes. *Environmental Toxicology and Chemistry* **14**, 61-67.
- Valega M., Lima A.I.G., Figueira E., Pereira E., Pardal M.A. & Duarte A.C. (2009) Mercury intracellular partitioning and chelation in a salt marsh plant, *Halimione portulacoides* (L.) Aellen: Strategies underlying tolerance in environmental exposure. *Chemosphere*, **74**, 530-536.
- Van AF, Clijsters H (1990) Effect of metals on enzyme activity in plants. *Plant Cell and Environment*, **13**, 195-206

- Van Der Linden W.E. & Beers C. (1973) Determination of the composition and the stability constants of complexes of Mercury (II) with amino acids. *Analytica Chimica Acta*, **68**, 143-154.
- Wang Y.D. & Greger M. (2004) Clonal differences in mercury tolerance, accumulation, and distribution in willow. *Journal of Environmental Quality*, **33**, 1779-1785.
- Vatamaniuk O.K., Mari S., Lang A., Chalasani S., Demkiv L.O. & Rea P. (2004) Phytochelatin synthase, a dipeptidyl transferase that undergoes multisite acylation with gamma-glutamylcysteine during catalysis. Stoichiometric and site-directed mutagenic analysis of AtPCS1-catalyzed phytochelatin synthesis. *Journal of Biological Chemistry*, **279**, 22449–60.
- Vatamaniuk O.K., Mari S., Lu Y.P. & Rea P.A. (1999) AtPCS1, a phytochelatin synthase from *Arabidopsis*: Isolation and *in vitro* reconstitution. *Proceedings of the National Academy of Sciences USA* **96**, 7110-7115.
- Webb S.M., Gaillard J.F., Ma L.Q. & Tu C. (2003) XAS speciation of arsenic in a hyper-accumulating fern. *Environmental Science & Technology*, **37**, 754-760.
- WHO/IPCS (1976): Mercury. Environmental Health Criteria No 1, World Health Organisation, International Programme on Chemical Safety (IPCS), Geneva, Switzerland, 1976.
- Yang X., Feng Y., He Z. & Stoffella P.J. (2005) Molecular mechanisms of heavy metal hyperaccumulation and phytoremediation. *Journal of Trace Elements in Medicine and Biology*, **18**, 339-353.
- Zhang H., Feng X.B., Larssen T., Qiu G.L. & Vogt R.D. (2010) In Inland China, Rice, Rather than Fish, Is the Major Pathway for Methylmercury Exposure. *Environmental Health Perspectives*, **118**, 1183-1188.
- Zhang W.H. & Tyerman S.D. (1999) Inhibition of water channels by HgCl₂ in intact wheat root cells. *Plant Physiology*, **120**, 849-857
- Zhou Z.S., Huang S.Q., Guo K., Mehta S.K., Zhang P.C. & Yang Z.M. (2007) Metabolic adaptations to mercury-induced oxidative stress in roots of *Medicago sativa* L. *Journal of Inorganic Biochemistry*, **101**, 1-9.
- UNEP United Nations Environment Programme. (2002) Global Mercury Assessment, Geneva, Switzerland. Available at:<http://www.unep.org/gc/gc22/Document/UNEP-GC22-INF3.pdf>
- US EPA (US Environment Protection Agency). Mercury Study Report to Congress; 1997. Available at: <http://www.epa.gov/mercury/report.htm>.



CHAPTER 2

Objectives

The Almadén mining area located in the south of Spain (Ciudad Real) has been for centuries the largest mercury (Hg) producing region in the world. Cessation of the production of Hg has imposed the necessity to promote other economic activities, such as agriculture and farming, which are undermined by the Hg content in soil. Consequently, it is important to evaluate the potential risk for human health and environment considering the uptake and distribution of Hg in crops suitable for the environmental conditions existing in Almadén. To this end, we propose the use of *Medicago sativa* (alfalfa) as alternative crop in the Almadén area because of the following properties: is one of the most important plants used as livestock forage due to its high protein content, is adapted to a wide array of climate conditions, can improve the fertility of degraded soil, and presents a relative tolerance to Hg. In addition, its physiological characteristics, such as the production of large root system and the high biomass at harvest make this plant very interesting for phytoremediation purposes. The use of alfalfa as alternative crop or as plant suitable for phytoremediation technologies requires a set of studies to **evaluate the plant behaviour under Hg stress**.

These studies will focus on the following:

1. Localization of Hg in root, stem and leaf tissues, and identification of the Hg species in alfalfa. This information will broaden our knowledge with regards to transport mechanisms, uptake and storage of the metal. In addition, similar data will be collected from natural plants grown in polluted soils, such as *Marrubium vulgare*, capable of colonizing metallurgic areas in Almadén.
2. Identification of phytochelatins (PCs) bound to Hg, since these biothiols are involved in heavy metal tolerance. Speciation of Hg will be carried out also in another crop species, such as *Zea mays* and *Hordeum vulgare*, to explore similar mechanisms of tolerance in other higher plants.
3. Study the influence of nitrogen fertilization on Hg uptake and oxidative stress responses to evaluate the impact of adequate nutrition in the tolerance of Hg, as part of agronomic practices normally followed to crop alfalfa for forage uses in Almadén area.

It is foreseen that the knowledge obtained with the experiments we propose will enhance our knowledge on detoxification and defense mechanism exerted by alfalfa plants against Hg. These experiments will allow the assessment of the alfalfa as a plant suitable for agriculture or phytoremediation uses in soils naturally polluted by Hg in the area of Almadén. Finally, the information gathered will also help to design pilot field trials to establish important agronomic parameters such as yield and food safety.



CHAPTER 3

Complexation of Hg with phytochelatins is important for plant Hg tolerance

ABSTRACT

Three-week-old alfalfa (*Medicago sativa*), barley (*Hordeum vulgare*) and maize (*Zea mays*) were exposed for 7 days to 30 μM of mercury (HgCl_2) to characterize the Hg speciation in root, with no symptoms of being poisoned. The largest pool (99%) was associated with the particulate fraction, whereas the soluble fraction (SF) accounted for a minor proportion (<1%). Liquid chromatography coupled with electro-spray/time of flight mass spectrometry showed that Hg was bound to an array of phytochelatins (PCs) in root SF, which was particularly varied in alfalfa (eight ligands and five stoichiometries), a species that also accumulated homophytochelatins. Spatial localization of Hg in alfalfa roots by microprobe synchrotron X-ray fluorescence spectroscopy showed that most of the Hg co-localized with sulfur in the vascular cylinder. Extended X-ray Absorption Fine Structure (EXAFS) fingerprint fitting revealed that Hg was bound *in vivo* to organic-S compounds, i.e. biomolecules containing cysteine. Albeit a minor proportion of total Hg, Hg-PCs complexes in the SF might be important for tolerance to Hg, as was found with *Arabidopsis thaliana* mutants *cad2-1* (with low glutathione content) and *cad1-3* (unable to synthesize PCs) in comparison with wild type plants. Interestingly, HPLC-ESI-TOFMS analysis showed that none of these mutants accumulated Hg-biothiol complexes.

Abbreviations – DEAE, diethylaminoethyl; DTT, dithiothreitol; GSH, glutathione; hGSH, homogluthahione; hPCs, homophytochelatins; MF, microsomal fraction; PCs, phytochelatins; PF, particulate fraction; SF, soluble fraction.

INTRODUCTION

Mercury (Hg) accumulation is considered a global environmental threat, and its trade is restricted due to its bioaccumulation and biomagnification in diverse ecosystems (Leonard *et al.* 1998). Mercury has no nutritional role, and exposure of biological systems to relatively low Hg concentrations results in serious toxicity (Nriagu, 1990). Although little is known about the precise mechanism of toxicity exerted by Hg in plants, cellular integrity and biological activity might be compromised due to its strong affinity for sulfhydryl residues of proteins and other biomolecules (Van Assche & Clijsters, 1990; Hall, 2002). Mercury has also been found to be a potent inducer of oxidative stress (Cho & Park, 2000; Rellán-Álvarez *et al.* 2006a), and an oxidative burst appeared in alfalfa root epidermal cells after a brief exposure to 30 μ M Hg (Ortega-Villasante *et al.* 2007), in spite of its limited redox activity (Schützendübel & Polle, 2002).

Mercury accumulates preferentially in roots (4- to 10-fold the concentration found in shoots) of several plant species such as *Pisum sativum* (Beauford *et al.* 1977), *Brassica napus* (Iglesia-Turiño *et al.* 2006), *Zea mays* (Rellán-Álvarez *et al.* 2006a), and *B. chinensis* (Chen *et al.* 2009). Therefore, most of the toxic effects of Hg are observed in roots. A large proportion of Hg was found associated with cell wall materials in *P. sativum* and *Mentha spicata* (Beauford *et al.* 1977), *Nicotiana tabacum* (Suszcynsky & Shann, 1995) and *Halimione portulacoides* (Valega *et al.* 2009). Although the mobility of Hg within the plant may be limited by root cell walls, the distribution in root cells or tissues is not presently clear. This objective can be achieved using techniques such as microprobe synchrotron X-ray fluorescence spectrometry (μ -SXRF), which is capable of providing spatially-resolved metal data (Punshon *et al.* 2009).

Once heavy metals enter the cell, additional defense mechanisms involve the synthesis of organic ligands that could form metal complexes with reduced biological activity. Among these compounds, phytochelatins (PCs) are known to bind Cd and other toxic elements by means of sulfhydryl residues (Cobbett & Goldsbrough 2002). Phytochelatins are synthesized from glutathione (GSH) and homologous biothiols by the enzyme phytochelatase (PCS; Grill *et al.* 1989; Vatamaniuk *et al.* 1999; Clemens *et al.* 1999 and Ha *et al.* 1999). When plants are exposed to heavy metals, PCS condenses the γ -glutamyl-cysteine (GC) moiety of a GSH molecule with the glutamic acid residue of a second GSH, releasing glycine and increasing the length of the PC molecule (Vatamaniuk *et al.* 2004, Clemens 2006).

Significant amounts of free PCs were detected in Hg-treated *Brassica napus* plants with high performance liquid chromatography coupled to mass spectrometry (HPLC-MS) after removal of Hg with a strong Hg-specific chelator (Iglesia-Turiño *et al.* 2006). Phytochelatins were also found in maize and alfalfa plantlets grown with Hg, but in lower amounts than in Cd-treated plants (Rellán-Álvarez *et al.* 2006a; Sobrino-Plata *et al.* 2009). *In vitro* studies using HPLC-MS also showed that small biothiols such as GSH and cysteine bind Hg (Krupp *et al.* 2008; Chen *et al.* 2009).

X-ray absorption spectroscopy (XAS) is a non-destructive technical approach that can be used for speciating metals in plant tissues (Aldrich *et al.* 2003, Gardea-Torresday *et al.* 2003; Pickering *et al.* 2003; De la Rosa *et al.* 2004). Understanding metal speciation is essential to clarify detoxification mechanisms in plants (Arruda & Azevedo 2009). Synchrotron-based techniques widely utilized to study metal chemical properties in a vast array of materials (*i.e.*, composites, semiconductors, etc.), are increasingly being used to characterise metal speciation in biological materials such as plants (Salt *et al.* 2002). Among different methods of analysis, X-ray Absorption Near Edge Spectroscopy (XANES) and Extended X-ray Absorption Fine Structure (EXAFS) provide information about a target atom (oxidation state, local geometry, local environment, co-ordination numbers and bond lengths) in close-to-natural-state plant tissues. Both techniques have been recently used to characterize the speciation of Hg in *Spartina foliosa* and *Eichhornia crassipes* (Riddle *et al.*, 2002; Rajan *et al.*, 2008; Patty *et al.*, 2009). However, fingerprint fitting of XANES and EXAFS spectra, the method used in this paper, require standards of metal-ligand complexes putatively occurring in plant tissues (Kim *et al.*, 2000).

In spite of the evidence pointing towards a role for PCs in Hg complexation in higher plants, only a small number of Hg-PC complexes have been found using HPLC-MS, in root extracts of *B. chinensis*, *Oryza sativa* and *Marrubium vulgare* (Chen *et al.* 2009; Krupp *et al.* 2009). In the present study, a combined approach using both *in vivo* analysis by XAS and HPLC coupled to a high-resolution mass analyzer (time-of-flight; TOFMS) was used to elucidate the plant components involved in the effective defense mechanisms utilized by three week old alfalfa (*Medicago sativa*), barley (*Hordeum vulgare*) and maize (*Zea mays*) plants exposed for 7 days to 30 μM of mercury (Hg, as HgCl_2). This high concentration of Hg was used in a short-term treatment to provide an adequate detection level of Hg with the techniques used in our studies, since the distribution and speciation of metals in non-hyperaccumulator plants is technically more challenging due

to the lower concentration of the analyte (Lombi & Susine, 2009). Moreover, a functional analysis with *Arabidopsis thaliana* mutants *cad2-1*, with diminished γ -glutamylcysteine synthetase activity (Cobbett *et al.* 1998), and *cad1-3*, defective in PCS activity (Howden *et al.* 1995), were used to evaluate Hg tolerance and Hg-biothiol complexes formation relative to wild-type Col-0 plants.

MATERIALS AND METHODS

Plant material

Alfalfa (*Medicago sativa* cv. Aragon), maize (*Zea mays* cv. Dekalb Paolo) and barley (*Hordeum vulgare*) seedlings were germinated and grown in a semi-hydroponic system as described by Sobrino-Plata *et al.* (2009) for alfalfa and as by Rellán *et al.* (2006a) for maize and barley. The plants grew for 12 days in a controlled environment chamber and were then treated with 30 μ M Hg (as HgCl₂) for 7 days. Once collected, plants were rinsed several times with 10 mM Na₂ EDTA solution to remove superficial Hg, and roots were harvested for tissue fractionation. Another portion of plants were used to determine total Hg concentration in tissues. In some experiments to detect more easily Hg by atomic absorption spectrophotometry in diethylaminoethyl (DEAE)-eluted fractions or by XAS spectroscopy in intact roots (see below), several batches of maize and alfalfa plantlets were grown in a pure hydroponic system with continuous aeration (Ortega-Villasante *et al.* 2005).

Tolerance to Hg assay

Functional experiments of Hg-complexation by PCs were performed with *Arabidopsis thaliana* mutants with altered biothiol content. Col-0, *cad2-1* and *cad1-3* seeds were grown for 12 d in square Petri dishes in solid Murashige-Skoog nutrient medium (0.6% phyto agar, Duchefa Biochemie B.V., Haarlem, The Netherlands) supplemented with 2% sucrose. Tolerance was assessed by measuring root growth after exposure to 10 μ M Hg, supplied in soaked 3MM filter paper (Whatman, Maidstone-Kent, UK) strips (10x1 cm) for 5 d in plates that were rotated 180° (roots-up position). Biothiol profile of mutant *A. thaliana* was studied in the leaves of plants (grown in a perlite-peat mixture for three weeks in short-days light regime), which were infiltrated under vacuum with water, 30 μ M Cd or 30 μ M Hg, and incubated for 48 h.

Tissue fractionation

Root tissue fractions were prepared following the procedure described by Lozano-Rodríguez *et al.* (1997). The homogenate was centrifuged at 10000 g for 30 min, and the pellet, consisting mainly of cell walls, intact cells and organelles, was labelled the Particulate Fraction (PF). The remaining supernatant was centrifuged again at 100000 g for 30 min. The pellet contained membrane fragments and constituted the Microsomal Fraction (MF). The supernatant contained all soluble components of the cell, constituting the so-called Soluble Fraction (SF). All steps were performed at 4°C, and the fractions were stored at -20°C for further analysis.

Anion exchange chromatography of root soluble fractions

The maize root SF was analyzed by anion exchange chromatography to determine the possible association of Hg to biothiols. An XK26 C-16/40 column (Pharmacia Biotech, Uppsala, Sweden) filled with DEAE fast flow Sepharose (Sigma-Aldrich, Saint Louis, MO) was equilibrated with 10 mM Tris-HCl washing buffer (pH 8.6) using a peristaltic pump (1.8 mL/min flow; Gilson, Middleton, WI). The column was loaded with 35 mL of SF and washed until a baseline elution was achieved by measuring absorbance at $\lambda=340$ nm with a UA-5 UV detector (Teledyne ISCO, Lincoln, NE). Elution was achieved using washing buffer supplemented with 0.5 M NaCl. 2.3 mL fractions were collected until the baseline was reached and stored at -20°C for further analysis.

Biothiol analysis

A 300 μ L aliquot of each DEAE chromatography fraction was used to determine the total biothiol content. 50 μ L of ice-cold 20% TCA was added to precipitate proteins, and the mixture was then centrifuged at 10000 g for 15 min at 4°C. The supernatant (100 μ L) was mixed with 400 μ L of reducing solution (1 M NaOH, 1 mg mL⁻¹ NaBH₄) and 200 μ L analytical-grade type II water (miliRO, Millipore, Bedford, MA). After acidification with 100 μ L 35% HCl, biothiols were detected after the addition of 600 μ L of Ellman's reagent (300 μ M DTNB in 0.5 M NaH₂PO₄, pH 7.5) by measuring the absorbance at 412 nm (Shimadzu UV-2401PC spectrometer, Kyoto, Japan). Biothiol concentration was calculated using a GSH standard curve. Biothiol profile of *A. thaliana* plants was analyzed by HPLC as described by Ortega-Villasante *et al.* (2005).

Mercury analysis

Solid samples of roots and cell wall fractions were dried at 40°C to constant weight and ground with mortar and pestle. Dried plant material (100 mg) was acid digested in 2 mL of the digestion mixture (HNO₃:H₂O₂:H₂O, 0.6:0.4:1 v:v) in an autoclave (Presoclave-75 Selecta, Barcelona, Spain) at 120°C and 1.5 atm for 30 min (Ortega-Villasante *et al.* 2007). Liquid samples (500 µL), including microsomal, soluble and DEAE chromatography fractions, were directly digested as described above after the addition of 300 µL HNO₃ and 200 µL H₂O₂. The digests were filtered through a polyvinylidene fluoride filter and diluted in miliRO water to 10 mL. Hg concentration was measured by Atomic Absorption Spectrophotometry, either with an Advanced Mercury Analyser 254 Leco (St. Joseph, Michigan, MI, USA) or with a Atomic Absorption Spectrophotometer Model 4000 equipped with a NaBH₄ cold vapor chamber MSH-20 (Perkin Elmer, Wellesley, MA, USA).

Preparation of biothiol and Hg-biothiol complex standard solutions

Biothiol stock standard solutions containing from 2 to 4 mM of GSH (M_m 307.3; Sigma-Aldrich, St. Louis, MO), hGSH (M_m 321.4; Bachem, Bubendorf, Switzerland), γ-(Glu-Cys)₂ (GC₂; M_m 482.5; GenScript Corporation, Scotch Plains, NJ), γ-(Glu-Cys)₂-Gly (PC₂; M_m 539.6, AnaSpec, San Jose, CA), γ-(Glu-Cys)₃-Gly (PC₃; M_m 771.9, AnaSpec), γ-(Glu-Cys)₄-Gly (PC₄; M_m 1004.1, AnaSpec), γ-(Glu-Cys)₂-Ala (hPC₂; M_m 553.6, GenScript Corporation), γ-(Glu-Cys)₃-Ala (hPC₃; M_m 785.9, Peptide 2.0 Inc., Chantilly, VA), and γ-(Glu-Cys)₄-Ala (hPC₄; M_m 1018.2, Peptide 2.0 Inc.) were prepared in analytical-grade type I water (Milli-Q Synthesis, Millipore). Aliquots of the stock solutions were immediately frozen in liquid N₂, lyophilized and stored at -80 °C. A 30 mM HgCl₂ (Merck, Darmstadt, Germany) stock solution was prepared in Milli-Q water, protected from light and stored at room temperature. Hg-biothiol complexes standard solutions were prepared just before usage by mixing appropriate amounts of Hg and biothiol stock standard solutions at different ratios (in µM; 25:50, 50:50, and 50:25) in 0.1% (v/v) of formic acid (50%; Sigma-Aldrich).

Biothiol and Hg-biothiol analysis by HPLC-ESI-TOFMS

Chromatographic separation was performed with an HPLC system (Alliance 2795, Waters, Milford, MA) following the procedure described by Rellán-Álvarez *et al.* (2006b) with some modifications. A reverse-phase monolithic column (Chromolith Performance RP-

18e, 3 x 100 mm, Merck, Darmstadt, Germany) was used. Injection volume was 50 μL for standard solution and 20 μL for root SF. Autosampler and column compartment temperatures were kept at 6 and 30°C, respectively. The mobile phase was built using three eluents: A (Milli-Q water), B (acetonitrile) and C (2% formic acid in water), all chemicals being HPLC-MS grade (Riedel-de Haën, Seelze, Germany). Samples were eluted (flow rate of 400 $\mu\text{L min}^{-1}$) with a gradient program: the initial conditions (95% A, 0% B and 5% C; min 0) were linearly changed to 85% A, 10% B and 5% C until min 5, and then changed to 45% A, 50% B and 5% C until min 6. After that, an isocratic step with the latter composition was applied until min 9. Then, to return to the initial conditions, a new linear gradient to 95% A, 0% B and 5% C was run until min 11, followed by a 4 min re-equilibration. The exit flow from the column was split with a T-connector (Upchurch Scientific, Oak Harbor, WA) that directed *ca.* 200 $\mu\text{L min}^{-1}$ into the electrospray ionization (ESI) interface of a time-of-flight mass spectrometer (TOFMS) micrOTOF II (Bruker Daltonics, Bremen, Germany). The TOFMS operated in negative ion mode at -500 and 3000 V of endplate and spray tip voltages, respectively. The orifice voltage was set at -90 and -150 V to acquire spectra in the mass-to-charge ratio (m/z) ranges of 50-1000 and 900-3000, respectively. In positive ion mode, endplate and spray tip voltages of -500 and 4500 V were used. The orifice voltage was set at 100 and 270 V to acquire spectra in the 50-1000 and 900-3000 m/z ranges, respectively. The nebulizer gas (N_2) pressure, drying gas (N_2) flow rate and drying gas temperature were 1.6 bar, 7.9 L min^{-1} and 180 °C. The mass axis was calibrated externally using Li-formate adducts (10 mM LiOH, 0.2% (v/v) formic acid and 50% (v/v) 2-propanol). The HPLC-ESI-TOFMS system was controlled with the software packages MicrOTOF Control v.2.2 and HyStar v.3.2 (Bruker Daltonics). Data were processed with Data Analysis v.3.4 (Bruker Daltonics). Ion chromatograms were extracted with a precision of $\pm 0.05 m/z$ units.

Synchrotron X-ray fluorescence microprobe (μ -SXRF)

Three week-old *Medicago sativa* primary roots were further analyzed by microprobe at beamline 2-3 at the Stanford Synchrotron Radiation Lightsource (SSRL). μ -SXRF mapping of Hg was collected by scanning a representative intact root in the microfocused beam at 13,500 eV sampled in $2 \times 2 \mu\text{m}$ pixels. Samples were rinsed several times with 10 mM Na_2 EDTA solution to remove Hg adhered to the root surface. Roots were then freeze-dried to preserve root tissue, placed in large ($\sim 3 \times 3$ cm) Al spacers bound with kapton tape, and stored at room temperature until analysis. The $K\alpha$ fluorescence line intensities of Hg (and other elements of interest, such as S) were

measured with a three-element Ge detector and normalized to the incident monochromatic beam intensity. HgCl₂ powder was used as a standard material for calibration. Data analysis was carried out with the software package SMAK version 0.45 (Webb, 2005).

Extended X-ray absorption fine structure (EXAFS)

Firstly, Hg-biothiol standards were prepared in a 2:1 ratio (ligand:Hg) in Mili-Q water, mixing i) pure hPCs (hPC₂, hPC₃ or hPC₄) (2 mM) and HgCl₂ (1 mM), ii) PCs (PC₂, PC₃ or PC₄) (0.5 mM) and HgCl₂ (0.25 mM), and iii) GSH or hGSH (4 mM) and HgCl₂ (2 mM). The aqueous solutions of Hg-biothiol complexes were mixed with 25% v/v glycerol to prevent the formation of ice crystals. The standard mixture was stored under liquid nitrogen until analysis. Spectra from the additional standard compounds: Hg (II) cysteine ligand (average of mercury cysteine and dicysteine), Hg acetate (HgAce), cinnabar (HgS red), metacinnabar (HgS black), methyl-Hg aspartate (MeHgAsp) and methyl-Hg methionine (MeHgMet) were also used for fit calculations (details can be found in Rajan *et al.* 2008). Hg L₃ edge X-ray absorption spectra for the hydroponic *Medicago sativa* root (average of five scans) and for the standard mixtures (average of three scans) were collected at beamline 9-3 at SSRL by monitoring the Hg L_{α1} fluorescence at 9988 eV. The tissue sample was ground in liquid nitrogen and placed in aluminium spacers. A 200 µl aliquot of the aqueous standard solution was placed in a Lucite sample holder. All samples were bound by kapton type and stored in liquid nitrogen. During the analysis, the samples were maintained at ≈ 10 K in a liquid helium flow cryostat and positioned at 45° to the incident beam. Calibration was accomplished by simultaneous collection of HgCl₂ with first edge inflection at 12284.4 eV. Data analysis was carried out with the software package SixPACK version 0.63 (Webb, 2005) following a standard method that consisted of preliminary examination of fluorescence channels and energy calibration of individual scans using a smoothed first derivative, followed by averaging of data. A linear background function was subtracted, and data were normalized to a unit step edge. To quantify the percentage of each Hg species present in alfalfa roots using the fingerprinting method, a least squares fit (LSF) was performed to fit the EXAFS (*chi*) of the experimental data to linear combinations of standard reference compounds, which were divided into four Hg coordination environments: inorganic sulphur bonding (Hg-S red and Hg-S black), organic sulphur bonding (Hg-PCs and Hg-Cys), oxygen-rich ligand bonding (carboxylic groups) (Hg-Ace) and methyl-Hg forms (Me-Hg-Asp and Me-Hg-Met). Single-component fits to the

data were carried out to exclude those contributing less than 1 %, and selected candidates of each group were fitted to get the relative proportion of Hg species. The reduced *chi*-square value (goodness of fit χ^2) provides information as to the quality of the standard fit to the spectra data (Kim *et al.* 2000).

Statistical analysis

Statistical significance was calculated by the Duncan's test of analysis of variance (at $p < 0.05$), using the SAS statistical software package.

RESULTS

Plant growth and Hg distribution in tissues

The growth of roots was not affected significantly in plants treated with 30 μM Hg for 7 days in a semi-hydroponic culture (Table 1), and no visual symptoms of toxicity appeared. Total root Hg concentrations were approximately 1,600, 500 and 800 $\mu\text{g g}^{-1}$ FW in barley, maize and alfalfa plants treated with Hg, respectively, whereas control plants had Hg concentrations below the detection limit ($< 0.05 \mu\text{g g}^{-1}$ FW). Shoot Hg concentration values were only approximately 2% of those found in roots (data not shown), in agreement with the known allocation of this toxic metal in plants grown under similar conditions (Sobrino-Plata *et al.* 2009; Valega *et al.* 2009). Therefore, we focused on Hg fractionation, speciation and allocation in root tissues.

Table 1. Fresh weight (mg plant^{-1}), and total and subcellular Hg concentration ($\mu\text{g g}^{-1}$ fresh weight) of roots from 3-week-old barley, maize and alfalfa plants treated with 0.0 (control) or 30 μM Hg (+Hg) for 7 days. In parentheses, the percentage of Hg distribution relative to the total is shown. Particulate Fraction, PF; Microsomal Fraction, MF; Soluble Fraction, SF. Data are average of three independent replicates (\pm SD). Data for MF and SF were originally measured on a total metal basis and then transformed into a $\mu\text{g g}^{-1}$ fresh weight basis.

	Root fresh weight		^a Hg concentration			
	Control	+Hg	Total	PF	MF ^b	SF
Barley	21 \pm 9	24 \pm 7	1599 \pm 217	1047 \pm 222 (66)	< 0.03	1.01 \pm 0.06 (0.06)
Maize	118 \pm 27	102 \pm 25	517 \pm 40	320 \pm 121 (61)	< 0.03	0.32 \pm 0.02 (0.06)
Alfalfa	500 \pm 204	440 \pm 133	816 \pm 184	757 \pm 36 (92)	< 0.03	0.69 \pm 0.01 (0.08)

^aMercury concentration in roots and subcellular fractions from control plants were below detection limits.

^bOnly traces of Hg (slightly below the quantification limit) were found in the microsomal fraction.

Subcellular fractionation and association of soluble Hg with biothiols in roots

Three subcellular fractions were isolated from root tissue: a particulate (PF), a microsomal (MF) and a soluble fraction (SF), and the Hg concentration of each fraction were

measured. The vast majority of Hg (approximately 99.9% in barley, maize and alfalfa) was found associated with the PF, which contains mainly cell walls (Table 1). A much smaller portion (approximately 0.1% in all cases) of Hg was found in the SF, whereas the Hg detected in the MF was just below the quantification limit (below 0.01%). Mercury concentrations were in the SF equivalent to approximately 1.0, 0.3 and 0.7 $\mu\text{g g}^{-1}$ FW of barley, maize and alfalfa respectively. Anion exchange DEAE-chromatography of SF revealed that Hg co-eluted with a peak containing most of the biothiols from maize root SF (Fig. 1); the amount of Hg recovered represents approximately 70% of the total Hg SF.

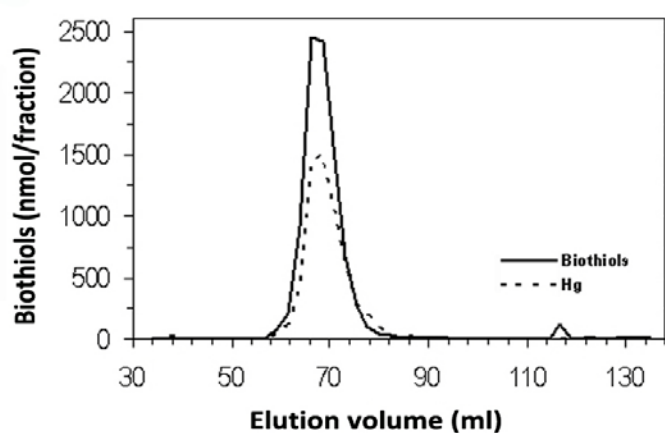


Fig. 1. FPLC-DEAE anion exchange chromatography of the Soluble Fraction from maize roots treated with 30 μM Hg. Samples collected were analyzed for biothiols reacting with Ellman's reagent (continuous line) or for Hg (dashed line) and plotted against elution volume. Data are representative of three independent experiments.

Detection of Hg-biothiol complexes by HPLC-ESI-TOFMS

Mass spectrometry-based analyses were carried out to identify the Hg species occurring in root SF, using an approach similar to that used recently by Krupp *et al.* (2008, 2009) and Chen *et al.* (2009). Hg-containing compounds were identified by the characteristic natural Hg isotopic composition (^{196}Hg , ^{198}Hg , ^{199}Hg , ^{200}Hg , ^{201}Hg , ^{202}Hg , and ^{204}Hg) using ESI-TOFMS (Chen *et al.* 2009). An array of biothiol and Hg-biothiol standard solutions was used to establish the HPLC-ESI-TOFMS analytical conditions, prepared at three concentration ratios (1:2, 1:1 and 2:1), with the following ligands: GSH, hGSH, (γ -Glu-Cys) $_2$ (GC $_2$), (γ -Glu-Cys) $_2$ -Gly (PC $_2$), (γ -Glu-Cys) $_2$ -Ala (hPC $_2$), (γ -Glu-Cys) $_3$ -Gly (PC $_3$), and (γ -Glu-Cys) $_3$ -Ala (hPC $_3$). Acidic chromatographic conditions were used, similar to

those established for the determination of reduced and oxidized GSH and hGSH (Rellán-Álvarez *et al.* 2006b), based on the fact that Hg-biothiol complexes are stable at pH 2.0 (Chen *et al.* 2009). Most biothiol ligands and Hg-biothiol complexes were detected both in negative and positive ionization. Since the ionization polarity could affect sensitivity to detect each Hg-biothiol complex, positive and negative ionizations were always used. Moreover, to detect the full array of possible Hg-complexes, TOFMS mass spectra were acquired in two different mass-to-charge ratio (m/z) ranges: 100-1000 and 1000-3000. Therefore, a total of four individual HPLC-ESI-TOFMS runs were carried out per sample (negative and positive mode, in two mass-to-charge ratios each), with high-resolution mass spectra acquired to obtain three-dimensional (time, m/z , and intensity) chromatograms.

The ion chromatograms of free biothiols were extracted at the exact m/z values of the $[M+H]^+$ and $[M-H]^-$ ions corresponding to the monoisotopic signals (Fig. 2A), and the ion chromatograms of Hg-biothiol complexes (Figs. 2B and 2C) were extracted at the exact m/z values of the $[M+H]^+$ and $[M-H]^-$ ions corresponding to the ^{202}Hg (most abundant isotope) signal. Results show that the HPLC-ESI-TOFMS method adequately resolved free biothiols and Hg-biothiol complexes (Fig. 2). Differences in retention times between the free and Hg-complexed biothiols were only found in the case of small biothiols such as GSH and hGSH. For instance, GSH eluted at 2.5 min (Fig. 2A) whereas $\text{Hg}(\text{GSH})_2$ eluted at 4.8 min (Fig. 2B). Fig. 2D shows an example of ESI-TOFMS spectra in the positive mode of one of the standards tested (Hg:hPC₂; 25:50 μM). When data were acquired in the 100-1000 m/z range, two main ions at m/z 554.1 and 754.1 were found. A close-up of the mass spectrum of the ion at m/z 554.1 shows that it corresponds to free $[\text{hPC}_2+\text{H}]^+$ (inset in Fig. 2D). However, the ion at m/z 754.1 and isotopic signature fit well with a single charged ion containing one Hg atom complex ($[\text{HghPC}_2+\text{H}]^+$; inset in Fig. 2D). When mass spectra were acquired in the 1000-3000 m/z range, two further ions at m/z 1307.2 and 1505.1 were found (Fig. 2E), with signal intensities one order of magnitude lower than that of $[\text{HghPC}_2+\text{H}]^+$. The ion at m/z 1307.2 had an isotopic signature characteristic of a single charged ion containing one Hg atom, and the m/z fit well with $[\text{Hg}(\text{hPC}_2)_2+\text{H}]^+$.

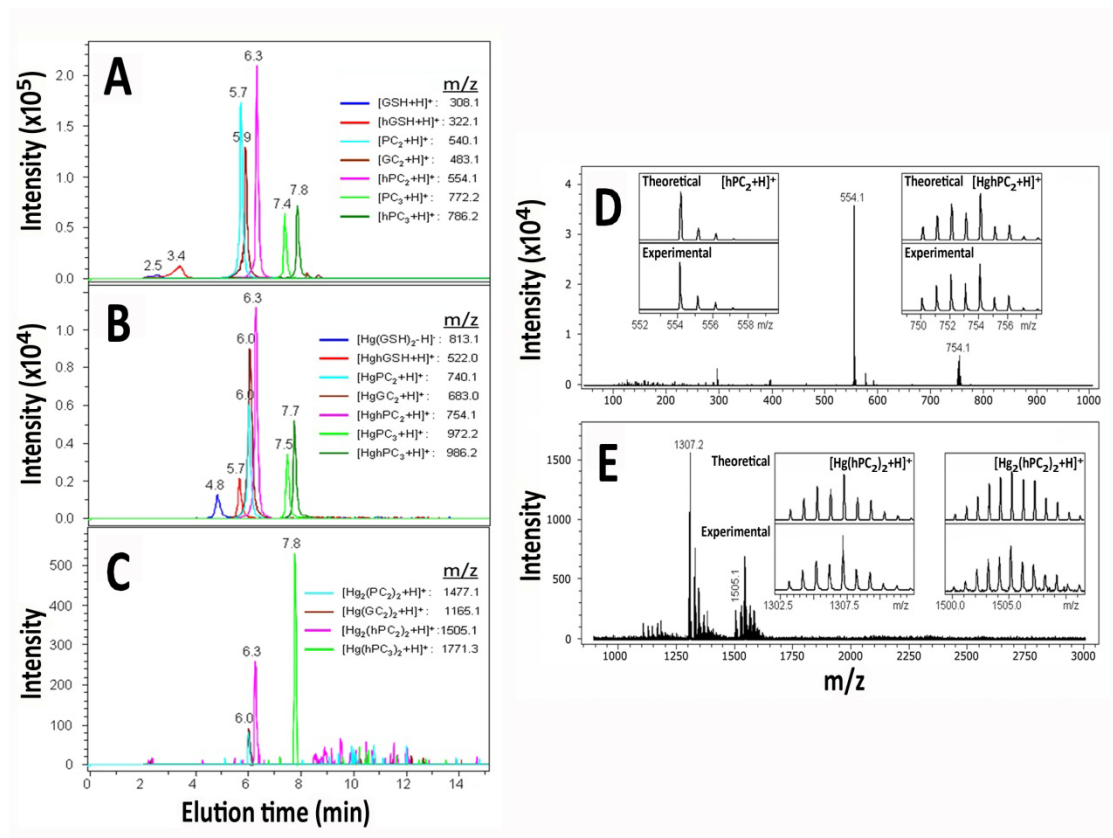


Fig. 2. HPLC-ESI-TOFMS analysis of biothiol ligands (50 μM) and Hg-biothiol complexes (mixture of Hg:biothiol; 25 μM :50 μM) standard solutions in 0.1% formic acid. Peaks corresponding to different biothiol ligands (**A**) and Hg-biothiol complexes of low m/z (50-1000 range; **B**) and high m/z (900-3000 range; **C**) are shown. Mass spectra of a Hg:hPC₂ mixture standard solution (25:50 μM in 0.1% formic acid) acquired in the 50-1000 (**D**) and 900-3000 (**E**) m/z ranges. Experimental and theoretical isotopic signatures of the identified ions are shown in insets.

The ion at m/z 1505.1 showed an isotopic signature characteristic of a single charged ion containing two Hg atoms, and the m/z fit well with $[\text{Hg}_2(\text{hPC}_2)_2+\text{H}]^+$ (Fig. 2E). The existence of two or more Hg atoms changes the fingerprint of the complex, as observed by comparing the isotopic signatures of $[\text{Hg}(\text{hPC}_2)_2+\text{H}]^+$ and $[\text{Hg}_2(\text{hPC}_2)_2+\text{H}]^+$ ions. A wide array of Hg-biothiol complexes was found in standard solutions prepared at three Hg-to-biothiol concentration ratios (1:2; 1:1 and 2:1) by HPLC-ESI-TOFMS. The m/z and retention time values of all free biothiol and Hg-biothiol ions detected are presented in Supplementary Table 1 (Appendix I). Independent of the proportions of Hg and PCs used in the standard preparation, the most frequent Hg-biothiol ions found corresponded to Hg-complexes with a 1:1 stoichiometry. Phytochelatins with a higher number of sulfhydryl residues such as PC₃ and hPC₃ also formed complexes with higher stoichiometries (4:2 or 2:1 Hg:ligand) in the case of the Hg-richest mixtures (e.g. the $[\text{Hg}_4(\text{hPC}_3)_2-2\text{H}]^{2-}$ ion;

Supplementary Table 1; appendix I). These heavily Hg-loaded complexes showed higher retention times than those of Hg-biothiol complexes with lower stoichiometries.

When the root SF of alfalfa, maize and barley plants treated with 30 μM Hg was analyzed using HPLC-ESI-TOFMS, a total of 28 Hg-containing ions were detected corresponding to 17 different Hg-complexes (ions were detected in positive mode, negative mode or in both), formed with up to six different biothiols (GC_2 , PC_2 , hPC_2 , hPC_3 , PC_4 , and hPC_4 ; summarized in Table 2).

Table 2. Mercury-containing ions detected in positive and negative mode HPLC-ESI-TOFMS analysis of root soluble fractions from 3-week-old barley, maize, and alfalfa plants treated with 30 μM HgCl_2 for 7 days. The identification of the ions detected along with their mass-to-charge ratio (m/z) and chromatographic retention times (t_R ; in minutes) are indicated. Data were obtained from 3 independent biological replicates.

Plant species	Formula species complex	t_R	Ion positive mode	Ion negative mode	m/z
Barley	Hg- GC_2	6.2	$[\text{HgGC}_2+\text{H}]^+$		683.1
		6.2		$[\text{HgGC}_2-\text{H}]^-$	681.1
	Hg- PC_2	6.3	$[\text{HgPC}_2+\text{H}]^+$		740.1
		6.3		$[\text{HgPC}_2-\text{H}]^-$	738.1
	Hg- PC_4	8.3		$[\text{HgPC}_{4ox}-\text{H}]^-$	1200.2
Maize	Hg- GC_2	6.2	$[\text{HgGC}_2+\text{H}]^+$		683.1
		6.2		$[\text{HgGC}_2-\text{H}]^-$	681.1
	$\text{Hg}_2-(\text{GC}_2)_2$	6.2		$[\text{Hg}_2(\text{GC}_2)_2-\text{H}]^-$	1361.2
Alfalfa	$\text{CH}_3\text{-Hg-hPC}_2$	6.0		$[\text{CH}_3\text{HghPC}_2-\text{H}]^-$	768.1
	Hg- GC_2	6.2		$[\text{HgGC}_2-\text{H}]^-$	681.1
	Hg- PC_2	6.2		$[\text{HgPC}_2-\text{H}]^-$	738.1
	Hg- <i>Unknown</i>	6.7		$[\text{Hg Unknown}]^-$	1084.2
		6.7		$[\text{Hg Unknown}]^-$	1165.2
		6.7		$[\text{Hg Unknown}]^-$	1834.3
		6.7		$[\text{Hg Unknown}]^-$	1834.3
	Hg-h PC_2	6.8	$[\text{HghPC}_2+\text{H}]^+$		754.1
	$\text{Hg}_2-(\text{hPC}_2)_2$	6.8		$[\text{Hg}_2(\text{hPC}_2)_2-\text{H}]^-$	1503.2
	$\text{Hg}_3-(\text{hPC}_2)_3$	6.8		$[\text{Hg}_3(\text{hPC}_2)_3-\text{H}]^-$	2255.3
	Hg-(h PC_{2ox}) ₂	7.7	$[\text{Hg}(\text{hPC}_{2ox})_2+2\text{H}]^2$		653.1
		7.7	$[\text{Hg}(\text{hPC}_{2ox})_2+\text{H}]^+$		1305.2
	Hg-h PC_3	8.0		$[\text{HghPC}_3-\text{H}]^-$	984.2
	Hg- PC_{4ox}	8.3	$[\text{HgPC}_{4ox}+\text{H}]^+$		1202.2
		8.3		$[\text{HgPC}_{4ox}-\text{H}]^-$	1200.2
	Hg-h PC_{4ox}	8.3	$[\text{HghPC}_{4ox}+\text{H}]^+$		1216.2
8.3			$[\text{HghPC}_{4ox}-\text{H}]^-$	1214.2	
Hg-(h PC_{3ox}) ₂	8.4	$[\text{Hg}(\text{hPC}_{3ox})_2+\text{H}]^+$		1767.3	
$\text{Hg}_2-(\text{hPC}_{3ox})_2$	8.4	$[\text{Hg}_2(\text{hPC}_{3ox})_2+\text{H}]^+$		1967.3	
Hg ₂ - PC_{4ox}	8.5		$[\text{Hg}_2\text{PC}_{4ox}-\text{H}]^-$	1400.2	
Hg ₂ -h PC_{4ox}	8.5		$[\text{Hg}_2\text{hPC}_{4ox}-\text{H}]^-$	1414.2	

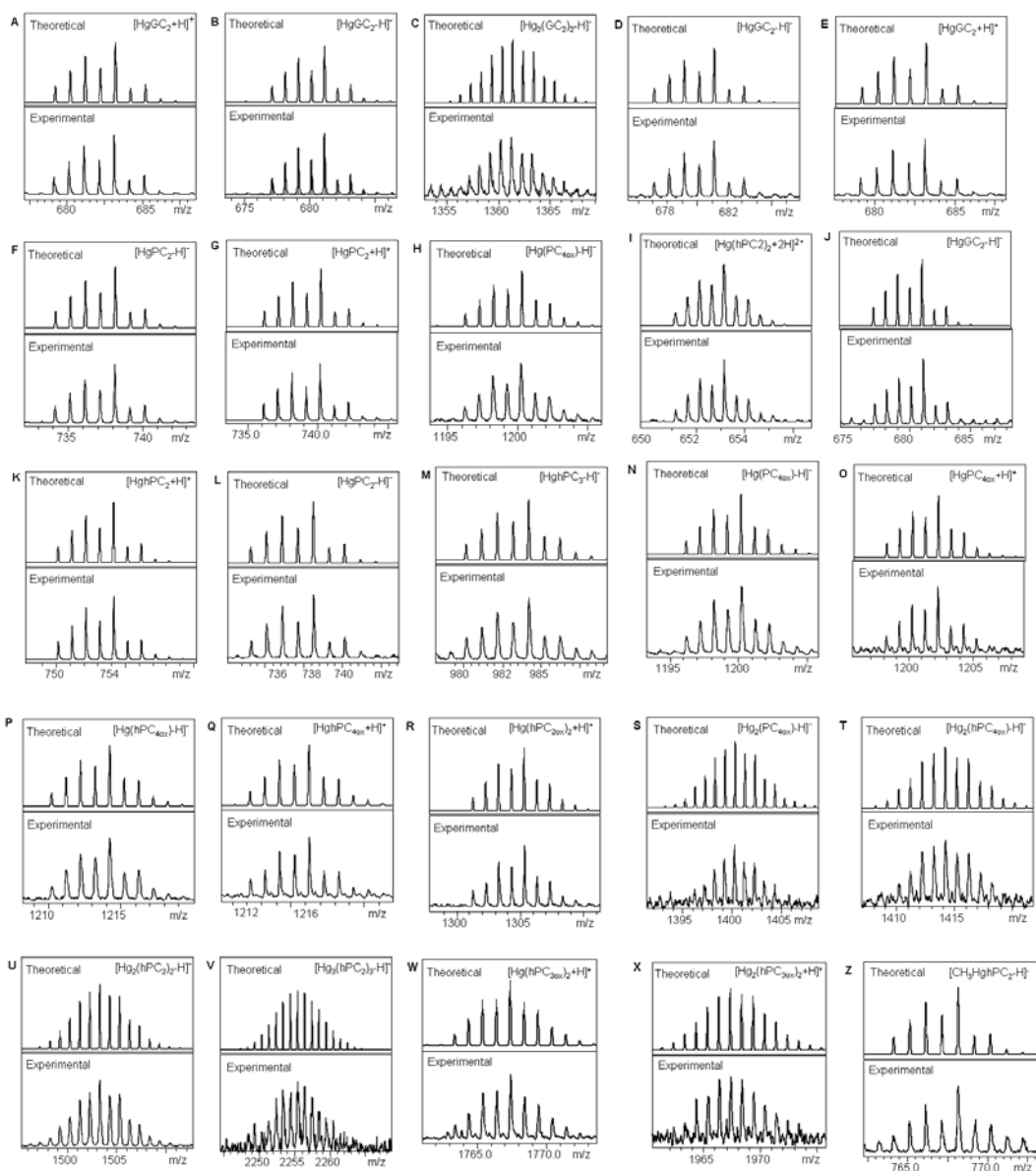


Fig. 3. Experimental and theoretical isotopic signatures of the identified Hg-containing ions found in the HPLC-ESI/TOFMS analysis of the root soluble fraction from 3-week-old alfalfa (A-R), barley (S-U) and maize (V-Z) plants treated with 30 μM HgCl_2 for 7 days.

Fourteen of the 17 Hg-containing complexes were unequivocally identified based on retention time, exact m/z , and isotopic signature (see fits between experimental and theoretical isotopic signatures in Fig. 3). In barley, three 1:1 Hg-complexes were found, one each with GC_2 , PC_2 and PC_4 . In maize, Hg formed only two complexes with GC_2 , having 1:1 and 2:2 stoichiometry. In alfalfa, up to 14 different Hg-biothiol complexes were found, one each with GC_2 ($HgGC_2$) and PC_2 ($HgPC_2$), four with hPC_2 ($HghPC_2$, $Hg(hPC_2)_2$, $Hg_2(hPC_2)_2$ and $Hg_3(hPC_2)_3$), three with hPC_3 ($HghPC_3$, $Hg(hPC_3)_2$ and $Hg_2(hPC_3)_2$), two with hPC_4 ($HghPC_4$ and Hg_2hPC_4), and two more with PC_4 ($HgPC_4$ and Hg_2PC_4). Additionally, we could detect a complex formed with methyl-Hg and hPC_2 (CH_3 -Hg- hPC_2) in alfalfa SF, not previously described in the literature. Therefore, the most abundant Hg-to-ligand stoichiometry found was 1:1. Moreover, some of the Hg-biothiol complexes having thiol groups not bound to Hg were found to occur in oxidized forms ($Hg(hPC_{2ox})_2$, $Hg(hPC_{3ox})_2$, $Hg_2(hPC_{3ox})_2$ and $Hg(hPC_{4ox})$), and eluted with a delay of approximately one min as compared with their reduced counterparts. Finally, three more Hg-containing ions were found in alfalfa at m/z 1084.2, 1165.2 and 1834.3, which could not be identified (Table 2). As an example, some chromatographic and MS data obtained for the three plant species are shown in Fig. 4. Barley root SF showed (in positive mode) two single charged ions containing one Hg atom at m/z 683.1 and 740.1, both eluting at 6.2 min, that had m/z and isotopic signatures matching those of $[HgGC_2H]^+$ and $[HgPC_2+H]^+$ ions, respectively (Fig. 4A). Maize root SF only showed two single charged Hg-containing ions, at m/z 683.1 (in positive mode) and 1361.2 (in negative mode), eluting at 6.2 min and with m/z and isotopic signatures fitting well with those of $[HgGC_2+H]^+$ and $[Hg_2(GC_2)_2-H]^-$ ions, respectively (Fig. 4B). Alfalfa root SF showed (in negative mode) two single charged ions containing one Hg atom, at m/z 1503.2 (at 6.8 min) and 2255.3 (at 6.7 min), that were identified as $[Hg_2(hPC_2)_2-H]^-$ and $[Hg_3(hPC_2)_3-H]^-$, respectively (Fig. 4C).

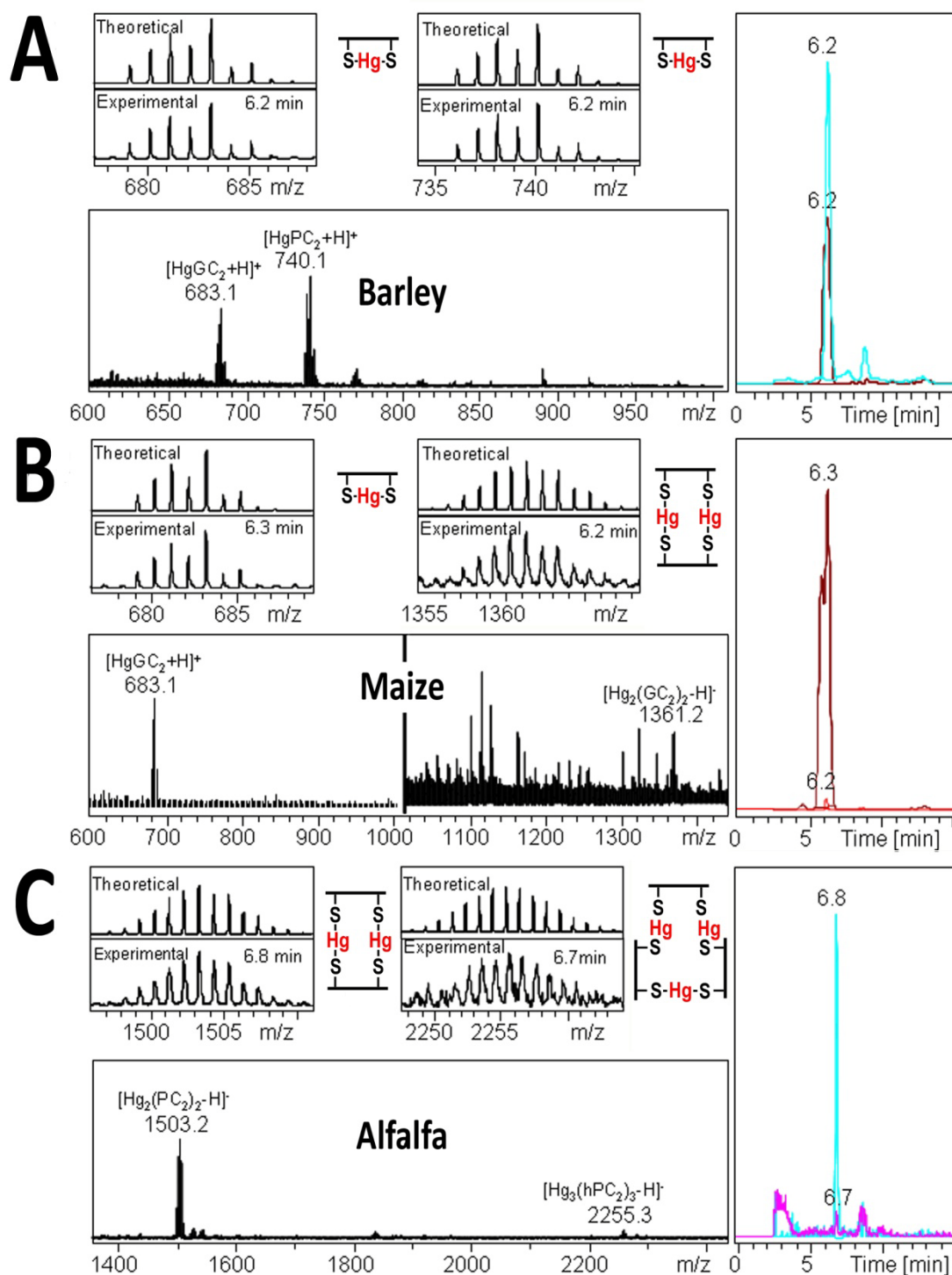


Fig. 4. Analysis of some Hg-phytochelatin complexes found in the root soluble fraction of 3-week-old barley (A), maize (B), and alfalfa (C) plants treated with 30 μ M HgCl₂ for 7 days. HPLC-ESI-TOFMS analyses were carried out in negative and positive modes, and data were acquired at different *m/z* ranges. On the left panels, chosen mass spectra extracted at the retention times indicated in the chromatograms shown on the right panels are displayed. Insets highlight experimental and theoretical isotopic signatures of the identified ions as well as a schematic diagram of the putative Hg-S bonds.

***In vivo* X-ray spectroscopy of Hg in alfalfa roots**

The spatial localization of Hg and S was studied in alfalfa roots treated with 30 μM Hg using $\mu\text{-SXRf}$ (Fig. 5A and 5B). The most intense Hg signals were found in the inner tissues, possibly at the vascular cylinder. At this location, there was significant overlap with Hg and sulfur (S; Fig. 5B; see overlay in Fig. 5C). The correlation between intensities of Hg and S was highly significant (r^2 of 0.84; see Fig. 5D).

To undertake the *in vivo* speciation of Hg in roots of 30 μM Hg-treated alfalfa plants, we performed XAS, which permits non-disruptive analysis in frozen root material. Confidence in the accuracy of the fit was increased by using a diverse standard library, taking into account the most probable Hg coordination environments in plants, since the goodness of the LSF approach depends on the standard compounds selected *a priori* (Beauchemin *et al.* 2002). A first LSF was performed in each group of standard mixtures (inorganic sulphur-Hg forms, biothiol and cysteine Hg ligand bonding, oxygen-rich ligand bonding and methyl-Hg forms) in order to exclude those standard compounds contributing less than 5 % in the fit. This preliminary survey showed that the spectra of the different HgPCs, and also the HgCys complexes were indistinguishable from each other. Therefore, we opted to use HghPC₂ and HgCys as representative standards for Hg-biothiol or Hg-organic sulphur (also protein) complexes. The Hg L₃ EXAFS spectra of the Hg model compounds plus the current sample are shown in Fig. 5E. Organic Hg-S coordination (HgCys and HghPC₂) and methyl-Hg forms (MeHgMet) accounted for 79% and 21%, respectively, of the total Hg in alfalfa roots (reduced *chi*-square 0.0909). The best LSF of the EXAFS spectra to the standards HgCys, HghPC and MeHgMet that represents the different Hg forms in alfalfa roots is shown in Fig. 5F.

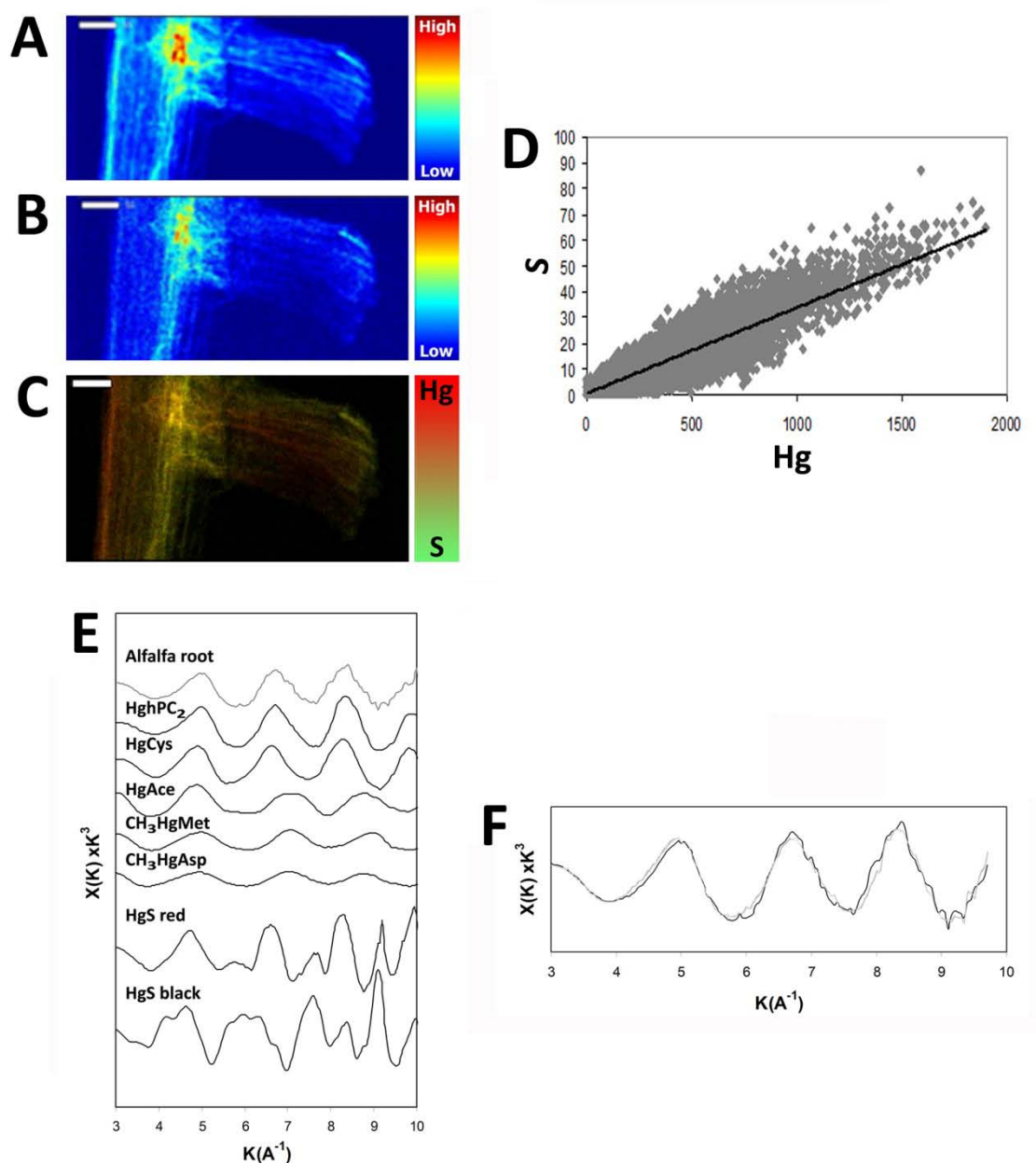


Fig. 5. X-ray spectroscopy to study Hg distribution and ligand association in three-week-old *Medicago sativa* roots treated with 30 μM Hg for 7 days in a pure-hydroponic system. (A) Elemental 2-D SXRF distribution of Hg; (B) distribution of sulfur; and (C) overlapping of Hg (red) and S (green); white scale bars equal 50 μm . (D) Correlation diagram of S relative to Hg, obtained from Fig. 5C as fluorescence line intensity (counts s^{-1}), after analysis by $\mu\text{-SXRF}$ (E) Hg L₃ EXAFS spectra of the Hg model compounds plus alfalfa root. (F) Linear fitting results for alfalfa root (black line: data, gray line: fit), showing the Hg L₃ EXAFS k^3 weighted spectra (reduced *chi*-square 0.0909). The components that contributed to the linear fit were HgCys (33.8%), HghPC (45.2%) and MeHgMet (21%).

Tolerance analysis of *A. thaliana cad1-3* and *cad2-1* mutants

To evaluate the relevance of Hg-PC complex formation for Hg detoxification and tolerance root growth inhibition, a biothiol profile was studied in *Arabidopsis thaliana* mutants with altered biothiol metabolism. *cad2-1* and *cad1-3* mutants were clearly less tolerant than the wild-type when exposed to 10 μM Hg for 4 d: root growth inhibition was over 80% in the mutants, whereas WT was inhibited by only 35% (Fig. 6).

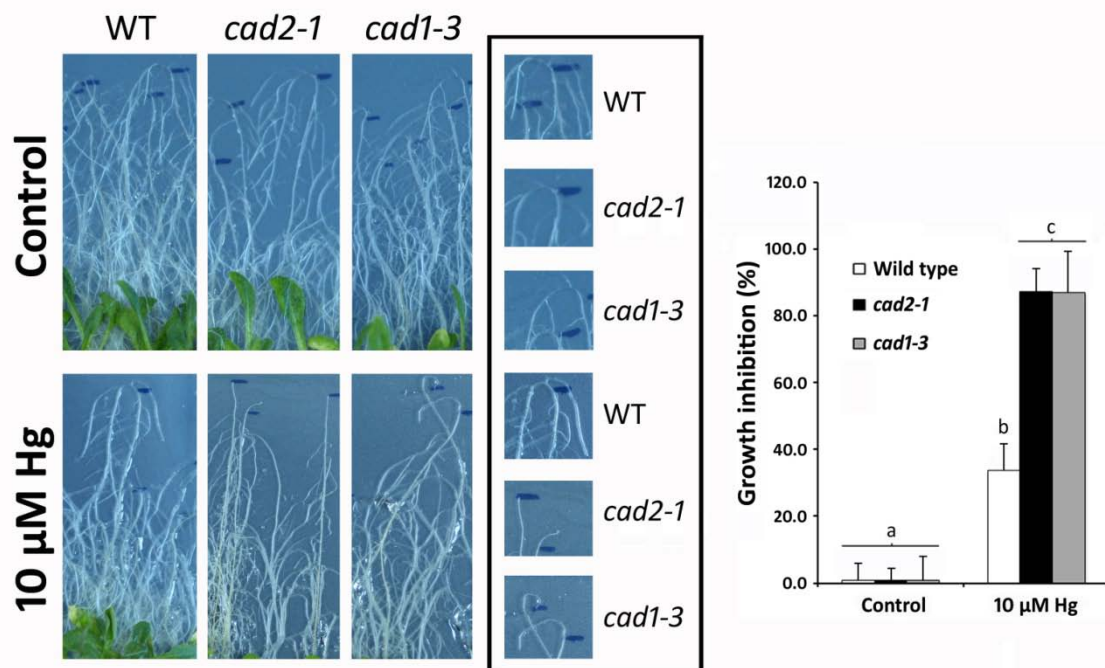


Fig. 6. Tolerance to Hg assay with *Arabidopsis thaliana* mutants altered in biothiol metabolism: Wild-type (Col-0), *cad2-1* (altered \square glutamyl cysteine synthase activity), and *cad1-3* (lacking PCS activity). Seven-days-old seedlings were turned roots-up and exposed to control (0) or 10 μM Hg by placing a 3MM filter paper strip close to the root apical tip. Close-ups of the root tips (insets in black rectangle) highlight the remarkable sensitivity of both mutants compared with the WT. Out-growth root length was measured from the blue mark and growth inhibition calculated after 5 d exposure (see graph on the right). Results are the average of 10 replicates, and different letters denote significant differences with $p < 0.05$.

The biothiol profile of each plant was analyzed by conventional HPLC in leaves infiltrated with 30 μM Cd or Hg for 48 h (Fig. 7). Cd-treated leaves of *cad2-1* mutant accumulated a lower amount of GSH (40%) and PCs (<31%) than Col-0, and no PCs were detected in leaves exposed to 30 μM Hg (Table 3). As expected, *cad1-3* did not accumulate PCs under Cd nor Hg stress, although a remarkable increase in GSH level was detected, over 150% the concentration found in Col-0 (Table 3).

Table 3. Concentration of biothiols (nmol g^{-1} FW) in *Arabidopsis thaliana* leaves infiltrated with 30 μM Cd or Hg for 48 h. In parentheses is the percentage of concentration relative to wild-type. Values are the mean of four independent replicates \pm standard deviation ($p < 0.05$).

Biothiol	Wild type	<i>cad2-1</i>	<i>cad1-3</i>
Control			
Cys	23.4 ^a \pm 4.8	21.5 ^a \pm 4.7 (92)	22.6 ^a \pm 9.7 (96)
GSH	153.8 ^a \pm 8.4	50.1 ^b \pm 10.3 (33)	142.1 ^a \pm 14.3 (92)
30 μM Cd			
Cys	19.7 ^a \pm 6.5	36.6 ^{ab} \pm 5.8 (186)	46.1 ^b \pm 12.8 (234)
GSH	142.5 ^a \pm 22.8	80.0 ^c \pm 22.4 (56)	316.1 ^d \pm 29.9 (222)
PC ₂	168.7 ^a \pm 38.7	52.5 ^b \pm 18.9 (31)	n.d.
PC ₃	346.7 ^a \pm 38.6	41.0 ^b \pm 14.7 (12)	n.d.
PC ₄	283.6 ^a \pm 48.6	25.6 ^b \pm 8.8 (9)	n.d.
PC ₅	73.9 ^a \pm 12.7	n.d.	n.d.
30 μM Hg			
Cys	25.0 ^a \pm 3.6	44.1 ^b \pm 2.2 (177)	65.6 ^c \pm 10.1 (263)
GSH	175.5 ^a \pm 12.4	52.0 ^b \pm 7.2 (30)	257.4 ^d \pm 21.9 (147)
PC ₂	60.4 ^a \pm 22.4	n.d.	n.d.
PC ₃	32.3 ^a \pm 9.3	n.d.	n.d.

^aDifferent letters denote significant differences compared with control wild-type samples.

HPLC-ESI-TOFMS analysis revealed that Hg-PC₂ complexes were only detected in Col-0 leaves ($[\text{HgPC}_2+\text{H}]^+$), whereas no traces of Hg-biothiol complexes could be detected in *cad2-1* or in *cad1-3* (data not shown). HPLC-ESI-TOFMS sensitivity was checked by the addition of Hg-GSH spikes to Col-0 leaves infiltrated with 30 μM Hg. We could only detect $[\text{Hg}(\text{GSH})_2-\text{H}]^-$ at m/z 813.1 with the highest spike concentration (25 μM Hg:50 μM GSH; Fig. 8B), whereas this ion was not detected in Col-0 leaves spiked with 2.5 μM Hg:5 μM GSH (Fig. 8C) nor in non-spiked 30 μM Hg-treated leaves (Fig. 8D).

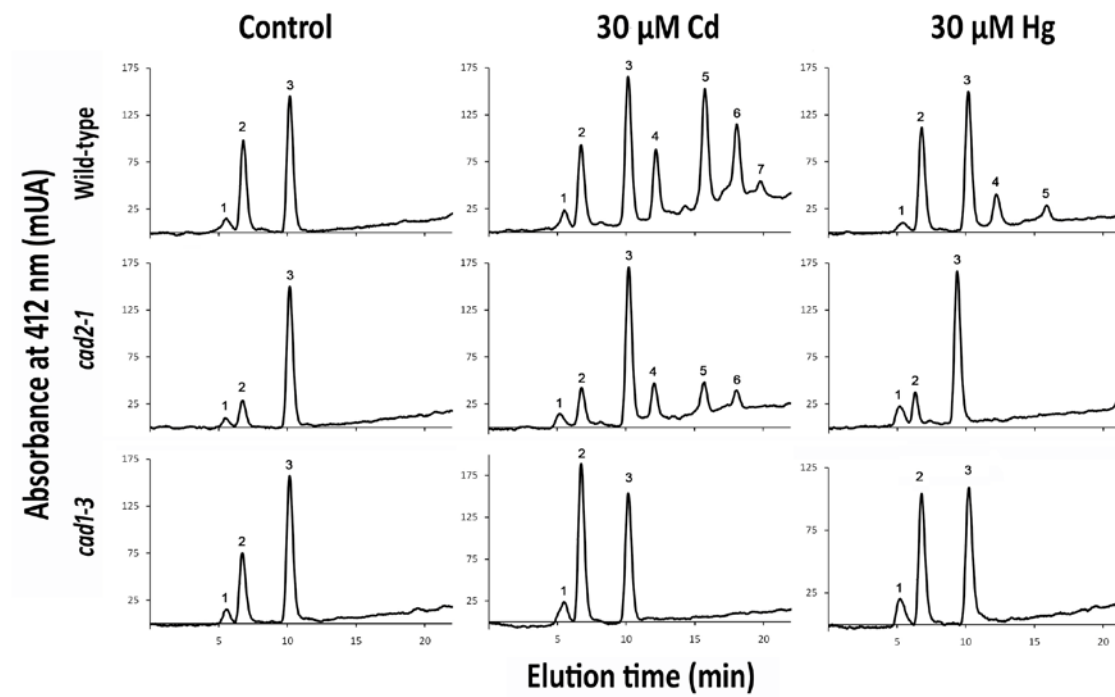


Fig. 7. Biothiol profile of *Arabidopsis thaliana* Col-0, *cad2-1* and *cad1-3* leaves infiltrated with control (0), 30 μ M Cd or 30 μ M Hg for 48 h. Peaks were identified by the elution of commercially available standards. Concentration was calculated by the integration of the internal standard N-acetyl-cysteine (Peak 3): Cys (1), GSH (2), PC₂ (4), PC₃ (5), PC₄ (6), and PC₅ (7).

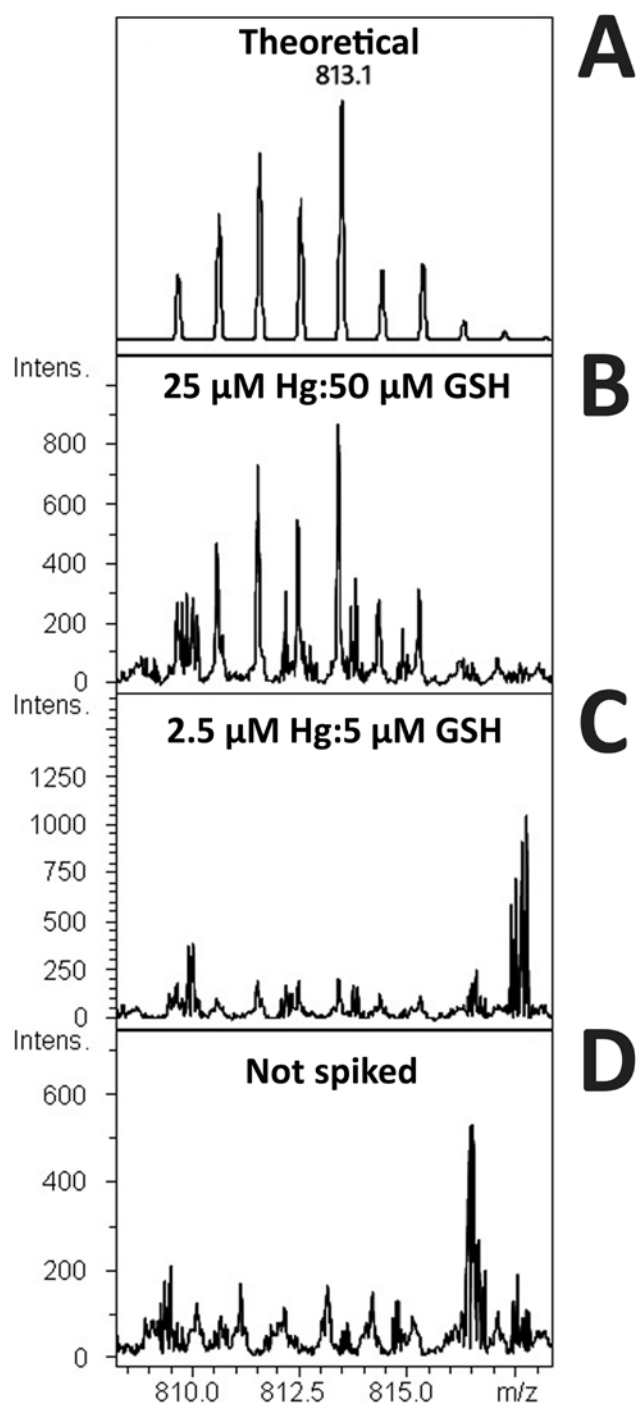


Fig.8 Assay to identify Hg-GSH complexes with respect to the detection limit of the HPLC-ESI-TOFMS analysis. Theoretical (A) isotopic signature of $[\text{Hg}(\text{GSH})_2-\text{H}]^-$ ion at m/z 813.1 found detected in *A. thaliana* Col-0 leaves infiltrated with 30 μM Hg for 48 h and spiked with 25 μM Hg:50 μM GSH (B), 2.5 μM Hg:5 μM GSH (C), and with deionized water (D).

DISCUSSION

Although plants examined in this study were treated with a high dose of Hg (30 μ M), they were not poisoned and effective defense mechanism(s) were exerted in agreement with our previous results (Sobrino-Plata *et al.* 2009). Roots were the major sink for Hg, as already described in these plant species (Rellán-Álvarez *et al.* 2006a; Sobrino-Plata *et al.* 2009). Several subcellular fractions were prepared from roots of Hg-treated alfalfa, maize, and barley plants. The largest amount of Hg accumulated in the root PF (up to 99%), with the SF representing a secondary pool, was in agreement with the distribution described in *Halimione portulacoides* using a similar experimental approach (Valega *et al.* 2009). Retention of heavy metals by materials associated with the cell wall and/or via complexation in the intracellular space has been described as important tolerance mechanisms to avoid its accumulation in cytosol and organelles (Hall, 2002). Thus, Hg has been found associated with the cell wall of different plant species (*Pisum sativum* and *Mentha spicata*, Beauford *et al.* 1977; *Nicotiana tabacum*, Suszcynsky & Shann, 1995). The chromatographic separation of maize SF by DEAE-FPLC revealed that the major proportion of soluble Hg was associated with biothiols, which agrees with the reported recovery of Cd in maize (Rauser & Meuwly 1995) and *Sedum alfredii* (Zhang *et al.* 2010) after a similar chromatographic separation of soluble Cd. These results highlight the relevance of biothiol ligands in Hg speciation in plants.

To identify the biothiol ligands involved in Hg complexation, root SFs of barley, maize and alfalfa plants exposed to 30 μ M Hg were analyzed in depth by HPLC-ESI-TOFMS. The HPLC-ESI-TOFMS analysis of the root SF of barley, maize and alfalfa plants exposed to 30 μ M Hg revealed that Hg was only found associated with PCs. No other Hg-containing substances were identified with our experimental settings, although other bioligands such as organic acids, nicotianamine or amino acids can be important in metal homeostasis (Sharma & Dietz, 2006). A wide array of Hg-PC complexes was found: three in barley, two in maize (one of them also present in barley), and 14 in alfalfa (two of them also present in barley). Ten novel Hg-PCs complexes formed with hPCs were unequivocally identified in alfalfa, a leguminous species capable of synthesizing GSH and hGSH, which has been reported to produce several kinds of PCs and hPCs in the presence of toxic metals, including Hg (Sobrino-Plata *et al.* 2009). The synthesis of hPCs depends apparently on the availability of hGSH as substrate, because phytochelatin synthase (PCS) does not distinguish between GSH or hGSH (Loscos *et al.* 2006).

The most common Hg-PC complexes detected in the three plant species studied were those formed with PCs having two γ -glutamylcysteine units (*i.e.* PC₂, hPC₂ and GC₂; Table 2), although up to 7 different Hg-PC complexes with hPC₃, PC₄ and hPC₄ were also found in alfalfa. Similarly, HgPC₂, HgGC₂, Hg(Ser)PC₂ and Hg(Glu)PC₂ were found to accumulate in *O. sativa*, whereas in *M. vulgare* only Hg(Glu)PC₂ was found by HPLC-ESI-MS/MS (Krupp *et al.* 2009). Although PC₃ and PC₄ were detected in root tissue extracts from *Brassica napus*, the major pool of biothiols corresponded to PC₂ (Iglesia-Touriño *et al.* 2006). Interestingly, the maize SF only contained the biothiol ligand GC₂, which is essentially in agreement with the findings of Meuwly *et al.* (1995), who reported that monocotyledonous plants such as maize preferentially accumulate GCs or des-Gly-phytochelatins after exposure to Cd.

Among the array of Hg-PC complexes detected in alfalfa, barley and maize, the SF mostly had 1:1 Hg to biothiol stoichiometry, as described in *B. chinensis* (Chen *et al.* 2009) and *O. sativa* and *M. vulgare* (Krupp *et al.* 2009). However, we also found Hg-PC complexes with higher stoichiometry such as 2:1, 2:2 and 3:3, mainly in alfalfa root SF (Table 2). Interestingly, there were several complexes that appeared in oxidized forms, such as Hg-(hPC_{3ox})₂ or Hg₂-hPC_{4ox}, that were more hydrophobic due to the loss of H, with an elution time delayed by one min relative to their reduced counterparts (Table 2). Similarly, Rellán-Álvarez *et al.* (2006b) observed that oxidized GSH and oxidized hGSH eluted approximately one minute later than GSH and hGSH. Nevertheless, the signal of the Hg-hPC_{2ox} and Hg-hPC_{3ox} was much weaker than Hg-hPC₂ or Hg-hPC₃ (Fig. 3). Chen *et al.* (2008) could detect only oxidized free PCs, whereas we could clearly find the free reduced ligands when conducting the experiment at nearly neutral pH and in the presence of reducing substances (data not shown). These precautions together with our enhanced detection capabilities by HPLC-ESI-TOFMS permitted us to detect up to 28 Hg-containing ions, particularly abundant in the alfalfa root SF (Table 2).

It is known that plants can reduce Hg²⁺ and accumulate methyl-Hg (Göthberg & Greger 2006). Spinach plants subjected to 0.2 μ M accumulated a relatively low proportion of methyl-Hg in roots and shoots (approximately 0.01% of total Hg), which suggests that some methylation may occur (Greger & Dabrowska 2010). Interestingly, a novel complex formed *in vivo* between methyl-Hg and hPC₂ was detected in the SF of alfalfa root (Table 2), albeit with a low MS signal intensity (Fig. 3). Despite the fact that we could not detect free methyl-Hg, it is feasible that methyl-Hg forms readily complexes with PCs, although

Krupp et al (2009) could not detect methyl-Hg-PCs complexes in *O. sativa* and *M. vulgare* plants treated with 45 μ M CH₃Hg.

The distribution of Hg was studied in alfalfa roots by μ -SXRF. The most intense Hg signal was located in the inner tissues of the vascular cylinder, and co-localised with S in the inner tissues (Fig. 5). Similarly, Patty *et al.* (2009) observed in Hg-treated *Spartina* spp. root tips that the inner tissues had the strongest signal. A high overlap of Hg and S localization was observed in alfalfa root, indicating that cells accumulating Hg also contained substances rich in S. Cadmium was also found to co-localize with S at the vascular bundle in *A. thaliana* roots (Isaure *et al.* 2006). X-ray fluorescence mapping of As and S in rice grains also showed that both elements were localized in the same embryo region, suggesting that As accumulated preferentially in protein and nutrient rich parts of the grain (Lombi *et al.* 2009). These studies suggest that S-containing metabolites might be important for the detoxification of toxic elements in plants.

Riddle *et al.* (2002) reported that Hg was coordinated mainly to organic S ligands using XANES in *E. crassipes*. In another study, Rajan *et al.* (2008) investigated Hg methylation in *E. crassipes*, and Patty *et al.* (2009) analyzed Hg binding in *S. foliosa* and *S. alterniflora*. In both cases, the authors concluded that most of the Hg was bound to S in a form similar to Hg-cysteine, and a smaller part (3-36%) was in a methylated-Hg form. Overall, these results are in agreement with our data because more than 79% of the Hg in alfalfa was found bound to organic S and 21% was methyl-Hg. Within the current technological limits of EXAFS and XANES, HgCys, HgGSH, HghGSH, HgPCs and HghPCs show very similar spectra because all of these compounds are bound to Hg *via* a sulfhydryl cysteine group of the biothiols and/or proteins, comparative spectral analysis that was undertaken for the first time in the present study. The more distant atoms in the molecule have limited influence on spectral properties (Beauchemin *et al.*, 2002). These results are in accordance with the detection of CH₃HgHPC₂ by HPLC-ESI-TOFMS in alfalfa root SF, as previously discussed.

The analysis of tolerance with Cd-sensitive *A. thaliana* mutants highlighted the importance of Hg-PC complexes for Hg homeostasis. Plants unable to accumulate PCs under Hg exposure, i.e. *cad2-1* and *cad1-3*, were much more sensitive, in agreement with Ha et al. (1999). The *cad2-1* mutant contains a defective γ -glutamylcysteine synthetase, which causes a severe depletion in GSH and PCs concentration upon Cd-stress (Cobbett *et al.* 1998), essentially following the same behavior as observed under Hg stress (Table 3

and Fig. 6). Interestingly, the concentration of GSH in *cad1-3* leaves was much higher under Cd and Hg stress than in Col-0, following the pattern described by Howden *et al.* (1995). However, no Hg-GSH complexes could be detected in Hg-treated *cad1-3*, in agreement with our previous observations that neither Hg-GSH nor Hg-hGSH complexes could be found in the SF of barley, maize and alfalfa roots, and with the findings in Hg-treated *B. chinensis*, *O. sativa* and *M. vulgare* (Chen *et al.* 2008; Krupp *et al.* 2009). We tested the sensitivity of our HPLC-ESI-TOFMS method by analyzing samples of *A. thaliana* Col-0 spiked with a 25 μM Hg:50 μM GSH mixture, and we observed the characteristic $[\text{Hg}(\text{GSH})_2\text{-H}]^-$ ion at m/z 813.1. The $\text{Hg}(\text{GSH})_2$ complex was not detected *in vivo*, in spite of being the endogenous GSH concentration found in 30 μM Hg-treated Col-0 leaves (257.4 nmol g^{-1} FW) 5-fold higher than the concentration of spiked GSH (Fig. 8). The absence of Hg-GSH complexes could be partially explained by the fact that PCs containing a larger number of sulfhydryl residues than GSH or hGSH will bind Hg more strongly, as Mehra *et al.* (1996) showed *in vitro* by circular dichroism and HPLC-UV/visible spectroscopy. These results imply that despite GSH accumulation under Hg stress, PCs are the biothiols that contribute to Hg detoxification in plants.

Phytochelatin synthase is synthesized by the condensation of a molecule of γ -glutamylcysteine on GSH that could contain the thiol group blocked by the transpeptidase activity of phytochelatin synthase (Vatamaniuk *et al.* 2000). Taking into account the strong affinity of Hg for thiol residues, an alteration of PCs and GSH metabolism catalysed by phytochelatin synthase might explain the restricted variety of PCs or hPCs variants found in plants exposed to Hg in comparison with those treated with Cd or As (Table 3; Cobbett & Goldsbrough, 2002, Haydon & Cobbett, 2007). In this sense, the absence of $\text{Hg}(\text{GSH})_2$ in all root SF and Hg-PC_3 in barley root SF, which should be expected in the canonical series of Hg-biothiol complexes, could also depend on the particular molecular stability (*i.e.* strength of bonds or susceptibility to oxidative modifications), and sub-cellular compartmentalization (*i.e.* vacuolar sequestration) occurring during the detoxification of Hg. Therefore, future work should be directed to characterize the dynamics of Hg-biothiol complexes formation using isotopic labeling and HPLC-ICPMS to quantify precisely their cellular concentration, information necessary to understand the contribution of each Hg species to detoxification.

In summary, plants accumulated several classes of Hg-PC complexes. Biothiols may constitute a sink of soluble Hg, although the major proportion of the toxic metal was found associated with the particulate fraction. Albeit a minor proportion of plant Hg,

Hg-PCs in the SF contribute to the ultimate fate of Hg in plants. It is plausible that Hg is mainly retained in the roots, interacting with cell wall components, and only when this barrier is overridden, soluble Hg binds to biothiols. EXAFS fingerprint fits suggest that the bulk of Hg is associated with thiols or cysteine, corresponding to cysteine-related components (probably proteins), which is in agreement with the data from μ -SXRF. Incidentally, the major structural protein in cell walls is extensin, a highly glycosylated protein which contains several residues of cysteine in a so-called Cys-rich domain (Baumberger *et al.* 2003). Therefore, as most Hg accumulates in the particulate fraction, speciation of Hg in cell wall components could be the major task for future work. The precise contribution of each compartment to the tolerance of plants is still in debate, and more sensitive and accurate techniques are needed to analyze the distribution of Hg at the subcellular level and to quantify the amount of Hg bound to the different ligands that accumulate in the plants.

ACKNOWLEDGEMENTS

The authors are grateful to Prof. C. Cobbett (University of Melbourne, Australia) and Prof. Ann Cuypers (Hasselt University, Belgium) for providing us *A. thaliana cad1-3* and *cad2-1* mutants, respectively. This work was supported by Fundación Ramón Areces (www.fundacionareces.es), the Spanish Ministry of Science and Innovation (CTM2005-04809/TECNO-REUSA, AGL2010-15151-PROBIOMET and AGL2007-61948), Comunidad de Madrid (EIADES S2009/AMB-1478), Junta Comunidades Castilla-La Mancha (FITOALMA2, POII10-0087-6458) and the Aragón Government (Group A03). The HPLC-ESI-TOFMS equipment was co-financed with EU FEDER funds. Portions of this research were carried out at the Stanford Synchrotron Radiation Lightsource, through the Structural Molecular Biology Program supported by the Department of Energy, Office of Biological and Environmental Research, and by the National Institute of Health, National Centre for Research Resources, Biomedical Technology Program. We thank Dr. FF del Campo, L Arroyo-Mendez, R Rellán-Álvarez, and S. Vazquez for technical advice and S Webb for help with μ -SXRF data collection.

REFERENCES

- Aldrich M.V., Gardea-Torresday J.L., Peralta-Videa J.R. & Parsons J.G. (2003) Uptake and reduction of Cr(VI) to Cr(III) by mesquite (*Prosopis* spp.): chromate-plant interaction in hydroponic and solid media studied using XAS. *Environmental Science Technology*, **37**, 1859–1864.
- Arruda M.A.Z. & Azevedo R.A. (2009) Metallomics and chemical speciation: towards a better understanding of metal-induced stress in plants. *Annals of Applied Biology*, **155**, 301–307.
- Baumberger N., Doesseger B., Guyot R., Diet A., Parsons R.L., Clark M.A., Simmons M.P., Bedinger P., Goff S.A., Ringli C. & Keller B. (2003) Whole-genome comparison of leucine-rich repeat extensions in *Arabidopsis* and rice. A conserved family of cell wall proteins form a vegetative and a reproductive clade. *Plant Physiology*, **131**, 1313–1326.
- Beauchemin S., Hesterberg D. & Beauchemin M. (2002) Principal component analysis approach for modeling sulfur K-XANES spectra of humic acids. *Soil Science Society America Journal* **66**, 83–91.
- Beauford W., Barber J. & Barringer A.R. (1977) Uptake and distribution of mercury within higher plants. *Physiologia Plantarum*, **39**, 261–265.
- Chen L., Yang L. & Wang Q. (2009) *In vivo* phytochelatin and Hg-phytochelatin complexes in Hg-stressed *Brassica chinensis* L. *Metallomics*, **1**, 101–106.
- Cho U.H. & Park J.O. (2000) Mercury-induced oxidative stress in tomato seedlings. *Plant Science*, **156**, 1–9.
- Clemens S. (2006) Evolution and function of phytochelatin synthases. *Journal Plant Physiology*, **163**, 319–332.
- Clemens S., Kim E.J., Neumann D. & Schroeder J.I. (1999) Tolerance to toxic metals by a gene family of phytochelatin synthases from plants and yeast. *The Embo Journal*, **18**, 3325–3333.
- Cobbett C.S., May M.J., Howden R. & Rolls B. (1998) The glutathione-deficient, cadmium-sensitive mutant, *cad2-1*, of *Arabidopsis thaliana* is deficient in γ -glutamylcysteine synthetase. *The Plant Journal*, **16**, 73–78.
- Cobbett C. & Goldsbrough P. (2002) Phytochelatin and metallothioneins: roles in heavy metal detoxification and homeostasis. *Annual Review Plant Biology*, **53**, 159–182.
- De la Rosa G., Peralta-Videa J.R., Montes M., Parsons J.G., Cano-Aguilera I. & Gardea-Torresday J.L. (2004) Cadmium uptake and translocation in tumbleweed (*Salsola kali*), a potential Cd-hyperaccumulator desert plant species: ICP/OES and XAS studies. *Chemosphere*, **55**, 1159–1168.
- Gardea-Torresday J.L., Gomez E., Peralta-Videa J.R., Tiemann K.J., Parsons J.G., Trolani H. & Yacaman M.J. (2003) Use of XAS and TEM to determine the uptake of gold and silver and nanoparticle formation by living alfalfa plants. *Proceedings of the 225th American Chemical Society National Meeting, Division of Environmental Chemistry*, **43**, 1016–1022.
- Göthberg A. & Greger M. (2006) Formation of methyl mercury in an aquatic macrophyte. *Chemosphere*, **65**, 2096–2105.
- Greger M. & Dabrowska B. (2010) Influence of nutrient level on methylmercury content in water spinach. *Environmental Toxicology and Chemistry*, **29**, 1735–1739.
- Grill E., Löffler S., Winnacker E.L. & Zenk M.H. (1989) Phytochelatin, the heavy-metal-binding peptides of plants, are synthesized from glutathione by a specific γ -glutamylcysteine dipeptidyl transpeptidase (phytochelatin synthase) *Proceedings of the National Academy of Sciences of the United States of America*, **86**, 6838–6842.
- Ha S.B., Smith A.P., Howden R., Dietrich W.M., Bugg S., O'Connell M.J., Goldsbrough P.B. & Cobbett C.S. (1999) Phytochelatin synthase genes from *Arabidopsis* and the yeast *Schizosaccharomyces pombe*. *The Plant Cell*, **11**, 1153–1164.

- Hall J.L. (2002) Cellular mechanisms for heavy metal detoxification and tolerance. *Journal Experimental Botany*, **52**, 631–640.
- Haydon M.J. & Cobbett C.S. (2007) Transporters of ligands for essential metal ions in plants. *New Phytologist*, **174**, 499–506.
- Howden R., Goldsbrough P.B., Andersen C.R. & Cobbett C.S. (1995) Cadmium-sensitive, *cad1* mutants of *Arabidopsis thaliana* are phytochelatin deficient. *Plant Physiology*, **107**, 1059–1066.
- Iglesia-Turiño S., Febrero A., Jauregui O., Caldelas C., Araus J.L. & Bort J. (2006) Detection and quantification of unbound phytochelatin 2 in plant extracts of *Brassica napus* grown with different levels of mercury. *Plant Physiology*, **142**, 742–749.
- Isaure M.P., Fayard B., Sarret G., Pairis S. & Bourguignon J. (2006) Localization and chemical forms of cadmium in plant samples combining analytical electron microscopy and X-ray spectromicroscopy. *Spectrochimica Acta Part B*, **61**, 1242–1252.
- Kim C.S., Brown G.E. & Rytuba J.J. (2000) Characterization and speciation of mercury-bearing mine waste using X-ray absorption spectroscopy. *Science of the Total Environment*, **261**, 157–168.
- Krupp E.M., Milne B.F., Mestrot A., Meharg A.A. & Feldmann J. (2008) Investigation into mercury bound to biothiols: structural identification using ESI-ion-trap MS and introduction of a method for their HPLC separation with simultaneous detection by ICP-MS and ESI-MS. *Annals of Bioanalytical Chemistry*, **390**, 1753–1764.
- Krupp E.M., Mestrot A., Wielgus J., Meharg A.A. & Feldmann J. (2009) The molecular form of mercury in biota: identification of novel mercury peptide complexes in plants. *Chemical Communications*, **28**, 4257–4259.
- Leonard T.L., Taylor G.E. Jr, Gustin M.S. & Fernandez G.C.J. (1998) Mercury and plants in contaminated soils: uptake, partitioning and emission to the atmosphere. *Environmental Toxicology Chemistry*, **17**, 2063–2071
- Lombi E., Scheckel K.G., Pallon J., Carey A.M., Zhu Y.G. & Meharg A.A. (2009) Speciation and distribution of arsenic and localization of nutrients in rice grains. *New Phytologist*, **184**, 193–201.
- Lombi E. & Susini J. (2009) Synchrotron-based techniques for plant and soil science: opportunities, challenges and future perspectives. *Plant and Soil*, **320**, 1-35.
- Loscos J., Naya L., Ramos J., Clemente M.R., Matamoros M.A. & Becana M. (2006) A reassessment of substrate specificity and activation of phytochelatin synthases from model plants by physiologically relevant metals. *Plant Physiology*, **140**, 1213–1221.
- Lozano-Rodríguez E., Hernández L.E., Bonay P. & Carpena-Ruiz R.O. (1997) Distribution of cadmium in shoot and root tissues of maize and pea plants: physiological disturbances. *Journal of Experimental Botany*, **48**, 123–128.
- Mehra R.K., Miclat J., Kodati V.R., Abdullah R., Hunter T.C. & Mulchandani P. (1996) Optical spectroscopic and reverse-phase HPLC analyses of Hg(II) binding to phytochelatin. *Biochemical Journal*, **314**, 73–82.
- Meuwly P., Thibault P., Schwan A.L. & Rauser W.E. (1995) Three families of thiol peptides are induced by cadmium in maize. *The Plant Journal*, **7**, 391–400.
- Nriagu J.O. (1990) Global metal pollution. *Environment*, **32**, 7–33.
- Ortega-Villasante C., Rellán-Álvarez R., del Campo F.F., Carpena-Ruiz R.O. & Hernández L.E. (2005) Cellular damage induced by cadmium and mercury in *Medicago sativa*. *Journal of Experimental Botany*, **56**, 2239–2251.
- Ortega-Villasante C., Hernández L.E., Rellán-Álvarez R., del Campo F.F. & Carpena-Ruiz. (2007) Rapid alteration of cellular redox homeostasis upon exposure to cadmium and mercury in alfalfa seedlings. *New Phytologist*, **176**, 96–107.

- Patty C., Barnett B., Mooney B., Kahn A., Levy S., Liu Y.J., Pianetta P. & Andrews J.C. (2009) Using X-ray microscopy and Hg L-3 XANES to study Hg binding in the rhizosphere of *Spartina* cordgrass. *Environmental Science Technology*, **43**, 7397–7402.
- Pickering I.J., Wright C., Bubner B., Ellis D., Persans M.W., Yu E.Y., George G.N., Prince R.C. & Salt D.E. (2003) Chemical form and distribution of selenium and sulphur in the selenium hyperaccumulator *Astragalus bisulcatus*. *Plant Physiology*, **131**, 1460–1467.
- Punshon T., Guerinot M.L. & Lanzirotti A. (2009) Using synchrotron X-ray fluorescence microprobes in the study of metal homeostasis in plants. *Annals of Botany*, **103**, 665–672.
- Rajan M., Darrow J., Hua M., Barnett B., Mendoza M., Greenfield B.K. & Andrews J.C. (2008) Hg L3 XANES study of mercury methylation in shredded *Eichhornia crassipes*. *Environmental Science Technology*, **42**, 5568–5573.
- Rauser W.E. & Meuwly P. (1995) Retention of cadmium in roots of maize seedlings. *Plant Physiology*, **109**, 195–202.
- Rellán-Álvarez R., Ortega-Villasante C., Álvarez-Fernández A., del Campo F.F. & Hernández L.E. (2006a) Stress responses of *Zea mays* to cadmium and mercury. *Plant and Soil*, **279**, 41–50.
- Rellán-Álvarez R., Hernández L.E., Abadía J. & Álvarez-Fernández A. (2006b) Direct and simultaneous determination of reduced and oxidized glutathione and homogluthathione by liquid chromatography electrospray/mass spectrometry in plant tissue extracts. *Analytical Biochemistry*, **356**, 254–264.
- Riddle S.G., Tran H.H., Dewitt J.G. & Andrews J.C. (2002) Field, laboratory, and X-ray absorption spectroscopic studies of mercury accumulation by water hyacinths. *Environmental Science Technology*, **36**, 1965–1970.
- Salt D.E., Prince R.C. & Pickering I.J. (2002) Chemical speciation of accumulated metals in plants: evidence from X-ray absorption spectroscopy. *Microchemical Journal* **71**, 255–259.
- Sharma S.S. & Dietz K.J. (2006) The significance of amino acids and amino acid-derived molecules in plant responses and adaptation to heavy metal stress. *Journal of Experimental Botany*, **57**, 711–726.
- Suszcynsky E.M. & Shann J.R. (1995) Phytotoxicity and accumulation of mercury in tobacco subjected to different exposure routes. *Environmental Toxicology Chemistry*, **14**, 61–67.
- Schützendübel A. & Polle A. (2002) Plant responses to abiotic stresses: heavy metal-induced oxidative stress and protection by mycorrhization. *Journal of Experimental Botany*, **53**, 1351–1365.
- Sobrino-Plata J., Ortega-Villasante C., Flores-Cáceres M.L., Escobar C., Del Campo F.F. & Hernández L.E. (2009) Differential alterations of antioxidant defenses as bioindicators of mercury and cadmium toxicity in alfalfa. *Chemosphere*, **77**, 946–954.
- Valega M., Lima A.I.G., Figueira E.M.A.P., Pereira E., Pardal M.A. & Duarte A.C. (2009) Mercury intracellular partitioning and chelation in a salt marsh plant, *Halimione portulacoides* (L.) Aellen: Strategies underlying tolerance in environmental exposure. *Chemosphere*, **74**, 530–536.
- Van Assche F. & Clijsters H. (1990) Effects of metals on enzyme activity in plants. *Plant Cell, and Environment*, **13**, 195–206.
- Vatamaniuk O.K., Mari S., Lang A., Chalasani S., Demkiv L.O. & Rea P. (2004) Phytochelatin synthase, a dipeptidyl transferase that undergoes multisite acylation with gamma-glutamylcysteine during catalysis. Stoichiometric and site-directed mutagenic analysis of AtPCS1-catalyzed phytochelatin synthesis. *Journal of Biological Chemistry*, **279**, 22449–60.
- Vatamaniuk O.K., Mari S., Lu Y.P. & Rea P.A. (1999) AtPCS1, a phytochelatin synthase from *Arabidopsis*: Isolation and *in vitro* reconstitution. *Proceedings of the National Academy of Sciences of the United States of America*, **96**, 7110–7115.
- Vatamaniuk O.K., Mari S., Lu Y.P. & Rea P.A. (2000) Mechanism of heavy metal ion activation of phytochelatin (PC) synthase - Blocked thiols are sufficient for PC synthase-catalyzed

transpeptidation of glutathione and related thiol peptides. *Journal of Biological Chemistry*, **275**, 31451-31459.

Webb S.M. (2005) Sixpack: A graphical user interface for XAS analysis using IFEEF IT. *Physica Scripta*, **115**, 1011–1014.

Zhang Z.C., Chen B.X. & Qiu B.S. (2010) Phytochelatin synthesis plays a similar role in shoots of the cadmium hyperaccumulator *Sedum alfredii* as in non-resistant plants. *Plant, Cell and Environment*, **33**, 1248-1255.



CHAPTER 4

CHAPTER 4

Mercury localization and speciation in hydroponic culture and natural plants**ABSTRACT**

The distribution and speciation of mercury (Hg) in roots, stems and leaves of plants was studied by X-ray absorption spectroscopy using a synchrotron light source. X-Ray Absorption Fine Structure (EXAFS) permitted the determination of Hg speciation by comparing the Hg L₃ edge EXAFS spectra of the samples with several reference ligands known to bind to this metal. We studied two kinds of plant materials, i) *Medicago sativa* treated in a pure hydroponic system with 30 μM HgCl₂; and ii) *Marrubium vulgare* collected in a naturally polluted soil in the Almadén Hg-mining area (Ciudad Real, Spain). Microprobe synchrotron X-ray fluorescence (μ-SXRF) showed that Hg accumulated principally at the root tip, whereas at the maturation zone Hg localized in the inner tissues. These results suggest that the root tip might be most permeable area to Hg. In stems and leaves Hg moved apparently following the vascular tissues. Speciation analysis showed that a high proportion of Hg was found associated with cysteine containing ligands, possibly biothiols and/or proteins. Transmission electron microscopy showed that dense particles accumulated in the cell walls of epidermal and vascular cells in root sections of *M. sativa*. In *M. vulgare* plants most Hg was accumulated in the epidermis of roots. XANES analysis indicated that most Hg was in an inorganic form (HgS_{red}) or cinnabar, indicating that Hg in natural samples would be less available, and it is possible that most Hg found in these plants occurred as adhered particles of soil or dust. The localization of some nutrients was also studied by μ-SXRF, showing that copper (Cu) was the nutrient that co-localized with Hg. On the other hand, iron (Fe) and calcium (Ca) content decreased, possibly due to alterations in their uptake in Hg stressed plants.

Key-words: mercury, SXRF, EXAFS, micro-tomography, X-ray absorption spectroscopy.

Abbreviations: a.s.l. above sea level

INTRODUCTION

Mercury and most of its compounds are highly toxic to humans and ecosystems, appearing naturally (i.e. of lithological origin) or as an introduced contaminant. Mercury is considered as a global pollutant because it is highly mobile and extremely persistent in the environment. The bioaccumulation and biomagnification properties of Hg lead to its concentration in the food chain, which can pose a serious threat to several human populations, as occurred in the Minamata disaster (Naito, 2008). Therefore, many national and international agencies and organizations, such as the United Nations Environment Programme, have targeted Hg for strict extraction, emission and trade controls (UNEP, 2011). In the environment, Hg can be found in several metal ores (e.g. cinnabar; HgS); as ions in solution forming inorganic (Hg^+ , Hg^{2+}) and organic (R-Hg^{2+}) salts; or in the monatomic metallic form (Hg^0). The chemical speciation of Hg affects the availability, and subsequently, the internal distribution in the organism and toxicity (UNEP, 2011). Therefore, the characterisation of Hg localization, concentration, and chemical speciation will provide valuable information about the detoxification pathways in plants (Punshon et al., 2009).

Several quantitative studies have shown rather conclusively that most of the Hg taken up by plants accumulated in roots, as measured by atomic absorption spectrophotometry (Du et al., 2005; Millán et al., 2006; Skinner et al., 2007; Esteban et al., 2008; Sierra et al., 2009). Transport and accumulation of metals in plants are regulated by several physiological processes involving transport of metals across the plasma membrane of root cells, xylem loading and translocation from root to shoot, detoxification and sequestration of metals at the vacuole (Hall, 2002). However, there is limited experimental data are currently available regarding Hg transport through plant membranes. It was described that the inorganic form of Hg (Hg^{2+}) is less permeable to plasma membranes, which would be the first cellular component affected; whereas methyl-Hg would permeate and affect cell organelles (Godbold and Huttermann, 1986). To this respect, it is well known the high affinity of Hg cations for sulfhydryl groups (-SH), contained in many proteins and important metabolites like glutathione (GSH), which might be critical to understand the toxic effects of Hg in plants (Clarkson, 1972). This chemical property may impose limitations in the mobility of Hg within plant tissues, as it might tend to bind different proteins located in the apoplast and plasma membrane, where Hg accumulates (Beauford et al., 1977).

Mercury absorption by plants may occur also *via* leaves possibly after surface adsorption of water soluble Hg forms and particulate Hg (Lindberg et al., 1992; Rea et al., 2001) or Hg⁰ uptake through the stomata (Iverfeldt 1991; Munthe et al., 1995). However, the mechanisms involved in atmospheric Hg uptake by leaves are not completely understood. Recent studies suggested that nonstomatal uptake was an important pathway by which Hg⁰ could be incorporated into leaf tissue (Stamenkovic and Gustin, 2009), so not all the atmospheric Hg is entirely controlled by stomata. An unspecific process, possible of biochemical nature, was proposed to be a principal limitation for the Hg⁰ uptake into leaves (Browne and Fang, 1983). Atmospheric Hg (Hg⁰) could diffuse through the cuticle similar to volatile lipophilic compounds (i.e. dimethyl-Hg; Liu, 2007).

In any case, more information is needed to improve our current knowledge. In particular, little is known regarding the distribution and the accumulation of Hg within the plant. Spatially resolved synchrotron source X-ray spectrometry can provide key knowledge about control uptake, transport and storage of essential and non-essential metals by plants (McNear et al., 2005; Isaure et al., 2006). SXRF have been demonstrated as potent analytical tool for localisation of metals in plant tissues since late 1990s. So far, there are only two studies focused on the localization of Hg at the tissues and cellular levels: Patty et al. (2009) used μ -SXRF mapping and TXM image in *Spartina* spp. and showed that the highest concentration of Hg in the root was localized in the tip area and in the inner tissues. At the cellular level, De Filippies and Pallaghy (1975) used scanning electron microscope (SEM) coupled to energy dispersive X-ray analysis (EDXA) to localize Hg in *Hordeum vulgare* root cells, revealing that Hg was localized almost entirely within the nucleus.

With respect to Hg speciation, X-ray absorption spectroscopy (XAS) analysis has been used to identify Hg coordination environment in plants. Riddle et al. (2002) concluded that Hg was bound ionically to oxygen ligands in roots, most likely to carboxylate groups corresponding to organic acid, and covalently to sulfur groups in shoot. However, Rajan et al. (2008) and Patty et al. (2009) found that Hg was mostly bound to S-containing ligands. This was indeed the case in alfalfa roots, where most Hg was found associated with Cys residues of proteins or phytochelatin (Carrasco-Gil et al. 2011).

The aim of this work was to study the localization and speciation of Hg in *Medicago sativa* and *Marrubium vulgare* grown under hydroponic and natural conditions, respectively. We used Synchrotron X-ray Fluorescence Microprobe (μ -SXRF) for Hg localization and Extended X-Ray Absorption Fine Structure (EXAFS) for Hg speciation; combination of

techniques used successfully to understand the dynamics of metals in plants used for phytoremediation (Gardea-Torresday et al., 2005). Transmission Electron Microscopy (TEM) analysis was also used to study Hg accumulation in *M. sativa* roots at the subcellular scale.

MATERIALS AND METHODS

Plant material

Alfalfa (*Medicago sativa* cv. Aragon) seedlings were germinated and grown in a pure hydroponic system (Fig. 1) with continuous aeration (Ortega-Villasante et al., 2005). The plants grew for 12 days in a controlled environment chamber and were then treated with 30 μ M Hg (as HgCl₂) for 7 days following the conditions described by Carrasco-Gil et al. (2011). Once collected, plants were rinsed several times with 10 mM Na₂ EDTA solution to remove superficial Hg. Another portion of plants were frozen under -80°C for EXAFS analysis or freeze-drying to preserve plant structure for SXRF analysis.



Fig 1. Pure hydroponic system for *M. sativa*.

Marrubium vulgare plants were collected from an abandoned metallurgic plant located in Almadenejos village, 12 km from Almadén (Cuidad Real, Spain) where six pairs of abandoned roasting furnaces are found in ruins (Fig 2). These furnaces were used to obtain primary mercury from cinnabar. Samples were collected at three points (P2, P4 and P6, see Fig. 2A) at 20 m spacing initiating from the highest point at 501 m a.s.l. and moving down the slope to the lowest point at 486 m a.s.l. from the furnaces corresponding to areas A1, A2 and A3. All the plant samples had the same age and

biomass in order to compare the results. This plant specie was chosen due to its dominance within the area of the abandoned metallurgic plant.

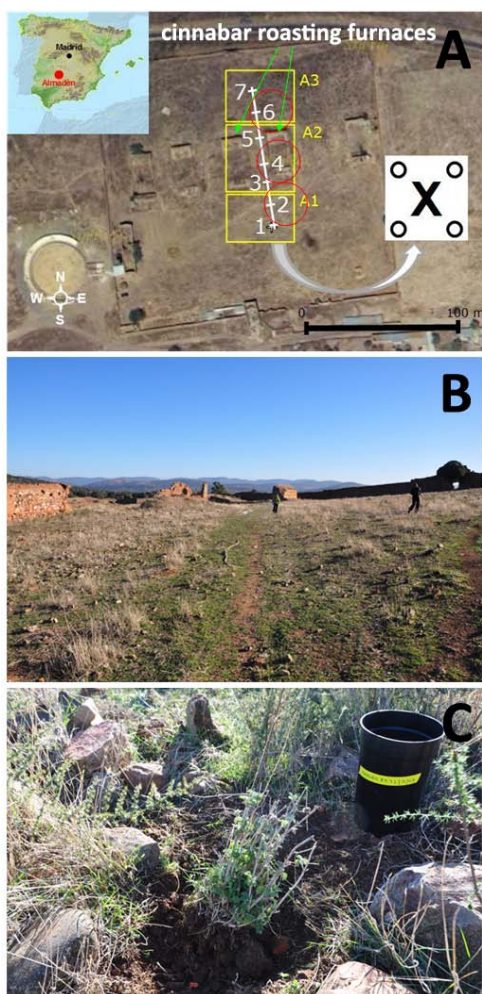


Fig. 2. Abandoned metallurgic plant located in Almadenejos (Ciudad Real, Spain). **A)** Aerial image of the experimental field plot showing the sampling points (red circles) in which the samples were collected; **B)** view of the experiment field plot; and **C)** collected *Marrubium vulgare* plants.

Mercury analysis

Plant samples were air-dried and ground to homogeneity with mortar and pestle. 100 mg of dried sample was acid digested in 2 mL of the digestion mixture ($\text{HNO}_3:\text{H}_2\text{O}_2:\text{H}_2\text{O}$, 0.6:0.4:1 v:v) in an autoclave (Presoclave-75 Selecta, Barcelona, Spain) at 120°C and 1.5 atm for 30 min (Ortega-Villasante *et al.* 2007). The digests were filtered through a polyvinylidene fluoride filter and diluted in miliRO water to 10 mL. Mercury concentration was measured using an Advanced Mercury Analyser 254 Leco (St. Joseph, Michigan, MI, USA) with a detection limit of $0.5 \mu\text{g kg}^{-1}$. Certified reference materials (CRM) were used to determine the accuracy of the measurements and validation.

Synchrotron X-ray fluorescence microprobe (μ -SXRF) and X-ray computed micro-tomography (SR- μ CT)

M. sativa and *M. vulgare* plants were analyzed by microprobe at beamline 2-3 at Stanford Synchrotron Radiation Lightsource (SSRL). μ -SXRF mapping of Hg was collected by scanning a representative intact root, stem and leaf in the microfocused beam above (12,300 eV) and below (12,250 eV) the edge of Hg sampled in $2.5 \times 2.5 \mu\text{m}$. Samples were freeze dried to preserve the tissue structure (Punshon et al. 2009). For root and stem cross section, freeze dried samples were cut to pieces of ~ 1 cm and placed in a silicon mold covered by the EPO-TEK 301-2FL resin that is a two component epoxy resin (A and B) and particularly adequate to maintain the redox state. The resin was prepared mixing A and B component in a 40.2:12.6 ratio respectively. Once the tissue pieces were embedded in the resin, silicon molds were put in the desiccator for degassing and full drying of the resin for 3 days at 24°C . After that, the pieces were taken out of the mold and thin sections ($60 \mu\text{m}$) were cut using a Leica cryo-microtome. Samples were placed in 3×3 cm Al spacers, bound with kapton tape, and stored at room temperature until analysis. The $K\alpha$ fluorescence line intensities of Hg (and other elements of interest, such as Fe, Ca, Mn, S, K and Zn) were measured with a three-element Ge detector and normalized to the incident monochromatic beam intensity. HgCl_2 powder was used as a standard material for calibration. Fluorescence microtomography data were collected as a function of a X axis position and a rotation angle using $3 \mu\text{m}$ translation step, 1° angular step and dwell times of 125 ms, resulting in a fluorescence sinogram image. Data analysis was carried out with the software package SMAK version 0.45 (Webb, 2005).

Extended X-ray absorption fine structure (EXAFS) and X-ray Absorption Near Edge Structure (XANES)

Mercury-biothiol standards were prepared in a 2:1 ratio (ligand:Hg) in Mili-Q water, mixing i) pure hPCs (hPC_2 , hPC_3 or hPC_4) (2 mM) and HgCl_2 (1 mM), ii) PCs (PC_2 , PC_3 or PC_4) (0.5 mM) and HgCl_2 (0.25 mM), and iii) GSH or hGSH (4 mM) and HgCl_2 (2 mM). The aqueous solutions of Hg-biothiol complexes were mixed with 25% v/v glycerol to prevent the formation of ice crystals. The standard mixture was stored under liquid nitrogen until analysis. Spectra from the additional standard compounds: Hg cysteine (HgCys), Hg acetate (HgAce), cinnabar (HgS red), metacinnabar (HgS black), methyl-Hg aspartate (MeHgAsp) and methyl-Hg methionine (MeHgMet) were also used for fit calculations (details can be found in Rajan *et al.* 2008). Hg-nitrate, Hg-

oxide and Hg-sulfate were purchased from Alfa Aesar's Puratronic (trace metal grade); ~15 mg reference material were diluted with ~70 mg boron nitride, mounted in a Teflon sample holder, and sealed with Kapton tape. The fresh tissue sample was ground in liquid nitrogen with acid-washed mortar and pestle, placed in Al spacers sealed with kapton tape, and stored in liquid nitrogen until analysis. A 200 μ l aliquot of the aqueous standard solution was placed in a Lucite sample holder. Samples were bound by kapton tape and stored in liquid nitrogen. Hg L₃ edge X-ray absorption spectra for the hydroponic *M. sativa* root (average of five scans) and for the Hg-biothiols standard mixtures (average of three scans) were collected at beamline 9-3 at SSRL by monitoring the Hg L _{α 1} fluorescence at 9988.9 eV. During the analysis, the samples were maintained at \approx 10 K in a liquid helium flow cryostat and positioned at 45° to the incident beam. Spectra for the hydroponic *M. sativa* stem (average of 25 scans) and leaf (average of 16 scans), and *M. vulgare* root and leaf (average of 20 scans) were collected at beamline 11-2 at SSRL under similar conditions. Calibration was accomplished by simultaneous collection of HgCl₂ with first edge inflection set to 12284.4 eV. Data analysis was carried out with the software package SixPACK version 0.63 (Webb, 2005) following a standard method that consisted of preliminary examination of fluorescence channels and energy calibration of individual scans using a smoothed first derivative, followed by averaging of scans. A linear background function was subtracted, and data were normalized to a unit step edge. To quantify the percentage of each Hg species present in alfalfa roots using the fingerprinting method, a least squares fit (LSF) was performed to fit the EXAFS (*chi*) of the experimental data to linear combinations of the above mentioned standard reference compounds, which were divided into four Hg coordination environments: inorganic sulphur bonding (Hg-S red and Hg-S black), organic sulphur bonding (Hg-PCs and Hg-Cys), oxygen-rich ligand bonding (carboxylic groups; Hg-Ace) and methyl-Hg forms (Me-Hg-Asp and Me-Hg-Met). Single-component fits to the data were carried out to exclude those contributing less than 5 %, and selected candidates of each group were fitted to get the relative proportion of Hg species. The reduced *chi*-square value (goodness of fit χ^2) provides information as to the quality of the standard fit to the spectra data (Kim et al. 2000).

Transmission X-ray Microscopy (TXM)

A cross section (60 μ M of thickness) of *M. vulgare* root was mounted in windows anchored by Kapton tape for TXM analysis. Images were obtained with the Xradia

NanoXCT full-field X-ray microscope at beamline 6-2 at SSRL, at 5.4 keV in absorption contrast.

Transmission Electronic Microscopy analysis (TEM)

Tissue samples were prepared following the procedure of vacuum-microwave combination for processing plant tissues for electron microscopy described by Giberson and Demaree (2001), with some modifications. The mature area of the fresh root, 5 cm from the tip, was cut into pieces of ~ 1 cm and placed in 2 mL Eppendorf tubes filled with 1000 μ l of fixative solution (2.5% glutaraldehyde in 50 mM sodium cacodylate buffer, pH 6). The samples were placed in a vacuum chamber for 5 h to improve the penetration of the fixative solution. Once the fixative solution was removed, the samples were rinsed with sodium cacodylate buffer three times, and dehydrated in a graded series of acetone (10, 30, 50, 70, 95, 100%), incubating the samples 30 min in each step. Dehydrated material was embedded in Spurr's resin, by incubating for 1 h in different mixtures with increased concentration of the resin (1:2, 2:1 and 1:0 resin:acetone v:v). In each embedding step, the samples were subjected to vacuum for 15 min, the the solution was changed twice. Completely embedded roots were placed in silicon molds to polymerize the resin in an oven at 70°C overnight.

RESULTS

Plant growth and Hg concentration in tissue

There was a significant inhibition of growth in roots and shoots, measured as organ length and fresh weight (Fig. 3). Also some visual symptoms of toxicity appeared, as a certain degree of leaf chlorosis (Fig. 1). The total concentration of Hg in plants treated with 30 μ M Hg was: $2,611.0 \pm 273.0$, 38.3 ± 0.45 , and 67.7 ± 0.5 μ g g^{-1} FW in roots, stems and leaves respectively. Control plants accumulated, as expected, much less Hg: < 0.1 , 2.0 ± 0.5 , and 8.0 ± 2.2 μ g g^{-1} FW in roots, stems and leaves respectively. It should be noted that the concentration of Hg measured in control roots was below the detection limit of the equipment used (< 0.05 μ g g^{-1} FW).

The total Hg concentration of *M. vulgare* natural plants increased from sampling point P2 to point P6, following the concentration gradient found in soil samples due to cinnabar furnace proximity (data not shown). Mercury concentration in roots was positively correlated to Hg concentration in shoots in samples collected in points P4 and P6, which was approximately three times higher than in shoot (Table 1). These plants did not displayed visual symptoms of toxicity (Fig. 2C).

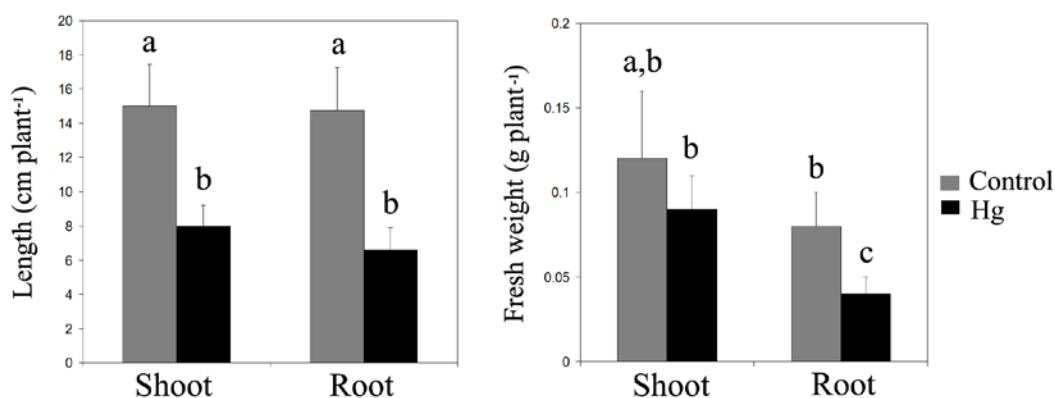


Fig 3. Length (cm plant⁻¹) and fresh weight (g plant⁻¹) of shoots and roots of three-week-old *M. sativa* grown in a pure-hydroponic system, treated with 0 μ M (control) and 30 μ M Hg for 7 days. Data are average of four independent assays (\pm SD). Different letters denote significant differences between treatments at $p < 0.05$.

Table 1. Total Hg concentration (mg kg⁻¹ DW) in leaf and root and ratio between Hg concentration in leaf and Hg concentration in root of *Marrubium vulgare* collected in a abandoned metallurgical plant in three different points (P2, P4 and P6)

	P2	P4	P6
Leaf	32.8 \pm 1.0	60.7 \pm 8.7	183.4 \pm 7.1
Root	36.7 \pm 0.7	203.5 \pm 4.7	501.9 \pm 3.2
Ratio	0.89	0.29	0.36

Localization of Hg and other elements in *Medicago sativa*

The spatial localization of Hg within the plant tissue was studied in root, stem and leaf of *M. sativa* plants using μ -SXRF. In roots, the most intense Hg signal was found in the inner tissue, at the vascular cylinder, and at the epidermis as observed in Fig. 4A. This spatial distribution was confirmed by transversal micro-tomography (SR- μ CT) imaging (Fig. 4B), which showed clearly that the strongest Hg signal was detected in the vascular cylinder. In addition, a third area with slightly less signal intensity was observed in the SR- μ CT image, which corresponded possibly with the endodermis.

A cross section of stems showed that Hg was located in circular areas of Hg around of the stem corresponding with the vascular bundles (Fig. 5A). In the stem, xylem and phloem packed together in these bundles, but the μ -SXRF resolution is not good enough to discriminate between phloem (outer layers of cells) and xylem (inner layers). A longitudinal image illustrated that the most intense Hg signal was found again in the vascular system (Fig. 5C). In leaves Hg accumulated in the veins (Fig. 5F). Interestingly,

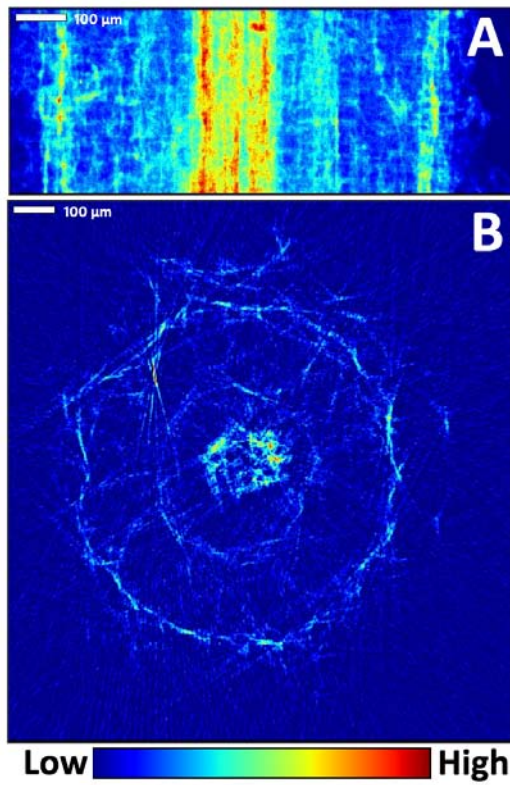


Fig 4. Hg distribution in three-week-old *M. sativa* primary root treated with 30 μM Hg for 7 days in a pure-hydroponic system using $\mu\text{-SXRF}$. **A)** Elemental 2D mapping of Hg distribution from a longitudinal section taken at 2.5 μm steps. **B)** micro-tomography of the same root showing a transversal analysis of Hg distribution.

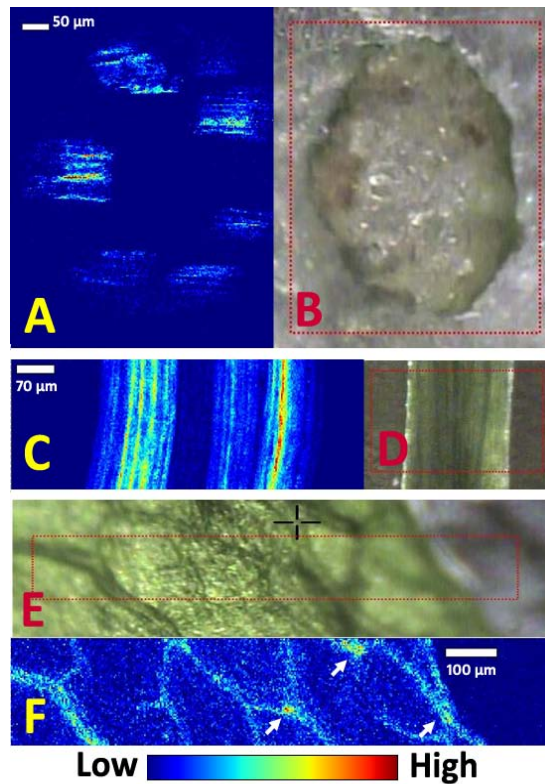


Fig 5. XRF Hg map (**A,C,F**) and visible (**B,D, E**) images of three-week-old *M. sativa* shoot treated with 30 μM Hg for 7 days in a pure-hydroponic system. **A,B)** Transversal 60 μm thick stem section. **C, D)** longitudinal image of the same stem; **E, F)** leaf. The red square in the optical images shows the region selected for XRF imaging.

there was some high Hg signal in little spots along the ribbing of the leaf (indicated by white narrows).

For a better understanding of root Hg and translocation in *M. sativa* plants, new $\mu\text{-SXRF}$ analysis was performed in different parts of the root tip in plants exposed to 30 μM Hg for different intervals. Results showed that in primary root tip (Fig. 6B), the most intense Hg signal was located in the region just behind the meristem, where cells are under division and elongation. Hg signal decayed in tissues located farther from the tip, but a certain high intensity signal was observed at the vascular cylinder. Therefore, more mature and differentiated cells accumulated less Hg (Fig. 4A). This Hg distribution was also observed in the secondary root tips, and also showed an intense Hg signal in the connection between primary and secondary root at the vascular cylinder (white arrows in Figs. 6A, 6C, 6D). Interestingly, Hg did not accumulate at the root cap (or calyptra) formed of dead cells (large white arrow, Fig. 6B). We also tested distribution of Hg in three-day-old *M. sativa* seedlings after a short-term exposure to 30 μM Hg for 5h and 24 h. XRF scanning showed that in the first hours Hg seemed to be distributed at the epidermis, as there was a intense signal over the root tip surface (Fig. 7A). However, Hg started to penetrate to the inner

tissues after 24 hours, and more intense signal was detected following the pattern described previously (Fig. 7B).

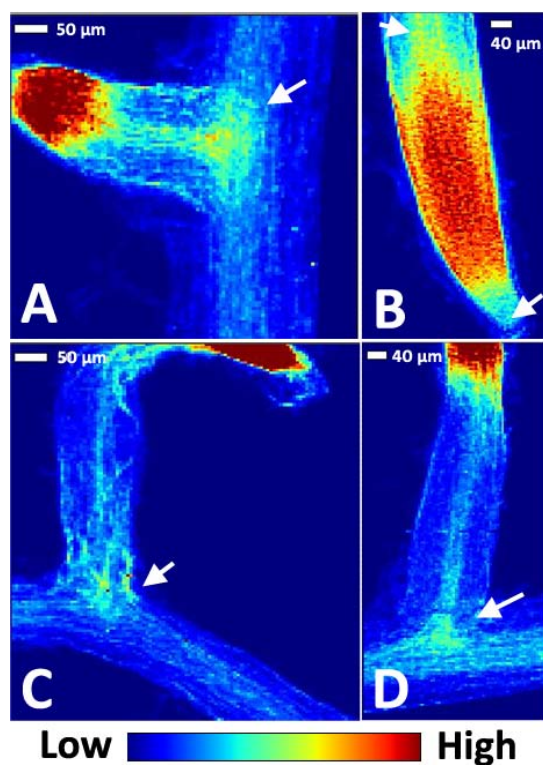


Fig. 6. μ -SXRF analysis to visualize distribution of Hg in three-week-old *M. sativa* root tips treated with 30 μ M Hg for 7 days in a pure-hydroponic system using. 2D mapping of Hg distribution in secondary root tips (**A**, **C**, **D**) and in a primary root tip (**B**).

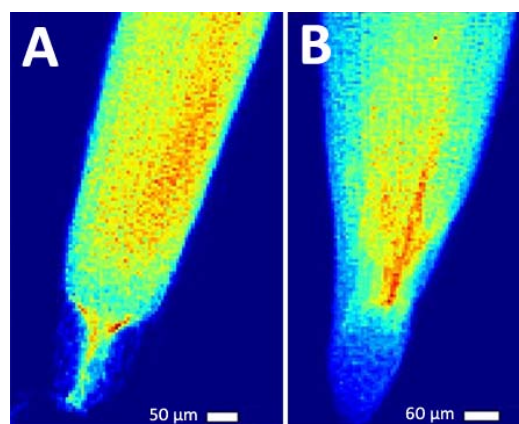


Fig. 7. Hg X-ray fluorescence (XRF) elemental map of three-day-old *M. sativa* primary root treated with 30 μ M Hg for 5 h (**A**) and 24 h (**B**).

The distribution of several essential nutrients: iron (Fe), zinc (Zn), calcium (Ca), copper (Cu), manganese (Mn) and potassium (K), was studied in alfalfa plants exposed to 30 μ M Hg. The distribution of these nutrients can be affected by Hg, as it is feasible that Hg entry plant cells through transporters or channels involved in their uptake, as has been shown for Cd (Küpper and Kochian, 2010). μ -SXRF mapping showed that Fe was localized in the external part of the root (Figs. 8A and 8B). However, Zn and Ca were distributed in the inner tissue at the vascular cylinder, and co-localized in part with an intense Hg signal. This information was confirmed with the μ -SXRF mapping of a cross section mature primary root (Fig. 8C). Moreover, X-ray fluorescence analysis in *M. sativa* root revealed that in the presence of Hg, the content of some nutrients like Fe, Mn, K and Ca were altered (Table 2). Plants treated with 30 μ M Hg suffered an increase in Fe counts s^{-1} , but a decrease in Mn and K, in different areas of the *M. sativa* root. Exposure to Hg also led

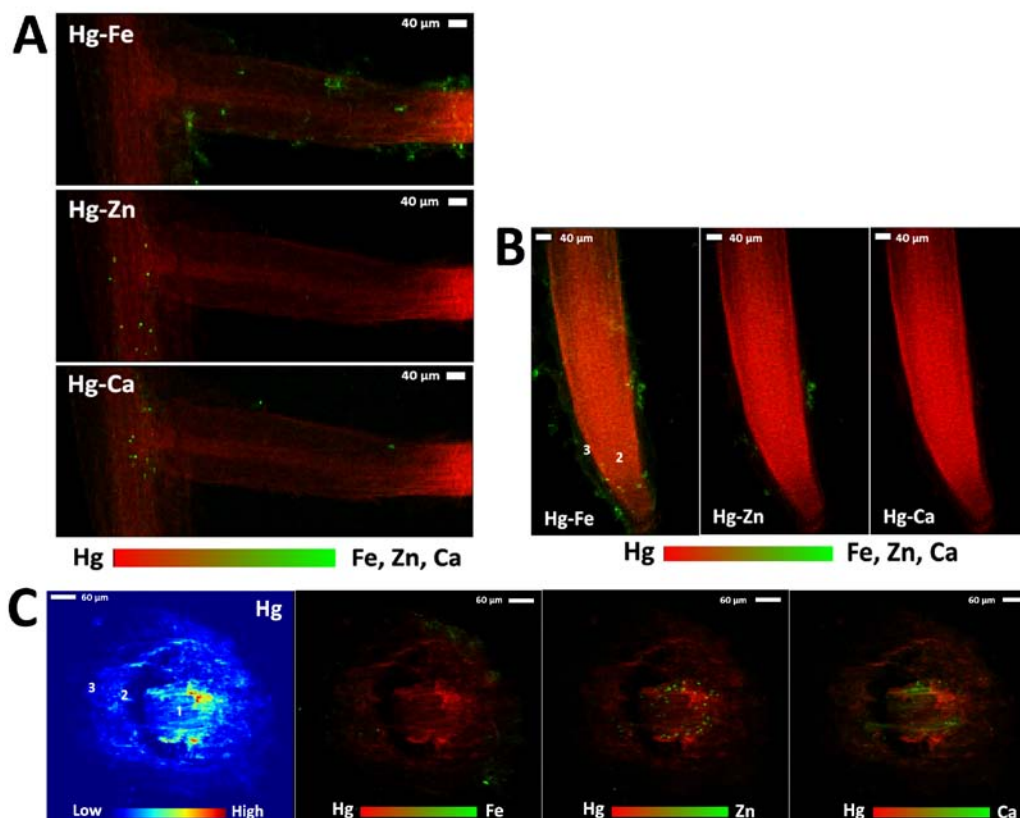


Fig. 8. X-ray fluorescence map of Hg (in red) overlapping with iron (Fe), zinc (Zn) and calcium (Ca) (in green) in emerged secondary root (**A**), a primary root tip (**B**) and a cross-section of a mature primary root (**C**), of three-week-old *M. sativa* root treated with 30 μM Hg for 7 days. Areas of the root were numbered to identify vascular cylinder (**1**), endodermis (**2**), and epidermis (**3**).

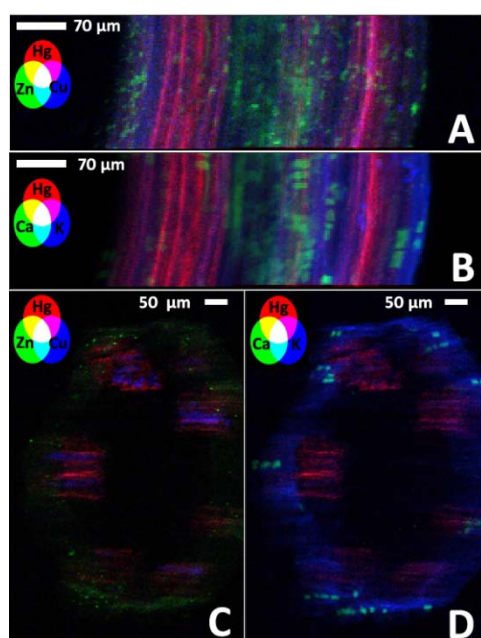


Fig. 9. **A, B** X-ray fluorescence map of Hg (in red) overlapping with zinc (Zn, in green), calcium (Ca, in green), copper (Cu, in blue), and potassium (K, in blue) in a stem longitudinal section; **C, D** Stem cross section (60 μm thickness), of three-week-old *M. sativa* treated with 30 μM Hg for 7 days.

to a notable increase in Ca counts s^{-1} in the root tip (Table 2). In stems, Zn, Ca and K were localized in the external part; possibly at epidermis, and also in the internal pith. However, Cu was localized with Hg at the vascular cylinder but they did not overlap (Fig. 9). Iron

signal was low to get its map of distribution. In leaves, Mn and K were co-localized with Hg in the veins, but Ca and Fe were distributed in spots around of the main veins and along the leaf area, respectively (Fig. 10).

Table 2. Maximum counts s^{-1} of Mn, K, Fe and Ca of the intensities extracted from each pixel in μ -SXRF mapping analysis of different areas of three-week-old *M. sativa* root treated with 0 μ M (control) and 30 μ M Hg for 7 days.

counts s^{-1}	Mature root		Emerged secondary root		Root tip	
	Control	30 μ M Hg	Control	30 μ M Hg	Control	30 μ M Hg
Mn	319	13	914	12	53	12
K	446	108	825	146	794	89
Fe	182	676	371	734	117	764
Ca	86	128	135	164	106	1106

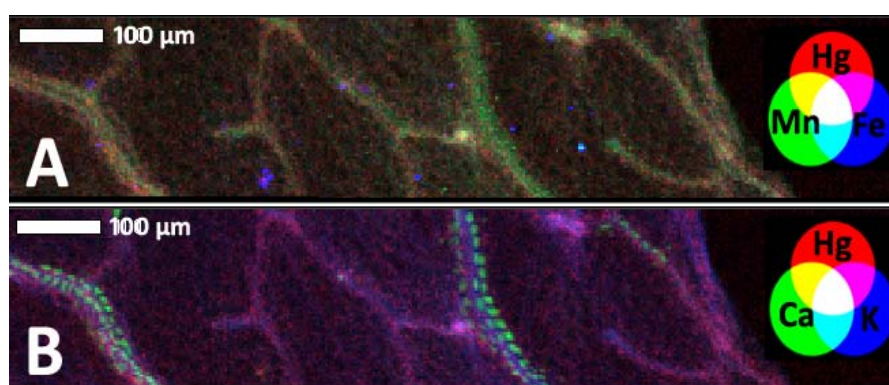


Fig. 10. X-ray fluorescence (XRF) map of Hg (in red) overlapping with manganese (Mn, in green) and iron (Fe, in blue) A), and calcium (Ca, in green), and potassium (K, in blue) B) in a leaf of three-week-old *M. sativa* treated with 30 μ M Hg for 7 days in a pure-hydroponic system.

Transmission electronic microscopy (TEM) analysis was performed on *M. sativa* root samples treated with 0 (control) and 30 μ M Hg for 7 days in three-week-old plants to locate Hg at the subcellular level. Under Electron-dense grains resulting from the metal presence were visible, especially on root treated with Hg (Fig. 11), in comparison with root plants grown in control conditions (Fig. 12). Distinctive granular deposits were observed in the intercellular space, in the cortical tissue of roots treated with 30 μ M Hg (Fig. 11B, C, D). Likewise, intracellular granular deposits in the cortical parenchyma cell were observed (Fig. 11E, F). However, Hg accumulation seemed to be symplastic in the cortical parenchyma cell in secondary root tip (Fig. 11G, H, I). Moreover, Hg was precipitated in the cytoplasm as large deposits located near the cell walls in the endodermis (Fig. 11J) and in the xylem (Fig. 11L, M, N). In addition, granular deposits were present in the intracellular space in the xylem (Fig. 11N). On the other hand, the root samples grown without Hg, did not showed distinctive deposits in none of these tissues (Fig. 12).

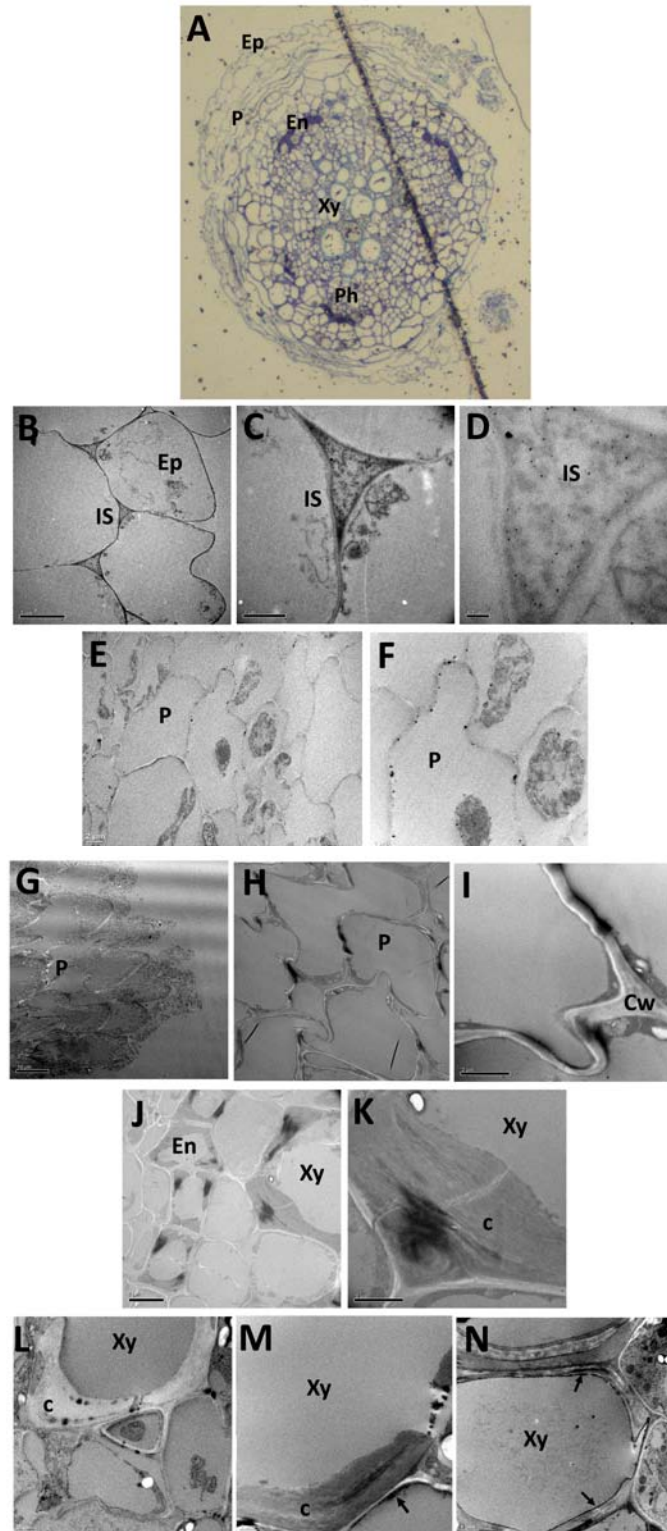


Fig. 11. (A) Visible microscopy to show typical transversal root section subjected to transmission electron microscopy study. (B-N) of a cross section *M. sativa* primary root treated with 30 μ M Hg for 7 days. TEM images show granular deposits corresponding to Hg accumulation in the intercellular space between epidermis and cortex (B, C, D); in the cortical symplast (E, F); cortical symplast of secondary root tip (G, H, I), in the cytoplasm near the cell wall in the endodermis (J) and in the xylem (L, M, N). c, cytoplasm; Cw, cell wall; En, endodermis; Ep, epidermis; IS, intercellular space; P, parenchyma cortical; Ph, phloem; Xy, xylem.

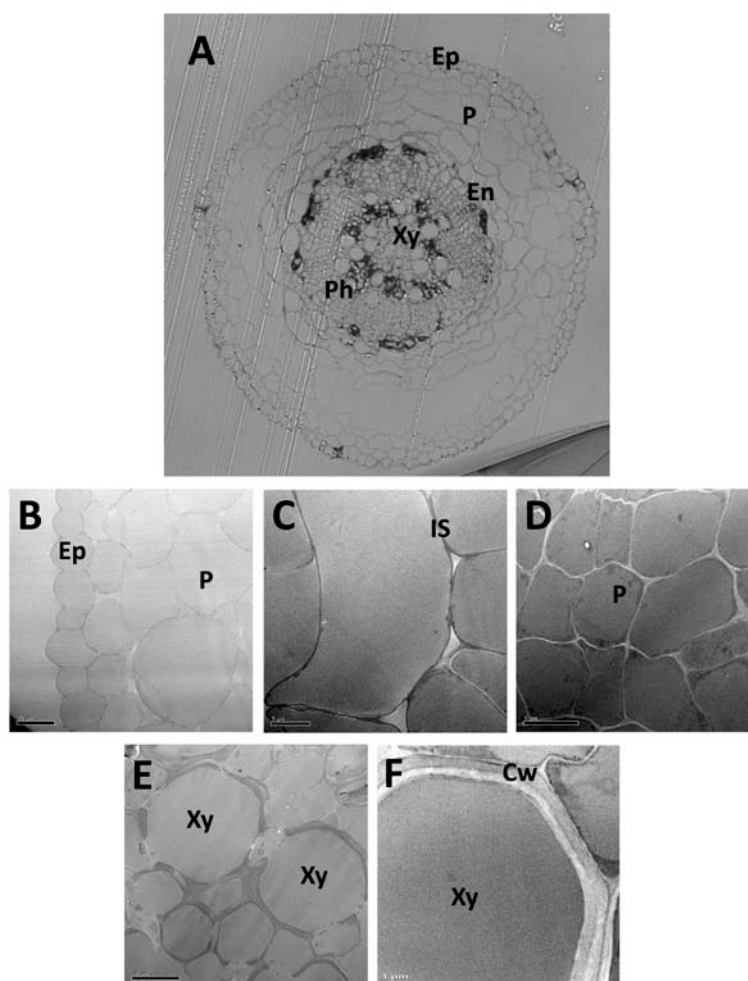


Fig. 12. (A) Visible microscopy of a cross section *M. sativa* primary root control used for transmission electron microscopy (B-F). TEM images show the absence of granular deposits in the different subcellular compartments studied: intercellular space between epidermis and cortex (B, C), cortical symplast (D), and xylem (E, F). Abbreviations are as shown in Fig. 11.

Mercury speciation in *Medicago sativa*

The chemical form of Hg in the bulk of *M. sativa* root, stem and leaf was investigated by Hg L₃-edge EXAFS spectroscopy. We selected spectrum references of putative ligands that would represent the most probable Hg coordination environments in plants: biothiols, (cysteine bonding), organic acids (oxygen-rich bonding), methyl-Hg (carbon bonding), and inorganic Hg (i.e. sulphides-Hg forms). A single LSF was performed in each standard mixture to exclude those standard compounds contributing less than 5 % in the fit. These preliminary measurements showed that the spectra of the different HgPCs, and also the HgCys complexes were indistinguishable from each other at the noise-to-signal ratio of the natural samples. Therefore, we opted to use HghPC₂ and HgCys as representative standards for Hg-biothiol or Hg-organic sulphur (including proteins) complexes. Moreover, the mayor contribution in the first single LSF was for HgAce as

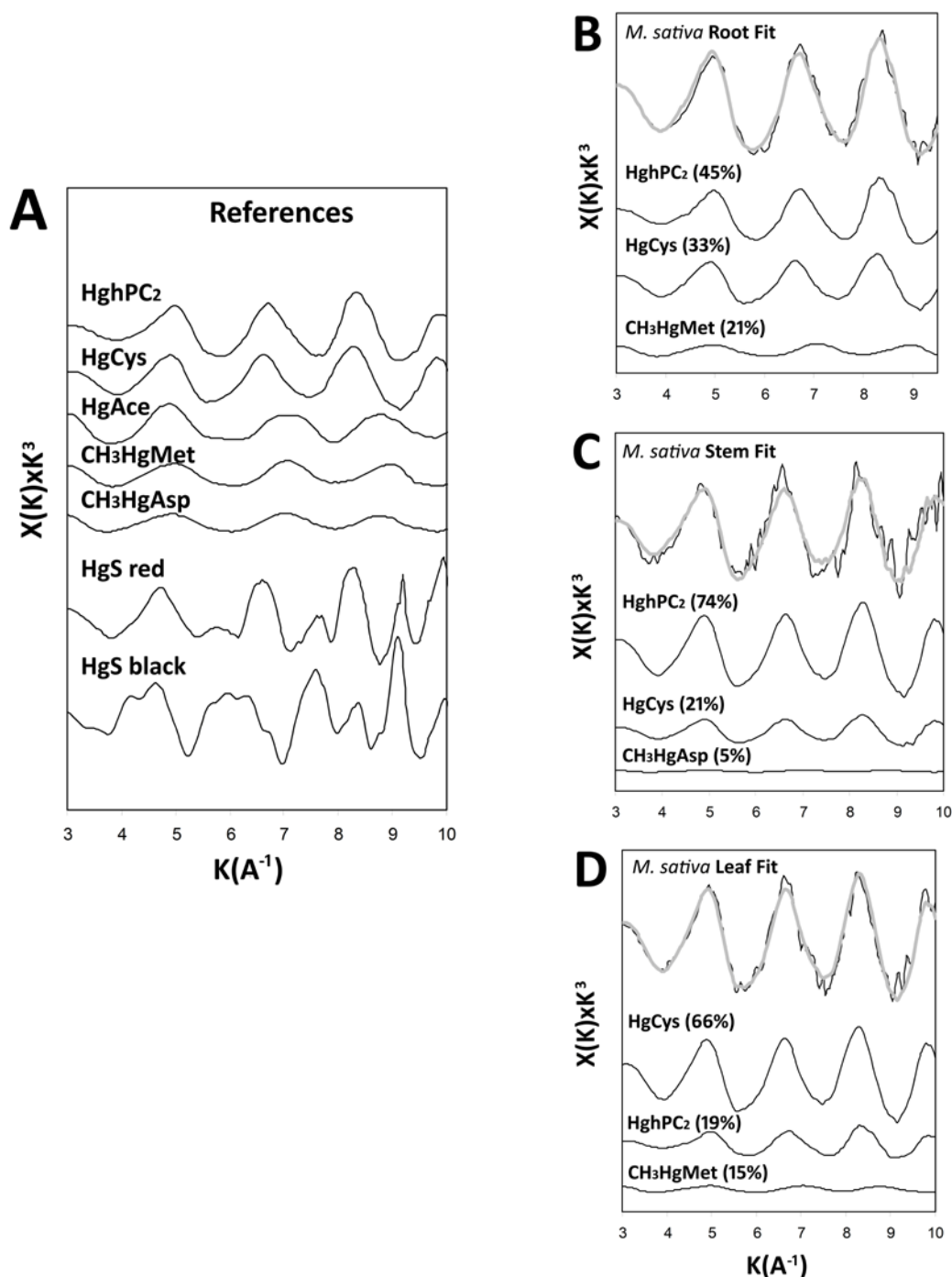


Fig. 13. Hg L₃ EXAFS spectra of the references used for the least square fitting of the samples (A) and linear fitting results for root (B), stem (C), and leaf (D) of three-week-old *M. sativa* treated with 30 μM Hg, showing the Hg L₃ EXAFS K₃ weighted spectrum (black line), the linear combination fit (gray line), and the components that contribute to the linear fit (% in parenthesis).

representative of oxygen-rich ligand bonding, CH₃HgMet and CH₃HgAsp as representative of methyl-Hg forms and HgSred and HgSblack as the most abundant inorganic Hg forms. The Hg L₃ EXAFS spectra of the Hg references used in the final LSF is shown in Fig. 13A, and the best fitting of roots, stems and leaves bulk-EXAFS spectra were displayed in Fig 13B, C and D respectively. This analysis revealed that in roots, stems and leaves the dominant forms of Hg were similar to HgPC₂ and HgCys, which corresponded to Hg-biothiol or Hg-organic sulphur complexes. This Hg coordination environment accounted for 79% in roots, 95% in stems and 85% in leaves of the total Hg in *M. sativa* plants. A minor percentage of Hg (5-21%) corresponded to methyl-Hg forms, CH₃HgMet in roots and leaves, and CH₃HgAsp in stem. The reduced *chi*-square that represents the goodness of the fit was 0.090, 0.441 and 0.128 for root, stem and leaf, respectively (Table 3).

Table 3. Relative proportion (%) of Hg species in three-week-old *M. sativa* root treated with 30 μ M Hg for 7 days, using Hg L₃ EXAFS k³ weighted as Least-Square Fitting method (Xmin= 3, Xmax= 9.5 for root and, Xmax= 10 for leaf and stem).

	Root	Stem	Leaf
Hg-S organic (%)	79	95	85
Me-Hg (%)	21	5	15
Goodness of fit (χ^2)	0.0909	0.441	0.128

Localization of Hg in *Marrubium vulgare*

The spatial localization of Hg was studied in a cross section of a *M. vulgare* root by μ -SXRF and TXM analysis. The sample was collected in the point P4 of the experimental plot. The most intense Hg signal in root using μ -SXRF was found in the external part, at the epidermis (crust) (Fig 14.B). However, Hg could not be observed in the inner tissue with the exception of a hot spot in the edge of the vascular cylinder. To complement this information, a mosaic TXM image of a delimited area of the root cross section was taken in absorption contrast showing dark areas in the epidermis at both sides assumably due to Hg (Fig. 14C). Moreover, a dark particle was co-localized with the hot spot of Hg in the μ -SXRF image. Other elements like iron (Fe), sulphur (S), manganese (Mn), potassium (K) and calcium (Ca) were studied by μ -SXRF mapping showing that they were mainly localized in the epidermis and also in the inner tissue, in the case of Ca (Fig. 14). μ -SXRF mapping of S was not possible due to the low counts s⁻¹.

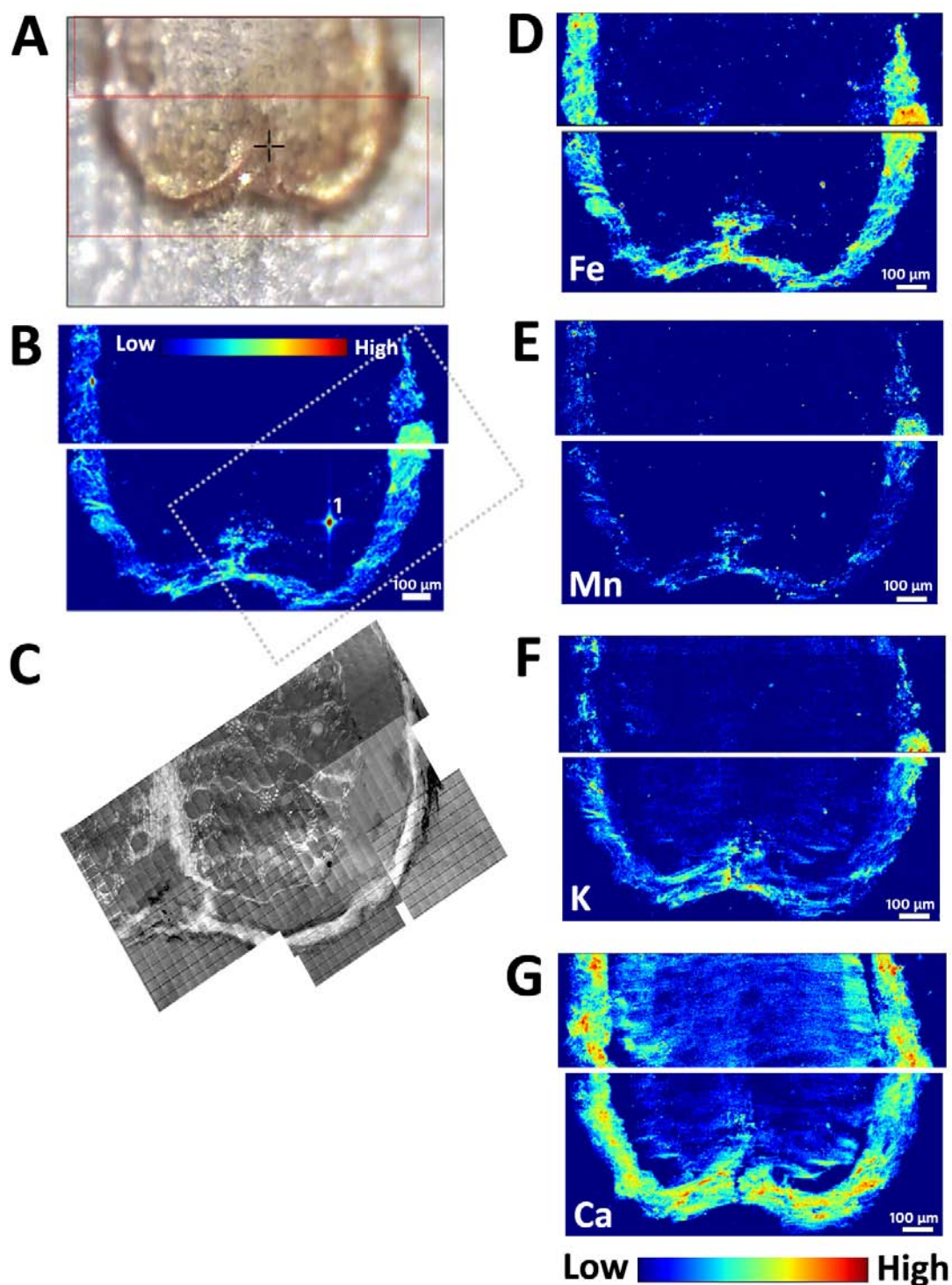


Fig. 14. Distribution of Hg, Fe, K, Mn and Ca in a 60 μm of thickness root cross section of *Marrubium vulgare* grown in an abandoned metallurgic plot. **A)** Optical image, **B)** X-ray fluorescence (TMX) map showing Hg distribution. **C)** TXM mosaic image taken at 5.4 KeV in absorption contrast shows dark areas due to the absorption by Hg. X-ray fluorescence imaging showing the distribution of **D)** Fe, **E)** K, **F)** Mn, and **G)** Ca. The red squares in **(A)** represent the mapped area in XRF image, and the grey square in **(B)** represents the mapped area in TXM image. Number 1 in **(B)** refers to the position where $\mu\text{-EXAFS}$ and $\mu\text{-XANES}$ spectra were collected (spectra shown in Fig. 16).

Mercury speciation in *Marrubium vulgare*

Hg L₃ EXAFS spectroscopy was used to identify the Hg species present in leaves and roots of *M. vulgare* plants collected in the points P2, P4 and P6 from the Hg-polluted soils. Several reference spectra representing the most probable Hg coordination environments in plants (biothiol and cysteine Hg and oxygen-rich bonding, methyl-Hg and inorganic sulphur-Hg forms) were fitted individually to each standard spectrum to exclude those standard compounds contributing less than 5 % in the fit. The final reference candidates used for the LSF were Hg₂PC₂ and HgCys, as representative standards for Hg-biothiol or Hg-organic sulphur complexes (proteins). HgAce was used as a representative of oxygen-rich ligand bonding, CH₃HgMet and CH₃HgAsp as representative of methyl-Hg forms, and HgSred and HgSblack as representative of inorganic sulphur-Hg species (Fig. 15A). The best fitting of roots and leaves bulk-EXAFS spectra are displayed in Fig 15B. The Hg L₃ EXAFS spectra of *M. vulgare* roots and leaves collected in P2 was very weak and very noisy, due to the lower Hg concentration in these samples were not analysed further. The mayor Hg form (60-80%) present in roots and leaves adjusted well with to HgSred and HgSblack, representing inorganic sulphur-Hg forms. A minor proportion of Hg was bound to organic S of biothiols or proteins (12-36%) and bound to methylated forms (3-10%). The proportion of Hg species was similar in roots from plants collected at points P4 and P6. Regarding leaves, P6 plants had similar proportion as found in roots, but there was a notable increase in the Hg-S organic forms in P4 plants, with a parallel diminution in the proportion of methylated Hg-forms. The μ -XANES and μ -EXAFS spectra obtained from spot 1 in the cross-section subjected also to μ -SXRF analysis (see Fig. 14B), bear a strong resemblance to the XANES and EXAFS spectra obtained from HgSred (cinnabar; Figs. 16A and 16B).

Table 4. Relative proportion (%) of mercury (Hg) species in *Marrubium vulgare* collected in a abandoned metallurgical plant in two different points (P6 and P4), using Hg L₃ EXAFS k³ weighted as Least-Square Fitting method (Xmin= 3, Xmax= 12).

Relative proportion (%)	Root P6	Leaf P6	Root P4	Leaf P4
Hg-PC	-	12.5	13.2	13.2
Hg-Cys ligand	16.5	-	-	23.5
Hg-S red	30	38.3	34.7	39
Hg-S black	44.3	42.2	42.3	21.1
Me-Hg-Asp	9.2	7	9.8	3.3
Hg-S organic	16.5	12.5	13.2	36.7
Hg-S inorganic	74.3	80.5	77	60.1
Me-Hg	9.2	7	9.8	3.3
Goodness of fit (χ^2)	0.53	0.824	0.553	0.479

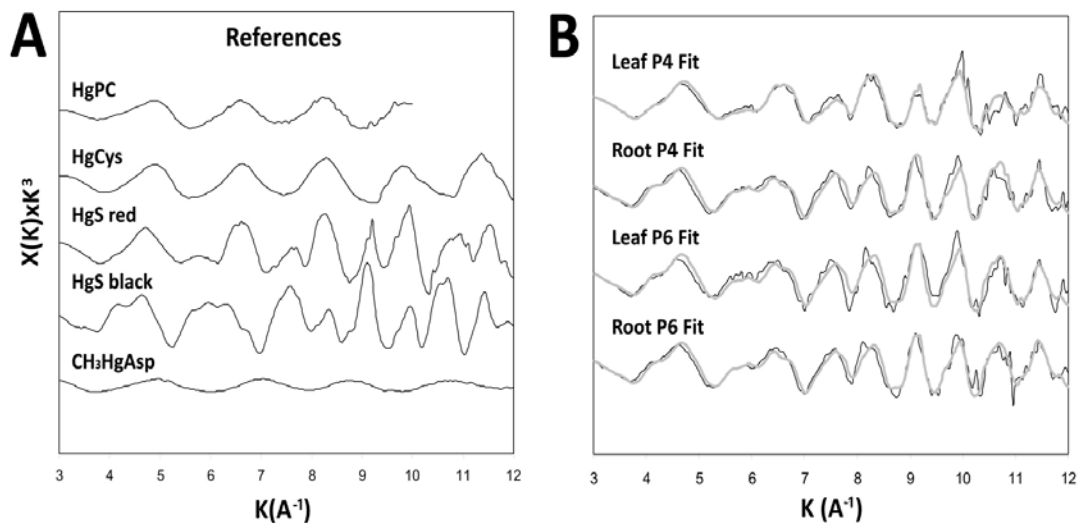


Fig. 15. Hg L₃ EXAFS spectra of the references used for the least square fitting of the samples **A**) and linear fitting results for leaf P4, root P4, leaf P6 and leaf P6, **B**) of *Marrubium vulgare* grown in an abandoned metallurgic plant showing the Hg L₃ EXAFS K³ weighted spectrum (black line), the linear combination fit (gray line).

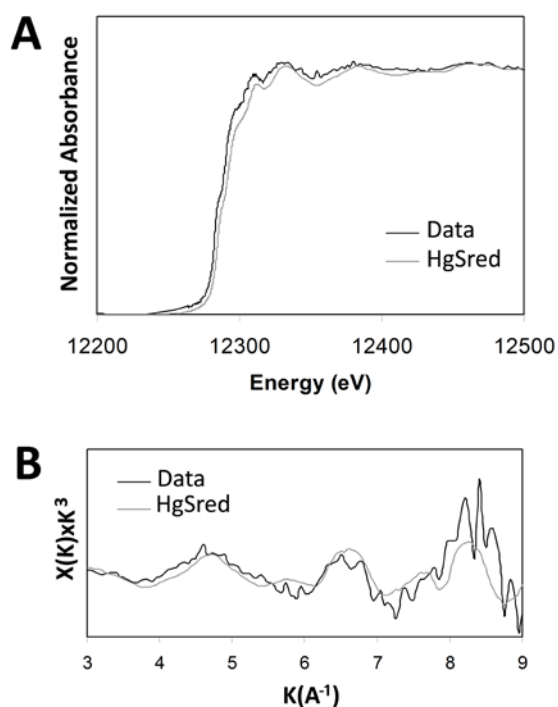


Fig 16. Overlays of normalized Hg L₃ μ-XANES (**A**) and μ-EXAFS (**B**) spectra collected in spot 1 of the root cross-section from *Marrubium vulgare* plants harvested in P6 subjected to μ-SXRF in Fig. 5 with normalized XANES and EXAFS spectra obtained from HgSred reference (cinnabar).

DISCUSSION

M. sativa plants treated with 30 μM Hg suffered visual symptoms of toxicity as reduction of organ growth, as was also described by Cho and Park (2000) and Sobrino-Plata et al. (2009). The high Hg concentration in root of *M. sativa* plants ($2,611 \pm 273 \text{ mg kg}^{-1} \text{ DW}$ equivalent to $44.5 \mu\text{mol g}^{-1} \text{ DW}$) can be explained by the fact that these plants were grown in pure-hydroponic system where Hg is in direct contact with the root tissue. This value is in the same order as the value of $89.65 \pm 5.11 \mu\text{mol g}^{-1} \text{ DW}$ obtained by Rellán-Álvarez et al. (2006) in roots of *Zea mays* exposed to 30 μM Hg. Leaf and stem Hg concentration values were 1.4% and 2.6% respectively of those found in roots of *M. sativa*. This is in agreement with the known allocation of this toxic metal in roots of alfalfa plants grown under similar conditions (Ortega-Villasante et al., 2005). It is well known that Hg is a rather immobile element that binds strongly with different cell components at the cell wall and biological membranes mainly (proteins and carbohydrates; Hall 2002), precluding the Hg translocation to the shoot as occur with other heavy metals (Beauford et al., 1976; Siegel et al., 1987). The small accumulation of Hg observed in stems and leaves of control plants might be due to a potential Hg volatilization from the nutrient solution containing of nearby plants which was absorbed by leaves without translocation to root (Suszcynsky and Shann, 1995).

Exposure to Hg altered the distribution of Fe, Mn, K and Ca in *M. sativa* roots. These results are in agreement with Godbold (1991), who observed that in the root tips of *Picea abies* seedlings exposed to Hg, the levels of K and Mn decreased dramatically and Fe levels increased due to an accumulation of Fe in cell walls of the root cortex. Shieh and Barber (1973) and De Filippis (1979) observed a K efflux in *Chlorella* exposed to Hg and methyl-Hg, in accordance with the lower K values observed in alfalfa seedlings treated with (Table 2). Godbold (1991) found that Hg may affect directly the plasma membrane integrity, which would cause an increase of Ca uptake. Therefore, changes in membrane integrity, or binding to membrane proteins (i.e. transporters) may impair their functionality, affecting the transport of other nutrients, such as K, Mn and Mg in roots.

The distribution of Hg was studied in the tissue of *M. sativa* roots, stems and leaves using μ -SXRF mapping. The most intense Hg signals detected in root were located in the tips and in the inner tissue, at the vascular cylinder. These results are in agreement with those observed by Patty et al. (2009) in *Spartina* spp., where the most concentrated area of Hg was localized in the tips and inner tissues of the root. Though the resolution

of μ -SXRF images is not enough to discern if Hg in root is localized in the xylem or in the phloem, it is feasible that Hg would be translocated to the areal part through the xylem, as Hg was also localized in the vascular tissues of the stems and in the veins of leaves. However, phloem cannot be discarded, as it is known the recycling of organic and inorganic substances between both conducts (Peuke, 2010).

It is probable that Hg use the water flow to enter in the root tissues through the tips of the roots. The cells just behind the apical meristem are dividing and elongating, forming the different root tissues following a radial pattern. These immature cells are less suberized, being more permeable to water. Therefore, the water together with different elements in solution, such as Hg^{2+} , can enter without any barrier throughout the root tip. Therefore, a large proportion of Hg reaches presumably the xylem *via* the root apoplast, whereas the symplasmic movement would be more difficult (Clemens et al., 2002). Recent studies have shown quite clearly that the movement of toxic metals, like Cd, depends on root structure. Developmental and physiological factors can affect greatly metal uptake, as was shown in plants grown in pure hydroponic, soil or aeroponic cultures, where different degree of suberisation modified the pattern of metal uptake and translocation (Redjala et al., 2010). The Casparian band in the endodermis cell walls is chemically different from the rest of the cell wall and is blocking the apoplastic diffusion of water and solutes into the vascular system. In general the solutes have to be taken up into the root symplast before they can enter the xylem (Tester and Leigh, 2001). TEM images showed significant Hg accumulation in the cytoplasm of endodermis and xylem cells near the cell wall (Fig 11J), suggesting that those cells constituted a barrier to Hg. Indeed, transversal SR- μ CT imaging showed that Hg accumulated in this location (Fig. 4B).

Cell walls constitute a large reservoir of metals in plant cells (Hall, 2002). By using a sub-cellular fractionation similar to the procedure described by Lozano-Rodriguez et al., (1997) for pea and maize treated with Cd, it was found that Hg was associated with cell walls of *Halimione portulacoides* (Valega et al., 2009), maize, barley and alfalfa (Carrasco-Gil et al., 2011). These results showed that up to a 90% of total Hg accumulated in the cell wall of roots. TEM images show that in *M. sativa* roots there were distinctive granular deposits in the intracellular space of epidermal cells and xylem, supporting the finding with the subcellular fractionation. The pattern of Hg distribution in root tissues resembles that of Cd, which was localized in the cell wall of cortical parenchyma in *Thlaspi caerulescens* (Vazquez et al., 1992a) and *Arabidopsis halleri* (Küpper et al., 2000), and in the intracellular space of *Phaseolus vulgaris* (Vazquez et al., 1992b).

Toxic metal ions are thought to enter the cells by the same uptake mechanisms involved in the transport of essential nutrients (Patra et al., 2004). In the case of Cd, Fe and Zn transporters and Ca channels may be used to allow Cd ions enter the root cells (Connolly et al., 2002; Perfus-Barbeoch et al., 2002). However, very little is known about possible transporters or channels involved in Hg uptake in plant cells. Our co-localisation analysis might help to focus future research to study specific transporters. For example, Cu localized in the same areas as Hg did in the stem of *M. sativa*. (Fig. 9C). This metal shares some chemical properties with Hg. Our data suggest that both metals could be transported in the same manner, implying that Cu transporters would be possible candidates to promote Hg uptake (Esteban et al., 2008). The rest of nutrients studied (Fe, Zn and Ca) did not apparently overlap, indicating that Hg would not compete with them for the uptake mechanisms.

There were some interesting “hot spots” accumulating metals in the leaves, according to the μ -SXRF image of Hg distribution in leaves (Fig. 5F). Trichomes apparently play a major role in storage and detoxification; in a study carried out by Salt (1995b) with *Brassica juncea* exposed to Cd, trichomes accumulated 40 times more Cd compared to the total leaf. The trichomes in *M. sativa* are distributed following the ribbing pattern of the leaf, implying that could play a similar role than Cd in Hg detoxification, as was observed in the trichomes of *Arabidopsis thaliana* plants exposed to Cd (Isaure et al., 2006). However, better resolution is needed to confirm these findings, and X-ray fluorescence should be captured in smaller steps (of at least 1 μ m width) to distinguish these epidermal structures (Punshon et al., 2009).

To date few studies have been focus to understand Hg speciation using X-ray synchrotron fluorescence spectroscopy. Riddle et al. (2002) used XANES to investigate the accumulation of Hg by *E. crassipes* and reported that Hg was coordinated mainly to organic S ligands in shoot. In other XANES studies, Rajan et al. (2008) studied Hg methylation in *E. crassipes*, and Patty et al. (2009) analysed Hg binding in *S. foliosa* and *S. alterniflora*. Both authors concluded that the major proportion of Hg was bound to S in a form similar to Hg-cysteine, and a smaller part (3-36%) was in a methylated form. This was in agreement with the results found in *M. sativa*, since more than 79% of the Hg was bound to organic S and 5-21% was in methyl Hg forms.

The bulk-EXAFS analysis of Hg coordination environments in the root did not revealed oxygen-rich ligand bonding corresponding with carboxyl groups of the cell wall. However, high proportion of Hg was associated with cysteine residues, possibly

corresponding to proteins and/or biothiols, in agreement with previous results (Carrasco-Gil et al., 2011). Several studies using mass spectrometry coupled with liquid chromatography showed that Hg occurred partially in roots as an array of Hg-PCs complexes in alfalfa, barley and maize (Carrasco-Gil et al., 2011), *B. chinensis* (Chen et al. 2009), *O. sativa* and *M. vulgare* (Krupp et al. 2009). It is possible that Hg bound to biothiols represents a minor proportion albeit important for Hg tolerance (Carrasco-Gil et al., 2011), so the major amount would be bound to proteins in the apoplast. Phytochelatins, and their precursor glutathione, constitute a group of biothiols that are thought to be involved in metal detoxification by means of their transport into plant cell vacuoles (Salt et al., 1995a). However, recent studies have shown that PCs also have the ability to undergo long-distance transport in the root-to-shoot and shoot-to-root directions (Chen et al., 2006; Gong et al., 2003). Therefore, it is a matter of discussion whether PCs may be involved in the long-distance transport of Hg, studies that will require more invasive techniques like mass spectrometry associated with isotopic labelling for accurate quantification. On the other hand, it is known the high affinity of Hg for the sulfhydryl residues of proteins (-SH or dithiol bridges; Clarkson, 1972), although few proteins interacting with Hg have so far being identified, and would be the target of future research.

With regards to *Marrubium vulgare* plants, Millan et al. (2011) carried out a study of the Hg concentration in the soil located in the abandoned metallurgic plant. They observed that soil concentration in that area was in the range of 5-1400 mg kg⁻¹, 10-7500 mg kg⁻¹ and 60-40000 mg kg⁻¹ corresponding to A1, A2 and A3 respectively (Fig. 2A). These workers observed that there was a significant high correlation between soil Hg concentration and Hg concentration in *M. vulgare* plants (Table 1), being the highest concentration near the furnaces where the cinnabar was stockpiled, and eventually ashes and waste mineral produced from roasting processes were dumped (Millan et al., 2011). Hg X-ray fluorescence analysis of *M. vulgare* root cross-sections showed that Hg was localized only in the epidermis tissue, concretely at the crust. Although we do not have spatial resolution image by μ -SXRF, EXAFS analysis suggest that also the Hg accumulated at the surface comes from soil particles deposition. The roughness of *M. vulgare* leaves, provide a reservoir chamber for deposition of particles of soil carried by the wind or atmospheric Hg (Hg⁰) that can be oxidized to Hg²⁺ in the outer tissue layers of the leaves. Several studies reported that a 90% of the Hg accumulated in the shoot of terrestrial originated from atmospheric depositions, whereas Hg translocation from root to shoot was less than <5% (Bishop et al., 1998; Ericksen et al, 2003; Lindberg et al., 1979;

Mosbaek et al., 1988). In general, Hg in leaf is located in epidermal and stomata cell walls, or adsorbed to the leaf surface, and rarely found in mesophyll or vascular tissue (Beauford et al., 1977; Cavallini et al., 1999; Amado Filho et al., 2002). The values of atmospheric Hg in Almadén area were larger than the concentration found in Hg mines in the Northern of Europe, possibly due to warmer Mediterranean climate that facilitates the vaporization of Hg⁰ (Higuera et al., 2006). In Almadén there are many ore deposits, mineral dumps and contaminated soils that are significant sources of gaseous Hg scattered in the area, which must be considered in further studies (Gustin, 2003; Ferrara, 1998).

XANES analysis revealed that more than 60% of the total Hg in *M. vulgare* was bound to inorganic S, similar to cinnabar (HgSred) and metacinnabar (HgSblack). This chemical species of Hg was found in the soils where the studied plants were collected (Millán et al., 2011). It is possible that part of the Hg signal from the μ -SXRF mapping of the root cross-section comes from soil particles containing HgSred adhered to the epidermis surface. In fact, the μ -EXAFS and μ -XANES analysis performed on the hot spot localized at the vascular cylinder edge revealed also the presence of HgSred. It is feasible that during the preparation of samples for synchrotron analyses some soil particles remained adhered, and were spread in the sample. Moreover, the most intense signal of Fe and Mn seems to be co-localized with Hg in the *M. vulgare* root. Soil analysis in the sampling area showed that between 3-30% of the total Hg was associated to crystalline Fe-Mn oxyhydroxides (Millán et al. (2011), so this confirms that part of the Hg accumulated in the epidermis comes from soil particles.

CONCLUSIONS

μ -SXRF showed that Hg was uptaken principally at the root tips, possibly following the water flow. More detailed study is required, like microtomography, to identify the tissues accumulating Hg. In addition, alternative techniques like X-ray (EDXA) coupled with scanning electron microscopy could help to dissect Hg localisation at the cellular level. The behavior of plants cultured hydroponically was consistent with a transport process involving uptake of Hg by roots, transport through the stem xylem to the shoot, where it is then distributed through the veins to the epidermis. However, Hg transport in natural plants seems to be quite different, since Hg is mainly retained in root without translocation from root to shoot, and apparently was due to inorganic Hg adhered to the surface. In addition, atmospheric Hg⁰ could be a relevant source of Hg accumulated in

leaves. New experiments should be directed to improve resolution and to augment the array of ligand references to understand the dynamics of Hg in plants.

ACKNOWLEDGEMENTS

This work was supported by Fundación Ramón Areces (www.fundacionareces.es), the Spanish Ministry of Science and Innovation (CTM2005-04809/TECNO-REUSA and AGL2010-15151-PROBIOMET). Junta Comunidades Castilla-La Mancha (FITOALMA2, POII10-0087-6458. Portions of this research were carried out at the Stanford Synchrotron Radiation Lightsource, through the Structural Molecular Biology Program supported by the Department of Energy, Office of Biological and Environmental Research, and by the National Institute of Health, National Centre for Research Resources, Biomedical Technology Program. We thank Wren Amos and Jennifer Cassano for sharing beam times and S Webb for help with μ -SXRF data collection.

REFERENCES

- Amado Filho G.M., Andrade L.R., Farina M. & Malm O. (2002) Hg localisation in *Tillandsia usneoides* L. (Bromeliaceae), an atmospheric biomonitor. *Atmospheric Environment*, **36**, 881-887.
- Beauford W., Barber J. & Barringer A.R. (1977) Uptake and distribution of mercury within higher plants. *Physiology Plantarum*, **39**, 271-275.
- Bishop K. & Dambrine E. (1995) Localization of tree water-uptake in scots pine and Norway spruce with hydrological tracers. *Canadian Journal of Forest Research-Revue Canadienne De Recherche Forestiere*, **25**, 286-297.
- Bowne C.L. & Fang S.C. (1978) Uptake of mercury vapor by wheat. *Plant Physiology*, **71**, 430-433.
- Carrasco-Gil S., Álvarez-Fernández A., Sobrino-Plata J., Millán R., Carpena-Ruiz R.O., LeDuc D.L., Andrews J.C., Abadía J. & Hernández L.E. (2011) Complexation of Hg with phytochelatin is important for plant Hg tolerance. *Plant, Cell and Environment* (in press).
- Cavallini A., Natali L., Durante M. & Maserti B. (1999) Mercury uptake distribution and DNA affinity in durum wheat (*Triticum durum* Desf.) plants. *Science of The Total Environment*, **243/244**, 119-127.
- Chen X.Y. & Kim J.Y. (2006) Transport of macromolecules through plasmodesmata and the phloem. *Physiologia Plantarum*, **126**, 560-571.
- Chen L., Yang L. & Wang Q. (2009) *In vivo* phytochelatin and Hg-phytochelatin complexes in Hg-stressed *Brassica chinensis* L. *Metallomics*, **1**, 101-106.
- Cho U.H. & Park J.O. (2000) Mercury-induced oxidative stress in tomato seedlings. *Plant Science*, **156**, 1-9.
- Clarkson T.W. (1972) The biological properties and distribution of mercury. *Biochemical Journal*, **130**, 61-63.
- Clemens S., Palmgren M.G. & Krämer U. (2002) A long way ahead: understanding and engineering plant metal accumulation. *Trends in Plant Science*, **7**, 309-315.
- Connolly E.L., Fett J.P. & Guerinot M.L. (2002) Expression of the IRT1 metal transporter is controlled by metals at the levels of transcript and protein accumulation. *Plant Cell*, **14**, 1347-1357.
- De Filippis L.F. (1979) The effect of heavy metal compounds on the permeability of *Chlorella* cells. *Z. Pflanzenphysiologie*, **92**, 39-49.

- De Filippis L.F. & Pallaghy C.K. (1975) Localization of zinc and mercury in plant cells. *Micron*, **6**, 111-120.
- Du X., Zhu Y.G., Liu W.J. & Zhao X.S. (2005) Uptake of mercury (Hg) by seedlings of rice (*Oryza sativa* L.) grown in solution culture and interactions with arsenate uptake. *Environmental and Experimental Botany*, **54**, 1-7.
- Ericksen J.A., Gustin M.S., Schorran D.E., Johnson D.W., Lindberg S.E. & Coleman J.S. (2003) Accumulation of atmospheric mercury in forest foliage. *Atmospheric Environment*, **37**, 1613-1622.
- Esteban E., Moreno E., Peñalosa J., Cabrero J.I., Millán R. & Zornoza P. (2008) Short and long-term uptake of Hg in white lupin plants: Kinetics and stress indicators. *Environmental and Experimental Botany*, **62**, 316-322.
- Ferrara R., Maserti B.E., Andersson M., Edner H., Ragnarson P., Svanberg S. & Hernandez A. (1998) Atmospheric mercury concentrations and fluxes in the Almadén district (Spain). *Atmospheric Environment*, **32**, 3897-3904.
- Gardea-Torresdey J.L., Peralta-Videa J.R., de la Rosa G. & Parsons J.G. (2005) Phytoremediation of heavy metals and study of the metal coordination by X-ray absorption spectroscopy. *Coordination Chemistry Reviews*, **249**, 1797-1810.
- Giberson R.T. & Demaree Jr R.S., eds (2001) *Microwave Techniques and Protocols*. Humana Press, Totowa, NJ.
- Godbold D.L. (1991) Mercury-induced root damage in spruce seedlings. *Water, Air, and Soil Pollution*, **56**, 823-831.
- Godbold D.L. & Hüttermann A. (1986) The uptake and toxicity of mercury and lead to spruce (*Picea abies* Karst. seedlings. *Water, Air, & Soil Pollution*, **31**, 509-515.
- Gong J.M., Lee D.A. & Schroeder J.I. (2003) Long-distance root-to-shoot transport of phytochelatin and cadmium in *Arabidopsis*. *Proceeding of the National Academy of Sciences, USA*, **100**, 10118-10123.
- Gustin M.S. (2003) Are mercury emissions from geologic sources significant? A status report. *The Science of The Total Environment*, **304**, 153-167.
- Hall J.L. (2002) Cellular mechanisms for heavy metal detoxification and tolerance. *Journal of Experimental Botany*, **52**, 631-640.
- Higuera P., Oyarzun R., Lillo J., Sánchez-Hernández J.C., Molina J.A., Esbrí J.M. & Lorenzo S. (2006) The Almadén district (Spain): Anatomy of one of the world's largest Hg-contaminated sites. *Science of The Total Environment*, **356**, 112-124.
- Isaure M.-P., Fayard B., Sarret G., Pairis S. & Bourguignon J. (2006) Localization and chemical forms of cadmium in plant samples by combining analytical electron microscopy and X-ray spectromicroscopy. *Spectrochimica Acta Part B: Atomic Spectroscopy*, **61**, 1242-1252.
- Iverfeldt A. (1991) Mercury in forest canopy throughfall water and its relation to atmospheric deposition. *Water and Soil Pollution*, **56**, 553-564.
- Kim C.S., Brown G.E. & Rytuba J.J. (2000) Characterization and speciation of mercury-bearing mine wastes using X-ray absorption spectroscopy. *Science of The Total Environment*, **261**, 157-168.
- Krupp E.M., Mestrot A., Wielgus J., Meharg A.A. & Feldmann J. (2009) The molecular form of mercury in biota: identification of novel mercury peptide complexes in plants. *Chemical Communications*, **28**, 4257-4259.
- Küpper H. & Kochian L.V. (2010) Transductional regulation of metal transport genes and mineral nutrition during acclimatization to cadmium and zinc in the Cd/Zn hyperaccumulator, *Thlaspi caerulescens* (Ganges population). *New Phytologist* **185**, 114-129.
- Küpper H., Lombi E., Zhao F.J. & McGrath S.P. (2000) Cellular compartmentation of cadmium and zinc in relation to other elements in the hyperaccumulator *Arabidopsis halleri*. *Planta*, **212**, 75-84.
- Lindberg S.E., Jackson D.R., Huckabee J.W., Janzen S.A., Levin M.J. & Lund J.R. (1979) Atmospheric emission and plant uptake of mercury from agricultural soils near the Almadén mercury mine. *Journal of Environmental Quality*, **8**, 572-578.

- Lindberg S.E., Meyers T.P., Jr, Turner R.R. & Schroeder W.H. (1992) Atmosphere-surface exchange of mercury in a forest: Results of modeling and gradient approaches. *Journal of Geophysical Research*, **97**, 2519-2528.
- Liu Z. (2007) Leaf epidermal cells: a trap for lipophilic xenobiotics. *International Journal of Plant Biology*, **48**, 1073-1078.
- Lozano-Rodríguez E., Hernández L.E., Bonay P. & Carpena-Ruiz R.O. (1997) Distribution of cadmium in shoot and root tissues of maize and pea plants: physiological disturbances. *Journal of Experimental Botany*, **48**, 123–128.
- McNear D.H., Peltier E., Everhart J., Chaney R.L., Sutton S., Newville M., Rivers M. & Sparks D.L. (2005) Application of quantitative fluorescence and absorption-edge computed microtomography to image metal compartmentalization in *Alyssum murale*. *Environmental Science & Technology*, **39**, 2210-2218.
- Millán R., Gamarra R., Schmid T., Sierra M.J., Quejido A.J., Sánchez D.M., Cardona A.I., Fernández M. & Vera R. (2006) Mercury content in vegetation and soils of the Almadén mining area (Spain). *Science of The Total Environment*, **368**, 79-87.
- Millán R., Schmid T., Sierra M.J., Carrasco-Gil S., Villadóniga M., Rico C., Ledesma D.M.S. & Puente F.J.D. (2011) Spatial variation of biological and pedological properties in an area affected by a metallurgical mercury plant: Almadenejos (Spain). *Applied Geochemistry*, **26**, 174-181
- Mosbaek H., Tjell J.C. & Sevel T. (1988) Plant uptake of airborne mercury in background areas. *Chemosphere*, **17**, 1227-1236.
- Munthe J., Hultberg H. & Iverfeldt A. (1995) Mechanisms of deposition of methylmercury and mercury to coniferous forests. *Water Air and Soil Pollution*, **80**, 363-371.
- Naito W. (2008) Ecological Catastrophe. In: *Encyclopedia of Ecology* (eds J. Sven Erik & F. Brian), pp. 983-991. Academic Press, Oxford.
- Ortega-Villasante C., Rellan-Alvarez R., Del Campo F.F., Carpena-Ruiz R.O. & Hernandez L.E. (2005) Cellular damage induced by cadmium and mercury in *Medicago sativa*. *Journal of Experimental Botany*, **56**, 2239-2251.
- Patra M., Bhowmik N., Bandopadhyay B. & Sharma A. (2004) Comparison of mercury, lead and arsenic with respect to genotoxic effects on plant systems and the development of genetic tolerance. *Environmental and Experimental Botany*, **52**, 199-223.
- Patty C., Barnett B., Mooney B., Kahn A., Levy S., Liu Y.J., Pianetta P. & Andrews J.C. (2009) Using X-ray Microscopy and Hg L-3 XANES To Study Hg Binding in the Rhizosphere of *Spartina Cordgrass*. *Environmental Science & Technology*, **43**, 7397-7402.
- Perfus-Barbeoch L., Leonhardt N., Vavasseur A. & Forestier C. (2002) Heavy metal toxicity: cadmium permeates through calcium channels and disturbs the plant water status. *Plant Journal*, **32**, 539-548.
- Peuke A.D. (2010) Correlations in concentrations, xylem and phloem flows, and partitioning of elements and ions in intact plants. A summary and statistical re-evaluation of modelling experiments in *Ricinus communis*. *Journal of Experimental Botany*, **61**, 635-656.
- Punshon T., Guerinot M.L. & Lanzirotti A. (2009) Using synchrotron X-ray fluorescence microprobes in the study of metal homeostasis in plants. *Annals of Botany*, **103**, 665-672.
- Rajan M., Darrow J., Hua M., Barnett B., Mendoza M., Greenfield B.K. & Andrews J.C. (2008) Hg L-3 XANES study of mercury methylation in shredded *Eichhornia crassipes*. *Environmental Science & Technology*, **42**, 5568-5573.
- Rea A.W., Lindberg S.E. & Keeler G.J. (2001) Dry deposition and foliar leaching of mercury and selected trace elements in deciduous forest throughfall. *Atmospheric Environment*, **35**, 3453-3462.
- Redjala T., Zelko I., Sterckeman T., Legué V. & Lux A. (2011) Relationship between root structure and root cadmium uptake in maize. *Environmental and Experimental Botany* (doi:10.1016/j.envexpbot.2010.12.010).
- Rellan-Alvarez R., Ortega-Villasante C., Alvarez-Fernandez A., del Campo F.F. & Hernandez L.E. (2006) Stress responses of *Zea mays* to cadmium and mercury. *Plant and Soil*, **279**, 41-50.

- Riddle S.G., Tran H.H., Dewitt J.G. & Andrews J.C. (2002) Field, laboratory, and X-ray absorption spectroscopic studies of mercury accumulation by water hyacinths. *Environmental Science & Technology*, **36**, 1965-1970.
- Salt D.E., Blaylock M., Kumar N., Dushenkov V., Ensley B.D., Chet I. & Raskin I. (1995a) Phytoremediation - a novel strategy for the removal of toxic metals from the environment using plants. *Bio-Technology*, **13**, 468-474.
- Salt D.E., Prince R.C., Pickering I.J. & Raskin I. (1995b) Mechanisms of cadmium mobility and accumulation in indian mustard. *Plant Physiology*, **109**, 1427-1433.
- Shieh Y.J. & Barber J. (1973) Uptake of mercury by *Chlorella* and its effect on potassium regulation. *Planta*, **109**, 49-60.
- Sierra M.J., Millán R. & Esteban E. (2009) Mercury uptake and distribution in *Lavandula stoechas* plants grown in soil from Almadén mining district (Spain). *Food and Chemical Toxicology*, **47**, 2761-2767.
- Skinner K., Wright N. & Porter-Goff E. (2007) Mercury uptake and accumulation by four species of aquatic plants. *Environmental Pollution*, **145**, 234-237.
- Sobrino-Plata J., Ortega-Villasante C., Flores-Caceres M.L., Escobar C., Del Campo F.F. & Hernandez L.E. (2009) Differential alterations of antioxidant defenses as bioindicators of mercury and cadmium toxicity in alfalfa. *Chemosphere*, **77**, 946-954.
- Stamenkovic J. & Gustin M.S. (2009) Nonstomatal versus Stomatal Uptake of Atmospheric Mercury. *Environmental Science & Technology*, **43**, 1367-1372.
- Suszczynsky E.M. & Shann J.R. (1995) Phytotoxicity and accumulation of mercury in tobacco subjected to different exposure routes. *Environmental Toxicology and Chemistry*, **14**, 61-67.
- Tester M. & Leigh R.A. (2001) Partitioning of nutrient transport processes in roots. *Journal of Experimental Botany*, **52**, 445-457.
- UNEP (2011) Toolkit for identification and quantification of mercury releases. Mercury Programme, UNEP DTIE, Chemicals Branch, Geneva, Switzerland.
- Valega M., Lima A.I.G., Figueira E., Pereira E., Pardal M.A. & Duarte A.C. (2009) Mercury intracellular partitioning and chelation in a salt marsh plant, *Halimione portulacoides* (L.) Aellen: Strategies underlying tolerance in environmental exposure. *Chemosphere*, **74**, 530-536.
- Vázquez M.D., Barceló J., Poschenrieder C., Mádico J., Hatton P., Baker A.J.M. & Cope G.H. (1992a) Localization of zinc and cadmium in *Thlaspi caerulescens* (Brassicaceae), a metallophyte that can hyperaccumulate both metals. *Journal of Plant Physiology*, **140**, 350-355.
- Vázquez M.D., Poschenrieder C. & Barceló J. (1992b) Ultrastructural effects and localization of low cadmium concentrations in bean roots. *New Phytologist*, **120**, 215-226.
- Webb S.M. (2005) Sixpack: A graphical user interface for XAS analysis using IFEEF IT. *Physica Scripta*, **115**, 1011-1014.

Attenuation of mercury phytotoxicity with a high nutritional level of nitrate in alfalfa plants grown in a semi-hydroponic system

ABSTRACT

Mercury (Hg) is one of the most dangerous pollutant heavy metals to the environment. Its accumulation in plants causes several negative effects, among them the induction of oxidative stress. Nitrogen (N) is one of the most limiting macronutrient for plants, which is fundamentally assimilated as NO_3^- after its reduction to NO_2^- by the enzyme nitrate reductase (NR), key step prior the formation of NH_4^+ . We studied the physiological effects of Hg (0, 6 and 30 μM) in alfalfa plants grown with low NO_3^- (2 mM; LN) and high (12 mM; HN) concentrations. Several parameters of oxidative stress such as lipid peroxidation, chlorophyll content, biothiol concentration and, ascorbate peroxidase (APX) and glutathione reductase (GR) activity were analysed, and showed that HN plants were less affected by Hg. Our results highlight the importance of the nitrogen nutritional status to improve tolerance to heavy metal stress.



CHAPTER 5

INTRODUCTION

Almadén (Ciudad Real, Spain) has been for centuries the largest mercury (Hg) mining area of the World. Cessation of the production of Hg has imposed the necessity to impulse other economic activities, such as agriculture and farming, which are undermined by the accumulation of Hg in local soils. Plants are able to extract metals, property that has been exploited to clean up polluted soils by using phytoremediation technologies. Intense research is conducted to understand tolerance mechanism in plants that might help to optimise such promising clean techniques (Clemens et al., 2002).

Depending on the chemical form, Hg may become extremely hazardous for the environment. The main species of Hg present in the environment are HgS, Hg²⁺, Hg⁰ and methyl-Hg. However, the ionic oxidized form (Hg²⁺) is predominant in agricultural soils (Han et al., 2006). The accumulation of Hg can induce visible injuries and physiological disorders in plants (Zhou et al., 2007), such as obstruction of water flow through the inhibition of plasma membrane aquaporins, alteration of mitochondrial activity, disruption of lipid membranes, alteration of photosynthesis and growth inhibition (Zhang and Tyerman, 1999; Patra and Sharma, 2000; Israr and Sahi, 2006; Cargnelutti et al., 2006). One of the earliest phytotoxic responses of plant cells to Hg exposure is the induction of oxidative stress, characterised by the oxidation of membrane lipids and proteins (Ortega-Villasante et al., 2005), and eventually causes cell poisoning and death (Ortega-Villasante et al., 2007). To cope with the oxidative stress induced by Hg, plant cells exposed to Hg concentration of 1-10 mg L⁻¹ showed an increase in the activity of antioxidant enzymes (Cho and Park, 2000). However when the concentration of Hg rose up to 50 mg L⁻¹, the protection effect disappeared (Ma, 1998). Plants have a complex antioxidant system, composed of antioxidant enzymes like ascorbate peroxidase (APX) and glutathione reductase (GR), and antioxidant metabolites like glutathione (GSH) and ascorbic acid (AA). In the presence of Hg, the activity of these antioxidant enzymes may be altered (Ortega-Villasante et al., 2007; Zhou et al., 2007; Sobrino-Plata et al., 2009; Elbaz et al., 2010). On the other hand, the accumulation of phytotoxic amounts of Hg and other metals in plants can produce inhibition of several enzymes through its binding to sulfhydryl groups, that may exist in catalytic domains or affect the structural integrity of the enzymes (Van and Clijsters, 1990). On the other hand, under oxidative stress some of these enzymes may increase their activity helping to maintain the redox balance of the cell (Foyer et al., 1997). Thus, the changes in enzymatic activity can be used to evaluate the heavy metal toxicity of

polluted soils. In particular, GR was extremely sensitive to Hg accumulated in the roots of alfalfa, and has been proposed as biomarker of Hg phytotoxicity (Sobrino-Plata et al., 2009).

On the other hand, nitrogen (N) is a very limiting macronutrient, which is normally assimilated as nitrate (NO_3^-). The assimilation of NO_3^- comprises its reduction in a two step process, firstly it is reduced to NO_2^- by the action of the cytosolic enzyme nitrate reductase (NR), and then the reduction to NH_4^+ thanks to the plastidial enzyme nitrite reductase (NiR; Wang et al. 2001). NH_4^+ is then incorporated to organic acids to form aminoacids. Within this complex process, NR is the first and limiting step (Campbell, 1999). Heavy metal polluted areas are commonly waste land with low N availability, so nitrogen fertilizer must be applied to improve the biomass yield of plants cultivated in this areas for phytoremediation purposes (Wong, 2003). A common agricultural practice is the addition of organic matter and NPK inorganic fertilizers containing NO_3^- (Barrutia et al., 2009). Therefore it is important to study the relation between NO_3^- nutritional status and heavy metals toxicity. Heavy metals may disturb N metabolic system with a significant decrease in the activities, as occurred to NR under Cd stress in pea plants (Hernández et al., 1996). Indeed, in pea plants treated with 50 μM Cd there was a severe diminution in NO_3^- assimilation, affecting NO_3^- and K uptake and NO_3^- reduction by NR (Hernández et al., 1997). Similar results were obtained in bean and tomato plants exposed to Cd, where the assimilation of NO_3^- and NH_4^+ was compromised (Gouia et al., 2000; Chaffei et al., 2004;).

On the other hand, recent studies have been carried out to evaluate the effects of N supply on Cd concentration in plants, showing the beneficial effect of N fertilization on metal uptake in plants grown in polluted soils (Du et al., 2009; Gao et al., 2010). Finkemeier et al. (2003) studied the inter-relation between N status and Cd toxicity in *Hordeum vulgare* roots and showed that the gene expression of phytochelatin synthase (PCS) and NRAMP metal transporters were up-regulated under N starvation. It is feasible that under N deficiency the detoxification mechanisms (for example production of phytochelatins) are over induced to prevent cellular damages, as stronger phytotoxic effects occurred under nutritional limiting conditions.

Prior to test the modulation of NO_3^- nutrition on plant performance in phytoremediation applications (i.e. tests in Almadén polluted soils), the effects of NO_3^- fertilization on Hg tolerance must be tested under controlled environment conditions. The objective of the present work was to study the effects of growing alfalfa plants

under two NO_3^- conditions (low and high) on Hg toxicity in a semi-hydroponic system using perlite as inert substrate. Hg distribution in plant, oxidative stress and N assimilation parameters were analysed. It should be noted that the information available about the interaction between NO_3^- nutrition status and Hg phytotoxicity is almost null.

MATERIAL AND METHODS

Plant material, growth conditions and treatments

Alfalfa (*Medicago sativa* cv. Aragon) seedlings were surface sterilized for 5 min in 5% (v/v) commercial bleach. After rinsing several times with sterile water, seeds were soaked overnight at 4°C and germinated on 1.5% (w/v) agar in square Petri dishes (10 x 10 mm), in complete darkness for 48 h at 28°C. Homogeneous selected seedlings were transferred to a semi-hydroponic system using a perlite inert substrate in plastic trays submerged in two modified Hoagland nutrient solution (Ortega-Villasante et al., 2005), one of them with low NO_3^- concentration (LN; 2 mM): (macronutrients [mM]: 1.0 KH_2PO_4 , 0.5 MgSO_4 , 0.1 NaCl , 0.9 $\text{Ca}(\text{NO}_3)_2$, 0.63 KNO_3 , 0.47 $\text{Mg}(\text{NO}_3)_2$, and micronutrients [μM]: 45.0 Fe (EDDHA), 18.0 MnSO_4 , 3.0 ZnSO_4 , 6.0 CuSO_4 , 23.5 H_3BO_3 , 2.0 $\text{Mo}_7\text{O}_{24}(\text{NH}_4)_6$) and the other one with high NO_3^- concentration (HN; 12 mM): (macronutrients [mM]: 1.0 KH_2PO_4 , 0.5 MgSO_4 , 0.1 NaCl , 5.4 $\text{Ca}(\text{NO}_3)_2$, 3.8 KNO_3 , 2.8 $\text{Mg}(\text{NO}_3)_2$, and micronutrients [μM]: 45.0 Fe (EDDHA), 18.0 MnSO_4 , 3.0 ZnSO_4 , 6.0 CuSO_4 , 23.5 H_3BO_3 , 2.0 $\text{Mo}_7\text{O}_{24}(\text{NH}_4)_6$). The plants grew for 12 days in a controlled environment chamber (16 h light (lamps of 120 Wm^{-2})/8 h darkness) at 25/18°C respectively and relative humidity, 75%. 0, 6 and 30 μM Hg was then supplied as HgCl_2 , and plants were collected after 7 days and rinsed several times with 10 mM Na_2EDTA solution to remove superficial Hg. Then length and fresh weight of roots and shoots were measured and stored at -80°C until analysis.

Mercury Analysis

Solid samples of roots and shoots were air dried and ground with mortar and pestle. Dried plant material (100 mg) was acid digested in 2 mL of the digestion mixture ($\text{HNO}_3:\text{H}_2\text{O}_2:\text{H}_2\text{O}$, 0.6:0.4:1 v:v) in an autoclave (Presoclave-75 Selecta, Barcelona, Spain) at 120°C and 1.5 atm for 30 min (Ortega-Villasante et al., 2007). Hg concentration was measured by Atomic Absorption Spectrophotometry using the Advanced Mercury Analyser 254 Leco (St. Joseph, Michigan, MI, USA) with a detection limit of 0.5 $\mu\text{g kg}^{-1}$. Certified Reference Materials (CRM) were used to determine the accuracy of the measurements and validation.

Nitrogen in plants

The nitrogen (N) in plant tissue was determined by Kjeldahl digestion, which converts organic N (proteins and nucleic acids) to inorganic ammonium (NH_4^+) with its posterior determination. The digestion was performed in a wet digester system B-440 (Buchi, Switzerland). Dry plant material was ground to powder using a mortar and pestle, and 0.05 g was transferred to the digestion tubes together with 10 ml of 98% H_2SO_4 (v/v) and 10 g of K_2SO_4 . The solution was heated at 410 °C for 1:30 h, and cooled for 30 min. NH_4^+ was distilled after the addition of 25 ml of 32% NaOH (v/w) in a K-355 distillation unit (Buchi, Switzerland). The concentration of NH_3 released in the resulting alkaline mixture was calculated by back titration of 2% H_3BO_3 (v/v) buffer adjusted to pH 4.65 with 0.02 M HCl, following the specifications of a KF Titrino Plus 870 equipment (Metrohm, Switzerland).

Oxidative stress indexes

Lipid peroxidation was estimated by measuring the concentration of the by-product malondialdehyde, which reacts with thiobarbituric acid. The resulting chromophore absorbs at 535 nm, and the concentration was calculated directly from the extinction coefficient of $155 \text{ mM}^{-1} \text{ cm}^{-1}$. Ground frozen tissue (0.1 g) was transferred to a screw-capped 1.5 ml Eppendorf tube, and homogenized following addition of 1 ml of TCA–TBA–HCl reagent (15% (w/v) trichloroacetic acid (TCA), 0.37% (w/v) 2-thiobarbituric acid (TBA), 0.25 M HCl, and 0.01% butylated hydroxytoluene). After homogenization, the samples were incubated at 90 °C for 30 min in a heating block, then chilled in ice, and centrifuged at 12,000 g for 10 min. Absorbance was measured in a UV-2401 PC spectrophotometer (Shimadzu Corporation, Japan) at 535 nm and 600 nm, the absorbance at last wavelength to correct non-specific turbidity.

For chlorophyll (Chl) determination, 0.05 g of frozen leaves were homogenized with 10 ml 80% (v/v) acetone using a mortar and pestle. Homogenates were filter through a paper filter and absorbance was measured in a UV-2401 PC spectrophotometer (Shimadzu Corporation, Kyoto, Japan) at 645 and 663 nm. Total chlorophyll concentration was calculated according to the formula by Arnon (Porra, 2002):

Total Chl ($\text{mg g}^{-1} \text{ FW}$) = $\text{Chla} + \text{Chlb}$, where:

$$\text{ChIa} \left(\frac{\text{mg}}{\text{g FW}} \right) = \left[(12.7 \times A_{663}) - (2.69 \times A_{645}) \right] \frac{\mu\text{g}}{\text{mL}} \times \frac{10 \text{ mL} \times \text{mg}}{0.05 \text{ g FW} \times 10^3 \mu\text{g}}$$

$$\text{ChIb} \left(\frac{\text{mg}}{\text{g FW}} \right) = \left[(22.90 \times A_{645}) - (4.68 \times A_{663}) \right] \frac{\mu\text{g}}{\text{mL}} \times \frac{10 \text{ mL} \times \text{mg}}{0.05 \text{ g FW} \times 10^3 \mu\text{g}}$$

Preparation of non-protein thiol standard solutions

Biothiol stock standard solutions containing 50 mM of glutathione (GSH), homoglutathione (hGSH), cysteine (Cys), N-acetyl cysteine (N-AcCys), and 2 mM of γ -(Glu-Cys)₂-Ala (hPC₂), and γ -(Glu-Cys)₃-Ala (hPC₃) were prepared in analytical-grade type I water (Milli-Q Synthesis, Millipore). Aliquots of the stock solutions were immediately frozen in liquid N₂, lyophilized and stored at -80 °C. Standards of 0.5 mM GSH, Cys and N-AcCys and standards of 0.1 mM hPC₂ and hPC₃ were injected in the HPLC to set the retention times.

Analysis on non-protein thiols

Non protein thiols were analysed by High Performance Liquid Chromatography (HPLC) following the procedure described by Ortega-Villasante et. (2005). 0.1 g of frozen tissue was ground in liquid N₂ and 15 μ l of 5 mM N-acetyl cysteine (N-AcCys) was spiked as internal standard (Howden et al. 1995) prior homogenization with 300 μ l of 0.25 N HCl to quantify the thiols. The homogenate was centrifuged twice for 15 min at 12 000 g and 4°C in Eppendorf tubes. The clear supernatant was transferred to a boron-silica glass injection vial. Separation and detection of the thiols was carried out using the method described by Meuwly et al. (1995) with some modifications. Extracts (100 μ l) were injected in a Mediterranean Sea18 column (5 μ m, 250 x 4.6 mm; Teknokroma, Spain), using an Agilent 1200 HPLC system (Santa Clara, CA, USA). The mobile phase was built using two eluents: A (dH₂O: acetonitrile (v/v) in 98:2 ratio plus 0.01 % TFA) and, B (dH₂O: acetonitrile (v/v) in 2:98 ratio plus 0.01 % TFA). The gradient program, as for % solvent B, was: 2 min, 0%; 25 min; 25%; 26 min, 50%; 30 min, 50%; 35 min, 0%; 45 min, 0% Thiols were detected after post-column derivatization with Ellman's reagent (1.8 mM DTNB (5,5-dithio-bis (2 nitrobenzoic acid) in 300 mM K-phosphate, 15 mM EDTA at pH 7.0), in a thermostatic 1.8 ml reactor at 38°C, as described by Rauser (1991). The derivative compound, 5-mercapto-2-nitrobenzoate, had and absorption maximum at 412 nm.

Determination of nitrate reductase activity *in vitro*

The *in vitro* nitrate reductase (NR) activity was analysed following the procedure described by Ramón et al. (1989). Intact frozen tissue (0.5 g) was homogenised in 1 ml or 0.5 ml extraction solution for shoot and root respectively, freshly prepared by mixing 10 ml extraction buffer-30mM MOPS at pH 7.5, 5 mM Na₂-EDTA, 10 mM DTT, 10 mM ascorbic acid, 0.6% PVP, 10 µl 100 mM PMSF and 1 ml protease inhibitors cocktail. After centrifugation (14,000g) for 15 min at 4°C, the supernatant was kept at ice-cold until enzymatic activity assay. NR activity was measured by adding 0.1 ml 100 mM KNO₃, 0.5 ml reaction buffer (100 mM KH₂PO₄/K₂HPO₄, 1 mM EDTA, pH 7.5) and 0.1 ml 1 mg ml⁻¹ NADH. The reaction was started by adding 0.1 ml of enzymatic extract and incubated for 15 min at 28°C. NO₂⁻ was analysed by the addition of 2 ml of freshly prepared colorimetric reagent (1% (v/v) sulphanilamide in 3 M HCl and 0.02% (w/v) N-(1-naphthyl) ethylenediamide dihydrochloride mixed in a 1:1 ratio). Homogenates were centrifuged at 1,000 x g for 15 min and absorbance was measured at 540 nm in a UV-2401 PC spectrophotometer (Shimadzu Corporation, Kyoto, Japan).

Glutathione reductase and ascorbate peroxidase

Glutathione reductase (GR) and ascorbate peroxidase (APX) activities were determined *in gel* after separation of protein extracts by non-denaturing electrophoresis in 10% polyacrylamide gels. Extracts were prepared from 0.5 g of intact frozen samples in 1 ml extraction solution, freshly prepared by mixing 10 ml extraction buffer-30mM MOPS at pH 7.5, 5mM Na₂-EDTA, 10 mM DTT, 10mM ascorbic acid, 0.6% PVP, 10 µl 100mM PMSF and 1 ml protease inhibitors cocktail. After centrifugation (14,000g) for 15 min at 4°C, the supernatant was stored as single use 100-200 µl aliquots at 80°C. Protein concentration in the extracts was preliminarily determined with the BioRad Protein Assay reagent, and the final loading for activity staining was adjusted after denaturing gel electrophoresis and Coomassie-blue staining (Laemmli, 1970). Protein loading for GR and APX analysis was 15 µg and 5 µg of shoot and root extracts, respectively. Gel slabs were incubated in GR staining solution (250mM Tris-HCl buffer at pH 7.5, supplemented with 0.2 mg ml⁻¹ thiazolyl blue tetrazolium bromide, 0.2 mg ml⁻¹ 2,6-dichlorophenol indophenol, 0.5 mM NADPH and 3.5 mM oxidised glutathione (Kaplan, 1969). APX was detected as described by Jimenez et al. (1998). Gel slabs were incubated for 20 min with 2 mM ascorbate and 2 mM H₂O₂ in 50 mM Na-phosphate buffer at pH 7.0. The APX activity was detected with 0.5 mM nitroblue tetrazolium (NBT) and 10 mM TEMED in 50 mM phosphate buffered at pH 7.8. A digital camera

(Kodak 290, USA) was used to take the gel pictures and they were processed by Kodak 1D Image Analysis Software (ver. 3.6). Selected regions of interest were of the same area and pixel intensity measured against the background. Data were given relative to the intensity of control samples. Only relevant differences are presented, and gels representative of three independent assays are shown.

Statistical analysis

Statistical analysis was performed using SPSS software for Windows (version 15.0), by using an ANOVA with Tukey test when the signification in Levene test was > 0.05 or Welch with Games-Howell test when the signification in Levene test was < 0.05 . Results were mean of at least three independent replicates \pm standard deviation, with significant differences between treatments at $p < 0.05$.

RESULTS

Mercury concentration and biometric parameters

Root Hg concentration was between 10 and 30 times higher than in shoot (Fig. 1). The treatments with Hg caused significant accumulation of Hg in shoot and root, increasing concomitantly with the higher doses of Hg in the nutrient solution. In addition, nitrate status affected the concentration of Hg in the organs, increasing with low NO_3^- supply. Significant differences were presented in root. It should be noted that shoot control accumulated between 7 and 10 $\mu\text{g g}^{-1}$ of Hg.

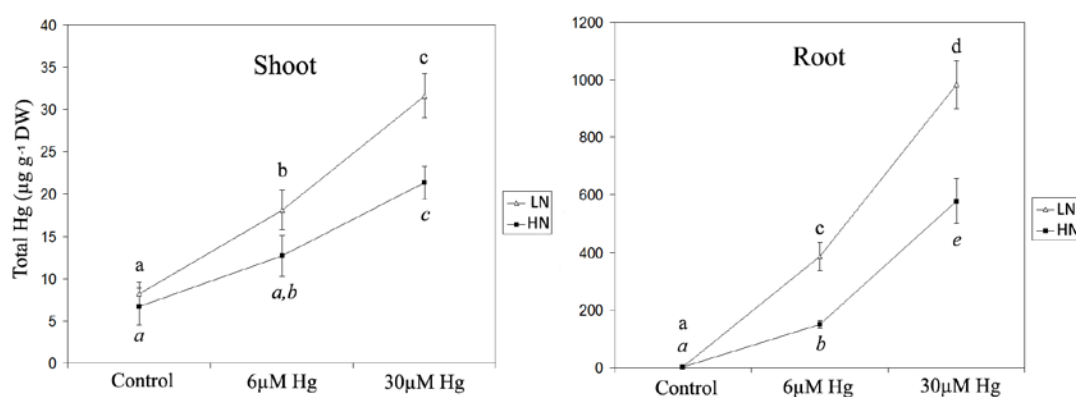


Fig. 1. Total Hg ($\mu\text{g g}^{-1}\text{DW}$) in shoot and root from 3-week-old *Medicago sativa* grown in low NO_3^- (LN; 2 mM) and high NO_3^- (HN; 12 mM) treated with 0 μM (control), 6 μM and 30 μM of Hg for 7 days. Data are average of five independent replicates (\pm SD). Different letters denote significant differences between treatments at $p < 0.05$. (Regular letter for LN and italics for HN).

Treatments with Hg had not appreciable effect on shoot biomass. However root length decreased with 6 and 30 μM Hg (*c.a.* 45%; data not shown). Regarding NO_3^- nutritional status, there were significant differences in shoot fresh weight between the LN and HN plants under control and 6 μM Hg conditions, whereas in plants treated with 30 μM Hg differences were minimal. However, the effects of NO_3^- on root fresh weight under Hg exposure were not significant in any of the combinations (Fig. 2). Similar pattern was observed by measuring shoot and root length, where the clearest differences in size between LN and HN occurred in plants treated with 6 μM Hg (data not shown).

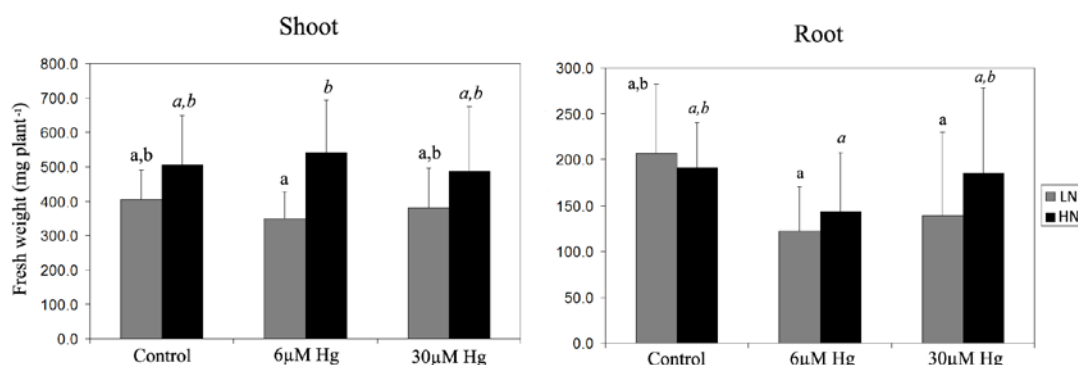


Fig. 2. Fresh weight (mg plant^{-1}) in shoot and root from 3-week-old *Medicago sativa* grown in low NO_3^- (LN; 2 mM) and high NO_3^- (HN; 12 mM) treated with 0 μM (control), 6 μM and 30 μM of Hg for 7 days. Data are average of at least three independent assays (\pm SD). Different letters denote significant differences between treatments at $p < 0.05$. (Regular letter for LN and italics for HN).

Nitrogen assimilation

In shoot, the accumulation of NH_4^+ increased as expected in plants grown with higher NO_3^- concentration. The exposure to 6 μM Hg did not varied substantially N assimilation, and only diminishes slightly in plants treated with 30 μM Hg (Fig. 3). A stronger diminution was found however in the roots of plants grown with 6 μM Hg with low NO_3^- supply, values that were similar in 30 μM Hg-treated plants (Fig. 3). Interestingly, plants grown in high NO_3^- supply suffered a more moderated decrease (Fig. 3). It should be noted that similar values of NH_4^+ concentration were found when expressed as a percentage per dry matter. This was expected, since there is an almost linear correlation of plant biomass relative to concentration of N in the nutrient solution. NR activity reflected a similar behaviour as was observed for NH_4^+ content in plants, being higher in plants grown with NO_3^- . Shoot NR activity was three-times greater than in root, indicating that in alfalfa the largest proportion of NO_3^- was assimilated in

the shoot (Fig. 4). None of the Hg-treatments affected NR activity in the shoot. However, in root some remarkable changes were detected: root NR activity augmented in plants exposed to 6 μM Hg, with c.a. two-fold higher activity in plants treated with high NO_3^- (Fig. 4). Finally, root NR activity decreased almost to control values with 30 μM Hg, showing a typical homeostasis response.

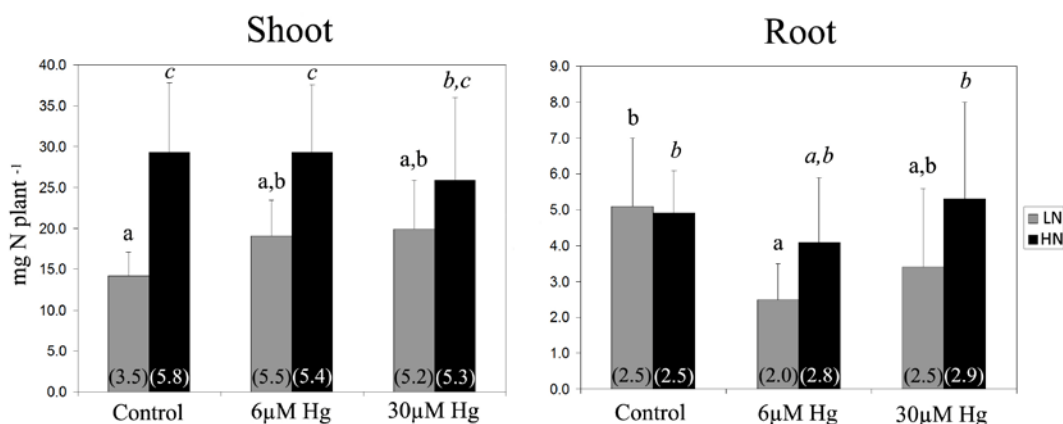


Fig. 3. Nitrogen accumulation (mg NH_4^+ plant⁻¹) and nitrogen percentage (%; in parenthesis) in shoot and root of 3-week-old *Medicago sativa* grown in low NO_3^- (LN; 2 mM) and high NO_3^- (HN; 12 mM) treated with 0 μM (control), 6 μM and 30 μM of Hg for 7 days. Data are average of at least three independent assays (\pm SD). Different letters denote significant differences between treatments at $p < 0.05$. (Regular letter for LN and italics for HN).

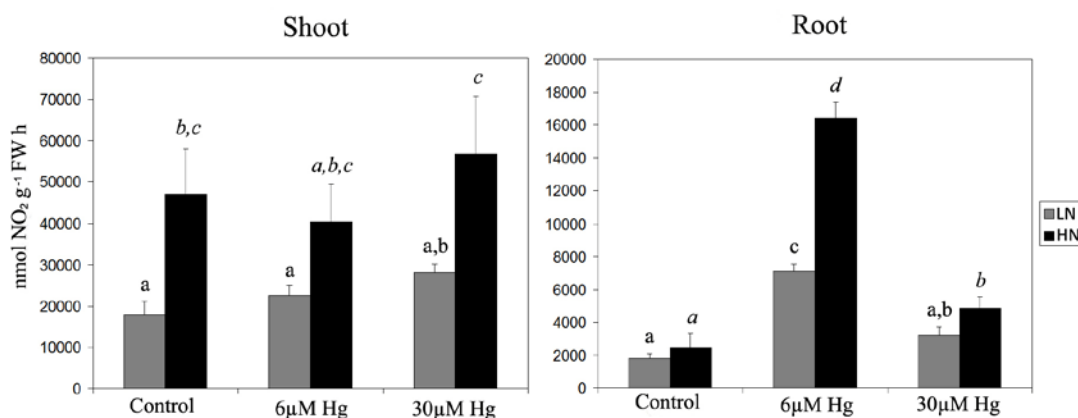


Fig. 4. Nitrate reductase activity (NR) ($\text{nmol NO}_2^- \text{g}^{-1} \text{FW h}$) in shoot and root of 3-week-old *Medicago sativa* grown in low NO_3^- (LN; 2 mM) and high NO_3^- (HN; 12 mM) treated with 0 μM (control), 6 μM and 30 μM of Hg for 7 days. Data are average of at least three independent replicates (\pm SD). Different letters denote significant differences between treatments at $p < 0.05$. (Regular letter for LN and italics for HN).

Stress indexes

Lipid peroxidation was evaluated by malondialdehyde (MDA) content in alfalfa plants. ANOVA analysis did not find differences or relation in shoot regarding to Hg and NO_3^- treatments. On the contrary, Hg treatments caused a clear increase in the MDA content

in root, which augmented in a metal concentration manner in plants supplied with high NO_3^- (Fig. 5). Moreover, in the absence of Hg low NO_3^- supply caused a significant increase in lipid peroxidation compared with high NO_3^- plants (Fig. 5). The concentration of chlorophyll was not affected by Hg exposure in plants treated with high NO_3^- concentration (Fig. 6). However, plants exposed 30 μM Hg and grown in low NO_3^- suffered a slight diminution in chlorophyll content.

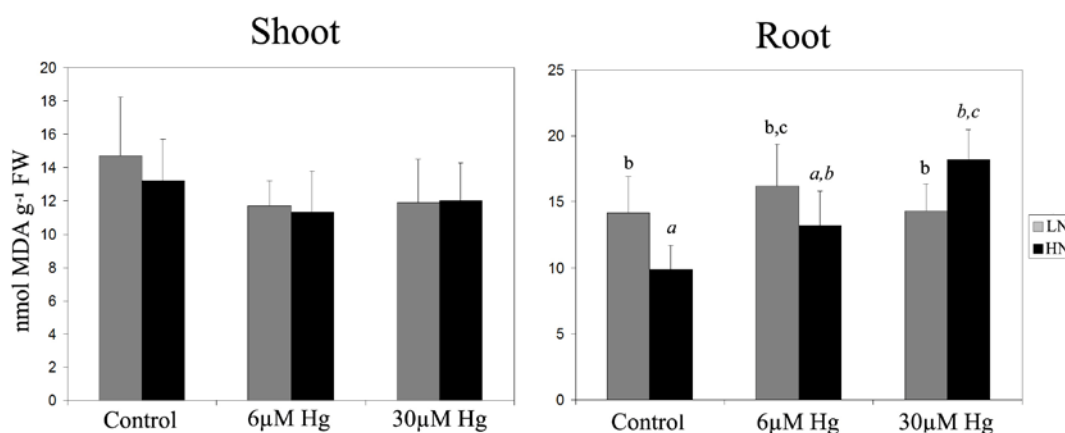


Fig. 5. Lipid peroxidation (nmol MDA g⁻¹ FW) in shoot and root of 3-week-old *Medicago sativa* grown in low NO_3^- (LN; 2 mM) and high NO_3^- (HN; 12 mM) treated with 0 μM (control), 6 μM and 30 μM of Hg for 7 days. Data are average of five independent replicates (\pm SD). Different letters denote significant differences between treatments at $p < 0.05$. (Regular letter for LN and italics for HN).

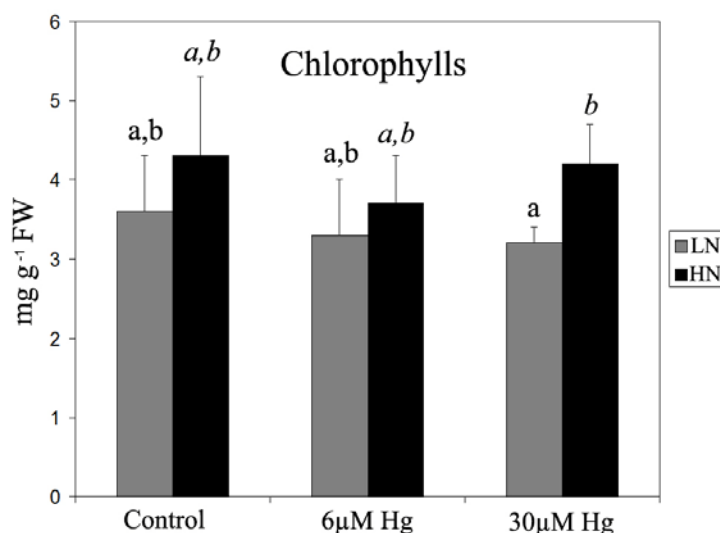


Fig. 6. Chlorophyll concentration (mg g⁻¹ FW) in leaves of 3-week-old *Medicago sativa* grown in low NO_3^- (LN; 2 mM) and high NO_3^- (HN; 12 mM) treated with 0 μM (control), 6 μM and 30 μM of Hg for 7 days. Data are average of five independent replicates (\pm SD). Different letters denote significant differences between treatments at $p < 0.05$. (Regular letter for LN and italics for HN).

APX activity increased only slightly under Hg stress in shoot and root, independently of the level of NO_3^- (Fig. 7). Similarly, shoot GR activity did not vary appreciably. However, root GR activity of plants with high NO_3^- decreased with 6 μM Hg until it was completely inhibited with 30 μM Hg (Fig. 7). Additionally, plants grown with high NO_3^- the inhibition of GR activity was more attenuated when treated with 6 μM Hg (Fig. 7).

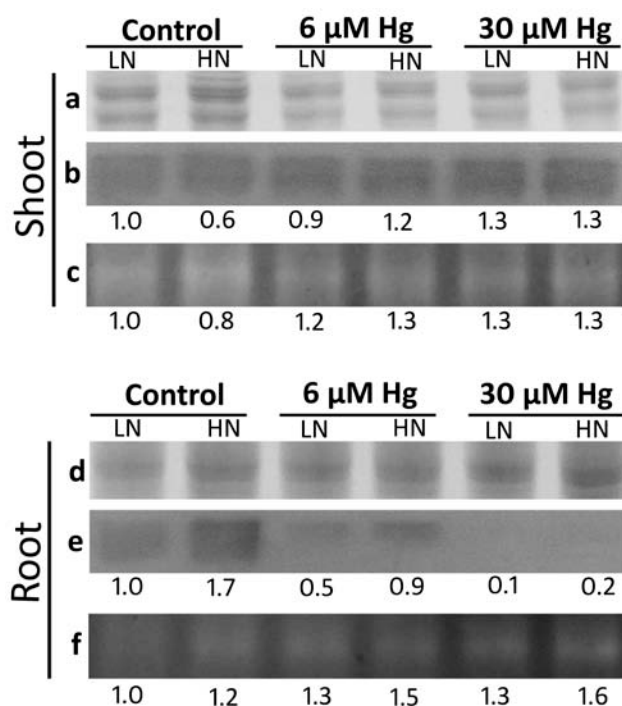


Fig. 7. Effect of Mercury on *in gel* Glutathione reductase (GR) and Ascorbate peroxidase (APX) activity in shoot and root of 3-week-old *Medicago sativa* grown in low NO_3^- (LN; 2 mM) and high NO_3^- (HN; 12 mM) treated with 0 μM (control), 6 μM and 30 μM of Hg for 7 days. **a, d)** coomassie-blue general staining of proteins to show equivalent loading of proteins, **b, e)** GR activity; and **c, f)** APX activity. To improve the visualization of differences between treatments, numbers below the band represent the relative fold-change against the LN control

Biothiols

The concentration of biothiols was determined to assess the effects of NO_3^- nutrition. As shown in Table 1, hGSH was the major biothiol in alfalfa and its concentration in shoot was between 2 and 3 times higher than in root. The exposition of plant to Hg increased slightly the content of hGSH in root. Differences in NO_3^- concentration did not produced differences in the biothiol content, except for root exposed to 6 μM Hg where a high NO_3^- supply caused an increase in hGSH content. ANOVA analysis did not find differences in the rest of thiols content with respect to Hg and NO_3^- treatments. Cysteine (Cys) in shoot, phytoquelatins (PC) or homophytoquelatins (hPC) in root and shoot were not detected in the plant extracts.

Table 1. Non-protein thiols content (nmol g⁻¹ FW) in shoot and root of 3-week-old *Medicago sativa* grown in low NO₃⁻ (LN; 2 mM) and high NO₃⁻ (HN; 12 mM) treated with 0 μM (control), 6 μM and 30 μM of Hg for 7 days. Concentration of each thiol peptide was calculated equivalent to the internal standard of N-Ac-Cys. Data are average of three independent replicates (± SD).

Thiol	NO ₃ ⁻	ROOT			SHOOT		
		Control	6 μM Hg	30 μM Hg	Control	6 μM Hg	30 μM Hg
Cys	LN	21.6±12.2	16.1±3.1	25.0±6.8	nd	nd	nd
	HN	17.4±2.8	16.8±4.5	25.5±7.1	nd	nd	nd
hGSH	LN	64.3±10.4 ^a	64.1±18.3 ^a	93.7±21.5 ^{a,b}	192.7±63.5	178.6±64.3	192.8±61.4
	HN	69.4±33.0 ^a	127.7±44.1 ^b	102.6±19.5 ^{a,b}	193.9±38.9	205.1±69.7	224.7±92.5
GSH	LN	31.7±15.7	29.0±9.9	39.8±9.7	27.9±10.9	25.8±9.5	18.9±5.4
	HN	27.9±12.2	29.5±11.5	29.9±9.9	41.3±6.2	21.1±7.2	18.8±3.5

n.d: no detected

Different letters denote significant differences between treatments at $p < 0.05$.

DISCUSSION

The concentration of Hg increased in plants following the concentration of Hg in the nutrient solution, being accumulated basically in the root. These results are in agreement with previous studies carried out with plants exposed to Hg (Beauford et al., 1976; Sinha et al., 1996; Rellán-Álvarez et al., 2006). The lower Hg content in shoot may be due to the fact that alfalfa plant is prone to restrict the movement of Hg to shoot by Hg immobilization in root, showing typical excluder behaviour (Briat and Lebrun, 1999). It is well known that Hg is a rather immobile element that binds strongly with different cell components at the cell wall and biological membranes (proteins and carbohydrates mainly; Hall 2002), precluding the Hg translocation to the shoot (Beauford et al., 1976; Siegel et al., 1987). Control plants grown with low and high NO₃⁻ accumulated a detectable level of Hg in shoot, result that could be explained by the potential volatilization of Hg from the nutrient solutions and its absorption by the leaves without translocation to root (Suszcynsky and Shann, 1995).

The higher content of NH₄⁺ in shoots than in roots (c.a. 5-times higher) and higher NR activity in shoots (also c.a. 5-times higher) indicate that alfalfa plants assimilate NO₃⁻ mostly in the shoot. These results were in agreement with the described behaviour of alfalfa plants at a vegetative development stage (Vance and Heichel, 1981). This decrease in shoot N content was reflected in the higher chlorophyll concentration of high NO₃⁻ plants. It is well known that chlorophylls are a good index of N nutritional status, as a severe depletion causes chlorosis (Evans, 1983; Bojovic and Marcovic, 2009). Under Hg exposure there were no changes in the amount of NH₄⁺ in shoots,

although NH_4^+ content was significantly lower in plants treated with low NO_3^- . As already commented, this could be due to the higher NO_3^- assimilation ratio in leaves. Hg would not affect NO_3^- metabolism and assimilation in shoot since Hg accumulates to a much less extent in this organ. With respect to the roots, under $6 \mu\text{M}$ Hg, alfalfa roots suffer a clear diminution of NH_4^+ content with low NO_3^- supply. Similarly, *Lycopersicon esculentum* plants treated with Cd suffered also a clear diminution of accumulation of NH_4^+ in plants treated with $50 \mu\text{M}$ Cd (Chaffei et al., 2004). Moreover, Hernández et al. (1997) found a rapid impairment of NO_3^- uptake and assimilation, reflected in a remarkable inhibition of NR under Cd stress.

It has been shown that NR activity was differently affected by Cd stress. In studies performed with *Silene cucubalus* exposed to less than $5 \mu\text{M}$ Cd (Mathys, 1975) and *Phaseolus vulgaris* exposed to the range of $10\text{-}100 \mu\text{M}$ Cd (Gouia, 2000), NR activity decreased with the concentration of Cd. However, Chugh et al. (1992) reported that NR activity was not affected by exposure to Cd concentrations below to $50 \mu\text{M}$ in *Pisum sativum*. In our case, NR activity augmented remarkably in the root of plants exposed to $6 \mu\text{M}$ Hg with high NO_3^- . This activation could be also detected in plants with low NO_3^- , but to a lesser degree. It is feasible that the presence of Hg altered the balance of NO_3^- in the plant, causing that a higher proportion of NO_3^- would be assimilated in the root. Only at the highly toxic dose of $30 \mu\text{M}$ Hg NR activity decreased to control values, possibly as a consequence of cell poisoning (Van and Clijsters, 1990). This interesting results should be studied using more sensitive analytical procedures to trace the uptake and assimilation of NO_3^- in the plants, perhaps by monitoring isotopically labelled NO_3^- (^{15}N), which would allow a dynamic study of the process under Hg stress.

To our knowledge, our study is the first describing the influence of different NO_3^- nutritional levels on the phytotoxic effects caused by Hg in higher plants. The only available information about the effect of NO_3^- nutrition on heavy metals uptake and accumulation describes the behaviour of Cd in several crop plants. Thus, Finkemeier et al. (2003) found that Cd accumulation was not affected in barley plants by the absence of NO_3^- in the growth medium. Hassan et al., (2005) evaluated the effect of different N species on Cd accumulation and phytotoxic effects in rice plants, and found that only plants fed with $(\text{NH}_4)_2\text{SO}_4$ accumulated less Cd and were more tolerant, possibly due to a decrease in Cd availability imposed by the lower solubility of CdSO_4 salts. However, these authors did not study the responses in plants depleted of N. More recent studies

showed that the concentration of Cd in two rice genotypes decreased in shoots but increased in roots under high N nutritional status (Du et al., 2009). On the contrary, a high NO_3^- concentration in the nutrient solution produced a decrease of Hg concentration in plants, being this effect stronger in roots.

The significant higher accumulation of Hg in the roots of low NO_3^- plants could not be explained completely in terms of a dilution effect, as there were not significant differences in biomass compared with high NO_3^- grown plants. Indeed, the only significant differences in biomass were found in shoot, where Hg accumulated to a lesser extent. Therefore, some tolerance mechanisms should be active to promote a diminution in Hg uptake in high NO_3^- treated alfalfa. One possibility might be the larger accumulation of hGSH in the roots of high NO_3^- plants exposed to 6 μM Hg: c.a. two-fold increase compared low NO_3^- plants (Table 1). Biothiols, and in particular phytochelatins are important ligands in Hg detoxification, as we described in our recent work (Carrasco-Gil et al., 2011). Although we tried to detect phytochelatins, we were unable to detect them in our experiment. We know that storage for a prolonged period of samples at -80°C causes a dehydration that affects the stability of phytochelatins, as occurred with our samples. To confirm this hypothesis we have planned new experiments to detect biothiols in fresh material, which will also allow us the detection of Hg-biothiol complexes in under low and high NO_3^- levels.

About the stress symptoms evaluated, plants grown with low NO_3^- were slightly more affected than plants treated with high NO_3^- . Thus, root lipid peroxidation was higher in plants exposed to 6 μM Hg, but at the higher dose of Hg there were no different between both NO_3^- levels. Several studies show the negative Hg effects on plant development and the induction of oxidative stress (Ortega-Villasante et al., 2005; Israr and Sahi, 2006; Israr et al., 2006; Rellán-Álvarez et al., 2006). The lipid peroxidation was similar in root and shoot, whereas in other studies carried out in *Lycopersicon esculentum* exposed to 10 and 50 μM Hg (Cho and Park, 2000) or in alfalfa exposed to 30 μM Hg (Ortega-Villasante et al., 2005) grown in pure hydroponic conditions, the lipid peroxidation in root was higher than in shoot.

On the other hand, the chlorophyll content was not affected by Hg exposition. This is in agreement with Cargnelutti et al. (2006) which reported that the presence of 0.5 and 50 μM Hg in *Cucumis sativus* L. seedling grown in a solid medium did not exert effect on the chlorophyll content. However, Cho and Park (2000) observed a decrease in the chlorophyll content of *Lycopersicon esculentum* exposed to 10 and 50 μM Hg for 10

and 20 days under pure-hydroponic conditions. It is feasible that the differences in the behaviour of stress parameters depend on the growth conditions, as was observed previously by Sobrino-Plata et al. (2009). Redjala et al. (2010) studied the relationship between root structure and Cd uptake in *Zea mays*. They reported that different cultivation methods, such as soil or hydroponic, produces differences in the maturation of root exodermis and endodermis with impact in Cd uptake. In a hydroponic system, the formation of root apoplastic barriers occurred farther from the root tip than in soil grown plants. Thus, root surfaces without suberization facilitate ion influx causing a higher Cd uptake rate, which in turn increased its phytotoxicity in a pure hydroponic system. Therefore, different root architecture may affect greatly the uptake and transport characteristics of metals under certain growth conditions and cultivation systems, as occurred in studies performed with a semi-hydroponic system.

There was not a clear effect of Hg on APX activity in alfalfa plants grown either in low or high NO_3^- . These results were basically in agreement with those described by Sobrino-Plata et al. (2009), who found a modest induction of APX in alfalfa plants grown in semi-hydroponic conditions. Again, only when plants were grown in a pure hydroponic system remarkable changes in APX was observed, as reported in maize roots grown under hydroponic conditions. These plants suffered an increase of activity with 6 μM Hg, but then it was inhibited with 30 μM Hg (Rellán-Álvarez et al., 2006). On the other hand, GR activity decreased considerably in roots with 6 μM Hg, and it was inhibited with 30 μM Hg. This enzyme contains a key cysteine rich domain prone to be blocked by Hg, rendering the enzyme inactive in the presence of Hg (Sobrino-Plata et al., 2009). This inhibition was also metal specific, since with Cd this effect was not observed. By contrast, in a study carried out by Israr (2006) with *Sebania drummondii* seedlings exposed to a range from 0 to 500 μM Hg, GR activity increased slightly with the Hg concentration. Interestingly, roots supplied with low NO_3^- showed lower GR activity than those with high NO_3^- , that was inhibited but to a lesser extent. This could be related to the concentration of Hg in plants, since roots with low NO_3^- accumulated higher Hg level, and thus the toxic effect of Hg would be more acute. Therefore, GR follows the general trend that low NO_3^- plants were more affected than high NO_3^- plants when treated with 6 μM Hg.

The plant ability to increase the antioxidant protection and then cope with the negative impact of the stress produced by heavy metals, seems to be more limited in low NO_3^- plants. Studies of heavy metal exposition such as Cu and Cd performed with *Pisum*

sativum (Bielawski and Joy, 1986) or with *Helianthus annuus* (Gallego et al., 1996) reported that the decrease of GR activity could be related to the reduction of the GSH levels. Indeed, in the present study we observed a remarkable increase in hGSH concentration in high NO_3^- plants, which could prevent oxidative damages as pointed out by lower lipid peroxidation observed in these plants. Our findings would imply a possible better redox adjustment of well-nourished plants exposed to a moderate dose of Hg.

CONCLUSIONS

The NO_3^- nutritional status of plants might be important to improve their tolerance to Hg. Oxidative stress indexes as lipid peroxidation and chlorophyll content together with GR antioxidant enzymatic activity were less affected with the high NO_3^- supply, in particular at moderate levels of Hg (6 μM). More work is needed to a better understanding of the mechanisms of tolerance involved. Such research will lead the way to optimise the use of plants in phytotechnologies that might help to clean up polluted or stabilise them to avoid erosion and loss of fertility, at first instance in the Almadén area.

REFERENCES

- Barrutia O., Epelde L., García-Plazaola J.I., Garbisu C. & Becerril J.M. (2009) Phytoextraction potential of two *Rumex acetosa* L. Accessions collected from metalliferous and non-metalliferous sites: Effect of fertilization. *Chemosphere* **74**, 259-264.
- Beauford W., Barber J. & Barringer A.R. (1976) Uptake and distribution of Hg within higher plants. *Physiologia Plantarum* **39**, 261-265.
- Bielawski W. & Joy K.W. (1986) Reduced and oxidized glutathione and glutathione reductase activity in tissues of *Pisum sativum*. *Planta* **169**, 267-.
- Bojović B. & Marković A. (2009) Correlation between nitrogen and chlorophyll content in wheat (*Triticum aestivum* L.) *Kragujevac Journal Science* **31**, 69-74.
- Briat J.F. & Lebrune M. (1999) Plant response to metal toxicity. C. Real. Academy of. Sciences. Paris 322, 43-54.
- Campbell W.H. (1999) Nitrate reductase structure, function and regulation: bridging the gap between biochemistry and physiology. *Annual Review of Plant Physiology and Plant Molecular Biology* **50**, 277-303.
- Cargnelutti D., Tabaldi L.A., Spanevello R.M., Jucoski G.D., Battisti V., Redin M., Linares C.E.B., Dressler V.L., Flores E.M.D., Nicoloso F.T., Morsch V.M. & Schetinger M.R.C. (2006) Mercury toxicity induces oxidative stress in growing cucumber seedlings. *Chemosphere* **65**, 999-1006.
- Carrasco-Gil S., Álvarez-Fernández A., Sobrino-Plata J., Millán R., Carpena-Ruiz R.O., LeDuc D.L., Andrews J.C., Abadía J. & Hernández L.E. (2011) Complexation of Hg with phytochelatins is important for plant Hg tolerance. *Plant, Cell and Environment* (in press).
- Chaffei C., Pageau K., Suzuki A., Gouia H., Ghorbel M.H. & Masclaux-Daubresse C. (2004) Cadmium toxicity induced changes in nitrogen management in *Lycopersicon esculentum* leading to a metabolic safeguard through an amino acid storage strategy. *Plant and Cell Physiology* **45**, 1681-1693.
- Cho U.H. & Park J.O. (2000) Mercury-induced oxidative stress in tomato seedlings. *Plant Science* **156**, 1-9.

- Chugh, L.K., Gupta, V.K., Sawhney S.K., 1992. Effect of cadmium on enzymes of nitrogen metabolism in pea seedlings. *Phytochemistry* **31**, 395-400.
- Clemens S., Palmgren M.G. & Krämer U. (2002) A long way ahead: understanding and engineering plant metal accumulation. *Trends in Plant Science* **7**, 309-315.
- Du Q., Chen M.X., Zhou R., Chao Z.Y., Zhu Z.W., Shao G.S. & Wang G.M. (2009) Cd toxicity and accumulation in rice plants vary with soil nitrogen status and their genotypic difference can be partly attributed to nitrogen uptake capacity. *Rice Science* **16**, 283-291.
- Elbaz A., Wei Y.Y., Meng Q., Zheng Q. & Yang Z.M. (2010) Mercury-induced oxidative stress and impact on antioxidant enzymes in *Chlamydomonas reinhardtii*. *Ecotoxicology* **19**, 1285-1293.
- Evans J.R. (1983) Nitrogen and photosynthesis in the flag leaf of wheat (*Triticum aestivum* L.). *Plant Physiology* **72**, 297-302.
- Finkemeier I., Kluge C. Metwally A., Georgi M., Grotjohann N., & Dietz K.J. (2003) Alterations in Cd-induced gene expression under nitrogen deficiency in *Hordeum vulgare*. *Plant Cell and Environment* **26**, 821-833.
- Foyer C.H., López-Delgado H., Dat J.F. & Scott I.M. (1997) Hydrogen peroxide and glutathione associated mechanisms of acclamatory stress tolerance and signalling. *Physiologia Plantarum* **100**, 241-254.
- Gallego S.M., Benavides M.P. & Tomaro M.L. (1996) Effect of heavy metal ion excess on sunflower leaves: evidence for involvement of oxidative stress. *Plant Science* **121**, 151-159.
- Gao X., Brown K.R., Racz G.J. & Grant C.A. (2010) Concentration of cadmium in durum wheat as affected by time, source and placement of nitrogen fertilization under reduced and conventional-tillage management. *Plant and Soil* **337**, 341-354.
- Gouia, H., Habib, M., Meyer, C. 2000. Effects of cadmium on activity of nitrate reductase and on other enzymes of the nitrate assimilation pathway in bean. *Plant Physiology and Biochemistry* **38**, 629-638.
- Hall J.L. (2002) Cellular mechanisms for heavy metal detoxification and tolerance. *Journal of Experimental Botany* **366**, 1-11.
- Han F.X., Su Y., Monts D.L., Waggoner C.A. & Plodinec M.J. (2006) Binding, distribution, and plant uptake of mercury in a soil from Oak Ridge, Tennessee, USA. *Science of The Total Environment* **368**, 753-768.
- Hernández L.E., Carpena-Ruiz R. & Gárate A. (1996) Alterations in the mineral nutrition of pea seedlings exposed to cadmium. *Journal of Plant Nutrition* **19**, 1581-1598.
- Hernández L.E., Gárate A. & Carpena-Ruiz R. (1997) Effects of Cadmium on the uptake, distribution and assimilation of nitrate in *Pisum sativum*. *Plant and Soil* **189**, 97-106.
- Howden R., Goldsbrough P.B., Andersen C.R., Cobbett C.S. (1995). Cadmium-sensitive, cad1 mutants of *Arabidopsis thaliana* are phytochelatin deficient. *Plant Physiology* **107**, 1059-1066.
- Israr M. & Sahi S.V. (2006) Antioxidative responses to mercury in the cell cultures of *Sesbania drummondii*. *Plant Physiology and Biochemistry* **44**, 590-595.
- Israr M., Sahi S., Datta R. & Sarkar D. (2006) Bioaccumulation and physiological effects of mercury in *Sesbania drummondii*. *Chemosphere* **65**, 591-598.
- Jiménez A., Hernández J.A., Ros-Barceló A., Sandalio L.M., del Río L.A. & Sevilla F. (1998) Mitochondrial and peroxisomal ascorbate peroxidase of pea leaves. *Physiologia Plantarum* **104**, 687-692.
- Kaplan J.C. & Beutler E. (1968) Electrophoretic study of glutathione reductase in human erythrocytes and leukocytes. *Nature* **217**, 256-.
- Laemmli U.K. (1970) Cleavage of structural proteins during the assembly of the head of bacteriophage T4. *Nature* **227**, 680-685.
- Ma C. (1998) Hg harm on cell membrane of rape leaf and cell endogenous protection effect. *Yingyong Shengtai Xuebao* **9**, 323-326.
- Mathys W. (1975) Enzymes of heavy metals resistant and non resistant population of *Silene cucubalus* and their interactions with some heavy metals *in vitro* and *in vivo*. *Physiologia Plantarum* **33**, 161-165.

- Meuwly P., Thibaul P., Schwan A.L. & Rauser W.E. (1995) Three families of thiol peptides are induced by cadmium in maize. *The Plant Journal*, **7**, 391–400.
- Ortega-Villasante C., Rellán-Álvarez R., del Campo F.F., Carpena-Ruiz R.O. & Hernández L.E. (2005) Cellular damage induced by cadmium and mercury in *Medicago sativa*. *Journal of Experimental Botany* **56**, 2239-2251.
- Ortega-Villasante C., Hernández L.E., Rellán-Álvarez R., Del Campo F.F. & Carpena-Ruiz R.O. (2007) Rapid alteration of cellular redox homeostasis upon exposure to cadmium and mercury in alfalfa seedlings. *New Phytologist* **176**, 96-107.
- Patra M. & Sharma A. (2000) Mercury toxicity in plants. *Botanical Review* **66**, 379-422.
- Porra R.J. (2002) The history of the development and use of simultaneous equation for the accurate determination of chlorophylls a and b. *Photosynthesis Research* **73**, 149-156.
- Rauser W.E. (1991) Cadmium-binding peptides from plants. *Methods in Enzymology*, **205**, 319-333.
- Redjala T., Zelko I., Sterckeman T., Legué V. & Lux A. Relationship between root structure and root cadmium uptake in maize. *Environmental and Experimental Botany*, **In Press**.
- Rellán-Álvarez R., Ortega-Villasante C., Álvarez-Fernández A., del Campo F.F. & Hernández L.E. (2005) Stress responses of *Zea mays* to cadmium and mercury. *Plant and Soil* **279**, 41-50.
- Schutzendubel A. & Polle A. (2001) Plant responses to abiotic stresses: heavy metal-induced oxidative stress and protection by mycorrhization. *Journal of Experimental Botany* **372**, 1351-1365.
- Siegel S.M., Siegel B.Z., Barghigiani C., Aratani K., Penny P., Penny D.A. (1987) Contribution to the environmental biology of Hg accumulation in plants. *Water, Air, and soil Pollution* **33**, 65-72.
- Sinha S., Gupta M. & Chandra P. (1996) Bioaccumulation and biochemical effects of mercury in the plant *Bacopa monnieri* (L). *Environmental Toxicology and Water Quality* **11**, 105-112.
- Sobrino-Plata J., Ortega-Villasante C., Flores-Cáceres M.L., Escobar C., Del Campo F.F. & Hernández, L.E. (2009) Differential alterations of antioxidant defenses as bioindicators of mercury and cadmium toxicity in alfalfa. *Chemosphere* **77**, 946-954.
- Suszcynsky E.M. & Shann J.R. (1995) Phytotoxicity and accumulation of mercury in tobacco subjected to different exposure routes. *Environment Toxicology Chemistry* **14**, 61-67.
- Van AF. & Clijsters H. (1990) Effects of metals on enzyme activity in plants. *Plant, Cell and Environment* **13**, 195-206.
- Vance CP & Heichel GH (1981) Nitrate assimilation during vegetative regrowth of alfalfa. *Plant Physiology* **68**, 1052-1056
- Wang YH, Garcin D.F, & Kochian L.V. (2001) Nitrate-induced genes in tomato roots. Array analysis reveals novel genes that may play a role in nitrogen nutrition. *Plant Physiology* **127**, 345-359.
- Wong, M.H. (2003) Ecological restoration of mine degraded soils, with emphasis on metal contaminated soils. *Chemosphere* **50**, 775–780
- Zhang W.H. & Tyerman S.D. (1999) Inhibition of water channels by HgCl₂ in intact wheat root cells. *Plant Physiology* **120**, 849-857.
- Zhou Z.S., Huang S.Q., Guo K., Mehta S.K., Zhang P.C. & Yang Z.M. (2007) Metabolic adaptations to mercury-induced oxidative stress in roots of *Medicago sativa* L. *Journal of Inorganic Biochemistry* **101**, 1-9.



CHAPTER 6

Influence of nitrate fertilisation on Hg uptake and oxidative stress parameters in alfalfa plants cultivated in a Hg-polluted soil

ABSTRACT

The Almadén area (Spain) holds one of the biggest deposits of mercury (Hg) in the world, where cinnabar and other mineral ores had been extracted in the last two millennia. The study was carried out in a green house with soil from an agricultural land plot located in Almadén, which contained an average Hg concentration of 12.4 mg kg⁻¹. We compared physiological stress parameters sensitive to Hg in alfalfa plants grown in Hg-polluted soils that were amended with two different fertilizers: without NO₃⁻ (PK) or with NO₃⁻ (NPK). Several parameters of oxidative stress, such as antioxidative enzymatic activities, lipid peroxidation, and chlorophyll content were analysed. Our results suggest that nitrogen supply prevents oxidative stress in roots, but may improve root development and increase the uptake of Hg from the soil above safety consumption limits. This work opens new perspectives towards phytoremediation applications with alfalfa plants, highlighting the importance of proper nitrogen fertilization to improve tolerance to the pollutant.

INTRODUCTION

Mercury poses a serious threat to the environment and to human health, and as a result of more strict environmental policies its ore extraction, metal processing and trade are under severe restrictions in the European Union (European Commission, 2008). Amalgamation of gold with Hg in mining, chlor-alkali industry, dye production, elaboration of lamps and electronic equipment are examples of uses of Hg responsible of severe environmental problems in many regions of the World (UNEP, 2011). The accumulation of Hg in several ecosystems is aggravated by its long-term persistence, which led to dramatic human health problems as occurred in Minamata Bay (Japan), caused by the bioaccumulation and biomagnification of Hg in the food chain (Dushenkov et al., 1997). Soils are the sink of Hg in polluted urban and agricultural areas, accumulation that may result in structure degradation, crop yield reduction, and poor quality of agricultural products (Long et al., 2002).

The present study was performed using soil from Almadén area (Ciudad Real, Spain), which constitutes the largest and most unusual natural concentration of Hg in the World, where mining activities had been carried out from Roman times to the present (Higuera et al., 2003). According to Huckabee et al. (1983) and Higuera et al. (1999, 2000), the major proportion of Hg existing in Almadén originates from bed rock weathering and erosion, anthropogenic dispersion from abandoned mineral dumps and metal extraction and refining. Hg is predominantly found in cinnabar form (HgS) but elemental Hg (Hg⁰) is also presented, which might disperse long distances *via* the atmosphere after volatilisation (Higuera et al., 2000). In spite of the low solubility of HgS, Hg may be mobilised and absorbed by plants and animals, as some studies have shown. Thus, the degree of Hg accumulation in the natural vegetation collected from Almadén ranges from 0.12 to more than 65 mg kg⁻¹ dry weight (DW; Huckabee et al. 1983). Millán et al. (2006) found that there was a high correlation between available Hg in soil and Hg accumulation in plants sampled in ten different locations in the Almadén mining area. For example, Hg accumulation in *Rumex induratus* and *Marrubium vulgare* was a function of Hg availability in tested plots (Moreno-Jimenez et al. 2006). Plants capable of surviving in areas with a high metal content need to develop tolerance strategies (Levitt, 1980). Exclusion is the most common mechanism of plant adaptation to metal toxicity, and is the common strategy of plants grown in Hg-polluted soils (Moreno-Jimenez et al., 2006). Nevertheless, Hg can accumulate in the aerial parts of the plants by several ways: i) translocation from the roots once Hg is taken up from the

soil normally as Hg^{2+} , ii) *via* the stomata from the atmosphere as volatile Hg^0 (or even as Hg^{2+}), iii) through by adsorption of particulate Hg deposited on leaves or stem surfaces (Lindberg et al., 1979; Frescholtz et al., 2003).

Due to changes in land usage after the banning of mining activities in Almadén, several crop plants are being introduced to develop new economic activities based on agriculture in polluted soils. Consequently, it is important to evaluate the potential risk for human health and the environment considering the uptake and distribution of Hg in suitable crops (Ferrara et al., 1998; Berzas et al., 2003, Higuera et al., 2003). With this aim, some studies were performed growing plants under greenhouse conditions in pots containing polluted soil from Almadén sites (Sierra et al., 2008a, 2008b, 2009). These studies revealed that crops like *Solanum melongea* or *Lavandula stoechas* should not represent a risk for consumers, whereas *Vicia sativa*, which is used as forage for livestock was near the established safety limit. Therefore, crops grown in Almadén soils may accumulate Hg in the harvested parts. Whenever alternative crops are introduced in the area it is mandatory a detailed evaluation of Hg translocation to avoid a possible impact to human population or animal through the food chain.

The accumulation of Hg in plants is influenced greatly by the Hg available in soils. Mercury is absorbed by the root system and is translocated to the shoot (Patra et al., 2004), although most portion of Hg absorbed remain immobilised in roots as has been observed by a number of studies (Rellán-Álvarez et al., 2006; Sobrino-Plata et al., 2009; Carrasco-Gil et al., 2011). It is thought that the high toxicity of Hg is mainly due to the high affinity for sulfhydryl groups ($-\text{SH}$) of proteins and other S-containing molecules (i.e. biothiols). Once Hg binds proteins, their tertiary and quaternary structures are disturbed, losing their function (Clarkson, 1972). Also, Hg affects the membranes of higher plants cells producing aquaporins inhibition, increasing in lipid peroxidation, modifying solute permeability, and even disrupting their structural integrity (Ma, 1998). Several visual symptoms develop under Hg stress: stunted seedling growth, reduction in the root growth; decrease in the stem length, and diminution in chlorophyll content (Patra and Sharma, 2000).

The induction of oxidative stress is one of the several phytotoxic effects of Hg that occur rapidly in plants exposed to Hg. Accumulation of moderate to high levels of Hg in the plants may stimulate the production of reactive oxygen species (ROS), which leads to damage of proteins and membrane lipids (Rellán-Álvarez et al., 2006; Ortega-Villasante et al., 2005). In addition, the onset of oxidative stress may produce the

alteration in the concentration of glutathione (GSH), an important antioxidant that forms part of the ascorbate-glutathione ROS scavenging pathway (Mittler, 2002). The toxic action of Hg compounds may also be related to an alteration of antioxidant enzyme activities such as superoxide dismutase (SOD), ascorbate peroxidase (APX), glutathione reductase (GR; Ortega-Villasante et al., 2005; Rellán-Álvarez et al., 2006; Zhou et al., 2007). Of these stress parameters, we have studied the responses of GR, enzyme very sensitive to Hg accumulation in alfalfa roots (Sobrino-Plata et al. 2009).

The use of soil amendments, some times are necessary to revegetate a degraded area or to establish a crop, but these treatments may influence metal bioavailability and phytoextraction processes (Cunningham and Ow, 1996). The information available about agronomic practices and Hg availability in soils is rather scarce. Studies showed that the additions of nitrogen alter soil solution equilibrium (Alloway, 1995), and root morphological parameters (Barber, 1995) increasing the potential Hg uptake. To our knowledge, there is only one report that evaluated the interactive effect of nitrogen fertilizers on Cd concentration in the grain of durum wheat in real conditions (Gao et al., 2010). Therefore, more information about this respect is needed to determine how nitrogen fertilization modify the ability of crops to uptake and translocate Hg, which depends greatly on species or cultivars.

Alfalfa (*Medicago sativa*) has been cultivated in Almadén for decades, used as forage for livestock feed because of its high levels of proteins (Llorca et al., 1999). Alfalfa is a leguminous plant that has the ability to assimilate atmospheric nitrogen (N₂) thanks to the association with symbiotic N₂-fixing bacteria (i.e. *Sinorhizobium meliloti*). Therefore, these plants are normally able to obtain their own nitrogen requirements, and are able to grown in poor soils. In fact, these plants are used to improve soil fertility, and decreases fertilization needs.

In the present work, we compared physiological stress parameters sensitive to Hg in alfalfa plants grown in Hg-polluted soils obtained from Almadén, that were amended with two different fertilizers: without NO₃⁻ (PK) or with NO₃⁻ (NPK). Thus, the Hg accumulation, chlorophyll concentration, non-protein thiols content, lipid peroxidation level and activity of GR and APX antioxidant enzymes were assessed.

MATERIAL AND METHODS

Physical and chemical soil analysis

The soil for this study was collected from “Castilseras”, a site where agricultural activities have been carried out. This plot is in the area of influence of “El Entredicho” mine located in Almadén (Ciudad Real, Spain). The soil was sampled in ten points along the plot collecting every sample from the first 30 cm. The soil was air dried and sieved to 2 mm. The texture of the soil was analysed according to UNE norms: 103-101 (1995) and 103-102 (1995). The soil pH was determined with a pH-meter Orion 525a in 2:1 distilled water:soil (v/v). Electrical conductivity was determined in 2:1 (v/v) extraction ratio of soil and distilled water using a Crison-MICRO CM 2200 conductivity/temperature meter. Organic matter was measured according to Walkey-Black (1934). The CEC was carried out according to Sierra et al. (2008b) using ammonium acetate. Total C/H/N was analysed using an Elemental Analyzer CHN-600 Leco (St. Joseph, Michigan, MI, USA) based on a dry combustion method. Available macronutrients were extracted with the procedure described by Soltampour and Schwab (1977) and analysed using inductively coupled plasma-mass spectroscopy (ICP-MS).

Experimental design, plants and growth conditions

The experiment was performed under greenhouse conditions. The soil sieved to 2 mm was mixed with perlite and sand in equal proportions (v/v) and placed in 48 pots with a total volume of 3 L. and then, they were watered with 0.5 L of water to initiate the drainage. Inorganic fertilisation was applied according to the nutritional requirements of irrigated alfalfa crops (Del Pozo, 1983). Half of the plants (24 pots) were fertilized with a NPK mixture (30:110:100; adequate NO_3^-), where nitrogen was added as NH_4NO_3 . A second batch (24 pots) was only fertilized with a PK mixture (110:100, poor NO_3^-). Phosphate and potassium were also added as K_2HPO_4 and KH_2PO_4 forms. Following the agronomic practices in Almadén area (MAPA, 1998), plants were sown in April. Two weeks before sowing, the pots were ground fertilized with phosphate and potassium doses. Nitrogen was applied at the moment alfalfa seedlings were sown to avoid excess drainage due to the high solubility of NH_4NO_3 .

Alfalfa (*Medicago sativa* cv. Aragon) seedlings were surface sterilized for 5 min in 5% (v/v) commercial bleach. After rinsing several times with distilled water, seeds were soaked overnight at 4°C. Fifteen homogeneous selected seedlings were transferred to

each pot where they were germinated. Periodic irrigations with tap water was performed according to the water requirements of the culture.

Sampling

Sampling was performed at two different growth stages: seedling (three weeks after sowing) and elongation (seven weeks after sowing), which was close to the first “cut in green” for forage uses. Soil and plants were collected in 12 pools formed by the mixing of four pots (see Fig.1). Plants were divided in shoot and root and placed into beakers and rinsed several times with 10 mM Na₂ EDTA solution to remove superficial Hg. Then length and fresh weight of roots and shoots were measured and stored at -80°C or air dried until analysis. The soils were air dried and stored at room temperature until analysis.

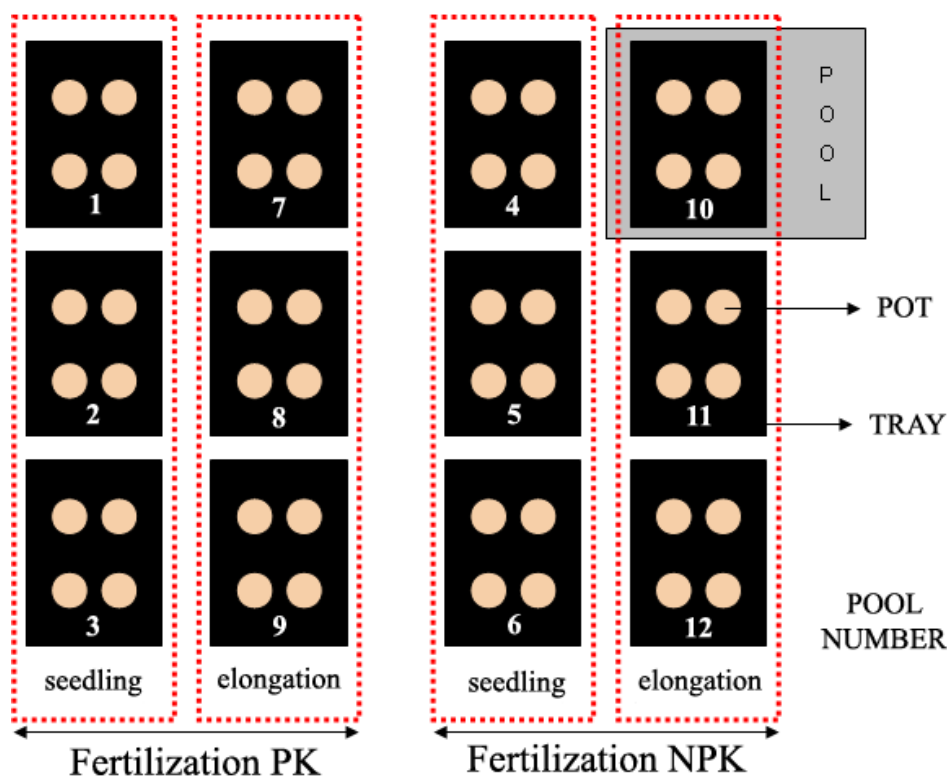


Fig. 1. Pots distribution in the greenhouse with respect to the fertilization applied and the growth stages sampled

Mercury determination

Solid samples of soil and plants (roots and shoot) were air dried and ground with mortar and pestle. Available Hg was extracted following the procedure described by Soltampour and Schwab (1977). Hg concentration was measured using an Advanced Mercury Analyser 254 Leco (St. Joseph, Michigan, MI, USA) with a detection limit of 0.5 $\mu\text{g kg}^{-1}$. Certified reference materials (CRM) were used to determine the accuracy of the measurements and validation: SRM 2709 (San Joaquin agricultural soil, 1.40 ± 0.08 mg

kg⁻¹ of Hg), BCR-CRM 62 (olive leaves, 0.28 ± 0.02 mg kg⁻¹ of Hg), BCR-CRM 150 (spiked skim milk powder, 0.0094 ± 0.0017 mg kg⁻¹ of Hg). The experimental value determined for 5 measurements of each BCR was: 1.34 ± 0.05 mg kg⁻¹, 0.30 ± 0.01 mg kg⁻¹, and 0.0102 ± 0.0009 mg kg⁻¹ respectively.

To evaluate the alfalfa capacity to uptake the Hg from the soil, bioaccumulation factor (BAF) was calculated as an index of Hg accumulation in plants. According to Tu and Ma (2002), the BAF factor is the ratio between the total Hg concentration in shoot or root and Hg available in soil. To study the mobility of Hg inside the plant the ratio between Hg concentration in shoot and Hg concentration in root was calculated according to Baker (1981).

Nitrogen in plants

The nitrogen (N) in plant tissue was determined by Kjeldahl digestion, which converts organic N (proteins and nucleic acids) to inorganic ammonium (NH₄⁺) with its posterior determination. The digestion was performed into the wet digester system B-440 (Buchi, Switzerland). Dry plant material was ground to powder using a mortar and pestle, and 0.05 g was transferred to the digestion tubes together with 10 ml of 98 %H₂SO₄ (v/v) and 10 g of K₂SO₄. The solution was heated at 410 °C for 1:30 h, cooled for 30 min. NH₄⁺ was distilled after the addition of 25 ml of a 32% NaOH (v/w) solution in a K-355 distillation unit (Buchi, Switzerland). The concentration of NH₃ released in the resulting alkaline mixture was calculated by back titration of a 2% H₃BO₃ (v/v) buffer adjusted to pH 4.65 with 0.02 M HCl, following the specifications of a KF Titrino Plus 870 (Metrohm, Switzerland).

Metal stress indexes

Lipid peroxidation was estimated by the formation of malondialdehyde, a by-product of lipid peroxidation that reacts with thiobarbituric acid. The resulting chromophore absorbs at 535 nm, and the concentration was calculated directly from the extinction coefficient of 1.563105 M cm⁻¹. Ground frozen tissue (0.1g) was transferred to a screw-capped 1.5 ml Eppendorf tube, and homogenized following addition of 1 ml of TCA–TBA–HCl reagent (15% (w/v) trichloroacetic acid (TCA), 0.37% (w/v) 2-thiobarbituric acid (TBA), 0.25 M HCl, and 0.01% butylated hydroxytoluene). After homogenization, samples were incubated at 90 °C for 30 min in a hot block, then chilled in ice, and centrifuged at 12 000 g for 10 min. Absorbance was measured in a UV-2401 PC spectrophotometer (Shimadzu

Corporation, Japan) at 535 nm and 600 nm, the last one to correct the non-specific turbidity.

Chlorophylls were extracted from 0.05 g of frozen leaves with 10 ml 80% (v/v) acetone using a mortar and pestle. Homogenates were filter and absorbance was measured in a UV-2401 PC spectrophotometer (Shimadzu Corporation, Kyoto, Japan) at 645 and 663 nm. Total chlorophyll concentrations were calculated according to the formula by Arnon (Porra, 2002):

Total Chlorophyll (mg g^{-1} FW) = Chlorophyll a + Chlorophyll b, where:

$$\text{Chla} \left(\frac{\text{mg}}{\text{g FW}} \right) = \left[(12.7 \times A_{663}) - (2.69 \times A_{645}) \right] \frac{\mu\text{g}}{\text{mL}} \times \frac{10 \text{ mL} \times \text{mg}}{0.05 \text{ g FW} \times 10^3 \mu\text{g}}$$

$$\text{Chlb} \left(\frac{\text{mg}}{\text{g FW}} \right) = \left[(22.90 \times A_{645}) - (4.68 \times A_{663}) \right] \frac{\mu\text{g}}{\text{mL}} \times \frac{10 \text{ mL} \times \text{mg}}{0.05 \text{ g FW} \times 10^3 \mu\text{g}}$$

Glutathione reductase and ascorbate peroxidase

Glutathione (GR) and ascorbate peroxidase (APX) activities were determined in gel after separation of protein extracts by non-denaturing electrophoresis in 10% polyacrylamide gels. Extracts were prepared from 0.5 g of intact frozen samples in 1 ml extraction solution, freshly prepared by mixing 10 ml extraction buffer-30mM MOPS at pH 7.5, 5mM $\text{Na}_2\text{-EDTA}$, 10 mM DTT, 10mM ascorbic acid, 0.6% PVP, 10 μl 100mM PMSF and 1 ml protease inhibitors cocktail. After centrifugation (14,000g) for 15 min at 4°C, the supernatant was stored as single use 100-200 μl aliquots at 80°C. Protein concentration in the extracts was preliminarily determined with the BioRad Protein Assay reagent, and the final loading for activity staining was adjusted after denaturing gel electrophoresis and Coomassie-blue staining (Laemmli, 1970). Protein loading for GR analysis was 15 μg and 10 μg of seedling and elongation shoot extract, and 5 μg and 3 μg . of seedling and elongation root extract, respectively. Protein loading for APX detection was 30 μg of seedling and elongation shoot extract and 7 μg of seedling and elongation root extract. GR activity was revealed with the procedure developed by Kaplan (1969), with minor modifications. Gel slabs were incubated in GR staining solution (250mM Tris-HCl buffer at pH 7.5, supplemented with 0.2 mg ml^{-1} thizolyl blue tetrazolium bromide, 0.2 mg ml^{-1} 2,6-dichlorophenol indophenol, 0.5 mM NADPH and 3.5 mM oxidised glutathione; GSSG). Bands corresponding to diaphorase activity (higher electrophoretic mobility than GRs), were identified by incubating a second gel in a staining solution without GSSG. The direct effect of Hg on GR activity was

evaluated by in vitro incubation of purified *S. cerevisiae* GR or leaf enzymatic crude extract. Samples were diluted to the appropriate activity (4-6 mU of purified GR) or extract protein content (15 µg), exposed to Hg (up to 1.0 mM), and incubated at room temperature for 1 h. Then, the proteins were separated by non-denaturing polyacrylamide gel electrophoresis, and GR activity was assayed in gel as described above.

APX was detected as described by Jimenez et al. (1998). Gel slabs were incubated for 20 min with 2 mM ascorbate and 2mM H₂O₂ in 50 mM Na-phosphate buffer at pH 7.0. The APX activity was detected with 0.5 mM nitroblue tetrazolium (NBT) and 10 mM TEMED in 50 mM phosphate buffered at pH 7.8. A digital camera (Kodak 290, USA) was used to take the gel pictures that were processed with Kodak 1D Image Analysis Software (version 3.6). Regions of interest (ROIs) were selected with the same surface and pixel intensity was adjusted to the background. Data were given relative to the intensity of control samples.

Preparation of non-protein thiol standard solutions

Biothiol stock standard solutions containing 50 mM of glutathione (GSH), homoglutathione (hGSH), cysteine (Cys), N-acetyl cysteine (N-AcCys), and 2 mM of γ -(Glu-Cys)₂-Ala (hPC₂), and γ -(Glu-Cys)₃-Ala (hPC₃) were prepared in analytical-grade type I water (Milli-Q Synthesis, Millipore). Aliquots of the stock solutions were immediately frozen in liquid N₂, lyophilized and stored at -80 °C. Standards of 0.5 mM GSH, Cys and N-AcCys and standards of 0.1 mM hPC₂ and hPC₃ were injected in the HPLC to set the retention times.

Analysis on non-protein thiols

Non-protein thiols were analysed by High Performance Liquid Chromatography (HPLC) following the procedure described by Ortega-Villasante et al. (2005). 0.1 g of frozen tissue was ground in liquid N₂ and 15 µl of 5 mM N-acetyl cysteine (N-AcCys) was spiked as internal standard (Howden et al. 1995) prior homogenization with 300 µl of a extraction buffer (0.1 M HCl, 1 M EDTA, 5% MPA, 1% PVPP) to quantify the thiols. The homogenate was centrifuged twice for 15 min at 12 000 g and 4°C in Eppendorf tubes. The clear supernatant was transferred to a boron-silica glass injection vial. Separation and detection of the thiols was carried out using the method described by Meuwly et al. (1995) with some modifications. Extracts (100 µl) were injected in a Mediterranean Sea18 column (5 µm, 250 x 4.6 mm; Teknokroma, Spain), using an

Agilent 1200 HPLC system (Santa Clara, CA, USA). The mobile phase was built using two eluents: A (dH₂O: acetonitrile (v/v) in 98:2 ratio plus 0.01 % TFA) and, B (dH₂O: acetonitrile (v/v) in 2:98 ratio plus 0.01 % TFA). The gradient program, as for % solvent B, was: 2 min, 0%; 25 min; 25%; 26 min, 50%; 30 min, 50%; 35 min, 0%; 45 min, 0%. Thiols were detected after post-column derivatization with Ellman's reagent (1.8 mM 5,5-dithio-bis, 2 nitrobenzoic acid in 300 mM K-phosphate, 15 mM EDTA at pH 7.0), in a thermostatic 1.8 ml reactor at 38°C, as described by Rauser (1991). The derivative compound, 5-mercapto-2-nitrobenzoate, had an absorption maximum at 412 nm. To identify the retention time of non-protein thiols of extract tissue before quantification, commercial biothiol standards (Cys, GSH, hGSH, hPC₂ and hPC₃) were run previously. Data were processed with the Agilent Chemstation software.

Statistical analysis

Statistical analysis was performed with the software package SPSS for Windows (version 15.0), by using an ANOVA with Tukey test when the significance in Levene test was > 0.05 or Welch with Games-Howell test when the significance in Levene test was < 0.05 . Results were mean of at least three independent replicates \pm standard deviation, with significant differences between treatments at $p < 0.05$.

RESULTS

Soil

According to the physical and chemical parameters showed in Table 1, the soil collected from Almadén had a loamy sand texture according to the USDA. This soil had pH 6.5 and a very low electric conductivity (EC); thus was classified as moderately acid and non saline (Porta et al., 1999). The organic matter content, the C/N ratio, the total nitrogen (N) and the cation exchange capacity (CEC) were low for agricultural soils. The content of Mg⁺², Na⁺ and K⁺ were low but the Ca²⁺ concentration was adequate for most agronomical crops (Tisdale et al., 1985). The total Hg concentration in the soil was 12.48 mg kg⁻¹ in average, being 0.007 mg kg⁻¹ the concentration of available Hg.

According to the experimental design used, total Hg concentration in the soil pots (Table 2) was within the range of 2.7-4.0 mg kg⁻¹, whereas available Hg was within the range of 2.2-6.6 µg kg⁻¹, representing less than 0.2% of the total Hg. After the experiment, NPK and PK did not alter both levels of Hg, remaining stable during the stages of growth (data not shown).

Table 1 Physical and chemical parameters of soil before start the experiment (texture, pH, OM and EC: n=5; rest of parameters: n=10)

Texture (%) Clay/Silt/Sand		12/15/72
pH		6.5
Electrical conductivity (EC) ($\mu\text{S cm}^{-1}$)		135.4
Organic matter (OM) (%)		1.38
C:H:N (%)		0.87:0.25:0.11
C/N ratio		7.9
Cation exchange capacity (CEC) ($\text{cmol}_c \text{ kg}^{-1}$)		11
Nutrients (mg kg^{-1})		
	Ca ²⁺	2720 \pm 215
	Mg ²⁺	180 \pm 24.1
	Na ⁺	28.2 \pm 5.6
	K ⁺	40.3 \pm 3.8
Total Hg (mg kg^{-1})		12.48 \pm 4.82
Available Hg (mg kg^{-1})		0.007 \pm 0.001

Table 2 Total Hg (mg kg^{-1}), available Hg ($\mu\text{g kg}^{-1}$) and available Hg (%) in the soil of the pots treated with a PK fertilizer (without NO_3^-) or a NPK fertilizer (with NO_3^-) after harvesting the alfalfa plants at different stage of growth (seedling and elongation). Data are average of three independent replicates (\pm SD).

Stage of growth	Fertilization	Total Hg (mg kg^{-1})	Available Hg ($\mu\text{g kg}^{-1}$)	Available Hg (%)
Seedling	PK	3.1 \pm 0.5	2.6 \pm 0.6	0.08
	NPK	4.0 \pm 0.3	2.2 \pm 0.1	0.06
Elongation	PK	2.7 \pm 0.8	6.6 \pm 1.2	0.24
	NPK	3.3 \pm 0.2	2.4 \pm 0.1	0.07

Mercury concentration and distribution in alfalfa plants

According to the data showed in Table 3, the Hg concentration in root was 5-7 times higher than in shoots at the seedling stage. This difference was attenuated in alfalfa at the elongation phase, being the Hg concentration in roots over 2.5-fold higher than in shoots. The Hg concentration decreased in roots and shoots during the elongation stage, possibly caused by a dilution effect due to the augment in plant biomass. It should be noted that nitrogen fertilization affected roots Hg concentration at the seedling stage, being significantly higher with NPK fertilization. However, the nitrogen status did not affect the Hg concentration in seedling shoots, and elongation shoot and root. To study the mobility of Hg inside the plant, the ratio between Hg concentration in shoots and roots was calculated. In all cases, the ratio was low (<0.5), confirming that Hg is mainly accumulated in the root (Table 3).

The bioaccumulation factor (BAF) was used as an index of Hg accumulation in plants to evaluate the alfalfa capacity to uptake Hg from the soil. BAF was calculated as a ration between the concentration of Hg in each organ and the concentration of Hg available in the soil (Table 3). As already stated, alfalfa plants showed a remarkable

Table 3 Total Hg (mg kg^{-1}) in root and shoot, ratio ($[\text{Hg}_{\text{shoot}}]/[\text{Hg}_{\text{root}}]$), and bioaccumulation factor BAF ($[\text{Hg}_{\text{organ}}]/[\text{Hg}_{\text{soil available}}]$) of alfalfa plants harvested at seedling and elongation growth stages, fertilized with NO_3^- (NPK) or without NO_3^- (PK). Data are average of three independent replicates (\pm SD), and different letters denote significant differences at $p < 0.05$.

Growth stage	Treatment	Hg (mg kg^{-1})		Ratio	BAF	
		Root	Shoot	Shoot/root	Shoot/soil	Root/soil
Seedling	PK	1.28 ± 0.41^a	0.24 ± 0.02^a	0.19	92.3	492.3
	NPK	2.12 ± 0.37^b	0.31 ± 0.04^a	0.14	140.9	963.6
Elongation	PK	0.28 ± 0.09^c	0.12 ± 0.02^b	0.43	18.9	42.4
	NPK	0.36 ± 0.03^c	0.12 ± 0.04^b	0.33	50.0	150.0

preference to accumulating Hg in roots, since BAF values were in the range of 2-7 times higher than in shoot depending on the stage of growth. With respect to fertilization, BAF values were much higher in alfalfa plants grown with the NPK fertilization, value that decreased in the elongation stage.

Biometric parameters

Plants did not show external symptoms of toxicity due to Hg exposure (i.e. chlorosis or darkened roots; Fig. 2C). However, nitrogen fertilization affected the length of plants: plants grown with NPK were significantly larger than plants grown with PK fertilization. However, in the elongation stage, the growth of PK treated plants almost

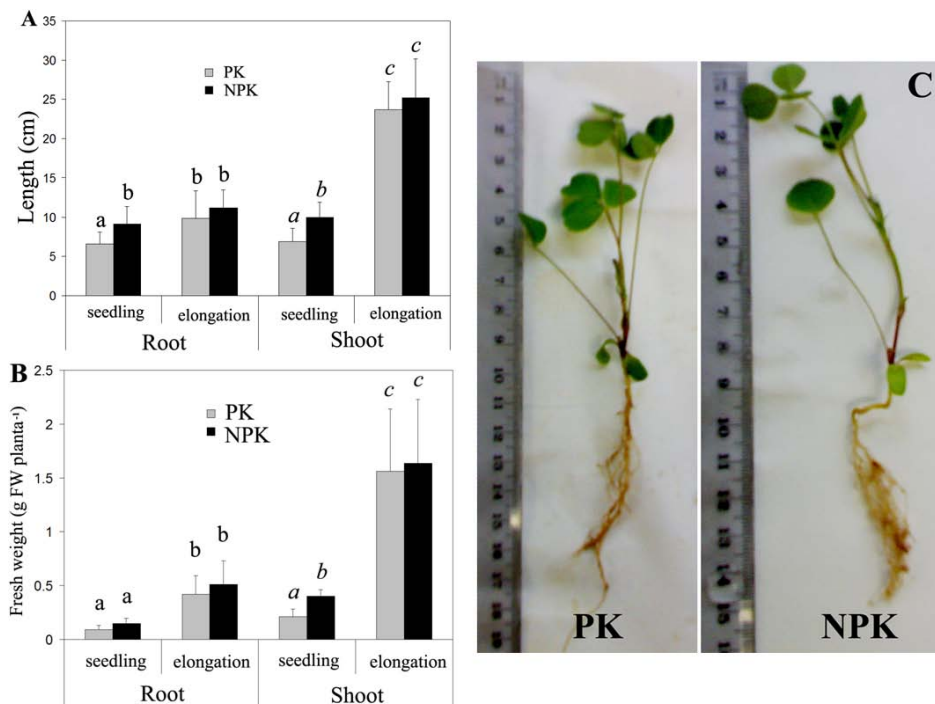


Fig. 2. Length (cm plant^{-1}) (A) and fresh weight (g plant^{-1}) (B) of roots and shoots of alfalfa plants harvested at seedling and elongation growth stages, fertilized with NO_3^- (NPK) or without NO_3^- (PK). (C) Detail of alfalfa plants collected at the seedling stage. Data are average of three independent replicates (\pm SD), and different letters denote significant differences at $p < 0.05$.

reached the size of NPK treated plants, when differences became not significant (Fig. 2A, 2C). The same trend was observed in the fresh weight of shoots and roots, which were higher alfalfa with NPK fertilization. However, this parameter was significantly different when shoots were compared (Fig. 2B, 2C).

Nitrogen content in alfalfa plants

Plants fertilized with NPK accumulated a significant higher amount of NH_4^+ per plant than those cultivated in soils only fertilized with PK at the seedling stage (Fig. 3A). However, in the elongation stage there were no differences in the amount of NH_4^+ per plant. When roots were sampled at the elongation stage, we observed that they were completely nodulated, with pinkish nodules possibly harbouring an effective nitrogen-fixation metabolism. Apparently, the collected soils had enough *Sinorhizobium meliloti* inoculum to allow the establishment of symbiotic N_2 -fixation, which would provide sufficient organic N to maintain the requirements for alfalfa plants in the absence of N fertilizer.

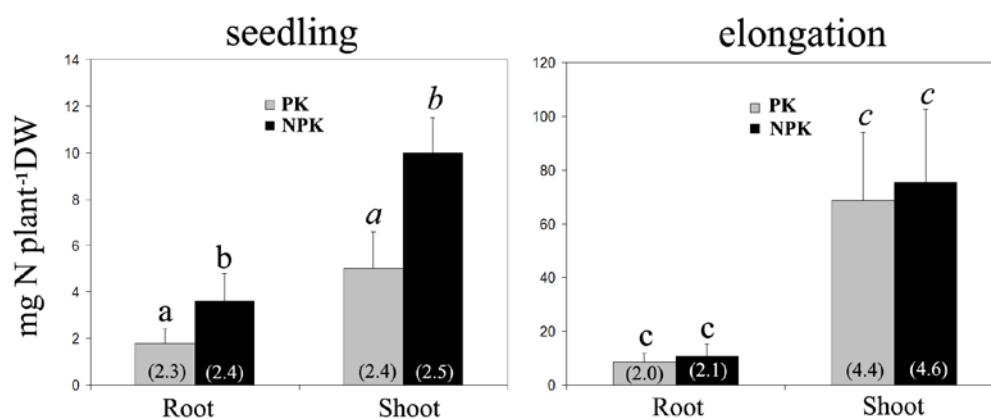


Fig. 3. Nitrogen content (mg NH_4^+ plant⁻¹) and nitrogen percentage (%; between parenthesis) in root and shoot of *Medicago sativa* harvested at seedling and elongation growth stages, fertilized with NO_3^- (NPK) or without NO_3^- (PK). Data are average of three independent replicates (\pm SD), and different letters denote significant differences at $p < 0.05$.

Oxidative stress parameters

The nitrogen fertilization did not affect significantly the concentration of chlorophyll in alfalfa plants, although there was a slightly diminution in the chlorophyll content of at the seedling stage with the PK treatment (Fig. 4). Malondialdehyde (MDA) content was determined as an index of lipid peroxidation in alfalfa root (Fig. 5). Results showed that MDA content was higher in plants fertilized with PK at the seedling stage. However, the differences in the MDA content between plants treated with or without NO_3^- were

lower at the elongation stage, indicating that the oxidative stress decreased in plants fertilized with PK when their biomass augmented.

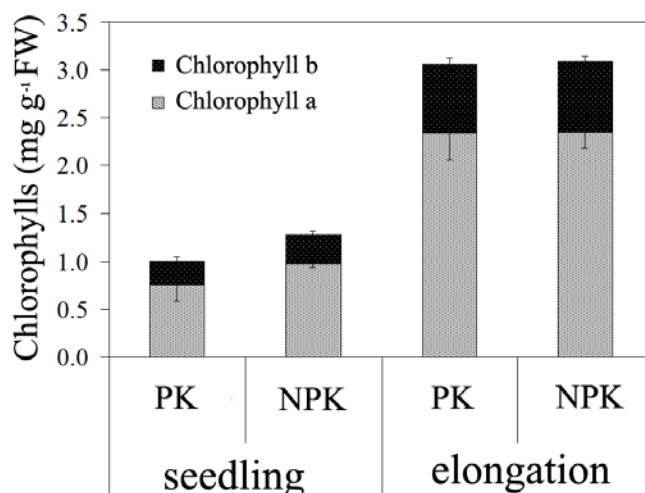


Fig. 4. Chlorophyll concentration (mg g^{-1} FW) in leaves of *Medicago sativa* harvested at seedling and elongation growth stages, fertilized with NO_3^- (NPK) or without NO_3^- (PK). Data are average of three independent replicates (\pm SD), and different letters denote significant differences at $p < 0.05$.

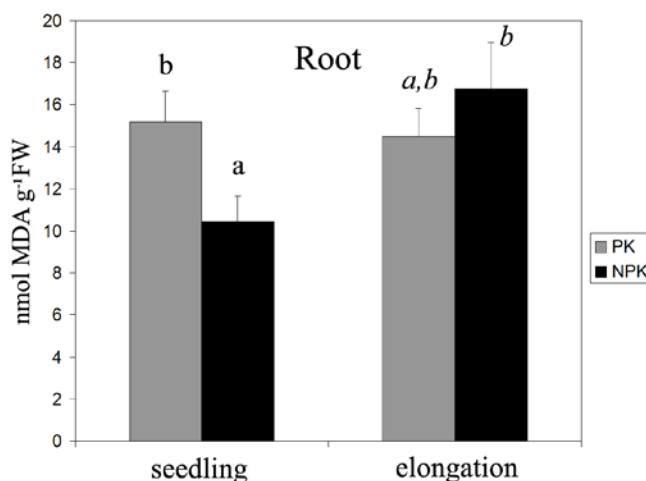


Fig. 5. Malondialdehyde content (nmol MDA g^{-1} FW) in root of *Medicago sativa* harvested at seedling and elongation growth stages, fertilized with NO_3^- (NPK) or without NO_3^- (PK). Data are average of three independent replicates (\pm SD), and different letters denote significant differences at $p < 0.05$.

The activity of APX and GR antioxidant enzymes was determined by in gel staining after non-denaturing polyacrylamide gel electrophoresis. Under the experimental conditions used, there was no difference in shoot of GR and APX activity with respect the fertilization at both growth stages (Fig. 6A). However, GR and APX activity in roots was remarkably higher in plants that were fertilized without NO_3^- (PK) compared with those that were fertilized with NO_3^- (Fig. 6B). This difference was better detected at the seedling growth stage (Fig. 6B).

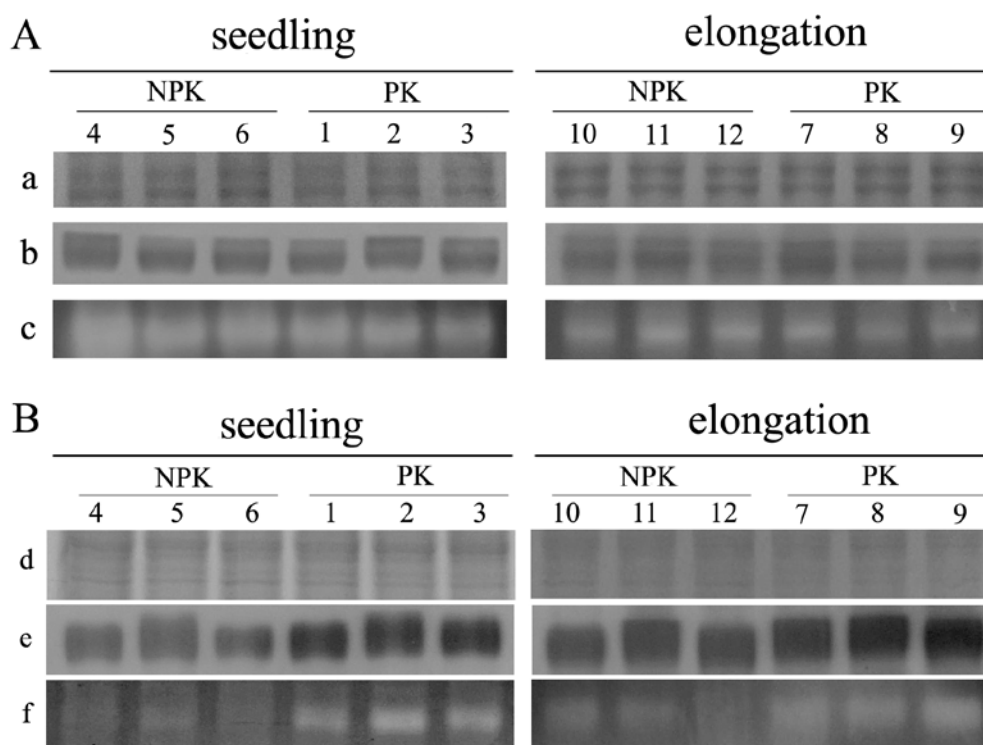


Fig. 6. Glutathione reductase (GR) and Ascorbate peroxidase (APX) *in gel* activity in shoot (**A**) and root (**B**) of *Medicago sativa* harvested at seedling and elongation growth stages, fertilized with NO_3^- (NPK) or without NO_3^- (PK). Numbers correspond to the pools sampled (see Fig 1). **a, d** Coomassie-blue general staining of proteins to show equivalent loading of protein; **b, e** GR activity; and **c, f** APX activity.

Analysis of non-protein thiols

The non-protein thiol content was analysed in shoots and roots of alfalfa seedling considering the different nitrogen nutritional status of the plants, as it is known the effect of adequate nitrogen fertilization in the assimilation and metabolism of sulphur containing metabolites in the plants (Kopriva and Rennenberg, 2004). Alfalfa plants accumulated homogluthathione (hGSH), a GSH homologous non-protein thiol that occurs in certain legume plants (Matamoros et al., 1999). At the seedling growth stage, shoot concentration of hGSH in plants treated with NPK was $384 \pm 85 \text{ nmol g}^{-1} \text{ FW}$, while in plants treated with PK was $347 \pm 33 \text{ nmol g}^{-1} \text{ FW}$. Therefore, it was slightly higher in plants fertilized with NO_3^- , although not significantly different ($p < 0.05$). hGSH content in roots was three times lower ($100 \text{ nmol g}^{-1} \text{ FW}$), and no differences were observed between NPK and PK fertilized plants. At the elongation stage, there were no differences between treatments, and the concentration was of the same order as in plants at the seedling stage (data not shown). There were no phytochelatins (nor the homologous non-protein thiols homophytochelatins) at any growth stage.

DISCUSSION

The physical and chemical characteristic of the soil obtained from Castilseras (Almadén, Spain) was adequate to sustain a crop of alfalfa, as this plant prefers slightly acidic and well-aerated soils. In addition, the low organic matter content, low C/N ratio and low CEC did not limit the growth of alfalfa (Ortega and Corvalan, 2004). The low content of nutrients, such as N, Mg^{2+} , Na^+ and K^+ , detected was probably due to losses caused by previous agricultural activities. Prior to soil collection for our experiments, cereals were cultivated for several seasons, causing a general depletion of nutrients in the area. It is well known that cereal exhaust the nutrients of soil, and supply of fertilizers and amendments is required for proper crop yield (Mengel and Kirby, 2001). The low N background found in the collected soil (0.11%), was then considered appropriated for our experiment to reproduce the conditions of a soil poor in nitrogen.

Hg is usually found in natural soil at levels ranging from 0.01 to 0.5 $mg\ kg^{-1}$ (Alloway, 1995). However the total Hg content of the initial soil used in this study was twenty five times higher. Taking into account that the study area belongs to a region rich in Hg deposits and with an intense and prolonged mining activities, the value of 12.48 $mg\ kg^{-1}$ would be considered normal, even moderate as there are plots in the Almadén that accumulates up to 34,000 $mg\ kg^{-1}$ (Gray et al., 2004; Bernaus et al., 2006). The concentration of available Hg in the initial soil was approximately 0.06% of the total Hg. These values were in agreement with previous studies, where available Hg represents 0.1% of total Hg in soils from Almadén (Moreno-Jimenez et al., 2006; Sierra et al., 2008b).

The range of total Hg concentration (2.7-4 $mg\ kg^{-1}$) and available Hg (2.2-6.6 $\mu g\ kg^{-1}$) measured in the soil used for the experiments contained in pots, was three times lower than the total Hg (12.48 $mg\ kg^{-1}$) and the Hg available (7 $\mu g\ kg^{-1}$) in the initial soil. This was due to the dilution of the original soil after it was mixed with perlite and sand in equal proportions (1:1:1), to avoid clogging and compaction. These results were similar to those found in a similar study performed by Sierra et al. (2008a) under greenhouse conditions with soil from Almadén.

The application of soil amendments to correct low fertility in polluted soils by mining activities may actually increase soluble Hg. These observations, however, are dependent on the amendment application rate, type of amendment and soil properties (Heeraman et al., 2001). By contrast, soil fertilization may decrease the Hg concentration in plants due to an increase in the biomass.

Interestingly, the addition of nitrogen fertilizer augmented significantly the concentration of Hg in alfalfa roots at the seedling stage, when the addition of NO_3^- led to a significant increase in biomass. This result is in agreement with Barrutia et al. (2009) who studied the influence of the fertilization (NPK+B) on metal up take in *Rumex acetosa* L. and *Rumex accessions* grown in a metalliferous soil with high levels of Zn, Pb and Cd. They observed that plants grown with fertilization accumulated more Zn and Cd than plants grown without fertilization. BAF parameter highlighted the increase effectiveness of NPK fertilized plants to remove Hg from the soil, as occurred with other metals (Tu and Ma 2002). Gao et al. (2010) evaluated the effect of nitrogen fertilizers on Cd concentration in the grain of durum wheat under field conditions, and found also that the supply of nitrogen fertilizer increased Cd uptake and accumulation in different parts of the plant, such as in the grain. In spite of the dilution effect related with an increase in biomass, common when plants are fed with NO_3^- , the increase in Hg accumulation should be explain in other basis. Well-nourished plants have an improved development of root architecture, which allows better extraction of nutrients and water (Lynch, 1995). In particular, nitrate availability induces lateral root elongation permitting in turn a higher capacity to uptake more NO_3^- (Mantelin and Touraine, 2004). Therefore, it is feasible that under adequate nutritional status plants would be able to augment Hg concentration.

Differences in biomass yield and Hg accumulation decreased (were in most cases not significant) between plants fertilized with NO_3^- or without NO_3^- at the elongation stage. This could be explained by the appearance of nodules in alfalfa roots, formed by the symbiotic interaction with an endogenous *Sinorhizobium meliloti* existing in the collected soil from Almadén. Consequently, N was not a limiting factor in PK-treated plants. This was indeed measured by the amount of NH_4^+ measured in the plants: At the seedling stage NPK-treated plants showed a significantly higher content of organic N, differences that were attenuated in the elongation stage.

Mercury accumulated to a higher extent in roots, as found in many wild and crop plants (Patra et al., 2004). The ratio between Hg concentration in shoot and Hg concentration in root, in all cases, was less than 0.5. According to Baker (1981), a ratio lower than 1, means that alfalfa presents excluder behaviour. Alfalfa is widely grown as forage for cattle. The alfalfa culture is harvested between the elongation and the 10 % of flowering because the protein content is optimum in those growth stages (Broderick, 1985). Regarding forage use, the accepted maximum Hg concentration relative to the feeding

stuff is less than 0.1 mg kg^{-1} (EC Directive 2002). According to this legislation, the concentration of Hg in shoots at elongation stage surpasses the legal limit, so precautions should be imposed to guarantee a safe consumption of edible parts of the plants.

With respect to the stress parameters measured in NPK and PK fertilized plants, lipid peroxidation was only higher in the roots of plants grown in the absence of NO_3^- at the seedling growth stage. Therefore, under N starvation an oxidative stress would be induced. In agreement with this observation, the activity of the antioxidant enzymes APX and GR was remarkably higher in the roots of PK-fertilized plants at the seedling stage. When the level of N was recovered in PK plants thanks to N_2 -symbiotic fixation at the elongation stage, both MDA concentration and APX and GR enzymatic activity were more similar to NPK-treated plants. It has been described that in the early stages of *Rhizobium* bacteria infection and nodule formation, leguminous roots experience a cellular redox imbalance. In such conditions, the antioxidant defence system is triggered, resulting in the over-expression of genes coding antioxidant enzymes, modulation of their enzymatic activity and accumulation of antioxidant metabolites (Gogorcena et al., 1997; Pauli et al., 2006).

CONCLUSIONS

The soil collected from Almadén is suitable for alfalfa crop cultivation. Despite the high total Hg concentration of the soil, only the 0.2 % is available for plants. Fertilisation with NO_3^- augmented plant biomass at the earliest developmental stages, but thanks to symbiotic N_2 -fixation plants without NO_3^- could also obtain sufficient N for an adequate normal biomass production. The largest pool of Hg was found retained in roots, with a rather low translocation to shoots, showing typical excluder behaviour. Nitrogen supply prevents oxidative stress in roots, but may improve root development and increase the uptake of Hg from the soil above safety consumption limits. It would be necessary to achieve a balance between the crop management and the accumulation of heavy metals. To confirm these results and provide a safe economic alternative to use Almadén plots for agricultural purposes, further studies should be performed at a pilot field scale in real conditions, paying special attention in the Hg accumulation in shoots during elongation and first steps of flowering stage.

ACKNOWLEDGEMENTS

This work was supported by Spanish Ministry of Science and Innovation (CTM2005-04809/TECNO-REUSA and AGL2010-15151-PROBIOMET), Fundación Ramón Areces (www.fundacionareces.es), Comunidad de Madrid (EIADES S2009/AMB-1478), Junta Comunidades Castilla-La Mancha (FITOALMA2, POII10-0087-6458). We thank M Jose Sierra and Juan Sobrino-Planta for technical advice and support in the experiments.

REFERENCES

- Alloway B.J. (1995) Heavy Metals in Soils, second ed. Blackie Academic & Professional, London.
- Arnon D.I. (1949) Copper enzymes in isolated chloroplasts-polyphenoloxidase in *Beta vulgaris*. *Plant Physiology*, **24**, 1-15.
- Baker A.J.M. (1981) Accumulators and excluders — strategies in the response of plants to heavymetals. *Journal of Plant Nutrition* **3**, 643–654.
- Barber S. A. (1995) Soil nutrient bioavailability: A mechanistic approach. 2nd edn. John Wiley and Sons, New York, USA.
- Barrutia O., Epelde L., Garcia-Plazaola J.I., Garbisu C. & Becerril J.M. (2009) Phytoextraction potential of two *Rumex acetosa* L. accessions collected from metalliferous and non-metalliferous sites: Effect of fertilization. *Chemosphere*, **74**, 259-264.
- Bernaus A., Gaona X., van Ree D. & Valiente M. (2006) Determination of mercury in polluted soils surrounding a chlor-alkali plant - Direct speciation by X-ray absorption spectroscopy techniques and preliminary geochemical characterisation of the area. *Analytica Chimica Acta*, **565**, 73-80.
- Berzas-Nevado J.J., García-Bermejo L.F. & Rodríguez-Martín R.C. (2003) Distribution of mercury in the aquatic environment at Almadén, Spain. *Environmental Pollution*, **122**, 261-271.
- Broderick G. A. (1985) Alfalfa silage or hay versus corn silage as the sole forage for lactating dairy cows. *Journal Dairy Science*, **68**, 3262.
- Carrasco-Gil S., Álvarez-Fernández A., Sobrino-Plata J., Millán R., Carpena-Ruiz R.O., LeDuc D.L., Andrews J.C., Abadía J. & Hernández L.E. (2011) Complexation of Hg with phytochelatin is important for plant Hg tolerance. *Plant, Cell and Environment* (in press).
- Clarkson T.W. (1997) The toxicology of mercury. *Critical Reviews in Clinical Laboratory Sciences*, **34**, 369-403.
- Cunningham, S.D., Ow, D.W., 1996. Promises and prospects of phytoremediation. *Plant Physiology*, **110**, 715-719
- Del Pozo, M. (1983) La alfalfa, su cultivo y aprovechamiento. *Ediciones Mundi-Prensa*, Madrid, Spain.
- Dushenkov S., Kapulnik Y., Blaylock M., Sorochisky B., Raskin I. & Ensley, B. (1997) Phytoremediation: a novel approach to an old problem, in: Wise, D.L. (Ed.), *Studies in Environmental Science*. Elsevier, pp 563-572.
- EC Directive (2002) Directive of The European Parliament and of the Council of 7 May 2002 on Undesirable Substances in Animal Feed 2002/32/EC.
- European Commission (2008) Options for reducing Mercury use in products and Applications, and the Fate of Mercury already Circulating in Society.
- Ferrara R., Maserti B.E., Andersson M., Edner H., Ragnarson P., Svanberg S. & Hernandez A. (1998) Atmospheric mercury concentrations and fluxes in the Almadén District (Spain). *Atmospheric Environment*, **32**, 3897-3904.
- Frescholtz T.F. & Gustin M.S. (2004) Soil and foliar mercury emission as a function of soil concentration. *Water Air and Soil Pollution*, **155**, 223-237.

- Gao X., Brown K.R. Racz G.J. & Grant C.A. (2010) Concentration of cadmium in durum wheat as affected by time, source and placement of nitrogen fertilization under reduced and conventional-tillage management. *Plant Soil*, **337**, 341-354.
- Gogorcena Y., Gordon A.J., Escuredo P.R., Minchin F.R., Witty J.F., Moran J.F. & Becana M. (1997) N₂ fixation, carbon metabolism, and oxidative damage in nodules of dark-stressed common bean plants. *Plant Physiology*, **113**, 1193-1201.
- Gray J.E., Hines M.E., Higuera P.L., Adatto I. & Lasorsa B.K. (2004) Mercury speciation and microbial transformations in mine wastes, stream sediments, and surface waters at the Almadén Mining District, Spain. *Environmental Science and Technology*, **38**, 4285-4292.
- Heeraman D.A., Claassen V.P. & Zasoski R.J. (2001) Interaction of lime, organic matter and fertilizer on growth and uptake of arsenic and mercury by Zorro fescue (*Vulpia myuros* L.). *Plant and Soil*, **234**, 215-231.
- Higuera P., Oyarzun R., Lunar R., Sierra J. & Parras J. (1999) The Las Cuevas deposit, Almadén district (Spain): an unusual case of deep-seated advanced argillic alteration related to mercury mineralization. *Mineralium Deposita*, **34**, 211-214.
- Higuera P., Oyarzun R., Munha J. & Morata D. (2000) Palaeozoic magmatic-related hydrothermal activity in the Almadén syncline, Spain: a long-lasting Silurian to Devonian process? *Transactions of the Institution of Mining and Metallurgy Section B-Applied Earth Science*, **109**, B199-B202.
- Higuera P., Oyarzun R., Biester H., Lillo J. & Lorenzo S. (2003) A first insight into mercury distribution and speciation in soils from the Almadén mining district, Spain. *Journal of Geochemical Exploration*, **80**, 95-104.
- Howden R., Goldsbrough P.B., Andersen C.R., Cobbett C.S. (1995). Cadmium-sensitive, cad1 mutants of *Arabidopsis thaliana* are phytochelatin deficient. *Plant Physiology* **107**, 1059-1066.
- Huckabee J.W., Sanz Diaz F., Janzen S.A. & Solomon J. (1983) Distribution of mercury in vegetation at Almadén, Spain. *Environmental Pollution Series A, Ecological and Biological*, **30**, 211-224.
- Jiménez, A., Hernández, J.A., Ros-Barceló, A., Sandalio, L.M., del Río, L.A., Sevilla, F. (1998) Mitochondrial and peroxisomal ascorbate peroxidase of pea leaves. *Physiology. Plantarium*, **104**, 687-692.
- Kopriva, S., Rennenberg, H. (2004). Control of sulphate assimilation and glutathione synthesis: interaction with N and C metabolism. *Journal of Experimental Botany*, **55**, 1831-1842.
- Kaplan, J.C., Beutler, E. (1968). Electrophoretic study of glutathione reductase in human erythrocytes and leukocytes. *Nature*, **217**, 256.
- Laemmli, U.K. (1970). Cleavage of structural proteins during the assembly of the head of bacteriophage T4. *Nature*, **227**, 680-685.
- Levit J. (1980) Responses of plants to environmental stresses, 2nd ed., 2 Academy Press, New York.
- Lindberg S.E., Jackson D.R., Huckabee J.W., Janzen S.A., Levin M.J. & Lund J.R. (1979) Atmospheric emission and plant uptake of mercury from agricultural soils near the Almadén mercury mine. *Journal of Environment Quality*, **8**, 572-578.
- Llorca, M., Masip, J., Ollé, F., (1999). La alfalfa deshidratada. Cultivo, transformación y consumo. *Ediciones Universidad de Lleida*, Spain.
- Long X.X., Yang X.E. & Ni W.Z (2002) Current status and perspective on phytoremediation of heavy metal polluted soils. *Journal of Applied Ecology*, **13**, 752-62.
- Lynch J. (1995) Root architecture and plant productivity. *Plant Physiology*, **109**, 7-13.
- Ma, C. (1998). Hg harm on cell membrane of rape leaf and cell endogenous protection effect. *Yingyong Shengtai Xuebao*, **9**, 323-326.
- Mantelin S. & Touraine B. (2004) Plant-growth promoting bacteria and nitrate availability: impacts on root development and nitrate uptake. *Journal of Experimental Botany*, **55**, 27-34.
- MAPA (Ministerio de Agricultura, Pesca y Alimentación), (1998). Calendario de siembra, recolección y comercialización. Madrid, Spain, 207pp
- Matamoros M.A., Moran J.F., Iturbe-Ormaetxe I., Rubio M.C. & Becana M. (1999) Glutathione and homoglutathione synthesis in legume root nodules. *Plant Physiology*, **121**, 879-888.

- Mengel K. & Kirby E.A. (2001) Principles of Plant Nutrition. 5th Edition, Kluwer Academic Publishers, Dordrecht, The Netherlands.
- Meuwly P., Thibault P., Schwan A.L. & Rauser W.E. (1995) Three families of thiol peptides are induced by cadmium in maize. *The Plant Journal*, **7**, 391–400.
- Millán R., Gamarra R., Schmid T., Sierra M.J., Quejido A.J., Sánchez D.M., Cardona A.I., Fernández M. & Vera R. (2006). Mercury content in vegetation and soils of the Almadén mining area (Spain). *Science of the Total Environment*, **368**, 79-87.
- Mittler R. (2002) Oxidative stress, antioxidant and stress tolerance. *Trends in Plant Science*, **7**, 405-410.
- Moreno-Jiménez E., Gamarra R., Carpena-Ruiz R.O., Millán R., Peñalosa J.M. & Esteban E. (2006) Mercury bioaccumulation and phytotoxicity in two wild plant species of Almadén area. *Chemosphere* **63**, 1969-1973.
- Ortega-Villasante C., Rellan-Alvarez R., Del Campo F.F., Carpena-Ruiz R.O. & Hernandez L.E. (2005) Cellular damage induced by cadmium and mercury in *Medicago sativa*. *Journal of Experimental Botany*, **56**, 2239-2251.
- Ortega, A., Corvalan, E. (2004). Diagnóstico de suelos. INTA EEA Salta.
- Patra M., Bhowmik N., Bandopadhyay B. & Sharma A. (2004) Comparison of mercury, lead and arsenic with respect to genotoxic effects on plant systems and the development of genetic tolerance. *Environmental and Experimental Botany*, **52**, 199-223.
- Patra M. & Sharma A. (2000) Mercury toxicity in plants. *Botanical Review*, **66**, 379-422.
- Pauli N., Pucciariello C., Mandon K., Innocenti G., Jamet A., Baudouin E., Hérouart D., Frenod P. & Puppo A. (2006) Reactive oxygen and nitrogen species and glutathione: key players in the legume–*Rhizobium* symbiosis. *Journal of Experimental Botany*, **57**, 1769–1776
- Porra R.J. (2002) The chequered history of the development and use of simultaneous equation for the accurate determination of chlorophylls *a* and *b*. *Photosynthesis Research*, **73**, 149-156.
- Porta J., Lopez-Acevedo M. & Roquero C. (1999) Edafología para la agricultura y el medio ambiente. 2ª edición. Ediciones Mundi-Prensa. Bilbao, Spain, 849 pp.
- Rauser W.E. (1991) Cadmium-binding peptides from plants. *Methods in Enzymology*, **205**, 319-333.
- Rellán-Álvarez R., Hernández L.E., Abadía J. & Álvarez-Fernández A. (2006) Direct and simultaneous determination of reduced and oxidized glutathione and homogluthathione by liquid chromatography-electrospray/mass spectrometry in plant tissue extracts. *Analytical Biochemistry*, **356**, 254-264.
- Howden R., Goldsbrough P.B., Andersen C.R. & Cobbett C.S. (1995) Cadmium-sensitive, cad1 mutants of *Arabidopsis thaliana* are phytochelatin deficient. *Plant Physiology*, **107**, 1059-1066.
- Sierra M.J., Millán R., Esteban E., Cardona A.I. & Schmid T. (2008a) Evaluation of mercury uptake and distribution in *Vicia sativa* L. applying two different study scales: Greenhouse conditions and lysimeter experiments. *Journal of Geochemical Exploration*, **96**, 203-209.
- Sierra M.J., Millán R. & Esteban E. (2008b) Potential use of *Solanum melongena* in agricultural areas with high mercury background concentrations. *Food and Chemical Toxicology*, **46**, 2143-2149.
- Sierra M.J., Millán R. & Esteban E. (2009) Mercury uptake and distribution in *Lavandula stoechas* plants grown in soil from Almadén mining district (Spain). *Food and Chemical Toxicology*, **47**, 2761-2767.
- Sobrino-Plata J., Ortega-Villasante C., Flores-Caceres M.L., Escobar C., Del Campo F.F. & Hernandez L.E. (2009) Differential alterations of antioxidant defenses as bioindicators of mercury and cadmium toxicity in alfalfa. *Chemosphere*, **77**, 946-954.
- Soltanpour P.N. & Schwab A.P. (1977) A new test for simultaneous extraction of macro and micronutrients on alkaline soils. *Communications in Soil Science and Plant Analysis*, **8**, 195–207.
- Tisdale S. L., Nelson W. L. & Beaton J. D. (1985) Soil fertility and fertilizers. 4th edn. Macmillan, New York.
- Tu C. & Ma L.Q. (2002) Effects of arsenic concentrations and forms on arsenic uptake by the hyperaccumulator ladder brake. *Journal of Environmental Quality*, **31**, 641–647.
- UNEP (2011) Toolkit for identification and quantification of mercury releases. Mercury Programme, UNEP DTIE, Chemicals Branch, Geneva, Switzerland.

Zhou Z.S., Huang S.Q., Guo K., Mehta S.K., Zhang, P.C. & Yang Z.M. (2007) Metabolic adaptations to mercury-induced oxidative stress in roots of *Medicago sativa* L. *Journal of Inorganic Biochemistry*, **101**, 1-9.



CONCLUSIONES

CONCLUSIONES

1. El Hg absorbido por las plantas de alfalfa, maíz y cebada expuestas a 30 μM fue acumulado principalmente en la raíz, concretamente más del 90% quedó retenido en la fracción particulada correspondiente con la pared celular. El análisis llevado a cabo mediante HPLC-ESI-TOFMS de la fracción soluble de los tres cultivos reveló que el Hg estaba asociado con fitoquelatinas. En total se identificaron 19 complejos Hg-PC, 14 de ellos en alfalfa, de los cuales 11 no habían sido descritos anteriormente en la literatura.
2. La síntesis de PCs parece importante para la tolerancia a Hg, como pudo mostrarse en plantas mutantes de *Arabidopsis thaliana* deficientes en la producción de fitoquelatinas, *cad1-3*, y con menor contenido de GSH, *cad2-1*.
3. El análisis EXAFS para determinar la especiación *in vivo* de Hg en plantas de alfalfa expuestas a 30 μM Hg mostró que un 79% estaba unido a Cys, y el 21% estaba en forma de metil-Hg. Las imágenes de la distribución espacial obtenidas mediante μ -SXRF revelaron que el Hg fue acumulado principalmente en los conductos vasculares de raíz, tallo y hoja. A nivel subcelular las imágenes de TEM apoyan la noción de que el Hg se acumula preferentemente en la pared celular de las células de la raíz.
4. Las plantas de alfalfa crecidas en un sistema hidropónico presentaron un comportamiento diferente en relación a la absorción de Hg de plantas silvestres de marrubio. El análisis mediante μ -SXRF indican que en alfalfa el Hg es absorbido principalmente a través de los ápices de las raíces, posiblemente siguiendo el flujo del agua. Sin embargo, en el marrubio el Hg es retenido en la epidermis de la raíz, concretamente en la corteza. El análisis EXAFS realizado en raíz y hoja indicó que más del 60% del Hg estaba unido a S inorgánico en forma de cinabrio y metacinabrio, posiblemente procedente de partículas de suelo adherida a la epidermis.
5. El estado nutricional del nitrato (NO_3^-) de las plantas podría ser importante para mejorar su tolerancia al Hg. Plantas de alfalfa que crecieron con altos niveles de NO_3^- , sufrieron un menor estrés oxidativo medido por un menor efecto en la peroxidación lipídica de raíz y un menor efecto inhibitorio sobre la actividad de GR. El estado nutricional de N se vio afectado, sobre todo en la raíz donde se apreció un aumento importante de la actividad de NR en plantas con alto NO_3^- .
6. El suelo muestreado en Almadén presentó condiciones adecuadas para el cultivo de la alfalfa. A pesar del alto contenido de Hg total en estos suelos, solo el 0.2% estaba

disponible para las plantas, el cual fue reflejado en la ausencia de síntomas de toxicidad en las plantas. La aplicación de un fertilizante NPK supuso un mayor crecimiento de la planta en la fase inicial de desarrollo (estadio de plántula). En esta fase, la aplicación de NO_3^- disminuyó los síntomas de estrés oxidativo ligados a un aumento de actividad de APX y GR, pero supuso una mayor acumulación de Hg que llegó a sobrepasar el límite legal de seguridad permitido.



APPENDIX I

Supplementary Table 1. Species observed, mass charge ratio (m/z) and retention time for LC—ESI/MS(TOF) analysis with positive and negative ionization modes of biothiols and Hg biothiols complexes standard solutions. The ratio Hg:ligand was (μM) 10:10; 10:20; 20:10. Identity of each complex was confirmed by the simulation of theoretical spectra with the MicrOtof Data Analysis Software. Ions are ordered by increasing m/z value.

m/z range	Hg:hPC ₂						t_R
	POSITIVE MODE						
	1:2		1:1		2:1		
	Species	m/z	Species	m/z	Species	m/z	
0-1000	[HghPC ₂ +2H+K] ²⁺	396.5	[HghPC ₂ +2H+K] ²⁺	396.5	[HghPC ₂ +2H+K] ²⁺	396.5	6.3
	[hPC ₂ +H] ⁺	554.1	[hPC ₂ +H] ⁺	554.1			6.3
	[HghPC ₂ +H] ⁺	754.1	[HghPC ₂ +H] ⁺	754.1			6.3
					[HghPC ₂ +H] ⁺	754.1	6.3
					[HghPC ₂ +H+Na] ⁺	776.1	6.3
					[HghPC ₂ +H+K] ⁺	792.0	6.3
1000-3000	[(hPC ₂) ₂ +H] ⁺	1107.2					6.3
	[(hPC ₂) ₂ +H+Na] ⁺	1129.2					6.3
	[(hPC ₂) ₂ +H+K] ⁺	1145.2					6.3
	[Hg (hPC ₂) ₂ +H] ⁺	1307.1	[Hg (hPC ₂) ₂ +H] ⁺	1307.2			6.3
	[Hg (hPC ₂) ₂ +H+Na] ⁺	1329.1	[Hg (hPC ₂) ₂ +H+Na] ⁺	1329.2			6.3
	[Hg (hPC ₂) ₂ +H+K] ⁺	1345.1					6.3
	[Hg ₂ (hPC ₂) ₂ +H] ⁺	1505.2	[Hg ₂ (hPC ₂) ₂ +H] ⁺	1505.1	[Hg ₂ (hPC ₂) ₂ +H] ⁺	1505.1	6.3
	[Hg ₂ (hPC ₂) ₂ +H+K] ⁺	1543.1	[Hg ₂ (hPC ₂) ₂ +H+Na] ⁺	1527.2	[Hg ₂ (hPC ₂) ₂ +H+Na] ⁺	1527.1	6.3
			[Hg ₂ (hPC ₂) ₂ +H+K] ⁺	1543.1		6.3	
NEGATIVE MODE							
0-1000	[hPC ₂ -H] ⁻	552.1	[hPC ₂ -H] ⁻	552.2	[hPC ₂ -H] ⁻	552.1	6.4
	[HghPC ₂ -H] ⁻	752.1	[HghPC ₂ -H] ⁻	752.1	[HghPC ₂ -H] ⁻	752.1	6.4
					[HghPC ₂ +Na-H] ⁻	774.1	6.4
					[HghPC ₂ +2Na-H] ⁻	796.1	6.5
1000-3000	[(hPC ₂) ₂ -H] ⁻	1105.2					6.4
	[Hg(hPC ₂) ₂ -H] ⁻	1305.1					6.4
	[Hg(hPC ₂) ₂ +Na-H] ⁻	1327.1					6.4
	[Hg ₂ (hPC ₂) ₂ -H] ⁻	1503.1	[Hg ₂ (hPC ₂) ₂ -H] ⁻	1503.1	[Hg ₂ (hPC ₂) ₂ -H] ⁻	1503.1	6.4
	[Hg ₂ (hPC ₂) ₂ +Na-H] ⁻	1525.1	[Hg ₂ (hPC ₂) ₂ +Na-H] ⁻	1525.1	[Hg ₂ (hPC ₂) ₂ +Na-H] ⁻	1525.1	6.5
			[Hg ₂ (hPC ₂) ₂ +2Na-H] ⁻	1547.1	[Hg ₂ (hPC ₂) ₂ +2Na-H] ⁻	1547.1	6.5
		[Hg ₃ (hPC ₂) ₃ -H] ⁻	2255.1			6.5	
		[Hg ₃ (hPC ₂) ₃ +Na-H] ⁻	2277.1			6.5	

<i>m/z</i> range	Hg:PC ₂						<i>t_R</i>
	POSITIVE MODE						
	1:2		1:1		2:1		
	Species	<i>m/z</i>	Species	<i>m/z</i>	Species	<i>m/z</i>	
0-1000	[HgPC ₂ +Na+2H] ²⁺	381.1	[HgPC ₂ +Na+2H] ²⁺	381.1	[HgPC ₂ +Na+2H] ²⁺	381.5	6.1
	[PC ₂ +H] ⁺	540.1	[PC ₂ +H] ⁺	540.1	[PC ₂ +H] ⁺	540.1	6.1
	[HgPC ₂ +H] ⁺	740.0	[HgPC ₂ +H] ⁺	740.1			6.1
	[HgPC ₂ +Na+H] ⁺	762.0					6.1
1000-3000			[Hg ₂ (PC ₂)+H] ⁺	1477.1			6.2
	[Hg ₂ (PC ₂)+Na+H] ⁺	1499.1					6.2
	[Hg ₂ (PC ₂)+K+H] ⁺	1515.0	[Hg ₂ (PC ₂)+K+H] ⁺	1515.1			6.2
NEGATIVE MODE							
0-1000	[PC ₂ -H] ⁻	538.1	[PC ₂ -H] ⁻	538.1	[PC ₂ -H] ⁻	538.1	6.0
	[HgPC ₂ -H] ⁻	738.1	[HgPC ₂ -H] ⁻	738.1	[HgPC ₂ -H] ⁻	738.1	6.2
	[HgPC ₂ +Na-H] ⁻	760.1	[HgPC ₂ +Na-H] ⁻	760.1	[HgPC ₂ +Na-H] ⁻	760.1	6.2
					[HgPC ₂ +2Na-H] ⁻	782.1	6.2
1000-3000	[PC ₂ -H] ⁻	1077.2					6.0
	[PC ₂ +Na-H] ⁻	1099.0					6.0
	[Hg(PC ₂) ₂ -H] ⁻	1277.1					6.1
	[Hg ₂ (PC ₂) ₂ -H] ⁻	1475.1	[Hg ₂ (PC ₂) ₂ -H] ⁻	1475.1	[Hg ₂ (PC ₂) ₂ -H] ⁻	1475.1	6.2
	[Hg ₂ (PC ₂) ₂ +Na-H] ⁻	1497.1	[Hg ₂ (PC ₂) ₂ +Na-H] ⁻	1497.1	[Hg ₂ (PC ₂) ₂ +Na-H] ⁻	1497.0	6.2
	[Hg ₂ (PC ₂) ₂ +2Na-H] ⁻	1519.1	[Hg ₂ (PC ₂) ₂ +2Na-H] ⁻	1519.0	[Hg ₂ (PC ₂) ₂ +2Na-H] ⁻	1519.0	6.2

m/z range	Hg:hPC ₃					t _R	
	POSITIVE MODE						
	1:2		1:1		2:1		
	Species	m/z	Species	m/z	Species	m/z	
0-1000	[HghPC ₃ +2H] ²⁺	493.5			[Hg(hPC ₃)+2H] ²⁺	493.6	7.8
	[HghPC ₃ +Na+2H] ²⁺	504.5			[Hg(hPC ₃)+Na+2H] ²⁺	504.6	7.8
	[hPC ₃ +H] ⁺	786.1			[hPC ₃ +H] ⁺	786.2	7.8
	[HghPC ₃ +H] ⁺	986.1	[HghPC ₃ +H] ⁺	986.1	[HghPC ₃ +H] ⁺	986.1	7.8
1000-3000	[HghPC ₃ +H] ⁺	986.1	[HghPC ₃ +H] ⁺	986.1	[HghPC ₃ +H] ⁺	986.1	7.8
	[Hg ₂ hPC ₃ +H] ⁺	1184.0	[Hg ₂ hPC ₃ +H] ⁺	1184.1			7.8
	[Hg(hPC ₃) ₂ +H] ⁺	1771.2	[Hg ₂ hPC ₃ +H+Na] ⁺	1206.1			7.8
NEGATIVE MODE							
0-1000	[HghPC ₃ -2H] ²⁻	491.6	[HghPC ₃ -2H] ²⁻	491.6			7.8
			[HghPC ₃ +Na-2H] ²⁻	502.6			7.8
			[HghPC ₃ +Na-2H] ²⁻	513.6			7.8
	[hPC ₃ -H] ⁻	784.2	[hPC ₃ -H] ⁻	784.2			7.9
	[hPC ₃ +Na-H] ⁻	806.16					7.9
	[HghPC ₃ -H] ⁻	984.2	[HghPC ₃ -H] ⁻	984.2			7.9
	[Hg(hPC ₃) ₂ -H] ⁻	1769.3					7.9
[Hg(hPC ₃) ₂ +Na-H] ⁻	1791.3					7.9	
[Hg(hPC ₃) ₂ +2Na-H] ⁻	1813.2					7.9	
1000-3000	[HghPC ₃ -H] ⁻	984.1	[HghPC ₃ -H] ⁻	984.1	[HghPC ₃ -H] ⁻	984.1	7.8
			[HghPC ₃ +Na-H] ⁻	1006.1	[HghPC ₃ +Na-H] ⁻	1006.1	7.8
			[HghPC ₃ +2Na-H] ⁻	1028.1			7.8
			[Hg ₄ (hPC ₃) ₂ -2H] ²⁻	1082.1	[Hg ₄ (hPC ₃) ₂ -2H] ²⁻	1082.6	8.4
			[Hg ₄ (hPC ₃) ₂ +Na-2H] ²⁻	1093.5	[Hg ₄ (hPC ₃) ₂ +Na-2H] ²⁻	1093.1	8.4
			[(Hg) ₂ hPC ₃ -H] ⁻	1182.0	[(Hg) ₂ hPC ₃ -H] ⁻	1182.0	8.4

<i>m/z</i> range	Hg:PC ₃					<i>t_R</i>	
	POSITIVE MODE						
	1:2		1:1		2:1		
	Species	<i>m/z</i>	Species	<i>m/z</i>	Species	<i>m/z</i>	
0-1000	[PC ₃ +2H] ²⁺	386.6					7.6
	[PC ₃ +Na+2H] ²⁺	397.6					7.6
	[HgPC ₃ +2H] ²⁺	486.6	[HgPC ₃ +2H] ²⁺	486.6			7.6
	[HgPC ₃ +Na ₂ +H] ²⁺	497.5	[HgPC ₃ +Na ₂ +H] ²⁺	497.6			7.6
	[HgPC ₃ +H] ⁺	972.1	[PC ₃ +H] ⁺	772.2	[PC ₃ +H] ⁺	772.2	7.6
					[HgPC ₃ +H] ⁺	972.1	7.6
1000-3000	[HgPC ₃ +H] ⁺	972.1	[HgPC ₃ +H] ⁺	972.1			7.5
	[HgPC ₃ +Na+H] ⁺	994.1	[HgPC ₃ +Na+H] ⁺	994.1	[HgPC ₃ +Na+H] ⁺	994.1	7.6
	[HgPC ₃ +Na+K+H] ⁺	1010.0					7.5
			[HgPC ₃ +2Na+H] ⁺	1016.1			7.5
			[HgPC ₃ +3Na+H] ⁺	1038.0			7.5
			[HgPC ₃ +4Na+H] ⁺	1060.0	[HgPC ₃ +4Na+H] ⁺	1060.0	7.5
			[Hg ₂ PC ₃ +H] ⁺	1170.1			8.4
		[Hg ₂ PC ₃ +Na+H] ⁺	1192.1			8.4	
NEGATIVE MODE							
0-1000	[PC ₃ -2H] ²⁻	384.6					7.4
	[PC ₃ -H] ⁻	770.2	[HgPC ₃ -2H] ²⁻	486.6	[HgPC ₃ -2H] ²⁻	484.6	7.6
	[PC ₃ +Na-H] ⁻	792.2	[PC ₃ -H] ⁻	770.2			7.4
	[HgPC ₃ -H] ⁻	970.1	[HgPC ₃ -H] ⁻	970.1	[HgPC ₃ -H] ⁻	970.1	7.5
	[HgPC ₃ +Na-H] ⁻	992.1	[HgPC ₃ +Na-H] ⁻	992.1	[HgPC ₃ +Na-H] ⁻	992.1	7.5
1000-3000	[HgPC ₃ -H] ⁻	970.1	[HgPC ₃ -H] ⁻	970.1	[HgPC ₃ -H] ⁻	970.1	7.6
	[HgPC ₃ +Na-H] ⁻	992.1	[HgPC ₃ +Na-H] ⁻	992.1	[HgPC ₃ +Na-H] ⁻	992.1	7.5
			[HgPC ₃ +2Na-H] ⁻	1014.1	[HgPC ₃ +2Na-H] ⁻	1014.1	7.5
			[HgPC ₃ +3Na-H] ⁻	1036.0			7.6
			[HgPC ₃ +4Na-H] ⁻	1058.0			7.6

<i>m/z</i> range	Hg:GC ₂					<i>t_R</i>	
	POSITIVE MODE						
	1:2		1:1		2:1		
	Species	<i>m/z</i>	Species	<i>m/z</i>	Species		<i>m/z</i>
0-1000			[GC ₂ +H] ⁺	483.1	[HgGC ₂ +2H+K] ²⁺	361.0	6.1
	[HgGC ₂ +H] ⁺	683.0	[HgGC ₂ +H] ⁺	683.1	[GC ₂ +H] ⁺	483.1	6.1
					[HgGC ₂ +H] ⁺	683.1	6.2
1000-3000			[Hg ₂ (GC ₂) ₂ +H] ⁺	1363.1			6.2
			[Hg ₂ (GC ₂) ₂ +Na+H] ⁺	1385.0			6.2
NEGATIVE MODE							
0-1000	[GC ₂ -H] ⁻	481.1	[GC ₂ -H] ⁻	481.1	[GC ₂ -H] ⁻	481.1	6.0
	[HgGC ₂ -H] ⁻	681.1	[HgGC ₂ -H] ⁻	681.1	[HgGC ₂ -H] ⁻	681.1	6.1
	[HgGC ₂ +Na-H] ⁻	703.0	[HgGC ₂ +Na-H] ⁻	703.0	[HgGC ₂ +Na-H] ⁻	703.0	6.2
1000-3000	[Hg(GC ₂) ₂ -H] ⁻	1163.1	[Hg(GC ₂) ₂ -H] ⁻	1163.1			6.1
	[Hg(GC ₂) ₂ +Na-H] ⁻	1185.1					6.1
	[Hg(GC ₂) ₂ +2Na-H] ⁻	1207.1					6.1
	[Hg ₂ (GC ₂) ₂ -H] ⁻	1361.1	[Hg ₂ (GC ₂) ₂ -H] ⁻	1361.0	[Hg ₂ (GC ₂) ₂ -H] ⁻	1361.0	6.2
	[Hg ₂ (GC ₂) ₂ +Na-H] ⁻	1383.1	[Hg ₂ (GC ₂) ₂ +Na-H] ⁻	1383.0	[Hg ₂ (GC ₂) ₂ +Na-H] ⁻	1383.0	6.2
	[Hg ₂ (GC ₂) ₂ +2Na-H] ⁻	1405.0					6.2
			[Hg ₂ (GC ₂) ₂ +3Na-H] ⁻	1427.0			6.2
			[Hg ₃ (GC ₂) ₃ -H] ⁻	2042.0			6.2

<i>m/z</i> range	Hg:GSH						<i>t_R</i>
	POSITIVE MODE						
	1:2		1:1		2:1		
	Species	<i>m/z</i>	Species	<i>m/z</i>	Species	<i>m/z</i>	
0-1000	[GSH+H] ⁺	308.1			[GSH+H] ⁺	308.1	2.4
			[Hg(GSH) ₂ +2H] ²⁺	408.1	[Hg(GSH) ₂ +2H] ²⁺	408.1	4.9
			[HgGSH+H] ⁺	508.1	[HgGSH+H] ⁺	508.0	4.8
			[Hg(GSH) ₂ +H] ⁺	815.1	[Hg(GSH) ₂ +H] ⁺	815.1	4.9
NEGATIVE MODE							
0-1000	[GSH-H] ⁻	306.1	[GSH-H] ⁻	306.1	[GSH-H] ⁻	306.9	2.3
					[HgGSH-H] ⁻	506.0	2.7
					[HgGSH+Na-H] ⁻	528.0	2.7
	[Hg(GSH) ₂ -H] ⁻	813.1	[Hg(GSH) ₂ -H] ⁻	813.1	[Hg(GSH) ₂ -H] ⁻	813.1	4.8
	[Hg(GSH) ₂ +Na-H] ⁻	835.1	[Hg(GSH) ₂ +Na-H] ⁻	835.1	[Hg(GSH) ₂ +Na-H] ⁻	835.1	4.8
			[Hg(GSH) ₂ +2Na-H] ⁻	857.1	[Hg(GSH) ₂ +2Na-H] ⁻	857.1	4.8
		[Hg(GSH) ₂ +3Na-H] ⁻	879.1	[Hg(GSH) ₂ +3Na-H] ⁻	879.0	4.8	
1000-3000	[Hg ₂ (GSH) ₄ -H] ⁻	1625.1					4.9
	[Hg ₂ (GSH) ₄ +Na-H] ⁻	1647.1					4.9

<i>m/z</i> range	Hg:hGSH						<i>t_R</i>
	POSITIVE MODE						
	1:2		1:1		2:1		
	Species	<i>m/z</i>	Species	<i>m/z</i>	Species	<i>m/z</i>	
0-1000	[hGSH+H] ⁺	322.1	[hGSH+H] ⁺	322.1			3.3
	[Hg(hGSH) ₂ +2H] ²⁺	422.1	[Hg(hGSH) ₂ +2H] ²⁺	422.1			5.6
	[HghGSH+H] ⁺	522.1	[HghGSH+H] ⁺	522.1	[HghGSH+H] ⁺	522.0	5.7
					[Hg(hGSH) ₂ +H] ⁺	843.1	5.8
NEGATIVE MODE							
0-1000	[hGSH-H] ⁻	320.1			[hGSH-H] ⁻	320.1	3.4
			[HghGSH-H] ⁻	520.1	[HghGSH-H] ⁻	520.1	5.7
			[Hg(hGSH) ₂ -H] ⁻	841.1	[HghGSH+Na-H] ⁻	841.1	5.7
			[Hg(hGSH) ₂ +Na-H] ⁻	863.1	[Hg(hGSH) ₂ +2Na-H] ⁻	863.1	5.8
			[Hg(hGSH) ₂ +2Na-H] ⁻	885.1	[Hg(hGSH) ₂ +3Na-H] ⁻	885.1	5.8
1000-3000			[Hg(hGSH) ₂ +3Na-H] ⁻	907.1			5.7



APPENDIX II

DATOS PERSONALES

Sandra Carrasco Gil

Fecha de nacimiento: 14 de enero de 1980 (Madrid)

Dirección: C/ Pisuerga nº52 Izq. 28670 V. de Odón. MADRID

Teléfonos: 630650022 (móvil)

Correo electrónico: sandra.carrasco.gil@gmail.com

DNI: 14307796W

TITULACIÓN ACADÉMICA

29 Sep/2005. **Certificado-Diploma de Estudios Avanzados** en el área de conocimiento *Edafología y Química Agrícola*, dentro del programa de doctorado *Tecnología Agroambiental*. Trabajo de investigación en "Influencia de los fertilizantes y abonos sobre la disponibilidad de mercurio en suelos de Almadén" (calif.:10.0).E.T.S.I. Agrónomos. Universidad Politécnica de Madrid.

1998-2002. **Licenciada en Ciencias Ambientales**. Universidad Europea de Madrid. Estudios cursados con Beca.

EXPERIENCIA PROFESIONAL

Oct/2006-Sep/2010. **Dpto Medio Ambiente, CIEMAT (Madrid)-Dpto. Biología, UAM**. Beca FPI 2+2 del Ministerio de Ciencia e Innovación.

Feb/2010-Abril/2010. **Estancia en Stanford Synchrotron Radiation Lightsource (SSRL)** perteneciente al SLAC National Accelerator Center (California, EEUU). Uso de la técnica XANES (X-ray absorption near-edge structure), EXAFS (extended X-ray absorption fine structure) y μ -SAXRF (synchrotron X-ray fluorescence microprobe).

Feb/2009-Jul/2009. **Estancia en Stanford Synchrotron Radiation Lightsource (SSRL)** perteneciente al SLAC National Accelerator Center (California, EEUU). Uso de la técnica XANES (X-ray absorption near-edge structure), EXAFS (extended X-ray absorption fine structure) y μ -SAXRF (synchrotron X-ray fluorescence microprobe).

Abr/2007-Jul/2010. **Estancias en el laboratorio de Fisiología de Estrés Abiótico en Plantas de la Estación Experimental de Aula Dei-CSIC**. Zaragoza (España). Uso de la técnica de cromatografía líquida acoplada a un masas (HPLC-MS/TOF).

Dic/2003- Abril/2006. Técnico Auxiliar de Medio Ambiente y Protección Civil.

Ayuntamiento de Brunete. Madrid.

Elaboración de planes de gestión ante incendios forestales en la interfaz urbano-forestal.

Elaboración del Plan Territorial de Protección Civil de Brunete (PLATERBRU).

Jun/2003-Nov/2003. Consultora Ambiental.

Ingeniería y Consultoría Ambiental. DRABA S.L. Las Rozas. Madrid.

Elaboración de Estudios de Impacto Ambiental de infraestructuras lineales.

Oct/2000-Oct/2002. Vendedora.

Decathlon España. S.A. Majadahonda. Madrid.

Venta y gestión interna (inventarios, pedidos, planificación).

FORMACIÓN COMPLEMENTARIA

Set/30/2009-Oct/2/2009. Curso de Postgrado del CSIC. Aplicación de la Radiación Sincrotrón a la Caracterización de Materiales.

Ene/2006. Curso de simulación de Incendios forestales FARSITE. Universidad de Lleida
Oct/2003-Jun/2004. Cursos de Doctorado dentro del programa de Tecnología Agroambiental.
E.T.S.I. Agrónomos. Universidad Politécnica de Madrid.

Degradación del Suelo y Tecnología de la Conservación (50 h).
Agricultura Ecológica y Protección al Medio Ambiente (50 h).
Análisis de Datos Aplicados en la Investigación en Agricultura y Economía Agraria (50 h).
Cómo Redactar Artículos de Investigación en Inglés para publicar en revistas científico-técnicas (50h).

PARTICIPACIÓN EN PROYECTOS I+D

2010-2013. PROSPECCIÓN DE BIOMARCADORES DE RESPUESTA A METALES (PROBIOMET).
Entidad financiadora: Ministerio de Ciencia e Innovación. Entidades participantes: UAM y Ciemat. Futura contratación con cargo a proyecto.

2007-2010. CARACTERIZACIÓN DE LOS MECANISMOS DE RESISTENCIA DE LAS PLANTAS A METALES PESADOS. Entidad financiadora: Fundación Ramón Areces. Entidades participantes: UAM, Ciemat, IMIDRA, Aula Dei-CSIC.

2006-2010. EVALUACIÓN DEL IMPACTO AMBIENTAL Y RECUPERACIÓN DEL MEDIO NATURAL EN EMPLAZAMIENTOS CONTAMINADOS (EIADES). Entidad financiadora: Comunidad de Madrid. Entidades participantes: IMIDRA, UCM, INIA, Ciemat, UAH, UPM, CSIC, UAM.

2007-2009. FITORREMEDIACIÓN DE EMPLAZAMIENTOS AFECTADOS POR MERCURIO EN LA COMARCA DE ALMADÉN CON PLANTAS DE USO AGRÍCOLA (FITOALMA). Entidad financiadora: Junta de Comunidades de Castilla-La Mancha. Entidades participantes: UCM, UAM, Ciemat.

2006-2009. RECUPERACIÓN DE SUELOS CONTAMINADOS POR MERCURIO: RECOMENDACIONES DE USOS DE SUELOS Y PLANTAS EN LA COMARCA DE ALMADÉN (REUSA). Entidad financiadora: Ministerio de Ciencia e Innovación. Entidades participantes: Ciemat, UAM, INIA, UAH, UPM y CSIC.

PARTICIPACIÓN EN CONGRESOS

Mercury localization and speciation in alfalfa (Medicago sativa) grown in hydroponic system. **S. Carrasco-Gil**, H. Siebner, J.C. Andrews, DL. LeDuc, R. Millán, L.E. Hernández. 11th International Conference of the Biogeochemistry of Trace Elements (ICOBTE). Florencia (Italia), 3-7 Julio, 2011. Comunicación oral. Enviada

Hard X-ray imaging of mercury accumulation in plants. J. C. Andrews, **S. Carrasco-Gil**, D. LeDuc, L. E. Hernández, R. Millán, Y. Liu, F. Meirer, S. Webb, P. Pianetta. The 10th International Conference on X-Ray Microscopy. Chicago (EEUU), 15-20 de agosto de 2010. Póster

Physiological effects of Hg in alfalfa plants grown in a soil contaminated with mercury with two different nitrogen nutritional statuses **S. Carrasco-Gil**, M. Estebaranz, D. Medel, LE. Hernández y R. Millán. SETAC Europe 20th Annual Meeting. Science and Technology for Environmental Protection. Sevilla (España), 23-27 de mayo de 2010. Póster

*Using Transmission X-ray microscopy, XAS, and μ -XRF to study Hg accumulation and transformation in *Spartina foliosa* and *Medicago sativa*.* C. Andrews, **S. Carrasco-Gil**, D. LeDuc,

C. Patty, R. Millán y L. E. Hernández. ACS American Chemical Society. Chemistry for Life. San Francisco (EEUU), 21-25 de marzo de 2010. Comunicación oral.

Soluble mercury is associated with phytochelatins in root. **Sandra Carrasco-Gil**, Ana Álvarez-Fernández, Rocío Millán, Ramón O. Carpena-Ruíz, Javier Abadía y Luis E. Hernández. Phytotechnology to promote sustainable land use and improve food safety. Ascona (Suiza), 11-16 octubre de 2009. Comunicación oral.

Soluble mercury is associated with phytochelatins in root. **Sandra Carrasco-Gil**, Ana Álvarez-Fernández, Rocío Millán, Ramón O. Carpena-Ruíz, Javier Abadía y Luis E. Hernández. XVIII Reunión de la Sociedad Española de Fisiología Vegetal (SEFV. XI Congreso Hispano-Luso de Fisiología Vegetal. Zaragoza (España), 8-11 de septiembre de 2009. Comunicación oral.

Influence of the nitrogen nutritional status in the stress responses to mercury in alfalfa (Medicago sativa). **Sandra Carrasco-Gil**, Rocío Millán, David Medel y Luis E. Hernández. Presentación del póster en: 10th International Conference of the Biogeochemistry of Trace Elements (ICOBTE). Chihuahua (Méjico), 13-16 Julio, 2009. Póster.

Influencia del estatus nutricional nitrogenado en la respuesta de estrés a mercurio en plantas de alfalfa (Medicago sativa). **Sandra Carrasco-Gil**, Rocío Millán, Luis E. Hernández. Presentación del póster en: XII Simposio Ibérico Sobre Nutrición Mineral de las Plantas-NUTRIPLANT. Granada (España), 22-24 Octubre, 2008. Póster.

Application of multi-sensor optical data for monitoring land uses within the mercury mining area of Almadén, Spain". Celia Rico, Thomas Schmid, Rocio Millán, María José Sierra, **Sandra Carrasco**. IEEE International Geoscience & Remote Sensing Symposium.. Boston, Massachusetts, (E.E.U.U), 6-11 julio de 2008. Comunicación oral.

Potencial Cultivation of Crops as an Alternative Economical Source in the Almadén Mining Area. **S. Carrasco**, M.J. Sierra, R. Millán, E. Esteban, T. Schmid, R.O. Carpena.. Presentación de la ponencia: 12 th International Congress on Energy and Mineral Resources. Oviedo (España), 7-11 Octubre, 2007. Comunicación oral.

Effect of soil amendmets and extractant solutions on soil with high Hg concentration" **S. Carrasco**, I. Carrasco, R. Millán, E.López-Samaniego and M.C. Díaz. Presentación del poster en: 9th International Conference of the Biogeochemistry of Trace Elements (ICOBTE). Pekín (China), 15 - 19 Julio, 2007. Póster.

Mercury accumulation in Cistus ladanifer under the influence of mining activities in Almaden area. **S. Carrasco**, O. Grebler, S. Vazquez, M.J. Sierra, R.O. Carpena and R. Millán. Presentación del Poster en: COST Action 859 Work Group 4 and Work Group 2 meeting. Vilnius (Lituania), 30 mayo–1 junio 2007. Póster.

Mercury absorption in several species of the genus cistus. **S. Carrasco**, O. Grebler, R. Millán, A.I. Cardona, S. Vazquez and G. León. Presentación del poster en: SETAC Europe 16th Annual Meeting. Oporto (Portugal), 20-24 Mayo, 2007. Póster.

Influence of the mining activities in soils of the rambla El Beal, Spain. E. Noruega, L.F. Rodriguez, R. Millán, F.J. Díaz, A. I. Cardona, G. García and **S. Carrasco**. Presentación del poster en: SETAC Europe 16th Annual Meeting. Oporto (Portugal), 20-24 Mayo, 2007. Póster.

Influence of the addition of fertilizers and organic matter on a mercury contaminated soil” S. Carrasco, R. Millán.. Presentación del poster en: SETAC Europe 16th Annual Meeting. La Haya (Holanda), 7–11 mayo 2006. Póster.

ASISTENCIA A JORNADAS / SEMINARIOS

Jornada anual del programa EIADES, Imidra, Finca “El Encín”, Alcalá de Henares (Madrid) 11 Noviembre de 2010. Ponencia bajo el título “Localización y especiación de mercurio en alfalfa (Medicago sativa): Implicaciones para su fitotoxicidad.

SSRL synchrotron BioXAS workshop, Menlo Park (California, EEUU) del 2 al 5 de junio de 2009

The European Environmental Bureau Conference on Mercury, Madrid 22 de abril de 2005.

PUBLICACIONES

Carrasco-Gil S., Álvarez-Fernández A., Sobrino-Plata J., Millán R., Carpena-Ruiz R.O., LeDuc D.L., Andrews J.C., Abadía J. & Hernández L.E. (2011). Complexation of Hg with phytochelatin is important for plant Hg tolerance. *Plant, Cell and Environment*. Enviada y aceptada

Millán R., Schmid T., Sierra M.J., **Carrasco-Gil S.**, Villadóniga M., Rico C., Ledesma D.M.S. & Puente F.J.D. (2011). Spatial variation of biological and pedological properties in an area affected by a metallurgical mercury plant: Almadenejos (Spain). *Applied Geochemistry*, **26**, 174-181

Millán R., Schmid T., Cardona A.I., Puente F.J.D., Sierra M.J., **Carrasco S.**, Rico C., Villadóniga M., Rodríguez V., Mejuto M. & García A. (2008). Suelos con altos contenidos de mercurio y estrategias de rehabilitación. *Infoenviro*, disponible en <http://www.infoenviro.es>

Sierra M.J., Millán R. & **Carrasco S.** (2007). Cambios de usos del suelo. En el libro: *Contaminación de Suelos. Tecnologías para su Recuperación*. Ciemat (eds), Pp. 473-485

Sierra M.J., Millán R. & **Carrasco S.** (2006). Cambios de usos del suelo. En el libro: *Procesos de Degradación y Recuperación de Suelos*. Ciemat (eds), Pp. 343-365

INFORMÁTICA

Windows vista y paquete Office 2007.

Adobe Photoshop 7.0